ATOM TRANSFER RADICAL POLYMERIZATION AND ITS CONTINUOUS PROCESSES

By

YOUQING SHEN, B. Sc., D. Sc.

A Thesis

Submitted to the School of Graduate Studies

In Partial Fulfillment of the Requirements

For the Degree of

Doctor of Philosophy

McMaster University

ATOM TRANSFER RADICAL POLYMERIZATION
AND
ITS CONTINUOUS PROCESSES

By

YOUQING SHEN
B.Sc., D. Sc.

ATOM TRANSFER RADICAL POLYMERIZATION AND ITS CONTINUOUS PROCESSES

DOCTOR OF PHILOSOPHY (2001)
(Chemical Engineering)

McMaster University
Hamilton, Ontario

TITLE: Atom Transfer Radical Polymerization and Its Continuous Processes

AUTHOR: Youqing Shen, B.S., D.Sc

SUPERVISORS: Professor Shiping Zhu and Professor Robert H. Pelton

NUMBER OF PAGES: XXII, 252

ABSTRACT

Atom transfer radical polymerization (ATRP), a transition metal-mediated living radical polymerization, has been developed as a powerful tool for synthesizing polymers of controlled structure, but its catalyst residue remains challenging. Described in this thesis is a comprehensive study on the ATRP applications in macromonomer preparation and the solutions to its catalyst residue problem by catalyst supporting. A novel continuous process for the production of polymers and block copolymers with controlled molecular weights has also been developed using packed column reactor technologies.

New versatile vinyl-containing initiators, 2′-vinyloxyethyl 2-bromoisobutyrate (VBIB) and 3′-vinyloxylpropyl trichloroacetamide (VTCA), were screened for the macromonomer synthesis of different vinyl monomer types by ATRP. Polymethacrylate and polystyrene macromonomers of well-controlled molecular weights were obtained without consumption of the initiators' vinyl moieties at monomer conversions lower than 80%. However, the ATRP of acrylates started to consume the vinyl moieties at medium conversions. Therefore, the polymerization of acrylates must be terminated at an early stage in order to obtain their macromonomers.

Three catalyst supporting systems have been developed to solve the catalyst contamination problem for batch ATRP. Firstly, the CuBr/HMTETA complex was supported onto silica gel by physical adsorption for ATRP of MMA in toluene. The supported complex mediated a living polymerization of MMA. The recycled catalysts had a high retention of catalyst activity and improved control over the polymer molecular

weights. Secondly the catalyst was immobilized on silica gel by covalent bonding for polar solvent/monomer systems. In this supporting method, the supporting spacer length was found to strongly affect the catalyst activity and control of the polymerization. The catalyst supported via three-unit PEG had highest activity and regulated the polymerization best. Longer or shorter spacer deteriorated catalyst activity and control of polymerization. Thirdly, the catalyst was grafted onto soluble and recoverable PE and PE-b-PEG supports to overcome the adverse effects of insoluble support. Catalyst directly grafted on the long PE chains had low activities, poor control over polymerization and low retention of the catalyst activity upon recycling. Using PEG as spacer to graft the catalyst onto the PE support minimized these adverse effects of the PE support. PE_{25}-PEG_4-TEDETA-CuBr effectively mediated the ATRP of MMA, and retained 90% activity of the fresh catalyst upon recycling with good polymer molecular weight control.

Catalyst recycling for batch ATRP was found laborious and time-demanding. A continuous ATRP using column reactors packed with silica gel supported CuBr/HMTETA was developed for homo- and block-copolymerization of MMA. The reactor showed good stability in both catalyst activity and molecular weight control of resulting PMMA. The polymerization in the reactor was still a living process. Thus, adjusting the MMA flow rate, which determined the monomer conversion, readily changed the molecular weight of PMMA. The block copolymerization of MMA with *n*-butyl methacrylate (nBMA) was carried out using two reactors in series. The produced block copolymers had little contamination of PMMA prepolymer. The chain length of nBMA block could be adjusted by the flow rate of nBMA in the second reactor.

ACKNOLEDGEMENT

I would like to thank my supervisors, Professor Shiping Zhu and Professor Robert H. Pelton, for their continuous guidance, constant support, encouragement and advice during my study. Their generous suggestions will be treasured in my life.

I also thank my supervisor committee members, Professor John Brash and Professor Yingfu Li and my Comprehensive II Examination Committee members, Professor Andrew N. Hrymak and Professor Heather Sheardown for their suggestions and remarks.

I must thank the members of Dr. Zhu's group, Leming Gu, Sam Zeng, Zhibin Ye, Ed Kolodka, Dr. Wenjun Wang, and others for their help during my study. It was a great pleasure to work with them. I also thank Doug Keller, the Polymer Institute's lab manager, for his constant assistance.

My appreciation also goes to Kathy Showkenik, Lynn Falkiner, Dianne Mallion, Paul Gatt, Gord Slater, and other department staff members for their help.

Finally I thank my wife, Zhen Duan, for her solid support for my study at McMaster.

PUBLICATIONS

This Ph.D. thesis is of sandwich style based on the following publications:

1. Y. Shen, S. Zhu and R. Pelton, "Atom transfer radical polymerization of methyl methacrylate mediated by copper bromide-tetraethyldiethylenetriamine grafted on soluble and recoverable poly(ethylene-*b*-ethylene glycol) supports"
   Macromolecules, accepted.
2. Y. Shen, S. Zhu and R. Pelton, "Effects of supporting spacer on the supported atom transfer radical polymerization of methyl methacrylate"
   Macromolecules **2001,** *34,* 5812-5818.
3. Y. Shen, S. Zhu and R. Pelton, "Soluble and recoverable support for copper bromide-mediated living radical polymerization"
   Macromolecules **2001,** *34,* 3182-3185.
4. Y. Shen, S. Zhu, F. Zeng, and R. Pelton "Supported atom transfer radical polymerization of methyl methacrylate mediated by CuBr-tetraethyldiethylene triamine grafted on silica gel"
   Journal of Polymer Science Part A: Polymer Chemistry, **2001**, *39*, 1051-1059.
5. Y. Shen, S. Zhu, and R. Pelton, "Packed column reactor for continuous atom transfer radical polymerization: methyl methacrylate polymerization using silica gel supported catalyst".
   Macromolecular Rapid Communication **2000**, *21*, 956-959.
6. Y. Shen, S. Zhu, F. Zeng, and R. Pelton, "Atom transfer radical polymerization of methyl methacrylate by silica gel supported copper bromide/multidentate amine"
   Macromolecules **2000**, *33,* 5427-5431.
7. Y. Shen, S. Zhu, F, Zeng, and R. Pelton, "Versatile initiators for macromonomer synthesis of acrylates, methacrylates and styrene by atom transfer radical polymerization"
   Macromolecules **2000**, *33*, 5399-5404.
8. Y. Shen, S. Zhu, F. Zeng and R. Pelton, " Synthesis of methacrylate macromonomers using silica gel supported atom transfer radical polymerization"
   Macromolecular Chemistry Physics **2000**, *201*, 1387-1394.
9. S. Zhu, Y. Shen and R. Pelton, "Supported controlled radical polymerization and continuous packed column reactor technology.

   US Patent 2,307,438.
10. Y. Shen, S. Zhu, F. Zeng and R. Pelton, "Atom transfer radical polymerization of alkyl methacrylate using T-triazine as ligand"
    Macromolecular Chemistry Physics **2000**, *201*, 1169-1175.

TABLE OF CONTENTS

LIST OF FIGURES

List of Tables

LIST OF SCHEMES

Chapter 1

Introduction to Atom Transfer Radical Polymerization

1.1 Background of Living Radical Polymerization

The control of macromolecular structure has recently been attracting both academic and industrial attention. It can lead to the development of new polymer products with improved and/or new materials properties. The only viable technique that offers appreciable control over macromolecular structure is living polymerization. Living polymerization is defined as a chain growth process without permanent chain termination and transfer reactions, and thus the polymer chains are always ready for further monomer propagation. Such polymerization provides end-group control and therefore enables synthesis of polymers of controlled molecular weights, various functionalities, and block copolymers by successive monomer addition.[1]

Living ionic polymerizations have been extensively studied and used.[2] Under optimal conditions, they can produce nearly mono-dispersed polymers with well-controlled molecular weights. However, living ionic polymerizations require very strict reaction conditions. They are very sensitive to moisture and other protonic chemicals. Therefore much effort must be made to dry the reaction systems and to purify the monomers and solvents. The versatility of living ionic polymerizations is also limited by incompatibility of their propagating centers with many functional groups. They are successful only in a limited number of monomers. For example, living anionic polymerization is successful in styrene, diene, methacrylates and some special acrylates (e.g. *tert*-butyl acrylate). The polymerizations of methacrylates and some acrylates by living anionic polymerization has to be at –78 °C or lower temperature to suppress the reaction of the anion with carbonyl groups. Therefore living ionic polymerizations are difficult for industrial applications.

Radical polymerization is the most important commercial process for the production of commodity polymers. It works for most vinyl monomers under mild conditions. Copolymerizations of different monomers provide an infinite number of copolymer products with properties depending on the comonomer types and compositions. Radical polymerization is not sensitive to water, and actually it is often carried out in aqueous media.[3] Therefore a living radical polymerization process is greatly desirable in terms of above advantages.

Living radical polymerization has been found very challenging compared with ionic polymerization. The free radical is a highly active, electrically neutral intermediate. It can thus undergoes various reactions (Scheme 1.1).[3] It can terminate with another radical by coupling or disproportionation or transfer reaction to monomer, polymer or solvent. The termination reactions are very rapid. The termination rate constant by recombination and/or disproportionation is about $k_t \approx 10^{8\pm1}$ (L/mol s), which is much higher than the

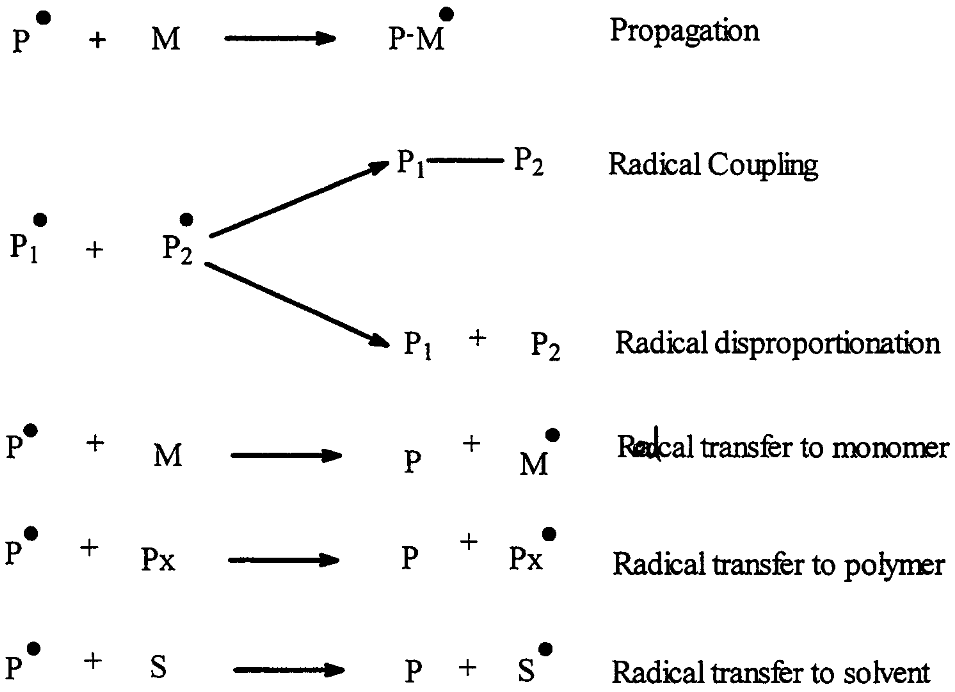

Scheme 1.1 Possible radical reactions

corresponding propagating rate constant, $k_p \approx 10^{3\pm1}$ (L/mol s). Therefore the lifetime of a free radical in a polymerization system is very short, usually less than 1 second.

Consequently the conventional free radical polymerization can not be living and only produces ill-defined polymer chains with uncontrolled molecular weight, broad molecular weight distribution and uncontrolled structure. It is also not possible for the conventional free radical polymerization to produce pure block copolymers and other functional polymers.

In a radical polymerization, transfer reactions to polymer and monomer are usually not significant and transfer reaction to solvent can be suppressed by selecting a proper solvent type. Therefore bimolecular radical recombination and disproportionation reactions are the main causes of the chain termination. In the polymerization kinetics, the propagation is first order, while the radical termination is second order with respect to radical concentration. Eq.1.1 expresses the ratio of radical termination to propagation rates. It shows that reducing the stationary radical concentration can suppress the contribution of radical termination.

$$\frac{R_t}{R_p} = \frac{k_t\,[P^\bullet]^2}{k_p\,[P^\bullet][M]} = \frac{k_t[P^\bullet]}{k_p[M]} \qquad \text{(Eq.1.1)}$$

1.2 The Concept of Reversible Activation/Deactivation in Living Radical Polymerization

The approach to reduce the stationary radical concentration and to protect the polymer chains is based on a reversible activation/deactivation process, which was firstly applied to living cationic polymerization.[4] Equation 1.2 illustrates the concept. In a radical polymerization system, while a polymer radical propagates monomers, it can also react with "deactivator", $D^\bullet$, to form an adduct (deactivation). The adduct, P-D, does not react with other radicals but can either thermally or chemically disassociate into a polymer radical for chain growth and a deactivator $D^\bullet$ (activation). This concept was first attempted to realize a living radical polymerization by using "iniferter" (*ini*tiator-trans*fer*-*ter*minator) [5] to reversibly protect the polymer chain ends. However, this "iniferter" strategy suffered high polydispersity and poor control over molecular weight. This process was greatly improved when stable nitroxide radicals, such as 2,2,6,6-tetramethylpiperidinyl-1-oxy (TEMPO),[6] were introduced to reversibly cap the propagating radicals, demonstrating a well-controlled polymerization of styrene (so called nitroxide-mediated living radical polymerization). Other persistent radials were

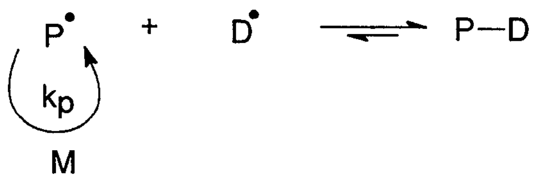

$P^\bullet$ -Polymer radical

$D^\bullet$ -Deactivator

(Eq. 1.2)

also reported.[7]

1.3 Atom Transfer Radical Polymerization (ATRP)

The reversible activation/deactivation process was further achieved by catalysis of metal complex, i.e. the metal complex-mediated living radical polymerization. It uses halogen atoms (mainly bromine or chlorine atoms) to protect the dormant polymer chains (Eq. 1.3).[8] This scheme was developed from atom transfer radical addition (ATRA) [9] in organic synthesis and thus was named atom transfer radical polymerization (ATRP).[8] Metal complex, MX_n/L_y, (e.g. copper(I) bromide), undergoes an one-electron oxidation with simultaneous abstraction of a halogen atom from the carbon-halide bond to generate a radical ($P^{\bullet}$) to propagate monomers. The radical, however, can also react with produced MX_{n+1}/L_y at the higher oxidation state (e.g. copper(II) dibromide) to resume the dormant state, P-X (the polymer chain end-capped with halogen atom). This process has been successfully used for a wide range monomers, including styrenic,[8,10] acrylates,[11] methacrylates,[8] acrylamides[12] and acrylnitrile[13] in bulk, in solution using organic or water [14,15] as solvent, in suspension[16] and in supercritical carbon dioxide.[17]

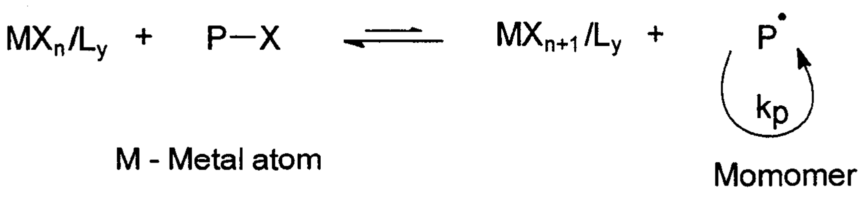

$$MX_n/L_y + P{-}X \rightleftharpoons MX_{n+1}/L_y + P^{\bullet} \circlearrowleft k_p \qquad \text{(Eq. 1.3)}$$

M - Metal atom

X - Br, Cl

L - Ligand

Table 1.1 The ATRP Systems

Metal	Ligand	Initiator
CuBr, CuCl	2,2`-Bipyridine	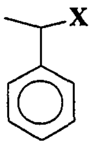
	Multidentate amine	
RuBr$_2$	PPh$_3$ + Al(OiPr)$_3$	
FeBr$_2$	PPh$_3$	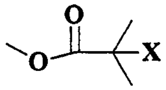
NiBr$_2$	PPh$_3$	
PdBr$_2$	PPh$_3$	
		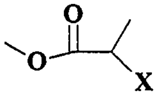
		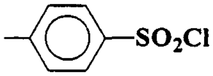

A typical ATRP system consists of an initiator, a metal halide (at low oxidation state) complexed with ligand(s), and a monomer. Various catalysts (Table 1.1) have been developed based on Cu(I),[18,19] Ni(II),[20,21] Ru(II),[22,23] Fe(II),[24] Rh(II)[25] elements, but Cu(I) and Ru(II) systems have been mostly studied. The ligands for copper-based catalysts are usually bipyridine or multidentate amines and ligands for other catalysts are usually PPh_3. The type of a ligand system (i.e. electronic, steric and solubility characters) greatly affects the catalyst activity and control of the polymer molecular weight. The initiator must match the monomer type to be polymerized. This issue will be discussed later. The initiators used in ATRP, structurally different from those used in the conventional free radical polymerization, are alkyl halides with activating groups such as aryl, carbonyl or nitrile groups on the α-position, e.g. 1-phenylethyl bromide, CCl_4, 2-chlorobutyrate or 2-bromobutyrate, methyl α-bromophenyl acetate and arenesulfonyl chloride.

1.4. ATRP Applications

1.4.1 Synthesis of Polymers with Controlled Molecular Weights

The first application of ATRP is the synthesis of various polymers with controlled molecular weights with very low polydispersity. For example, the molecular weight distribution of polystyrene (PS) prepared by ATRP could be as narrow as that of PS standard synthesized by living anionic polymerization.[26] The molecular weights of PS also agreed with the theoretical values calculated by the $[M]_0/[I]_0$ ratio.

In an ATRP process, fast initiation and fast deactivation of living chains are essential for synthesizing low-polydispersed polymers. The fast initiation requires that the initiation reaction must be much faster than propagation so that all the polymer chains grow simultaneously. A slow initiation yields a mixture of long chains (those starting to propagate early) and short chains (those starting to propagate later) and thus the polydispersity cannot be low. Therefore, the initiator used has to match the monomer type. The criterion is that the carbon-halide bond in the initiator (R-X) must be equal to or more active than that in the dormant propagating chain (P-X). A practical way to select an initiator for a given monomer type is to have an initiator that contains similar alkyl group as the dormant propagating chain. For example, 1-phenylethyl halide is good for styrene polymerization,[8] and α-halopropionate is good for acrylates, while they are poor initiators for methacrylates.

Equation 1.4 [19,27,28] relates the polydispersity to the factors in an ATRP system. As we can see that fast deactivation rate (k_d) results in a low dispersity. Firstly, a fast deactivation decreases the stationary radical concentration and thus decreases radical terminations. Secondly, radical propagation is very fast. It usually takes less than 0.1 second for a free radical to propagate 1000 units. Therefore a slow deactivation will allow a radical to propagate with too many monomer units at each activation/deactivation cycle and thus some polymer chains may have very high molecular weights while others may have low molecular weight. Ideally the fewer units a radical propagates during one activation/deactivation cycle, the narrower the polydispersity becomes.

$$\frac{Mw}{Mn} = 1 + \left(\frac{Kp[R\text{-}X]}{Kd[CuX_2]}\right)\left(\frac{2}{Conv} - 1\right) = 1 + \left(\frac{Rp[R\text{-}X]}{Rd\,[M]}\right)\left(\frac{2}{Conv} - 1\right)$$

(Eq. 1.4)

Kp-Propagation rate constant

Kd-Deactivation rate constant

[R-X]-Initiator concentration

[CuX_2]-Deactivator concentration

Conv-Conversion

Eq. 1.4 also shows that high polymerization rate will lead high polydispersity. Therefore, as long as the polymerization rate is within an acceptable range, a lower temperature is preferred in order to have low polydispersity of the polymers.

1.4.2 Synthesis of Block Copolymers [29-32]

Various block copolymers among different monomers have been synthesized by ATRP. One of the methods is "macroinitiator method", in which the first monomer is polymerized by an initiator with proper R-X, yielding polymer chains with end carbon-halide bonds (P-X) (macroinitiator). The P-X then initiates the second monomer to produce AB block copolymers. If a di-functional initiator is used, an ABA triblock copolymer can be prepared.

The strategy of synthesizing well-defined block copolymers is to use a proper order of monomer additions or to use a halide-exchange method. The former is related to the fast-initiation requirement discussed above. For example, PMMA-macroinitiator can initiate MA or St polymerization and yields well-defined block copolymers, while the reverse order, that is to use PMA or PS macroinitiator to initiate MMA polymerization, yields highly polydispersed block copolymers contaminated with unreacted macroinitiators. The halide-exchange method,[29] which uses alkyl-bromide as initiator and uses copper chloride as catalyst, can break this order. For example, catalyzed with CuCl, bromo-ended PMA (PMA-Br) can initiate MMA polymerization, producing PMA-PMMA block copolymers with low polydispersity.

1.4.3 Synthesis of Star Polymers [33,34]

The third application of ATRP is to synthesize star polymers. When a compound having several initiator moieties (carbon-halide bonds) is used as an initiator, the ATRP yields multi-armed star polymers. For example, Compounds A and B (Scheme 1.2) can be used to prepare 3- or 4- armed star polymers, respectively. Different from linear polymers, the measured molecular weights of star polymers by GPC are lower than their calculated values because the molecular hydrodynamic volumes are smaller than their corresponding linear polymers with the same molecular weights.

1.4.4 Synthesis of Hyperbranched Polymers

Hyperbranched polymers have the similar branching structure as dendrimers, but are much easier to synthesize. ATRP provides a new efficient approach to synthesize hyperbranched polymers from vinyl monomers. When a monomer having carbon-halide group (Scheme 1.3) is polymerized by ATRP, every unit incorporated into the polymer chains also introduces a new branching site, as shown in Scheme 1.3. Finally such a polymerization will produce three-dimensional structure without crosslinking. Because of their highly condensed chain structure, hyperbranched polymers have much smaller gyration volumes than linear polymers of the same molecular weight.

1.4.5 Synthesis of End-Functionalized Polymers [35-39]

When an alkyl halide compound contains a functional group such as hydroxyl, amino or vinyl group as initiator, the functional group will be attached to the polymer chain end. These end-functionalized polymers are useful for supermolecular construction. There were also two reports for the synthesis of end-unsaturated-functionalized polystyrene by ATRP in literature.[38,39] Vinyl chloroacetate and allyl bromide were used as initiators to prepare polystyrene macromonomers. The vinyl terminated polystyrene copolymerized with N-vinylpyrrolidinone and yielded hydrogels of poly(N-vinylpyrrolidinone-g-styrene).[38]

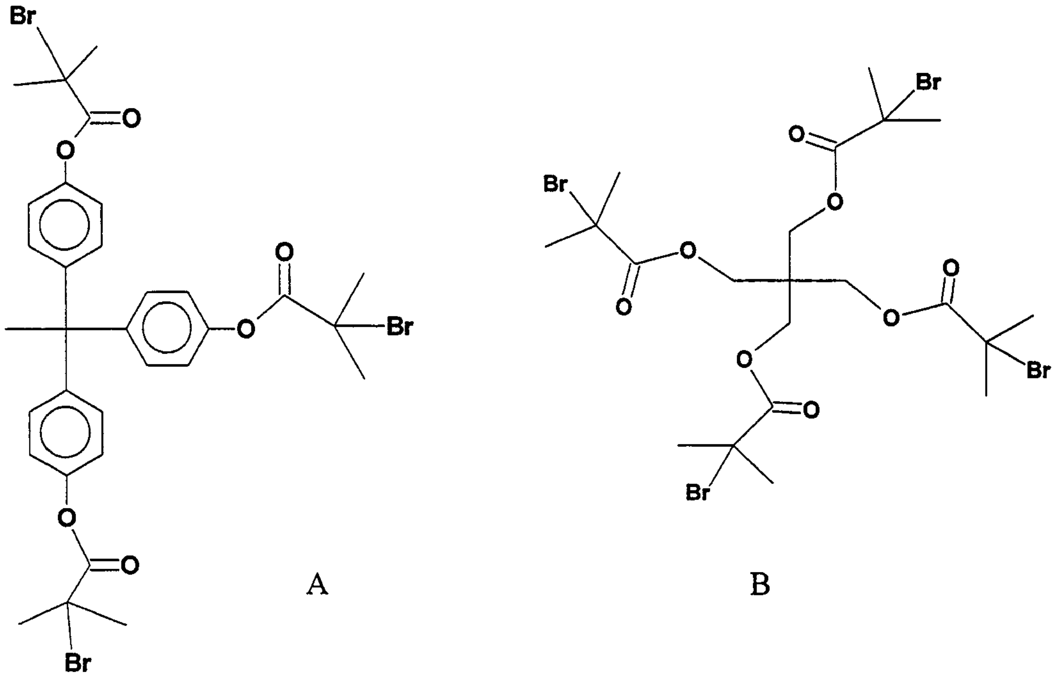

A

B

Scheme 1.2. The initiators for synthesizing star polymers

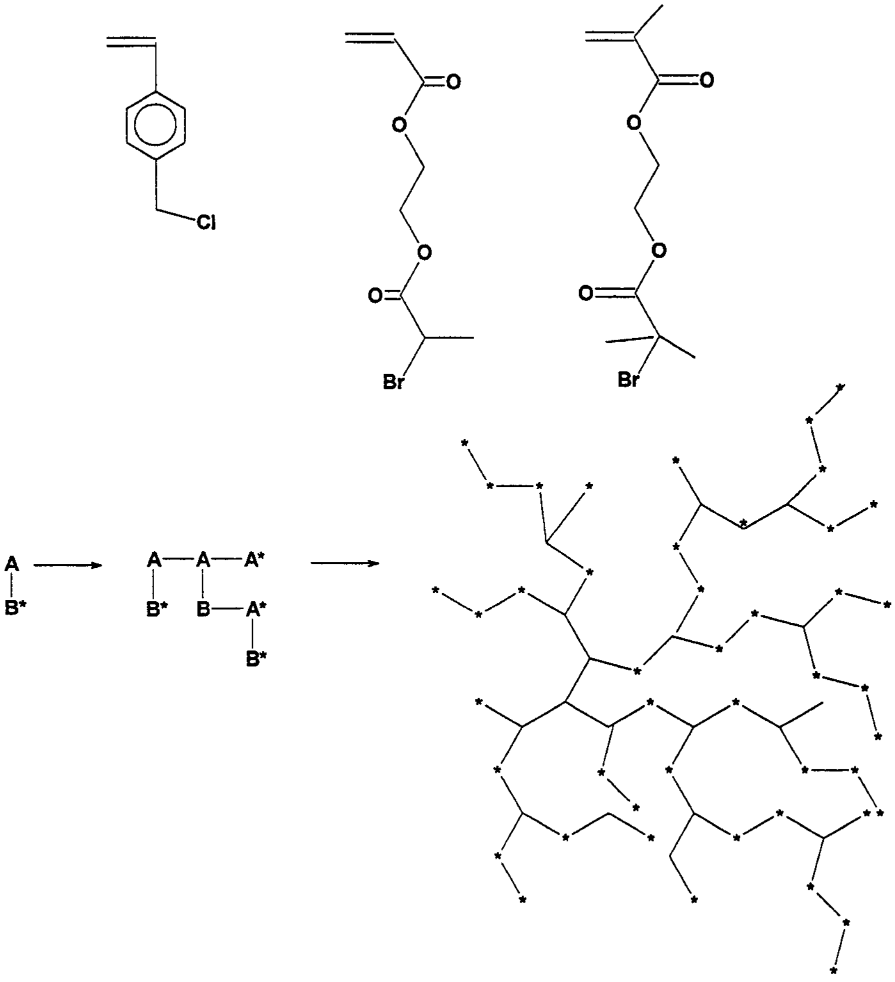

Scheme 1.3. The monomers and polymerization for hyperbranched polymers

*- initiation sites

1.5 Challenges of ATRP

ATRP is a new powerful tool to synthesize specialty polymers of low molecular weights, usually less than 10^5. A challenging problem for ATRP is its low catalyst efficiency and thus high catalyst concentration is often required. In a typical ATRP recipe, the initiator to catalyst ratio is usually 1. The metal halide is about 0.1~1% (molar) of the monomer. This catalyst finally goes to the product, resulting in a high concentration of catalyst residue in the product. This residual catalyst not only deeply colors the product but also may make the product toxic. Therefore, post-purification is required to remove the catalyst from the product prepared by ATRP, usually by passing the polymer/catalyst mixture through silica or alumina gel or resins.[40] The catalyst is thus wasted and this post-treatment is time-consuming and costly. Therefore a great challenge of ATRP is to develop processes to directly reduce the concentration of the catalyst residue in the final product to avoid the post purification.

Catalyst supporting has been developed to solve this problem. The idea is that the catalyst immobilized on insoluble particles can be easily removed from the polymer solution, and ideally can be recycled. ATRP catalysts were immobilized onto particles by complexation with their ligands grafted on particles (Scheme 1.4).[41,42] However, the catalysts supported on particles were found not effectively to mediate the ATRP process. The molecular weights of polystyrene and PMMA prepared by ATRP with CuBr supported on silica gel or crosslinked polystyrene particles via Schiff-base were much higher than predicted with high polydispersities (Figure 1.1).[41] Copper bromide

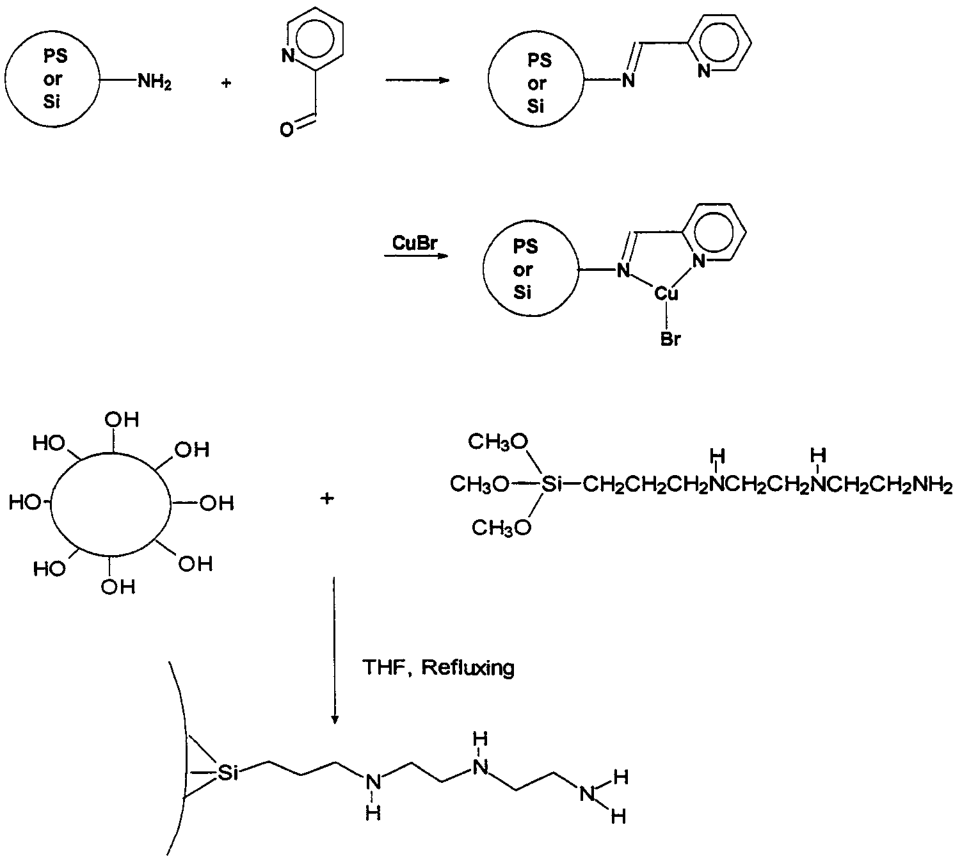

Scheme 1.4. Catalyst immobilization by ligand grafting first

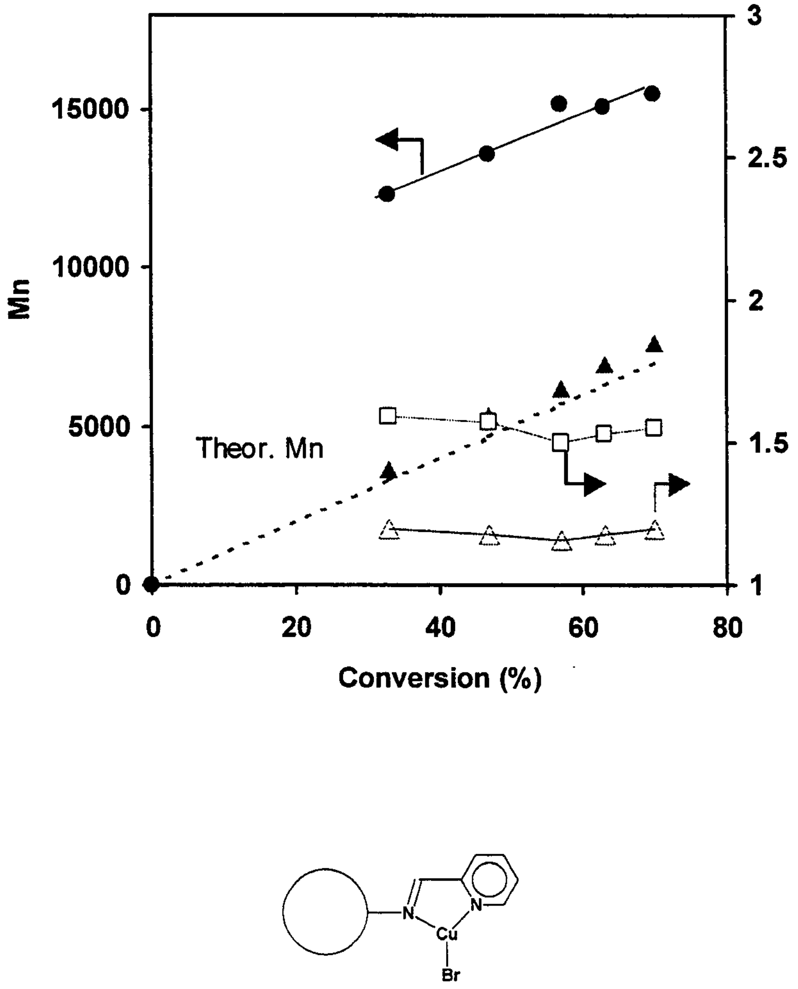

Figure 1.1. PMMA molecular weight development catalyzed by immobilized CuBr on silica gel particles (●, □); unimmobilized catalyst (▲, Δ)

immobilized on multidentate amine-functionalized silica gel was found not to mediate the living polymerizations of MMA, MA and styrene.[42] The reason for this adverse effect of catalyst support is that the catalyst diffusivity was substantially reduced after the catalyst was immobilized on large particles (relatively to a molecule). Consequently the generated radicals could not be deactivated quickly enough and thus propagated with monomers as in a conventional free radical polymerization. Therefore, catalyst supporting for ATRP is a good concept, but it remains unsuccessful until now.

1.6 Objectives of This Thesis

Macromonomers are polymers having terminal unsaturated groups for further polymerization. They are important intermediates for supermolecular-structure construction including comb-branched graft copolymers, star-shaped copolymers. For example, well-defined comb-branched graft copolymers can be synthesized by macromonomer copolymerization with chain length and density of the pendant side chains easily adjustable by varying the molecular weight of the macromonomer and the comonomer composition.[43] Though ATRP has been developed as a powerful tool for synthesizing polymers of well-controlled chain structure, its application in macromonomer preparation has not been well studied. Therefore, the first objective of this thesis is to explore the applications of ATRP in the synthesis of macromonomers.

ATRP is a promising process for industrial applications because of its mild reaction conditions, but one of the major challenges that impede the applications is the catalyst residue problem. As discussed in Section 1.5, the high concentration of catalyst residue not only deeply colors the product and affects polymer properties, but also may leach out gradually from the product and thus make the product toxic. Therefore, the catalyst residue must be lowered to a certain level. Purification by passing the product solution through a column packed with silica gel, alumina or resins is currently used in lab scale. This purification is time-consuming and costly, and wastes catalyst. The catalyst supporting is a possible solution to this problem. Catalysts immobilized on insoluble particles can be readily separated from the product and be recovered for second use. Even though there were two reports about catalyst support of CuBr for ATRP, these attempts were unsuccessful. The supported catalysts did not effectively mediate the polymerization and could not control the polymer molecular weight satisfactorily. Accordingly, the second objective of this thesis is to develop new catalyst supporting systems for ATRP to solve the catalyst residue problem and investigate the major factors that affect catalytic performance.

Batch processes for supported catalyst system, which involve laborious catalyst recycling, are not efficient and cost-effective for industry uses due to a large amount of solvents required. Continuous processes are often desirable in industry because of their high efficiency, low cost and good quality control. Therefore the third objective of this thesis is to develop a continuous process for ATRP for industry applications.

1.7 References

1. Szwarc, M. *Nature* **1956,** *176*, 1168.
2. Hsieh, H. L. and Quirk, R. P. *Anionic Polymerization: Principles and Practical Applications*, Marcel-Dekker, New York, **1996**; Jerome, R., Teyssie, Ph., Vuillemin, B., Zundel, T., Zune, C. *J. Polym. Sci. Polym. Chem.* **1999,** *37*, 1.
3. Moad, G.; Solomon, D. H. *The Chemistry of Free Radical Polymerization;* Pergamon, Oxford, **1995.**
4. Matyjaszewski, K. and Lin, C. H. *Makromol. Chem. Macromol Symp.,* **1991,** *47,* 221; Puskas, J.E.; Kaszas, G. and Litt, M. *Macromolecules* **1991**, *24,* 5278
5. Quirk, R. P.; Kinning, D. J.; Fetters, L. J. in "*Comprehensive Polymer Science, vol. 7*", Pergamon Press, London **1989**, Aggarwal, S. L (ed)., P1.
6. Moad, G.; Rizzardo, E.; Solomon, D. H. *Macromolecules* **1982,** *15,* 905.; Georges, M. K.; Veregin, R. P. N.; Kazmaier, P. M.; Hamer, G. K. *Macromolecules* **1993,** *26*, 2987.
7. Otsu, T.; Matsumoto, A; Tazaki, T. *Polym. Bull.* **1987,** *17,* 323.
8. Matyjaszewski, K. *J. Macro. Sci.- Pure Appl. Chem.* **1997**, *A34*, 1785; Wang, J.; Matyjaszewski, K. *Macromolecules* **1995**, *28*, 7901.
9. Curran, D. P. In *Comprehensive Organic Synthesis;* Trost, B.M., Fleming, I., Eds.; Pergamon: Oxford, **1991**; *Vol. 4*, 715.
10. Matyjaszewski, K., Patten, T. E.; Xia, J. *J. Am. Chem. Soc.* **1997**, *119*, 674.
11. Xia, J. Gaynor, S. G. and Matyjaszewski, K. *Macromolecules* **1998**, *31*, 5958; Davis, K. A.; Paik, H.; and Matyjaszewski, K. *Macromolecules* **1999**, *32*, 1767.

12. Eodorescu, M.; Matyjaszewski, K. *Macromol. Rapid Commun.* **2000,** *21*, 190.
13. Matyjaszewski, K; Jo, S. M.; Paik, H-j; Shipp, D. A. *Macromolecules* **1999,** *32*, 6431.
14. Wang, X.-S.; Jackson, R.A.; Armes, S.P. *Macromolecules* **2000,** *33*, 255; Wang, X.-S. and Armes, S. P. *Macromolecules*; **2000**; *33,* 6640;
15. Zeng, F; Shen, Y.; Zhu, S. and Pelton, R. *J. Polym. Sci. Part A: Polym. Chem.* **2000,** *33*, 3821.
16. Nishikawa, T.; Kamigaito, M. K. and Sawamoto, M. *Macromolecules* **1999,** *32*, 2204.
17. Xia, J.; Johnson, T.; Gaynor, S. G.; Matyjaszewski, K.; DeSimone, J. *Macromolecules* **1999,** *32*, 4802.
18. Matyjaszewski, K *Macromolecular Symposia* **2000,** *152*, 29.
19. Matyjaszewski, K. "Mechanism aspects of atom transfer radical polymerization" in "*Controlled Radical Polymerization*", Matyjaszewski, K. (ed), *ACS Symposium Series* **1997**, *685*, p258.
20. Granel, C.; Teyssie, Ph.; Dubois, Ph.; Jerome, Ph. *Macromolecules* **1996,** *29*, 8576.
21. Uegaki, H.; Kotani, Y.; Kamigaito, M.; Sawamoto, M. *Macromolecules* **1998,** *31*, 6756.
22. Kato, M; Kamigaito, M.; Sawamoto, M.; Higashimura, T. *Macromolecules* **1995**, *28*, 1721.
23. Sawamoto, M. and Kamigaito, M. *J. Macro. Sci-Pure Appl. Chem* **1997,** *A34*, 1803.
24. Matyjaszewski, K.; Wei, M.; Xia, J.; McDermott, N. E. *Macromolecules* **1997**, *30*, 8161.

25. Moineau, G.; Granel, C.; Dubois, Ph.; Jerome, R. and Teyssie, Ph. *Macromolecules* **1998**, *31*, 542.

26. Patten, T. E., Xia, J., Abernathy, T. Matyjaszewski, K. *Science* **1996**, *272*, 866.

27. Matyjaszewski, K.; Lin, C-H. *Macromol. Chem. Symp.* **1991**, *47,* 221.

28. Litvinienko, G. Muller, A.H.E *Macromolecules* **1997**, *30*, 1253.

29. Shipp, D.A.; Wang, J-L.; Matyjaszewski, K., *Macromolecules* **1998**, *31,* 8005.

30. Zhang, X. and Matyjaszewski, K. *Macromolecules* **1999**, *32*, 1763.

31. Davis, K. A. and Matyjaszewski, K. *Macromolecules* **2000**, *33*, 4039.

32. Matyjaszewski, K., Shipp, D.A.; Mcmurtry, G. P.; Gaynor, S.G.; Pakula, T. *J. Polym. Sci. Part. A: Polym. Chem.* **2000**, *38*, 2023.

33. Matyjaszewski, K., Miller, P. J.; Pyun, J.; Kickelbick, G. and Diamanti, S. *Macromolecules* **1999**, *32,* 6526.

34. Hovestad, N. J.; Koten, G. van, Bon, S.A.F.; and Haddleton, D. M. *Macromolecules* **2000**, *33,* 4048.

35. Haddleton, D. M.; Waterson, C.; Derrick, P. J.; Jasieczek, C. B. and Shooter, A. J. *Chem. Commun.* **1997**, 683.

36. Coessens, V.; Matyjaszewski, K. *Macromol. Rapid Commun.* **1999**, *20*, 127.

37. Malz, H.; Komber, H.; Voigt, D.; Hopfe, I.; Pionteck, J. *Macromol. Chem. Phys.* **1999**, *200*, 642.

38. Matyjaszewski, K.; Beers, K. L.; Kern, A.; Gaynor, S. G. *J. Polym. Sci.: Part A: Polym. Chem.* **1998**, *36*, 823.

39. Nakagawa, Y. and Matyjaszewski, K. *Polym. J.* **1998**, *30*, 138.

40. Matyjaszewski, K.; Pintauer, T.; Gaynor, S. *Macromolecules* **2000,** *33,* 1476.

41. Haddleton, D. M.; Kukulj, D. and Radigue, A. P. *Chem. Commun,* **1999**, 99.

42. Kickelbick, G.; Paik, H.; and Matyjaszewski, K. *Macromolecules* **1999,** *32,* 2941.

43. Shinoda, H.; Miller, P. J.; Matyjaszewski, K. *Macromolecules* **2001,** *34,* 3186.

Chapter 2

Macromonomer Synthesis by Atom Transfer Radical Polymerization

2.1 Introduction to Macromonomer Synthesis

Macromonomers are polymers that have unsaturated terminal groups for further polymerization or copolymerization. They are important precursors for supermolecular construction including the syntheses of well-defined graft copolymers, polymer brushes and star polymers.[1]

Even though the conventional free radical polymerization is sometimes used to synthesize macromonomers,[2] living polymerization is preferred for macromonomer synthesis since it can well control the polymer molecular weight with low polydispersity. The macromonomer synthesis strategies by living polymerization can be classified as end-functionalization methods that use vinyl-containing capping agents and initiation methods that use functional initiators. The end-functionalization method involves either coupling living polymer chains with a termination reagent,[3-5] or reacting functional polymers with an unsaturated compound, e.g. ω-hydroxyl polymer with acryloyl chloride.[6] The main challenge for this approach is that usually not all end groups can be capped. For the living chain coupling, the active centers of polymer chains must be stable to avoid side reactions. Therefore, this method is only applicable for limited systems. The initiation method using vinyl-containing initiators is preferred for macromonomer synthesis since it can guarantee that each polymer chain has one terminal vinyl group. The challenge for this method is to select a proper vinyl-containing initiator so that the vinyl moiety will not be consumed during the macromonomer preparation.

Living anionic polymerization has been widely used for synthesizing macromonomers.[7] It is capable of producing polymers with well-controlled polymer chains with low polydispersity. However, the main drawback of living anionic polymerization is its high sensitivity to moisture and other protonic agents and low reaction temperature.

Recently, atom transfer radical polymerization (ATRP) mediated by metal complex has succeeded in polymerizing various types of monomers in a "living" manner.[8-14] ATRP was also found useful in synthesizing functionalized polymers, such as polymers with terminal hydroxyl group.[15-17] However there has been little study on the macromonomer synthesis by ATRP. Matyjaszewski et. al. reported the synthesis of polystyrene macromonomers using vinyl chloroacetate [18] and allyl bromide [19] as initiators, but these initiators were lack of activity for methacrylates. In this work, a new set of vinyl-containing initiators was evaluated for the ATRP of methacrylates, acrylates and styrene, producing polymers with terminal vinyl groups, as shown in Scheme 2.1. 2′-Vinyloxyethyl 2-bromoisobutyrate (VBIB) polymerized styrene, methyl methacrylate (MMA), 2-(*N,N*-dimethylamino)ethyl methacrylate (DMAEMA), methyl acrylate (MA), and butyl acrylate (BA) and yielded macromonomers with controlled molecular weights

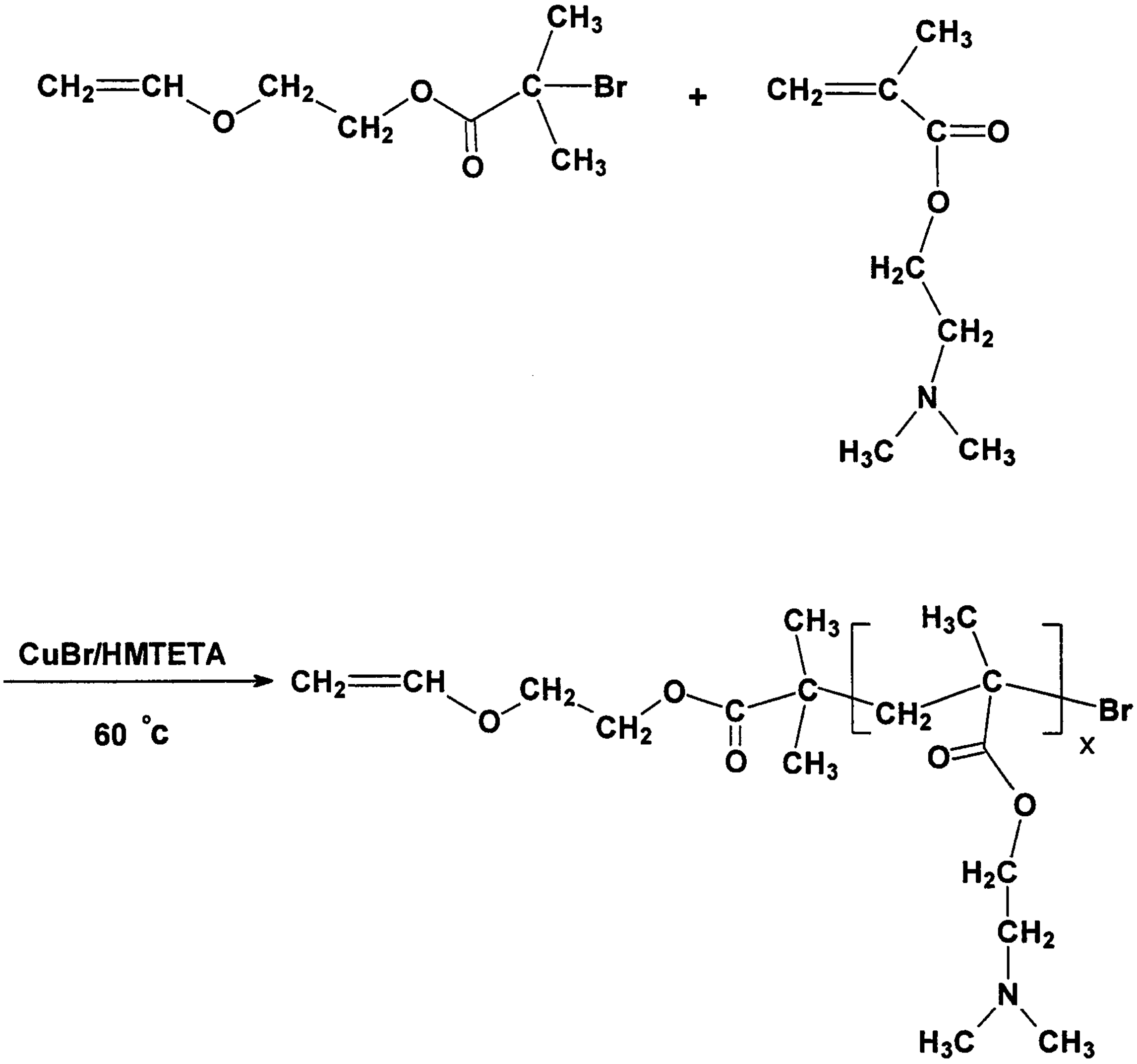

Scheme 2.1. Macromonomer synthesis by ATRP

and narrow molecular weight distributions. 3′-Vinyloxypropyl trichloroacetamide (VTCA) also initiated well-controlled polymerizations of DMAEMA and MMA. VTCA initiator is particularly useful for preparing hydrophilic DMAEMA macromonomers because the initiator moiety attached to the polymer end is stable in water.

2.2 Experimental Section

2.2.1 Materials

Styrene (St), methyl acrylate (MA), n-butyl acrylate (BA), methyl methacrylate (MMA) and 2-(*N,N*-dimethylamino)ethyl methacrylate (DMAEMA) from Aldrich were distilled under vacuum and stored at –15 °C before use. γ-Butyrolactone (γBL), 1,1,4,7,10,10-hexamethyltriethylenetetramine (HMTETA), CuBr, ethylene glycol vinyl ether (EGVE), 3-aminopropanol vinyl ether (APVE), 2-bromoisobutyryl bromide, trichloroacetyl chloride, 2-bromopropionyl bromide also from Aldrich were used as received. THF was distilled over CaH_2.

2.2.2 Initiator Syntheses

2.2.2.1 2′-Vinyloxyethyl 2-Bromoisobutyrate (VBIB)

Ethylene glycol vinyl ether (EGVE) (10 g, 0.113 mol) and triethylamine (19 ml, 0.136 mol) were dissolved in THF (250 ml). The solution was cooled in an ice-water bath. 2-Bromoisobutyryl bromide (BIBB) (14.0 ml, 0.113mol) in 50 mL of THF was added dropwise to this solution with stirring. The mixture was further stirred for 2h at room temperature (EGVE reacted with BIBB to yield VBIB and HBr, and HBr was absorbed by triethylamine). Triethylamine hydrogen bromide salt was filtered. THF in the filtrate was removed under vacuum at room temperature. The residual was dissolved in $CHCl_3$ and washed with water (50 mL) for three times. The aqueous parts were combined and shaken with fresh $CHCl_3$ (50 mL). The $CHCl_3$ solution was dried over anhydrous $CaCl_2$ overnight. After filtering off the drying agent, $CHCl_3$ was distilled out under vacuum. A brown liquid was obtained. Further distillation under high vacuum gave a colorless liquid. Yield 20.8 g. ^{1}H-NMR(in ppm): 6.40-6.51 (q, =C$\underline{H}$-, 1H), 4.00-4.23 (m, C$\underline{H}_2$=, 2H), 4.36-4.41 (t, -$OCH_2C\underline{H}_2$-OC(O)-, 2H), 3.88-3.93 (t, =CH-O-$C\underline{H}_2CH_2$, 2H), 1.92 ppm (s, -C$\underline{H}_3$, 6H).

2.2.2.2 2′-Vinyloxyethyl 2-Bromopropionate (VBP)

EGVE (5 g, 0.0567 mol) reacted with 2-bromopropionyl bromide (5.94 mL, 0.0567 mol) in the presence of triethylamine (9.5 mL) following a procedure similar to the VBIB synthesis. The final product was a colorless liquid. Yield: 9.7g. ^{1}H-NMR: 6.40-6.51 (m, =C$\underline{H}$, 1H), 4.5~4.25 (m, -C$\underline{H}_2$OC(O)-, and –OC(O)C$\underline{H}$(Br)CH_3, 3H), 4.00-4.23 (m, C$\underline{H}_2$=, 2H), 1.80 -1.84 (d, -C$\underline{H}_3$, 3H).

2.2.2.3 3′-Vinyloxypropyl 2-Bromoisobutyramide (VBIBA)

3-Aminopropanol vinyl ether (10.1g, 0.1 mol) and triethylamine (17 mL) mixture in THF (250 mL) reacted with 2-bromoisobutyryl bromide (12.36 mL, 0.1 mol). Following the same procedure as in the VBIB synthesis yielded a brown solid. The solid was purified by dissolving in THF and passing silicon gel. After removing THF by vacuum at room temperature, a yellowish viscous liquid was obtained. Yield: 13.0g. ^{1}H NMR (in ppm): 6.37-6.47 (q, $=C\underline{H}$-O-, 1H), 3.96-4.20 (m, $C\underline{H}_2$=, 2H), 3.71-3.77 (t, -$OC\underline{H}_2$-, 2H), 3.31-3.40 (q, -$C\underline{H}_2$NHC(O)-), 1.89~1.8 (m, -$CH_2C\underline{H}_2CH_2$- and –$C\underline{H}_3$, 8H), 7.08 (broad, -N$\underline{H}$C(O), 1H).

2.2.2.4 3′-Vinyloxypropyl Trichloroacetamide (VTCA)

3-Aminopropanol vinyl ether (10.1 g, 0.1 mol) and triethylamine (17 mL) mixture in THF (250mL) reacted with (11.2 mL, 0.1 mol) trichloroacetyl chloride by the same procedure as of the VBIB synthesis. A brown solid was obtained. The solid was purified by dissolving it in THF and passing it through silicon gel. After removing THF by vacuum at room temperature, a yellowish viscous liquid was obtained. Yield: 12.8g. ^{1}H-NMR (in ppm): 6.37-6.47 (q, $=C\underline{H}$-O-, 1H), 4.01–4.24 (m, $C\underline{H}_2$=, 2H), 3.78-3.84 (t, -$OC\underline{H}_2$-, 2H), 3.45-3.54 (q, -$C\underline{H}_2$NHC(O)-), 2.0~1.9 ppm (m, -$CH_2C\underline{H}_2CH_2$-, 2H), 7.32 ppm (broad, -N$\underline{H}$C(O)-).

The molecular structures of the initiators and the ligand HMTETA are shown in Scheme 2.2.

2.2.3 Polymerization

Required amounts of monomer, CuBr, HMTETA and γBL (added only in solution polymerization) were added to a clean tube. The tube was sealed with rubber septum and cooled in ice water. The solution was bubbled with ultra high purity nitrogen for 10 min. Then the initiator previously purged with nitrogen was added with syringe. The tube was immersed into an oil bath at a set temperature. The polymerization was stopped by cooling the tube in ice. The mixture was diluted with THF immediately. The contents in the tube were divided in two parts – one used for determining conversion by weight and the other for determining molecular weight and polydispersity. For conversion measurements the solution was poured into petroleum ether (for MMA, DMAEMA and St polymerization). The polymer was precipitated and dried in a vacuum, and then weighted to measure conversion. In the BA and MA cases, the polymer solution was dried directly without adding petroleum ether. The other portion of solution was passed through the silica gel to remove the catalyst. The polymer was also precipitated in petroleum ether and dried for characterization.

2.2.4 Measurements

Nuclear Magnetic Resonance (NMR) Spectroscopy: Proton (^1H) NMR spectra were recorded on a Bruker ARX-200 spectrometer at 200 MHz. ^1H NMR chemical shifts in $CDCl_3$ were reported downfield from 0.00 ppm using trace of $CHCl_3$ signal at 7.23 ppm as an internal reference.

Molecular Weight Measurements: Number and weight average molecular weights (M_n and M_w, respectively) were determined by gel permeation chromatography (GPC) using THF-2% (v/v) triethylamine as solvent at 25 °C with RI detector. Narrow polystyrene standards (Polysciences) were used to generate a calibration curve. Data were recorded and manipulated using the Windows based Millennium 2.0 software package.

Initiators

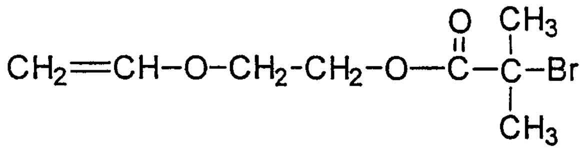

$CH_2{=}CH{-}O{-}CH_2{-}CH_2{-}O{-}C({=}O){-}C(CH_3)_2{-}Br$

2'-vinyloxyethyl 2-bromoisobutyrate (VBIB)

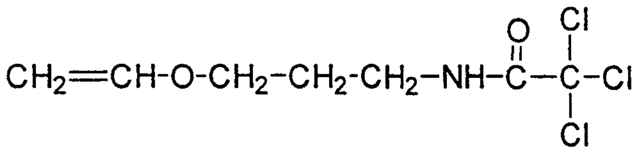

$CH_2{=}CH{-}O{-}CH_2{-}CH_2{-}CH_2{-}NH{-}C({=}O){-}CCl_3$

3'-vinyloxypropyl trichloroacetamide (VTCA)

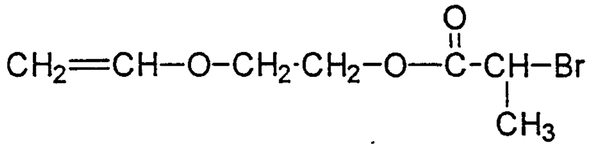

$CH_2{=}CH{-}O{-}CH_2{-}CH_2{-}O{-}C({=}O){-}CH(CH_3){-}Br$

2'-vinyloxyethyl 2-bromopropionate (VBP)

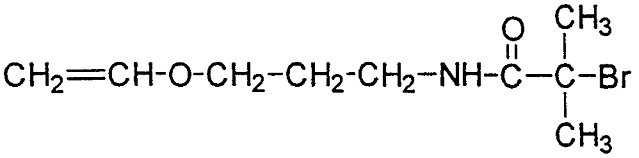

$CH_2{=}CH{-}O{-}CH_2{-}CH_2{-}CH_2{-}NH{-}C({=}O){-}C(CH_3)_2{-}Br$

3'-vinyloxypropyl 2-bromoisobutyramide (VBIBA)

Ligand

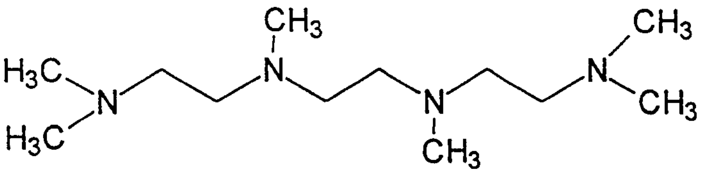

HMTETA

Scheme 2.2 The molecular structures of the initiators and ligand used in this work

2.3 Results and Discussion

2.3.1. Evaluation of Initiators

The four initiators bearing vinyloxyl group were first evaluated for the polymerizations of DMAEMA and MMA by using CuBr combined with hexamethyltrimethylenetetramine (CuBr/HMTETA) as catalyst. The results are summarized in Table 2.1.

All of the four initiators initiated the polymerizations of DMAEMA and MMA. However, VBP and VBIBA had poor control over the polymer molecular weight. The molecular weights of the resulting polymers were much higher than the calculated values, suggesting low initiator efficiencies. By contrast, VBIB and VTCA produced polymers with molecular weights close to their theoretical values. The polydispersities of the polymers prepared with VBIB and VTCA were also very low. The high polydispersity of polymers prepared with VBP and VBIBA was due to their slow initiation reactions. It was observed that upon adding VBIB or VTCA, the polymerization solution immediately turned bright green, suggesting the rapid formation of Cu^{2+}. However, when VBIBA or VBP was added to the polymerization solution, the solution gradually turned green after being heated to 60 °C. Therefore, VBIB and VTCA were selected as initiators for the further macromonomer synthesis studies.

Table 2.1. MMA and DMAEMA polymerization with different initiators catalyzed by CuBr/HMTETA at 60 °C

Initiator	Monomer	Time (min)	Conv.	Mn (Theor.)	Mn (exp.)	Mw/Mn
VBIB	MMA[a]	30	0.77	7700	7482	1.23
VBP	MMA[a]	50	0.83	8300	19300	1.62
VBIBA	MMA[a]	60	0.82	8200	22300	1.67
VTCA	MMA[a]	210	0.71	7100	8400	1.12
VBIB	DMAEMA[b]	40	0.66	10362	9485	1.12
VBP	DMAEMA[b]	60	0.67	10520	38400	1.59
VBIBA	DMAEMA[b]	60	trace	-	-	-
VTCA	DMAEMA[b]	120	0.63	9891	9100	1.09

a: in γBL, γBL/MMA = 0.5 (w/w); b: bulk

Monomer/initiator/CuBr/HMTETA=100/1/1/1 (molar).

2.3.2 Polymerizations of Methacrylates

The kinetics of DMAEMA and MMA polymerizations with VBIB and VTCA as initiators were investigated to examine whether the vinyl groups in the initiators were consumed during the macromonomer preparation. With both initiators, the bulk DMAEMA polymerization proceeded smoothly at 60 °C up to 80% conversion. The linear plots of $\ln([M]_o/[M])$ versus time indicate the first order kinetics and constant radical concentrations during the polymerization (Figure 2.1). The polymerization rate with VCTA was slower than that of VBIB. The apparent propagation rate constant, k^{app}, was 0.0252 min^{-1} for VBIB, compared to 0.0107 min^{-1} for VTCA. This was due to a low radical concentration in the VTCA system because of the formed stronger C-Cl bond.

The molecular weights of polyDMAEMA, measured by GPC and NMR ($M_{n,NMR} = M_{monomer} \times r$, r is the intensity ratio of polymer backbone to terminal vinyl group, see discussion below), increased linearly with monomer conversion up to 80% and were very close to their theoretical values with both initiators (Figure 2.2). The molecular weight distributions of the polymers prepared with VBIB were below 1.2, even lower with VTCA as initiator.

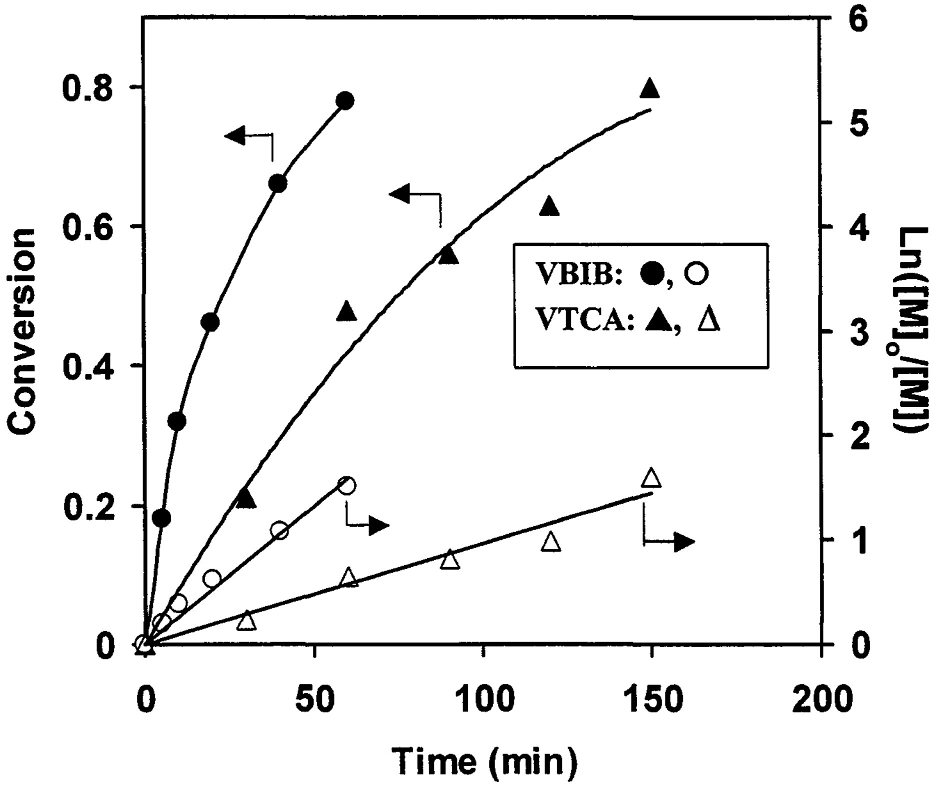

Figure 2.1. Bulk polymerization of DMAEMA initiated by VBIB and VTCA at 60 °C with CuBr/HMTETA/Initiator/DMAEMA = 1/1/1/100 in molar.

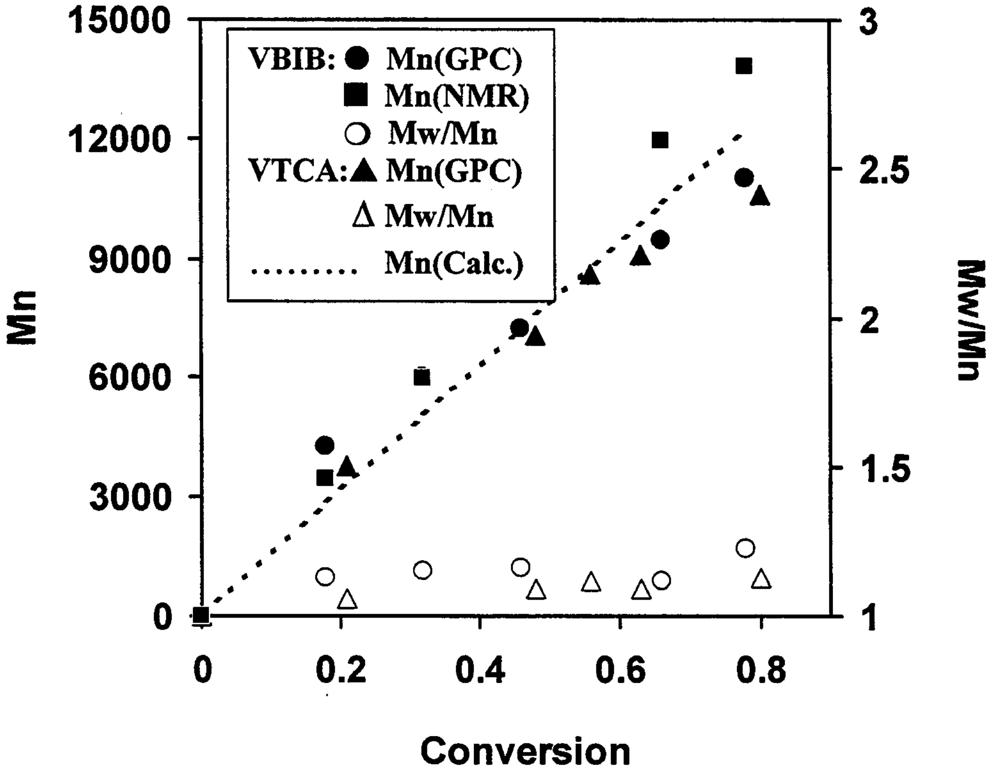

Figure 2.2 PolyDMAEMA molecular weight and molecular weight distribution versus DMAEMA conversion. See Figure 2.1 for conditions.

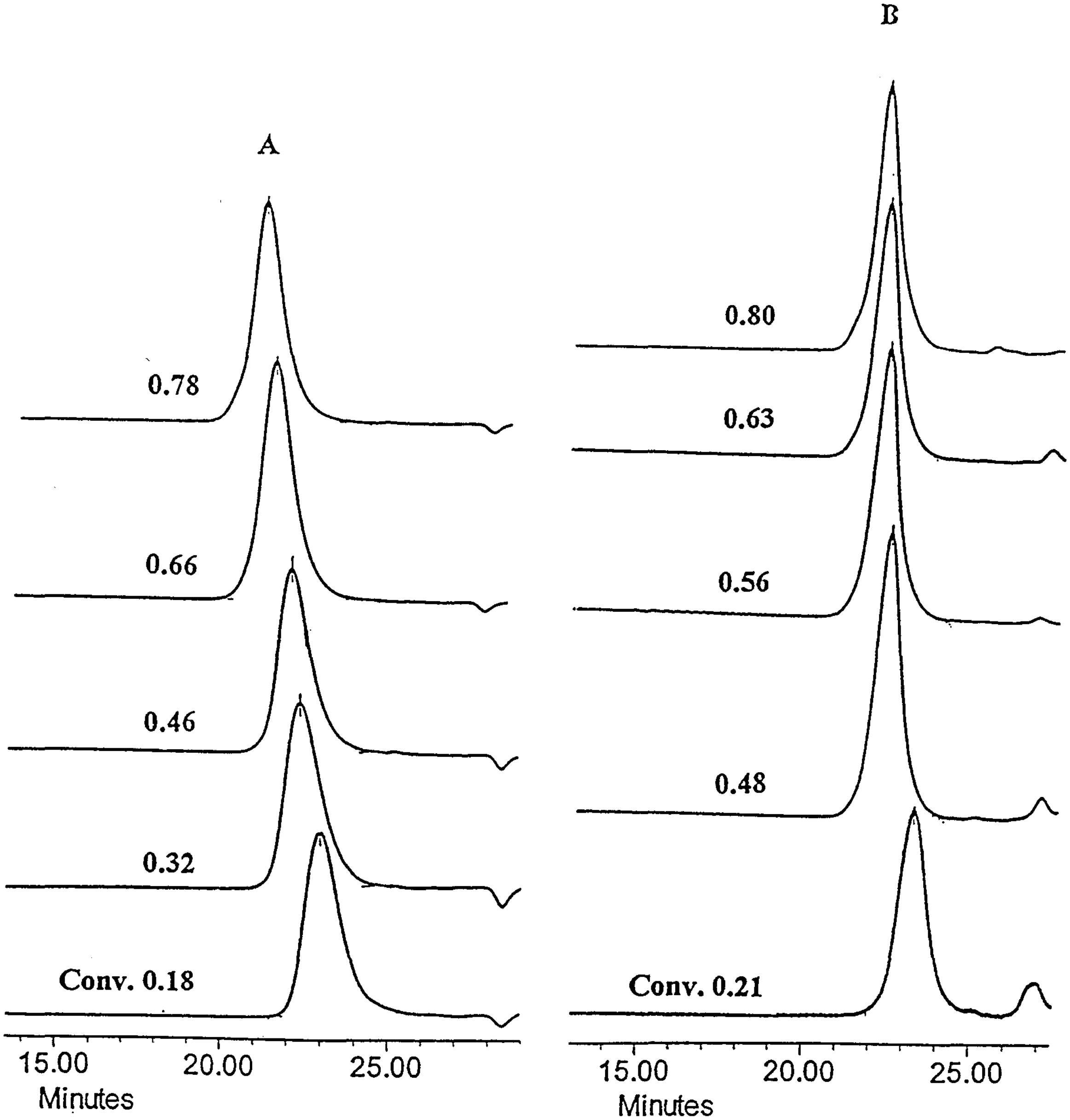

Figure 2.3. GPC traces of polyDMAEMA at different conversions prepared with (A) VBIB or (B) VTCA as initiator. See Figure 2.1 for conditions.

Figure 2.3 shows the GPC traces of polyDMAEMA prepared with the two initiators. The GPC traces of all the samples at different conversions were a typical Gaussian distribution without any shoulder peak, which was observed in the MA polymerization (see Section 2.3.3). This observation suggested that the vinyl group of the initiator moiety was not polymerized during the ATRP of DMAEMA mediated by CuBr/HMTETA.

The results for the MMA polymerization are shown in Figure 2.4. Because the T_g of PMMA is higher than 60 °C, the MMA polymerization was carried out either in THF or in γ-butyrolactone (γBL). The polymerization in THF was heterogeneous. The catalyst was only partially dissolved. Upon heating, some bright green crystals were precipitated from the solution. In contrast, when γBL (an inert 5-membered cyclic ester with high polarity) was used as solvent, the polymerization mixture was homogenous with a persistent green color throughout the polymerization.

With VBIB or VTCA as initiator, the MMA polymerization in both THF and γBL proceeded smoothly up to 80 % conversion at 60 °C in first order kinetics (Figures 2.4 and 2.5). The MMA polymerization rate in γBL was much faster than that in THF. This may be due to the high catalyst concentration in γBL because of the good solubility of copper bromide in γBL. The polymerization in γBL with VTCA was slower than with VBIB due to the formation of C-Cl bond, which is more difficult to be abstracted by CuBr than the C-Br bond.

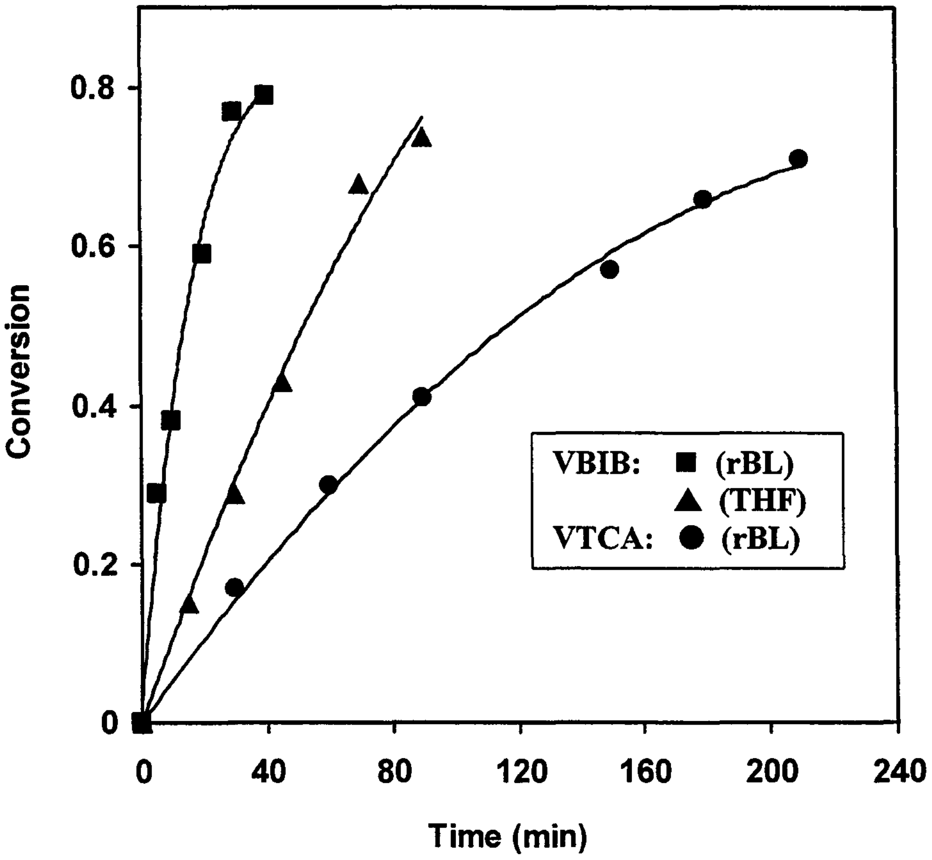

Figure 2.4. Solution polymerization of MMA initiated by VBIB and VTCA in γBL or in THF at 60 ^{0}C. CuBr/HMTETA/Initiator/MMA = 1/1/1/100 in molar, THF(or γBL)/MMA = 0.5(w/w).

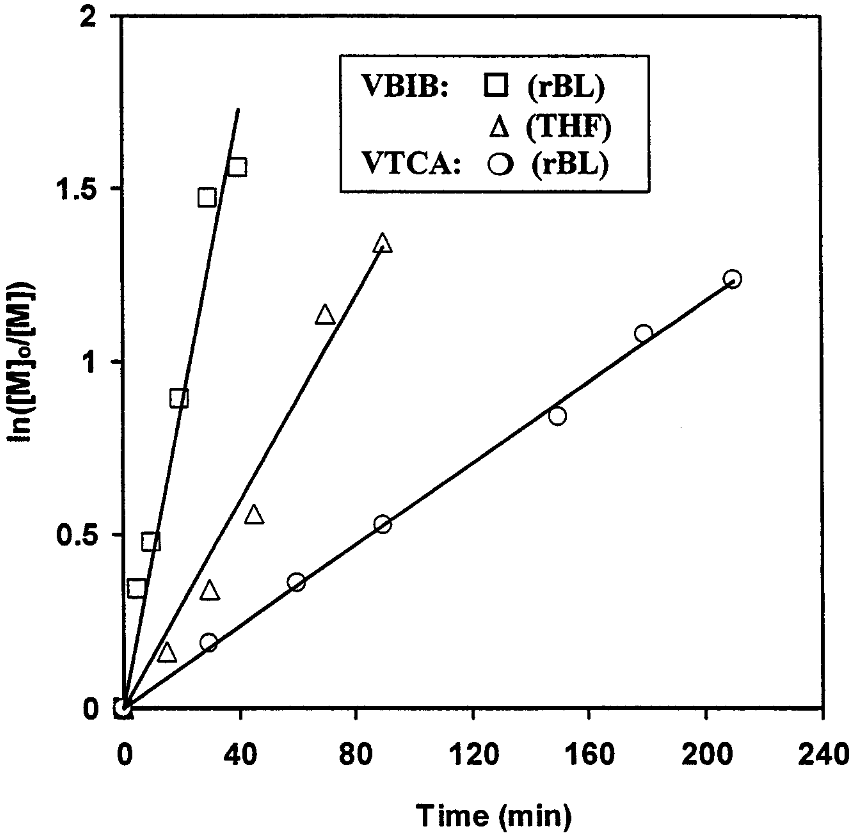

Figure 2.5. Kinetic plots for ATRP of MMA initiated by VBIB and VTCA in THF or γBL. See Figure 2.4 for the experimental conditions.

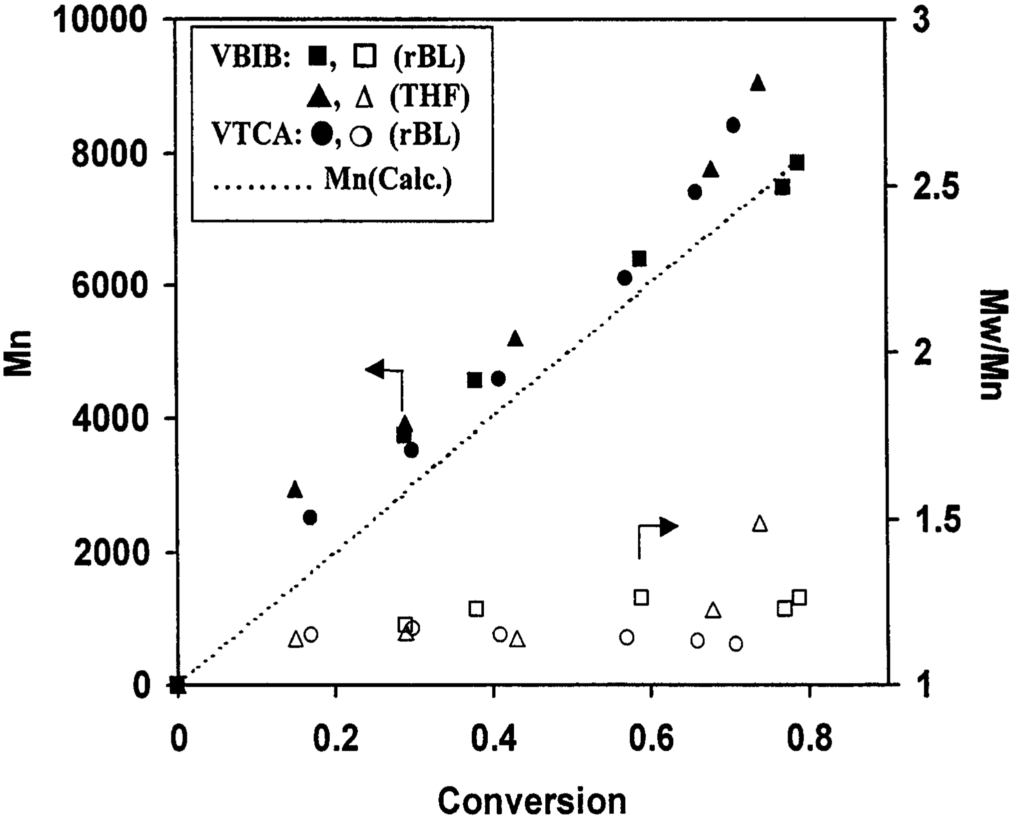

Figure 2.6. PMMA molecular weight and molecular weight distribution versus MMA conversion with VBIB and VTCA as initiators in THF or γBL. See Figure 2.4 for the experimental conditions.

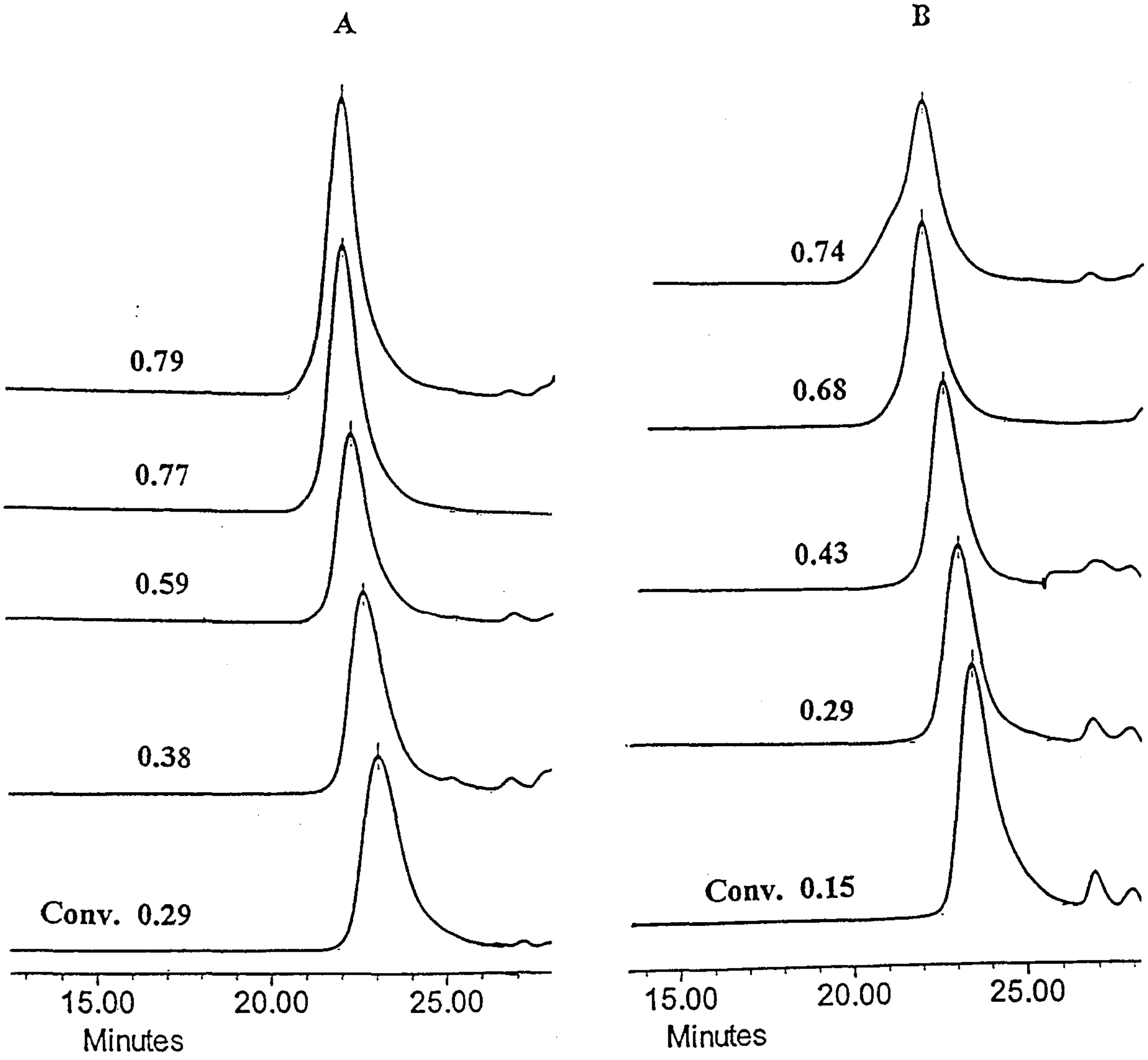

Figure 2.7. GPC traces of PMMA prepared in (A) γBL and (B) THF with VBIB as initiator. See Figure 2.4 for the experimental conditions.

The molecular weights of PMMA were very close to the calculated values and increased linearly with the conversion up to 70% in THF and 80% in γBL (Figure 2.6). When the conversion was higher than ca. 70% in THF, both the molecular weight and molecular weight distribution of PMMA increased sharply. Figure 2.7 shows the GPC traces of PMMA prepared in γBL and THF with VBIB as initiator. In THF, there appeared a shoulder peak at the high molecular weight region at high monomer conversions. The molecular weight corresponding to the shoulder peak was about twice of the major peak. This high molecular weight polymer population may be produced by coupling reactions of propagating radicals with terminal vinyl moieties, which yield polymer chains with doubled molecular weight. The detail of the reaction will be discussed below. With γBL as solvent, no shoulder peak was observed up to 80% conversion.

2.3.3 Polymerizations of Acrylates

The ATRP of MA initiated by VBIB at 60 °C and 80 °C are shown in Figure 2.8. At the early stage, the $\ln([M]_o/[M])$ *vs.* time plots were linear. However, the polymerization began to bend down from the first order kinetics at about 60% conversion at 80 °C and about 40% at 60 °C, indicating a decrease in radical concentration at higher MA conversion. The molecular weights of PMA prepared at both temperatures increased linearly at low conversions, but increased sharply at the conversions where the polymerizations began to deviate from the first order reaction (Figure 2.9). The BA polymerization at 80 °C was very similar to the MA polymerization at the same temperature with a comparable polymerization rate (Figures 2.10 and 2.11).

Figure 2.12 shows the GPC traces of PMA prepared at 60 and 80 °C. At low conversions, the GPC traces did not have any shoulder peak. The molecular weight distributions were relatively narrow with polydispersities about 1.2. With the reaction proceeding, a shoulder peak appeared at the high molecular weight region and its intensity increased with conversion. The Mn of the shoulder peak was about twice of that of the low molecular weight region. Similar GPC traces were also found in the BA polymerization. This shoulder peak appearing at high MA or BA conversion was generated by the reaction of acrylate radical with terminal vinyl group (Scheme 2.3), which produced polymers with doubled molecular weights relative to the original polymer chains. At the same times, the produced radicals ($-CH_2-\dot{C}H-O$) could react with $CuBr_2$ to form carbon-bromine ($CH_2-CH(Br)-O$) bonds. This kind of C-Br was too stable to be re-activated by Cu(I)Br to become a propagating radical (Scheme 2.3). This conclusion was tested by the ATRP of vinyl 2-hydroxyl ether with the same catalyst.[20] As a result, such a reaction became radical termination. The radical concentration thus decreased, as observed in Figures 2.8 and 2.10. Therefore, in order to obtain well-defined acrylate macromonomers, the polymerization should be stopped at low conversions before the reaction of the vinyl moieties becomes significant.

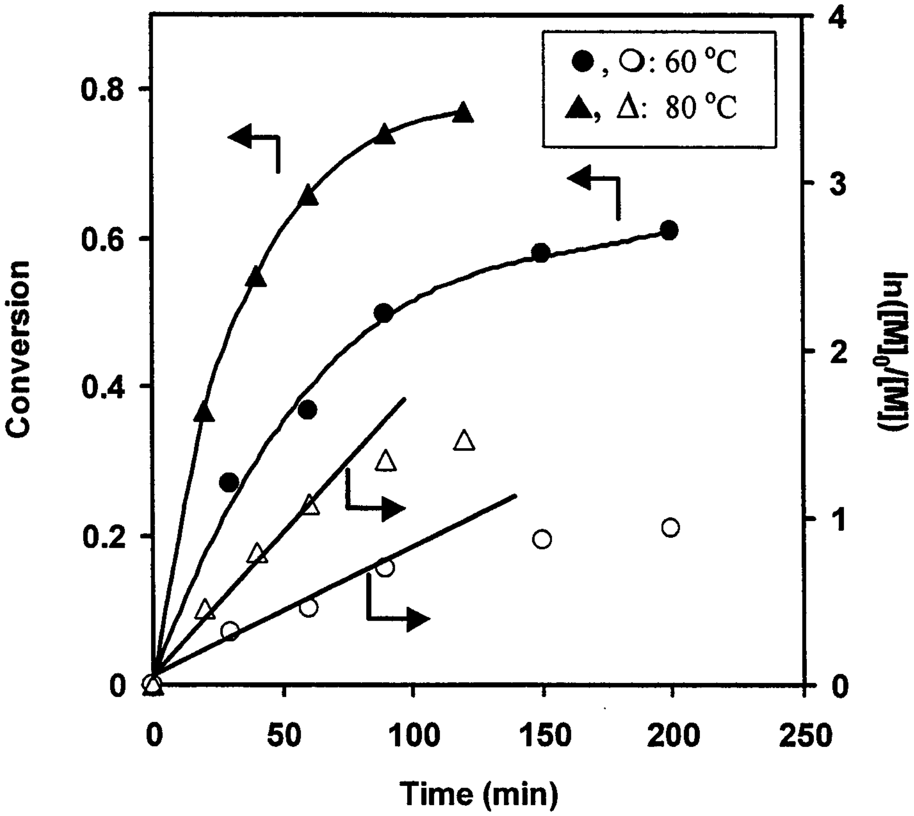

Figure 2.8. MA polymerization initiated by VBIB at 60 and 80 °C in γBL. CuBr/HMTETA/VBIB/MA = 1/1/1/100 in molar and γBL/MA = 0.5 (w/w)

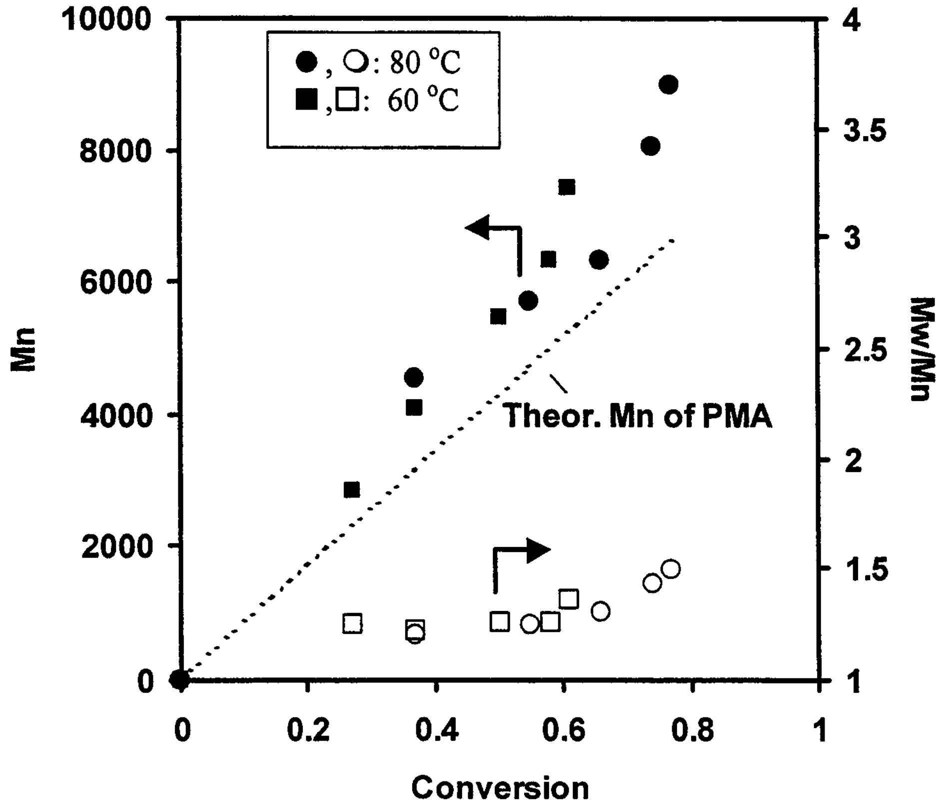

Figure 2.9. PMA molecular weight and molecular weight distribution versus MA conversion initiated by VBIB at 60 and 80 °C. See Figure 2.8 for conditions.

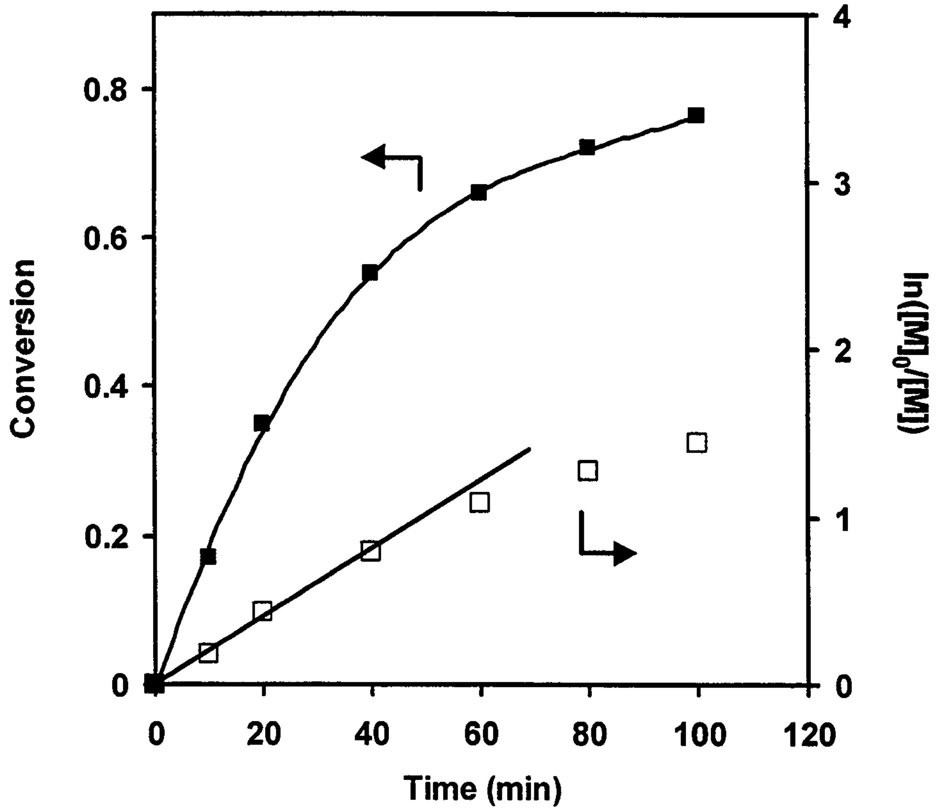

Figure 2.10 BA polymerization initiated by VBIB at 80 °C with CuBr/HMTETA/VBIB/BA = 1/1/1/100 in molar and γBL/BA = 0.5 (w/w).

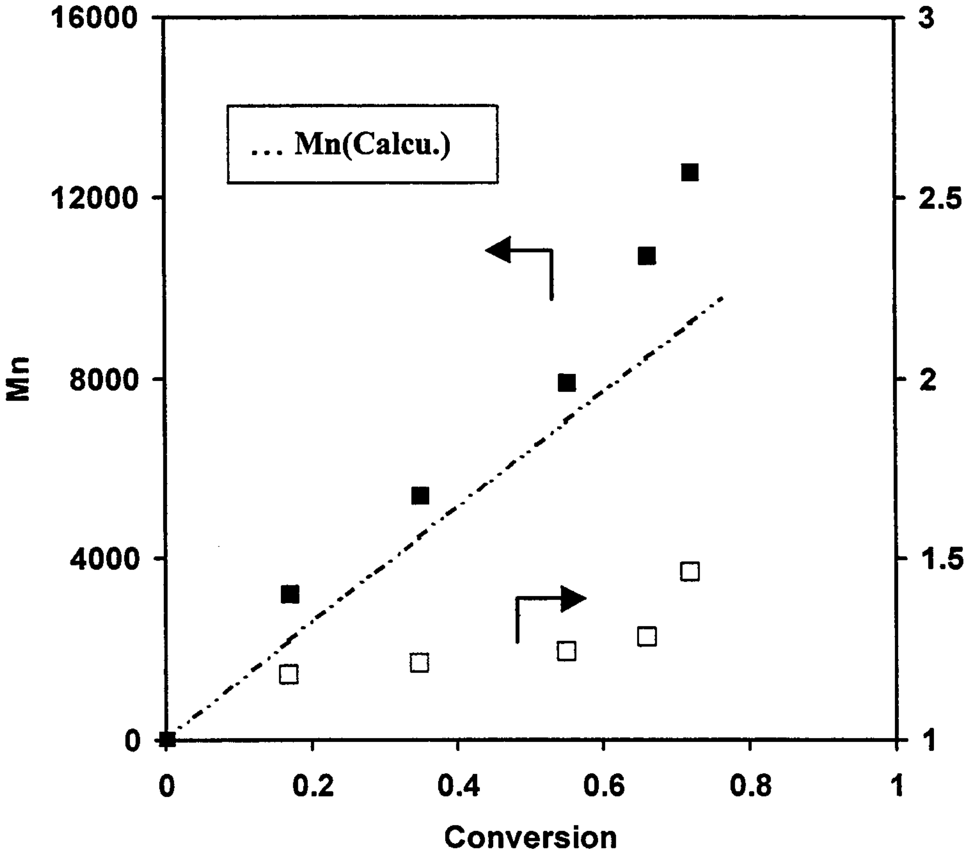

Figure 2.11. PBA molecular weight and molecular weight distribution versus BA conversion initiated by VBIB at 80 °C. See Figure 2.10 for conditions.

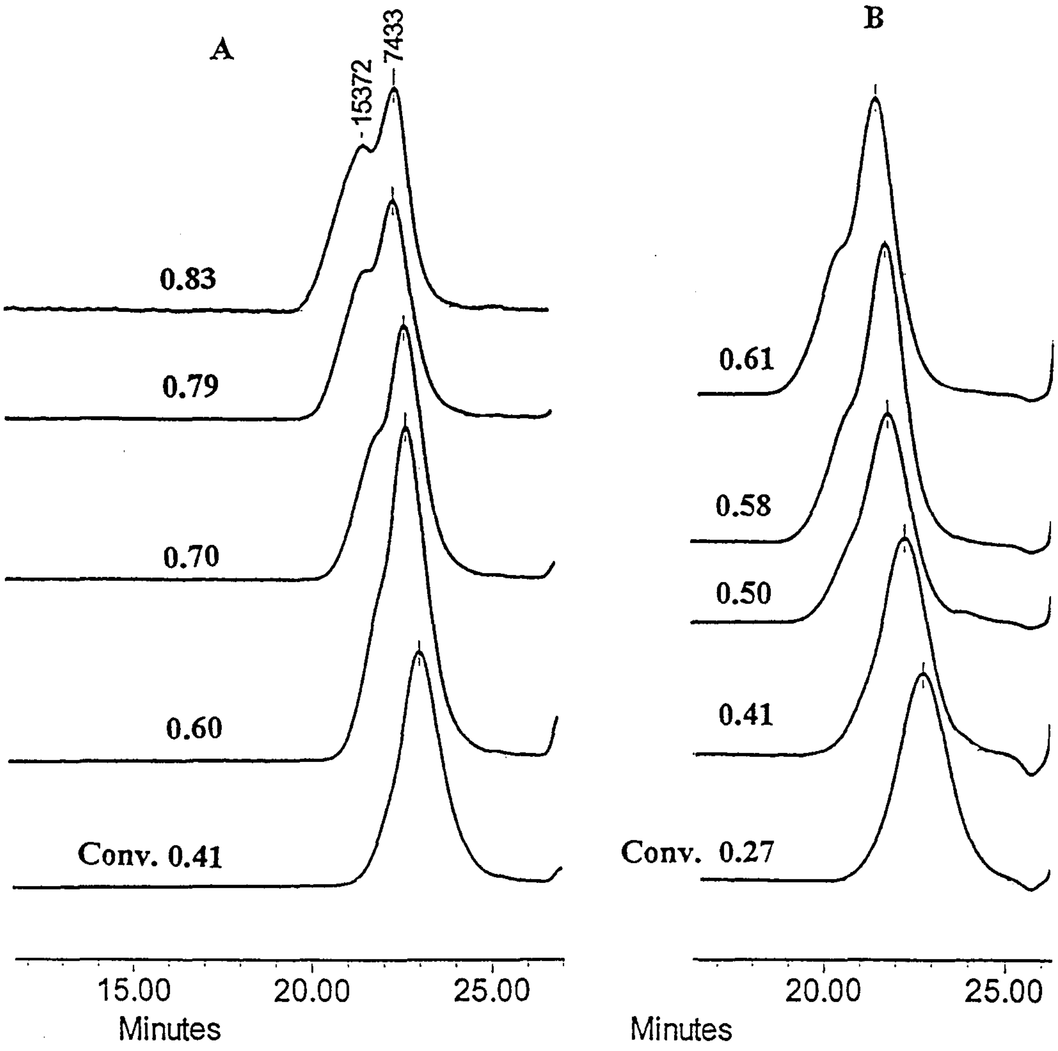

Figure 2.12. GPC traces PMA obtained from the ATRP of MA at (A) 80 and (B) 60 °C initiated by VBIB in γBL. See Figure 2.8 for the experimental conditions.

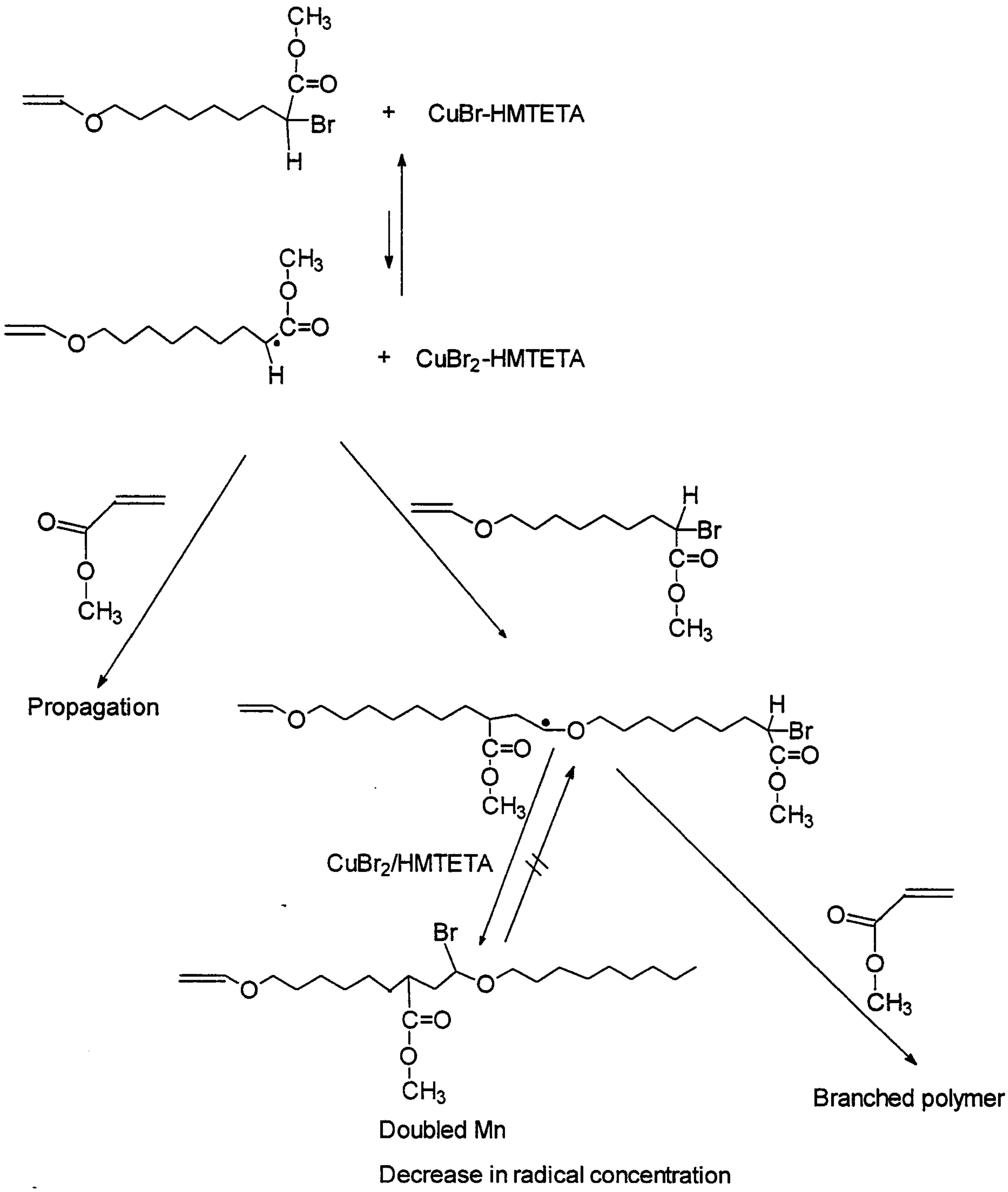

Scheme 2.3. The reaction of propagating radicals of acrylate with terminal unsaturated groups

2.3.4 Styrene polymerization

The styrene ATRP mediated by CuBr/HMTETA with VBIB (St/CuBr/HMTETA/VBIB = 100/1/1/1, γBL/St = 0.5(w/w)) is shown in Figure 2.13. γBL was also used as solvent to obtain a homogenous media and to lower reaction temperature. The solution was homogenous throughout the polymerization with a persistent green color. The polymerization also proceeded in first order kinetics and gave 78% conversion in four hours at 100 °C. The polystyrene molecular weights increased linearly with conversion and were comparable to their calculated values (Figure 2.14). The molecular weight distributions were about 1.1. The GPC traces (Figure 2.15) showed no sign of shoulder peak even up to 80% conversion. These observations indicated that during the ATRP process of styrene, the vinyl end groups were not consumed. Well-defined polystyrene macromonomers with terminal vinyloxyl group were thus prepared.

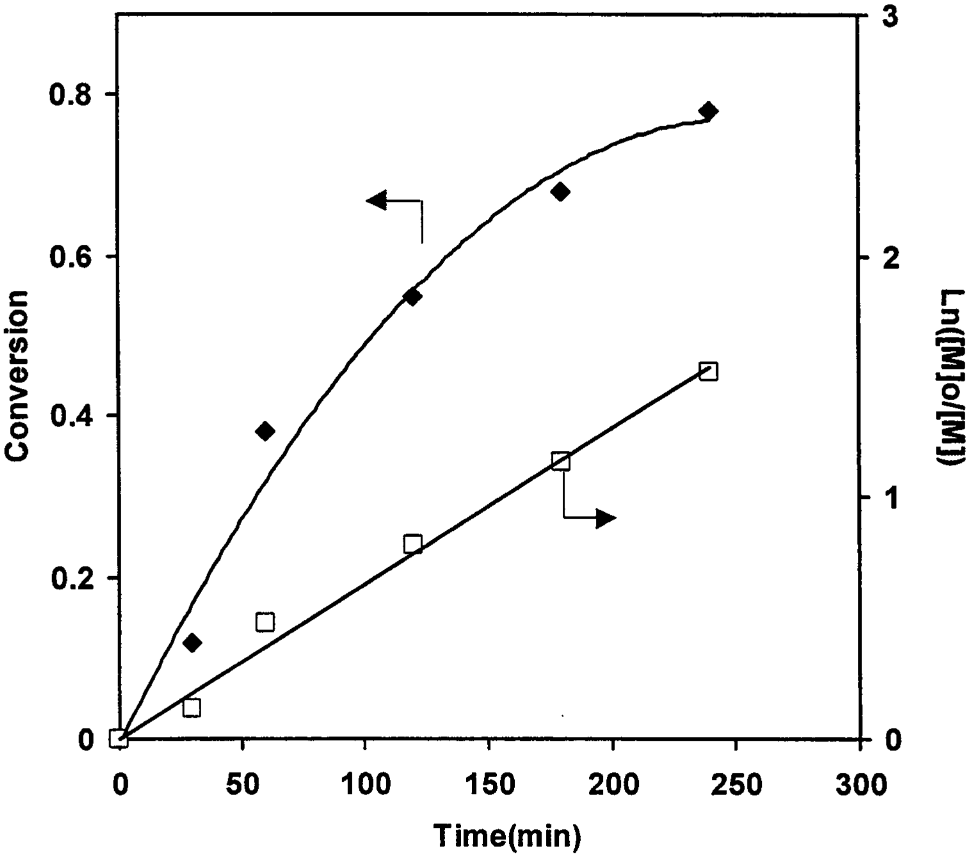

Figure 2.13. ATRP of styrene initiated by VBIB in γBL at 100 °C with CuBr/HMTETA/VBIB/St = 1/1/1/100 in molar and γBL/St = 0.5 (w/w).

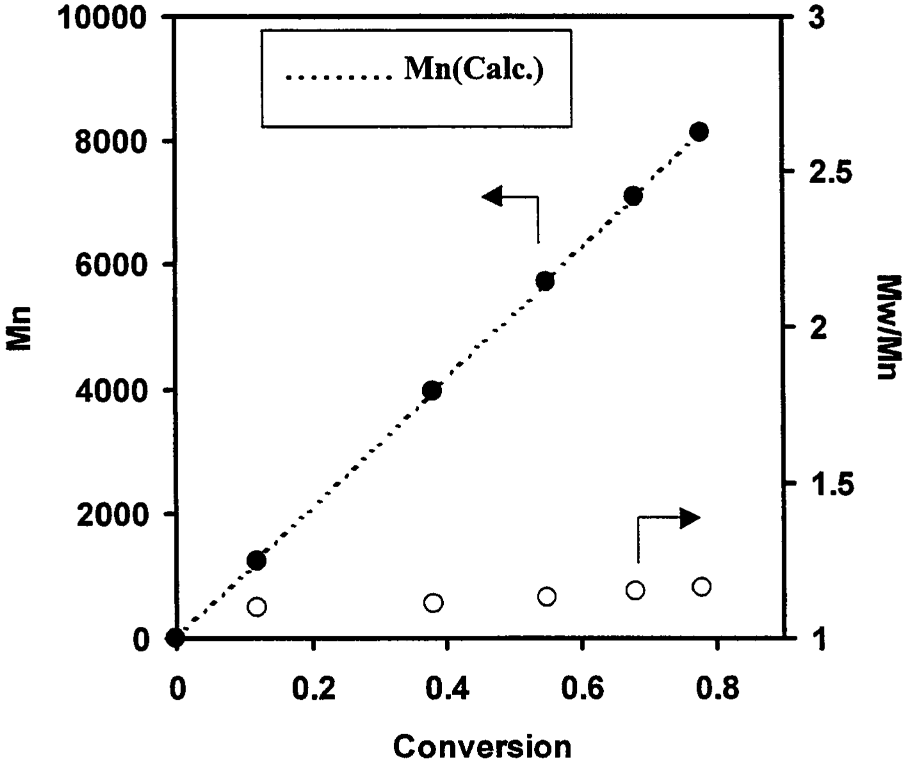

Figure 2.14. PS molecular weight and molecular weight distribution versus St conversion initiated by VBIB. See Figure 2.13 for the experimental conditions.

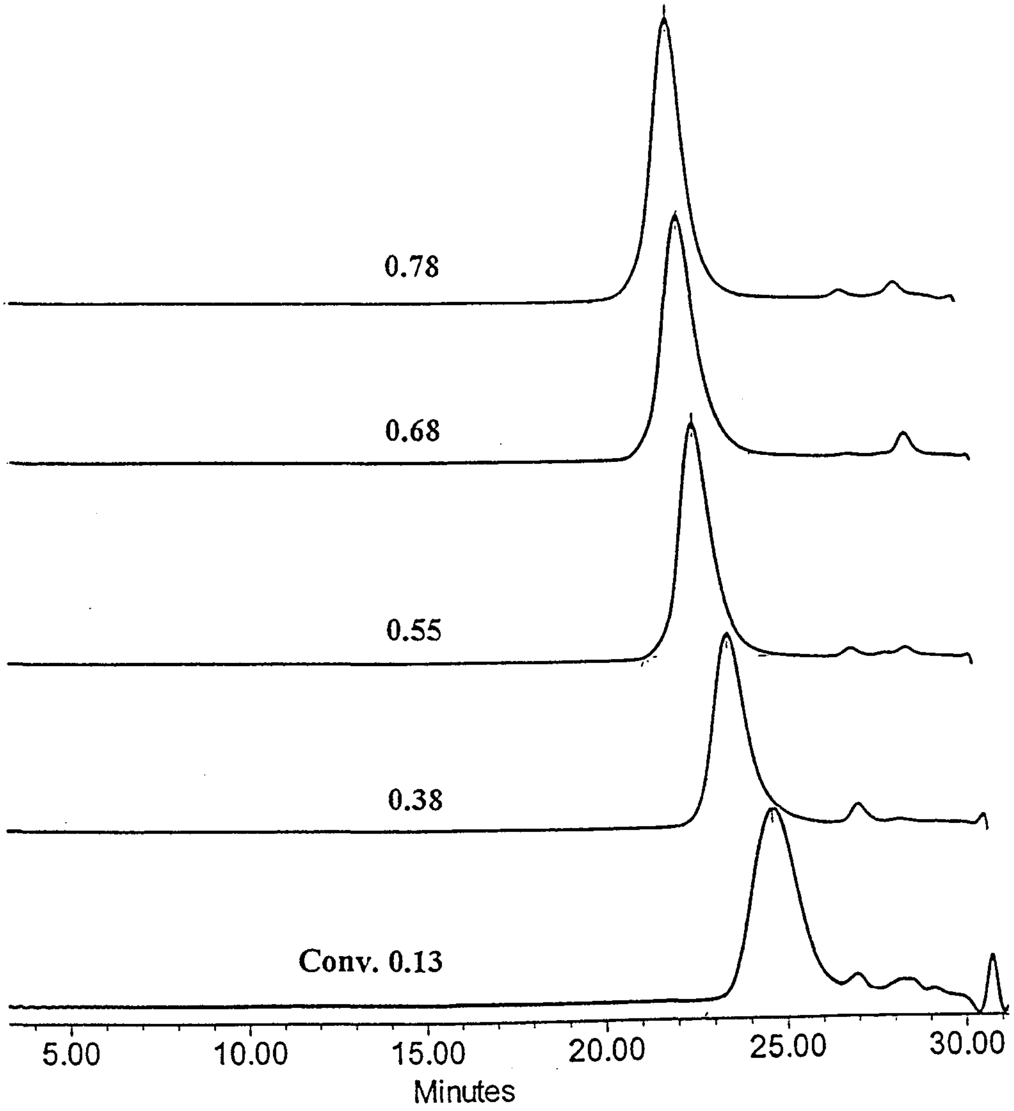

Figure 2.15. GPC traces of PS obtained from the ATRP of St at 100 °C. See Figure 2.13 for the experimental conditions.

2.3.5 Characterization of the Macromonomers

The macromonomers were characterized with NMR and the typical spectra are shown in Figures 2.16 A-D. Besides the polymer backbone signals assigned in the figures, there were signals ascribed to the terminal groups. For each of the polymers except for polystyrene, there was a same tetrad signal at 6.50~6.30 ppm attributed to the methine proton of the vinyl group ($=C\underline{H}-$). The methylene proton signals of the vinyl group ($C\underline{H}_2=CH-$) were overlapped by those of ester group ($-COOC\underline{H}_2-$) in polyDMAEMA and PBA. In polystyrene, the methine signal was overlapped by the benzene ring signals, but the tetrad signal of methylene proton ($C\underline{H}_2=$) in the vinyl group appeared clearly at 3.9-4.2 ppm. These signals were also found in PMMA and PMA. These observations proved that the prepared polymers contained the vinyl groups from the initiators.

The molecular weights of the polymers could also be estimated from the NMR measurements. The molecular weights were calculated by the intensity ratio of signal $-COOC\underline{H}_2-$ (for polyDMAEMA, PBA) or $-COOC\underline{H}_3$ (for PMMA and PMA) to the vinyl methine proton ($=C\underline{H}$) or the intensity ratio of the benzene ring signal to the vinyl methylene proton ($C\underline{H}_2=$) signal (for polystyrene). The calculated molecular weights by NMR of polyDMAEMA prepared by the VBIB-initiated ATRP of DMAEMA were also shown in Figure 2.2. The NMR measured molecular weights were slightly higher than the theoretical values and those by GPC. The PMMA and PS molecular weights by

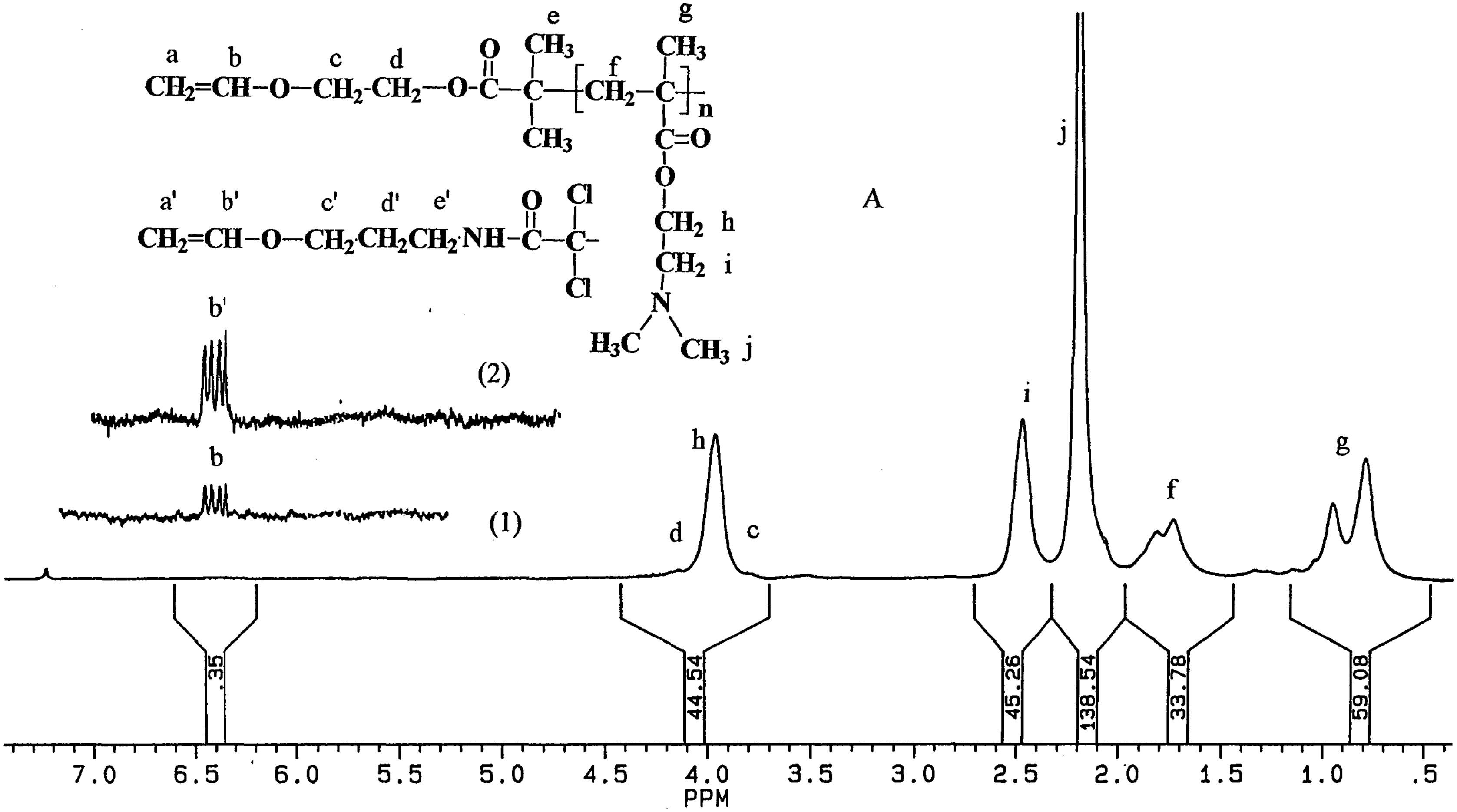
a b c d e g
CH2=CH–O–CH2·CH2–O-C(=O)–C(CH3)(CH3)–[CH2–C(CH3)]n
f
C=O
O
CH2 h
CH2 i
N
H3C CH3 j
a' b' c' d' e'
CH2=CH–O–CH2·CH2CH2·NH–C(=O)–C(Cl)(Cl)–
A
b'
(2)
b
(1)
d
h
c
i
j
f
g
.35
44.54
45.26
138.54
33.78
59.08
7.0
6.5
6.0
5.5
5.0
4.5
4.0
3.5
3.0
2.5
2.0
1.5
1.0
.5
PPM

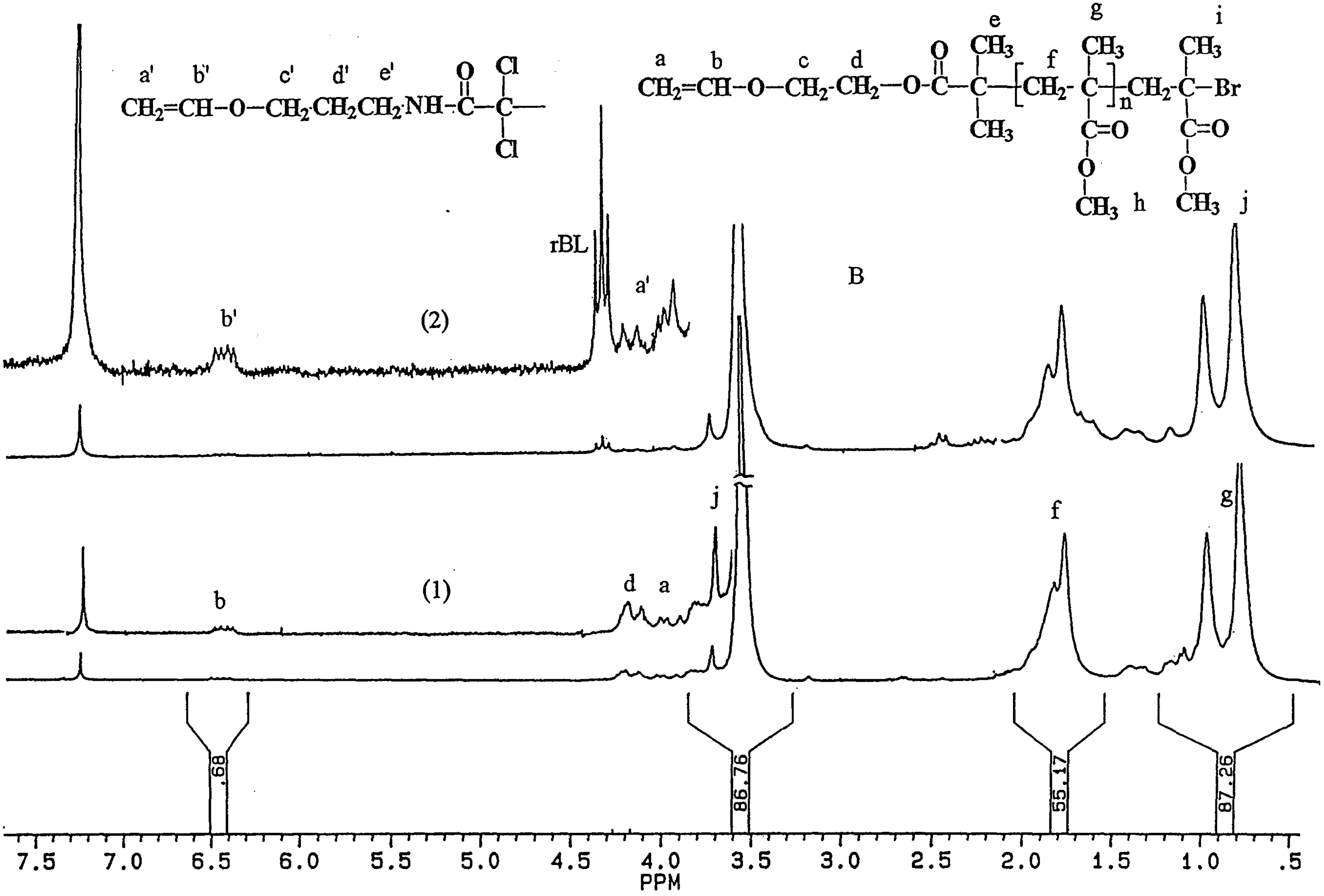
a' b' c' d' e'
CH2=CH−O−CH2·CH2CH2·NH−C(=O)−CCl2−
a b c d e f g i
CH2=CH−O−CH2·CH2−O−C(=O)−C(CH3)2−[CH2−C(CH3)(C=O−O−CH3)]n−CH2−C(CH3)(C=O−O−CH3)−Br
h j
rBL
a'
b'
(2)
B
j
d a
b
(1)
f
g
.68
86.76
55.17
87.26
7.5 7.0 6.5 6.0 5.5 5.0 4.5 4.0 3.5 3.0 2.5 2.0 1.5 1.0 .5
PPM

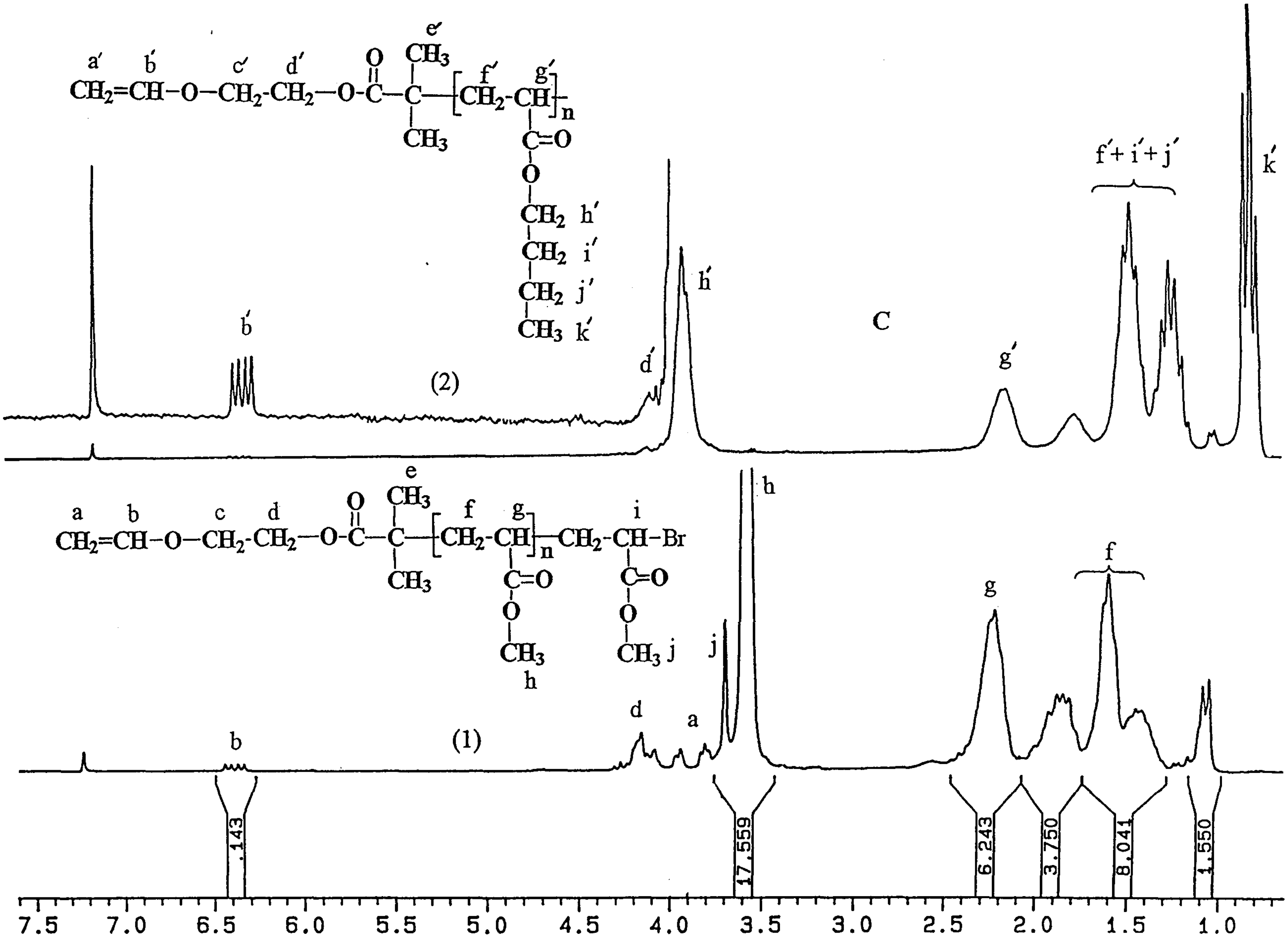
a' b' c' d' e' f' g'
CH2=CH-O-CH2-CH2-O-C(=O)-C(CH3)2-[CH2-CH]n-
C=O
O
CH2 h'
CH2 i'
CH2 j'
CH3 k'
b'
(2)
d'
h'
C
g'
f'+i'+j'
k'
a b c d e f g i
CH2=CH-O-CH2-CH2-O-C(=O)-C(CH3)2-[CH2-CH]n-CH2-CH-Br
C=O
O
CH3 h
C=O
O
CH3 j
b
(1)
d
a
j
h
g
f
.143
17.559
6.243
3.750
8.041
1.550
7.5
7.0
6.5
6.0
5.5
5.0
4.5
4.0
3.5
3.0
2.5
2.0
1.5
1.0

D

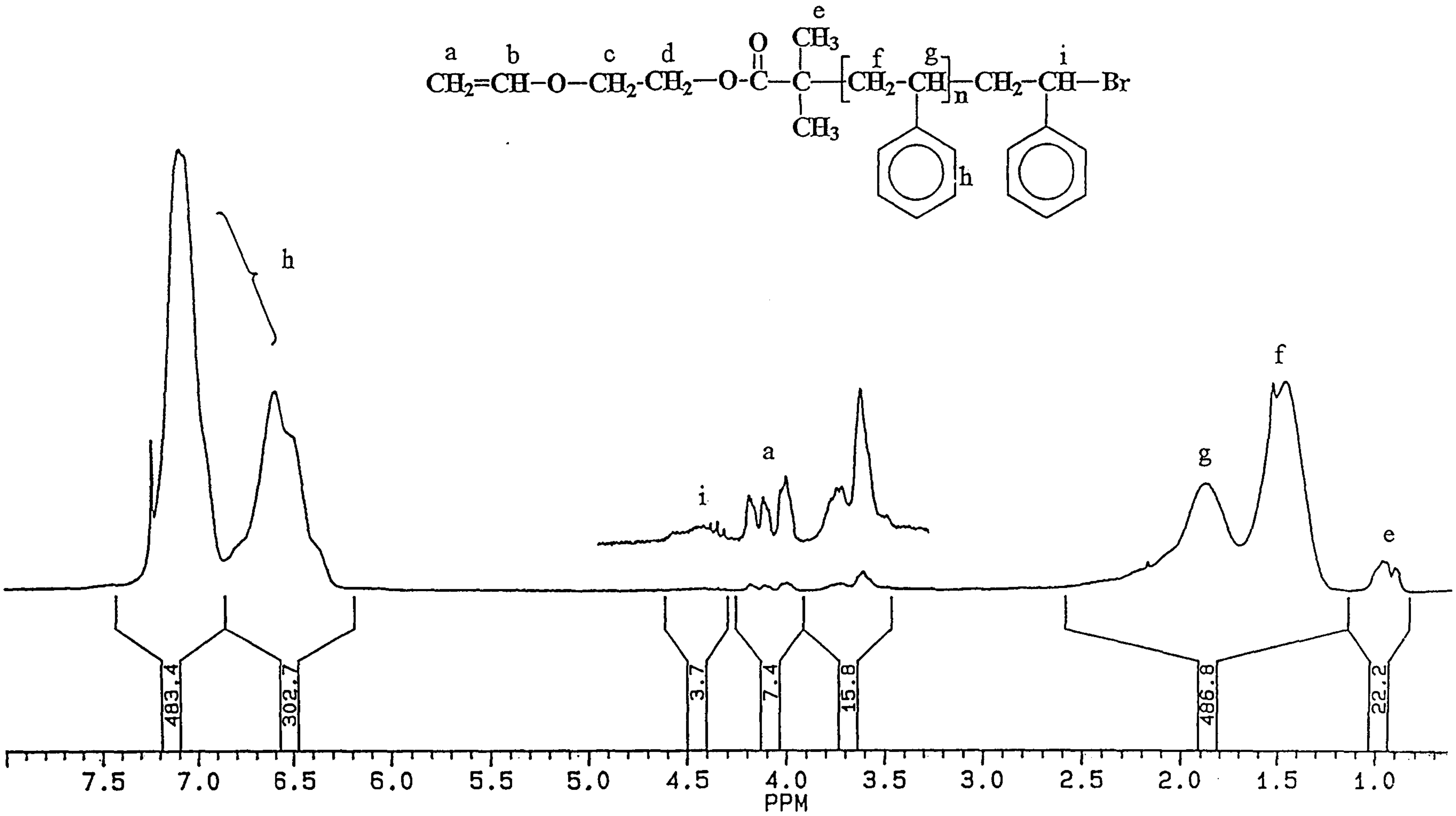

a
b
c
d
e
f
g
i
h
$CH_2=CH-O-CH_2-CH_2-O-C(=O)-C(CH_3)_2-[CH_2-CH]_n-CH_2-CH-Br$
h
i
a
g
f
e
483.4
302.7
3.7
7.4
15.8
486.8
22.2
7.5
7.0
6.5
6.0
5.5
5.0
4.5
4.0
3.5
3.0
2.5
2.0
1.5
1.0
PPM

Figure 16 ^{1}H-NMR spectra of prepared macromonomer.

A: Poly(DMAEMA): (1)CuBr/HMTETA/VBIB/DMAEMA=1/1/1/100; 60 °C, 40 min;
(2) CuBr/ HMTETA /VTCA/DMAEMA = 1/1/1/100; 60 °C, 120 min;

B: PMMA: (1) CuBr/ HMTETA /VBIB/MMA = 1/1/1/100; 60 °C in THF, 45 min; (2) CuBr/ HMTETA /VTCA/DMAEMA = 1/1/1/100; 60 °C in γBL, 180 min;

C: (1) PMA, CuBr/ HMTETA/VBIB/MA = 1/1/1/100; 80 °C, 20 min; (2) PBA, CuBr/ HMTETA /VBIB/BA = 1/1/1/100, 60 °C, 20 min;

D: Polystyrene, CuBr/ HMTETA /VBIB/St = 1/1/1/100, 100 °C in γBL, 120 min.

NMR were also agreeable with those by GPC. The PMA and PBA molecular weights obtained at low conversions were also comparable with the GPC results, suggesting that at this stage the vinyl groups in the initiator moieties were not consumed.

2.4 Conclusion

With CuBr/HMTETA as catalyst/ligand, VBIB was an effective ATRP initiator for preparation of vinyl-terminated macromonomers of PMMA, polyDMAEMA, PMA, PBA and PS. In the MMA, DMAEMA and St polymerization, the vinyl group in the initiator moiety was stable until very high conversion. However, in the polymerization of acrylates, the initiator vinyl group was consumed at low conversions. The ATRP of acrylates needed to be terminated in its early stage in order to prepare the acrylate macromonomers. VTCA also initiated the MMA and DMAEMA polymerization and yielded narrow macromonomer samples.

2.5 References

1. Yamashita, Y., Ed.; *Chemistry and Industry of Macromonomers*; Huthig & Wepf: Basel, Switzerland, **1993.**
2. Serizawa, T.; Chen, M, Q.; Akashi, M. *Journal of Polymer Science: Part A: Polymer Chemistry*, **1998**, *36*, 2581.
3. Quirk, R. P.; Yoo, T. *Polym. Preprints.* **1999**, *40*, 77.
4. Quirk, R. P., Yoo, T. *Polym. Bull.* **1993,** *31*, 29.
5. Wesdemiotis, C.; Arnould, M. A.; Lee, Y. and Quirk, R. P. *Polym. Preprints* **2000,** *41*, 629.
6. Hirao, A., Hayashi, M., Nakahama, S. *Macromolecules* **1996,** *29*, 3353.
7. Hsieh, H. L. and Quirk, R. P. *Anionic Polymerization: Principles and Practical Applications*, Marcel-Dekker, New York, **1996**.
8. Matyjaszewski, K. Ed. *Controlled Radical Polymerization;* American Chemical Society: Washington, DC **1997**; ACS Symp. Ser. Vol. 685.
9. Kato, M; Kamigaito, M; Sawamoto, M; Higashimura, T. *Macromolecules* **1995,** *28*, 1721.

10. Wang, J. S.; Matyjaszewski, K. *Macromolecules* **1995**, *28*, 7901.

11. Percec, V.; Barboiu, B; Neumann, A.; Ronda, J.C.; Zhao, M. *Macromolecules* **1995**, *29*, 3665.

12. Haddleton, D. M.; Jasieczek, C. B.; Hannon, M. J.; Shooter, A. J. *Macromolecules* **1997**, *30*, 2190.

13. Destarac, M; Bessiere, J. M; Boutevin, B. *Macromol. Rapid Commun.* **1997**, *18*, 967.

14. Moineau, G.; Granel, C.; Dubois, Ph.; Jerome, R.; Teyssie, P. *Macromolecules* **1998**, *31*, 542.

15. Haddleton, D. M.; Waterson, C.; Derrick, P. J.; Jasieczek, C. B. and Shooter, A. J. *Chem. Commun.* **1997**, 683.

16. Coessens, V.; Matyjaszewski, K. *Macromol. Rapid Commun.* **1999**, *20*, 127.

17. Malz, H.; Komber, H.; Voigt, D.; Hopfe, I.; Pionteck, J. *Macromol. Chem. Phys.* **1999**, *200*, 642.

18. Matyjaszewski, K.; Beers, K. L.; Kern, A.; Gaynor, S. G. *J. Polym. Sci.: Part A: Polym. Chem.* **1998**, *36*, 823.

19. Nakagawa, Y. and Matyjaszewski, K. *Polym. J.* **1998**, *30*, 138.

20. The polymerization of 2-dimethylaminoethyl vinyl ether was tried with the same catalyst system. 19.8 mg CuBr, 31.6 mg HMTETA, 2 ml dimethylaminoethyl vinyl ether, 1 ml γ-BL and 20 μl ethyl 2-bromoisobutyrate were charged to tube and degassed by nitrogen. The mixture was heated at 60 ^{0}C for 24 h. No polymer was isolated. Then 1.5 degassed MA was injected to the polymerization media. Also no

polymerization was found. The same result was obtained using 2-hydroxylethyl vinyl ether as monomer.

Chapter 3

Supported Atom Transfer Radical Polymerization by Catalyst Adsorption

3.1 Introduction to Catalyst Supporting for ATRP

Atom transfer radical polymerization (ATRP) has made significant progress [1] since it was first developed in 1995.[2-6] Various systems based on Cu,[1,4,7,8] Ru,[3,9] Fe,[10] Ni,[11-13] and Rh[14] have been developed for ATRP of styrenic, acrylic, and methacrylic monomers in organic and aqueous media.[15-16] ATRP is very useful for synthesizing functional polymers of low molecular weight. For example, polymers with allyl,[17,18] vinyl,[19,20] and hydroxyl groups [21-23] were readily prepared with molecular weights less than 10^5.

The major disadvantage of ATRP is its low catalyst efficiency and thus the high catalyst concentration used. In a typical ATRP recipe, the initiator to catalyst ratio is usually 1/1, which is one catalyst molecule mediating one polymer chain. The metal halide usually is about 0.1~1% (molar) of the monomer and it finally goes to the products. This residual catalyst not only deeply colors the product, but also it may make the product toxic. Therefore, an additional purification is required to remove the catalyst from the product, usually by passing the mixture solution through a column of silica or alumina gel or adsorbing with resins.[24] This post-treatment is not only time-demanding but also costly due to catalyst waste.

A possible solution to this problem is to support catalyst onto a solid that can be readily removed from the product, and ideally be reused. Recently, ruthenium(II) catalyst supported onto amine-functionalized silica gel was successfully used for the heterogeneous ATRP of methyl methacrylate (MMA), which displayed typical living polymerization characteristics.[25]

Cu-based catalysts are most versatile for ATRP of various monomers. However, supporting CuBr for heterogeneous ATRP is not very successful. CuBr was supported by a Schiff base ligand to amino-functionalized silica gel and crosslinked polystyrene for styrene and MMA polymerizations. The polymerizations by these catalysts showed limited living characters.[26] The polymer molecular weights were significantly higher than predicted and the polydispersities were high (>1.5).[26] Copper bromide immobilized by multidentate amine-functionalized silica gel did not mediate living polymerizations of MMA, MA and styrene.[27]

Chapter 2 shows that copper bromide-hexamethyltriethylenetetramine (HMTETA) complex was an excellent catalyst for the ATRP of MMA, 2-(*N,N*-dimethylamino)ethyl methacrylate (DMAEMA), styrene (St) and methyl acrylate (MA). When we purified the products prepared by ATRP in Chapter 2 by passing the polymer-catalyst mixture solutions through a column of silica gel, we noticed that the blue color from the catalyst complex was retained at the very top layer of the silica gel in the column. This suggests that copper halide-HMTETA complex has a strong affinity to silica gel. We therefore supported the catalyst complex onto silica gel by physical adsorption for ATRP. Compared to grafting methods, this adsorption approach is much simpler and does not require special chemicals or tedious procedures.

This chapter reports the use of the silica gel supported copper bromide-HMTETA complex for the living polymerization of MMA. The supported catalysts were recycled twice with good retention of the catalyst activities. The controllability of the catalyst systems over the polymer molecular weight was even better after recycling.

3.2 Experimental Section

3.2.1 Materials

MMA (Aldrich, 99.9%) was distilled under vacuum and stored at –15 °C before use. 1,1,4,7,10,10-Hexamethyltriethylenetetramine (HMTETA, 99%), CuBr (99.999%), methyl (±) α-bromophenylacetate (MBP, 97%) were used as received from Aldrich. Toluene was distilled from CaH_2. Silica gel was supplied by SiliCycle Inc (230-400 mesh, average pore diameter of 60 Å). It was boiled in deionized water for 5 h, air dried and then dried in vacuum.

3.2.2 Measurements

Nuclear Magnetic Resonance (NMR) Spectroscopy: ^{1}H-NMR spectra were recorded on a Bruker ARX-200 spectrometer at 200 MHz. ^{1}H-NMR chemical shifts in

$CDCl_3$ were reported downfield from 0.00 ppm using residual $CHCl_3$ signal at 7.23 ppm as an internal reference.

Molecular Weight Measurements: Number and weight average molecular weights (M_n and M_w, respectively) were determined by gel permeation chromatography at the flow rate of 1.0 mL/min relative to polystyrene using THF-2% (v/v) triethylamine as solvent at 25 °C with RI detector. Data were recorded and manipulated using the Waters Millennium software package.

3.2.3 Polymerization

A typical polymerization process was as follows: CuBr and silica gel were added to a Schlenk flask. The flask was degassed by five vacuum-nitrogen cycles. Degassed MMA, toluene and HMTETA were added to the flask and the mixture was bubbled with nitrogen for 5 min with stirring. The mixture became blue upon the ligand addition. The blue silica particles quickly settled down to the bottom of the flask once the stirring stopped and the upper solution layer became colorless. Degassed initiator (MBP) was dropwise introduced to the flask with stirring. The blue particles turned green. The flask was then immersed in an oil bath at 90 °C with sufficient stirring. At different time intervals, solution mixture (~0.05 mL) was withdrawn from the flask with a nitrogen-purged syringe. The mixture was diluted with $CDCl_3$. The conversion was estimated from the ^{1}H-NMR intensity ratio of $OC\underline{H}_3$ signals from the polymer (3.60 ppm) and monomer (3.75 ppm). A small amount of this solution was injected to GPC to measure the polymer molecular weight and polydispersity.

3.2.4 Catalyst Recycle

After the polymerization is complete, the flask was lifted from the oil bath and left still for an hour. The upper layer solution was carefully removed via cannula with nitrogen pressure. The remaining solid in the flask was washed twice with degassed toluene (total 20 mL) under nitrogen. Then the same amount of the degassed MMA, toluene, and initiator, as in the first polymerization run, were charged to the flask. The polymerization procedure was repeated.

3.3 Results and Discussion

3.3.1 Atom Transfer Radical Polymerization of Methyl Methacrylate by Silica Gel Supported Copper Bromide/Multidentate Amine

3.3.1.1 Catalyst Adsorption onto Silica Gel Surface

The adsorption of the catalyst on silica gel surface was studied by using $CuBr_2$-HMTETA as a model because the complex has an adsorption band at 740 nm that can be used to determine the concentration of the complex. Figure 3.1 shows the UV-Vis spectra of the $CuBr_2$-HMTETA solution in toluene-MMA (1:1) in the presence of silica gel at different times. The absorbency of the peak at 740 nm decreased very quickly upon addition of silica gel. Figure 3.2 shows the fraction of $CuBr_2$-HMTETA in solution as a function of time. The concentration of $CuBr_2$-HMTETA in solution decreased sharply once the silica gel was added. About 3% of the complex originally charged remained in the solution after 5 min of addition of silica gel and less than 0.1% of $CuBr_2$-HMTETA was in solution after 25 min. This result indicates that the catalyst complex has a strong affinity to the silica gel surface.

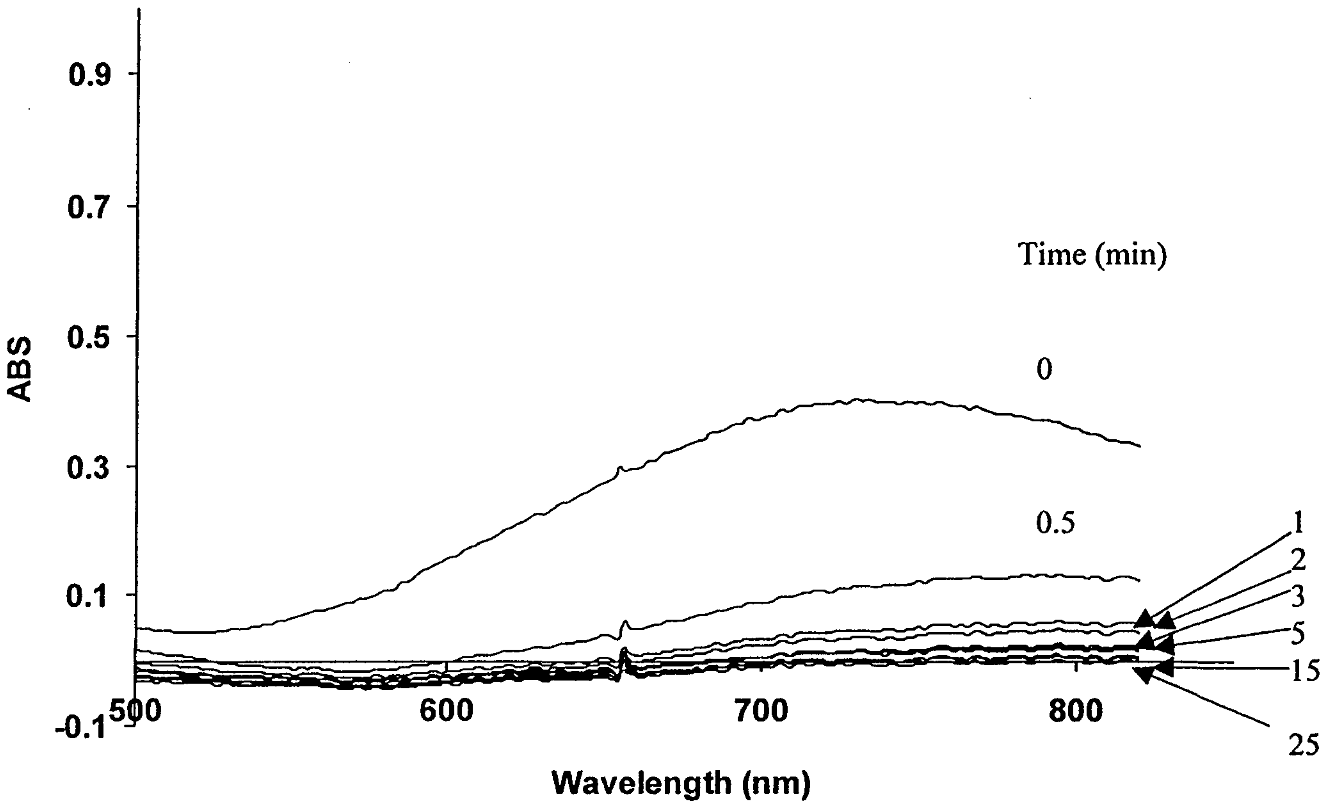

Figure 3.1 UV-Vis spectra of $CuBr_2$-HMTETA solution in the presence of silica gel at different time

Solution: toluene (50 mL)-MMA (50 mL), CuBr (10 mg), HMTETA (16 mg), γ-butyrolactone (2 mL)

Silica gel: 200 mg

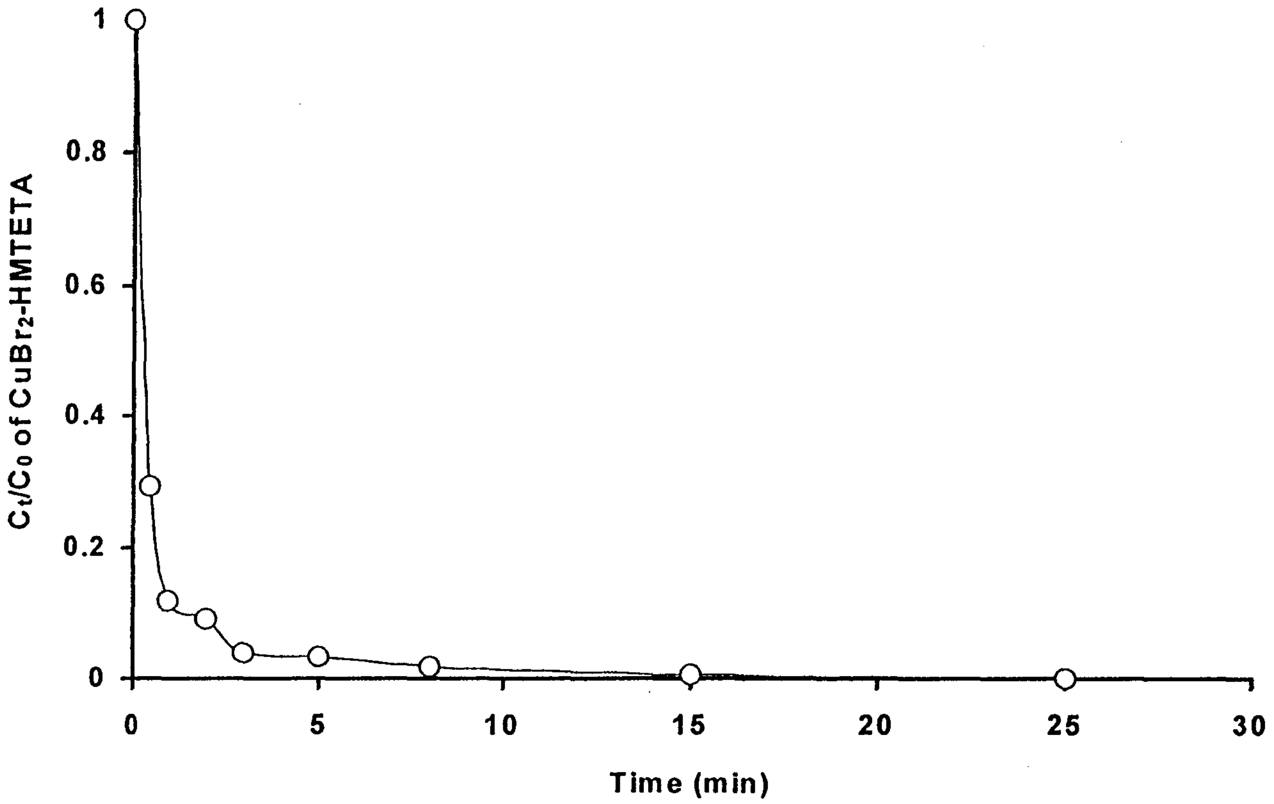

Figure 3.2. The fraction of $CuBr_2$-HMTETA in solution at different time after adding silica gel

See Figure 3.1 for experimental conditions

3.3.1.2 Effects of Silica Gel on the MMA Polymerization

When silica gel was added to the copper-HMTETA complex MMA-toluene solution, it immediately became blue. The blue particles immediately turned green upon addition of the initiator. The mixture gradually became viscous at 90 °C. Figure 3.3 shows the MMA polymerizations with and without silica gel. The polymerizations proceeded at almost the same polymerization rate with and without silica gel. Both the $\ln([M]_o/[M])$ *vs.* time plots are linear, indicating first order kinetics in monomer and the constant radical concentrations throughout the polymerizations. This demonstrates that the MMA polymerizations proceeded without detectable chain termination. The HMTETA/CuBr molar ratio had a minor effect on the polymerization. Doubling the ligand content slightly accelerated the polymerization.

Figure 3.4 shows the molecular weight and molecular weight distribution as a function of conversion. With or without silica gel, the molecular weight distributions of the resulting PMMA were all very narrow with polydispersities below 1.1 at the early stage. The polydispersities increased slightly with conversion, but most remained lower than 1.3. These polydispersities were much lower than those with ruthenium catalysts supported on amine-modified silica gel.[25] The better controllability of silica gel supported CuBr-HMTETA may result from more effective deactivation ability of $CuBr_2$. The PMMA molecular weights in Figure 3.4 increased linearly with conversion. This clearly confirms that the polymerization mediated by silica gel supported CuBr-HMTETA preceded without detectable terminations.

The PMMA molecular weights, however, were much higher than predicted. The calculated initiator efficiencies (Mn_{calc}/Mn_{GPC}) were about 0.5 throughout the polymerization. Since the initiator efficiencies were also low in the unsupported polymerization of the same system, the low initiator efficiency was evidently not caused by the silica gel support. Increasing the ligand/CuBr ratio to 2 did not improve the initiator efficiency. Since plots of $\ln([M]_o/[M])$ *vs.* time in Figure 3.3 are linear, i.e. constant radical concentration throughout the polymerization, the low initiator efficiencies must be caused by the consumption of some initiators at the very beginning by side radical reactions because of high radical concentration at the beginning of polymerization.

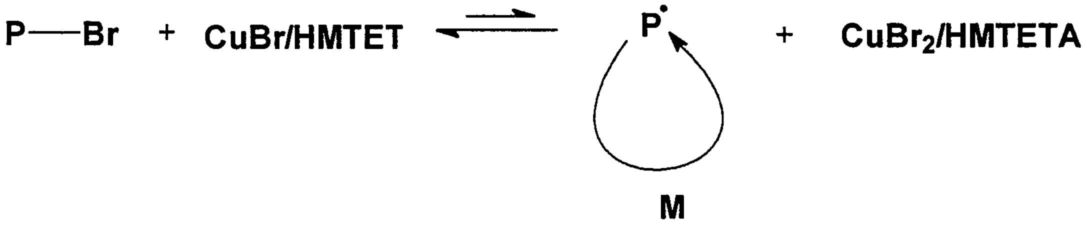

Eq. 3.1

Eq. 3.1 indicates that reducing CuBr concentration can reduce the radical concentration and thus may minimize initiator side reactions, and thereby increase the initiator efficiency. The polymerization was thus carried out at reduced level of catalyst. Figure 3.5 shows the MMA polymerizations with [CuBr]/[I] ratios of 0.5 and 1, respectively. The polymerization rate with [CuBr]/[I] = 0.5 was lower than that with

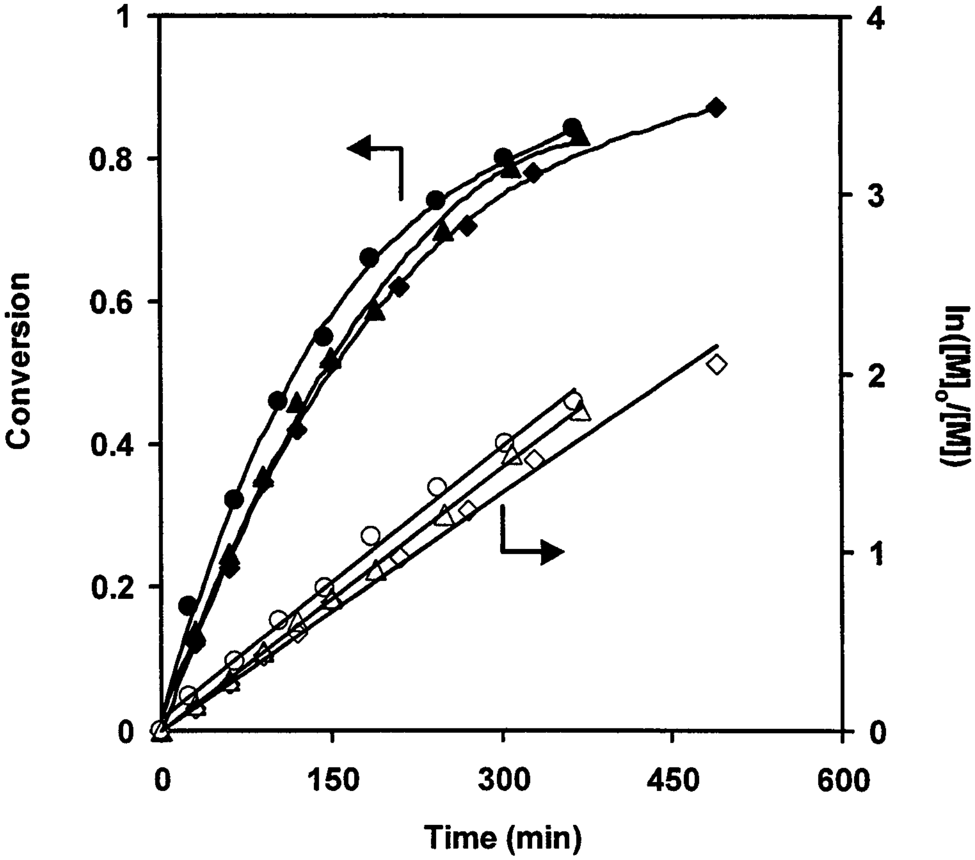

Figure 3.3 MMA Polymerization catalyzed by CuBr-HMTETA with or without silica gel. 90 °C, toluene/MMA = 2 (w/w) and [MMA]/[CuBr]/[Initiator] = 100:1:1:1(molar). [HMTETA]/[CuBr]=1, no silica gel (▲, △); [HMTETA]/[CuBr]=1, silica gel/CuBr =2(w/w) (◆, ◇); [HMTETA]/[CuBr]=2, silica gel/CuBr=2 (w/w) (●, ○).

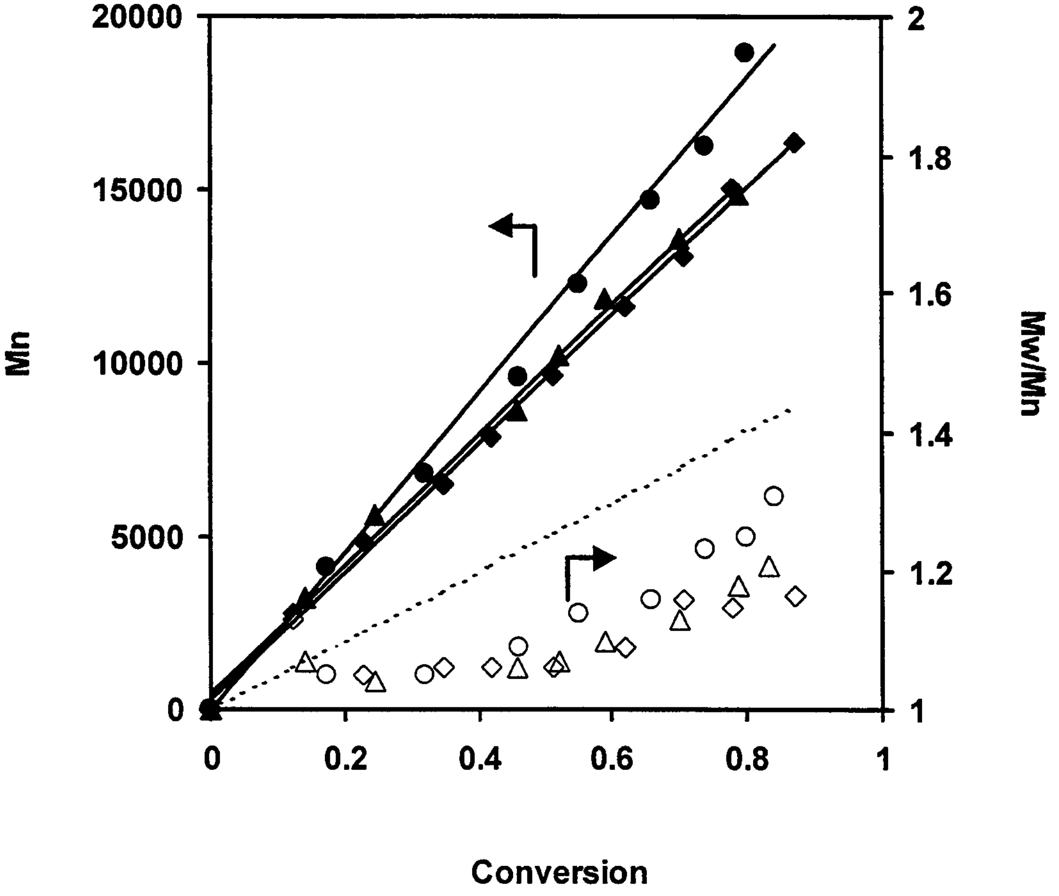

Figure 3.4. PMMA molecular weight and polydispersity as a function of conversion in the MMA polymerization with and without silica gel. Same experimental conditions as in Figure 3.3.

[HMTETA]/[CuBr]=1, no silica gel (▲, Δ); [HMTETA]/[CuBr]=1(molar), silica gel/CuBr =2(w/w) (◆, ◇); [HMTETA]/[CuBr](molar)=2, silica gel/CuBr=2 (w/w) (●,O).

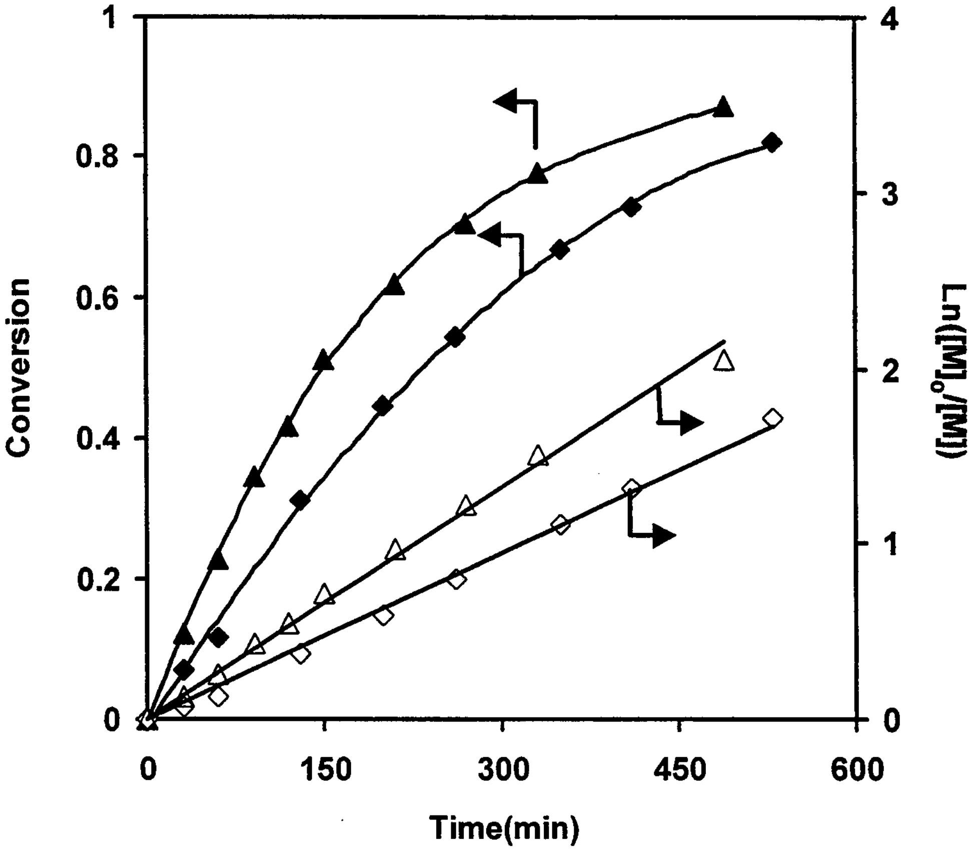

Figure 3.5 Polymerization of MMA with different CuBr/MBP ratios catalyzed by CuBr-HMTETA/2-silica gel

90 °C, toluene/MMA=2 (w/w), [MMA]/[Initiator] = 100:1(molar), and silica gel/CuBr=2 (w/w); [HMTETA]/[CuBr]=1, [CuBr]/[I]=1:1(molar)(▲, Δ); 0.5:1 (◆, ◇).

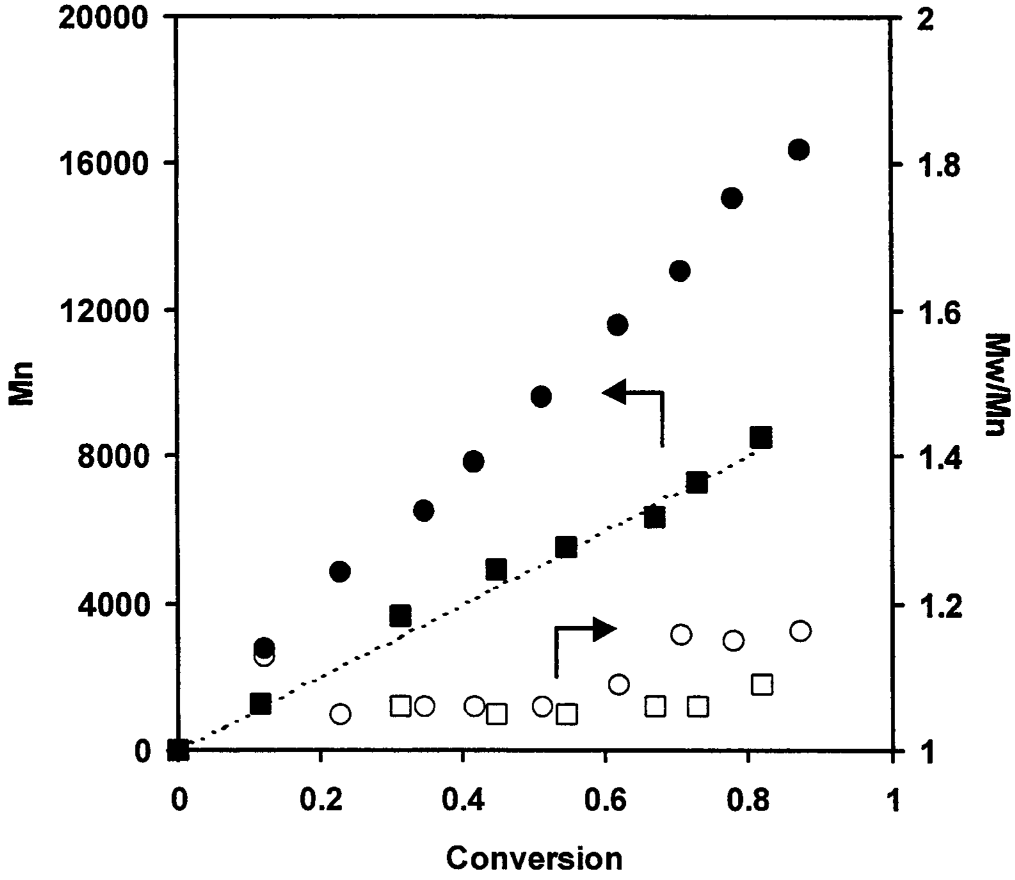

Figure 3.6 PMMA molecular weight and polydispersity as a function of conversion in the MMA polymerization with different CuBr/initiator ratios catalyzed by CuBr-HMTETA/2-silica gel. See Figure 3.5 for experimental conditions.

[CuBr]/[I]= 1:1 (molar) (●, ○), 0.5:1 (■,□).

[CuBr]/[I] = 1. The concentration of propagation species in the [CuBr]/[I]=0.5 system calculated from the slope of $\ln([M]_0/[M])$ *vs* time plot in Figure 3.5 was about 0.69 of that of [CuBr]/[I]=1 system. Figure 3.6 shows PMMA molecular weight and polydispersity vs. MMA conversion at different copper bromide concentrations. Clearly reducing the CuBr level by half produced PMMA with molecular weights close to predicted. The initiator efficiencies approached to 1 and the polydispersities of PMMA were about 1.1. This comparison indicates that lowering the catalyst concentration reduced radical concentration at the early stage and thus minimized the radical side reactions.

3.3.1.3 Effect of Silica Gel/CuBr Ratio

The MMA polymerizations with silica gel to CuBr ratios (w/w) of 2, 5, and 10 are shown in Figure 3.7. All of the polymerizations were in the first order reaction with respect to the monomer. The polymerization rate increased as the silica gel/CuBr ratio increased from 2 to 5, but remained constant when it was further increased to 10. The increase in the polymerization rate at high silica gel levels might be caused by slower deactivation reaction by $CuBr_2$ due to lower $CuBr_2$ concentration on the silica gel surface in the presence of a large amount of silica gel.

Figure 3.8 shows the dependence of molecular weight and polydispersity of PMMA on the MMA conversion with different silica gel levels. The PMMA molecular weights increased linearly with the conversion in all the polymerization runs. With silica gel/CuBr = 2 (w/w), the molecular weights agreed well with the theoretical values, but the molecular weights were higher than predicted at silica gel/CuBr ratios of 5 and 10.

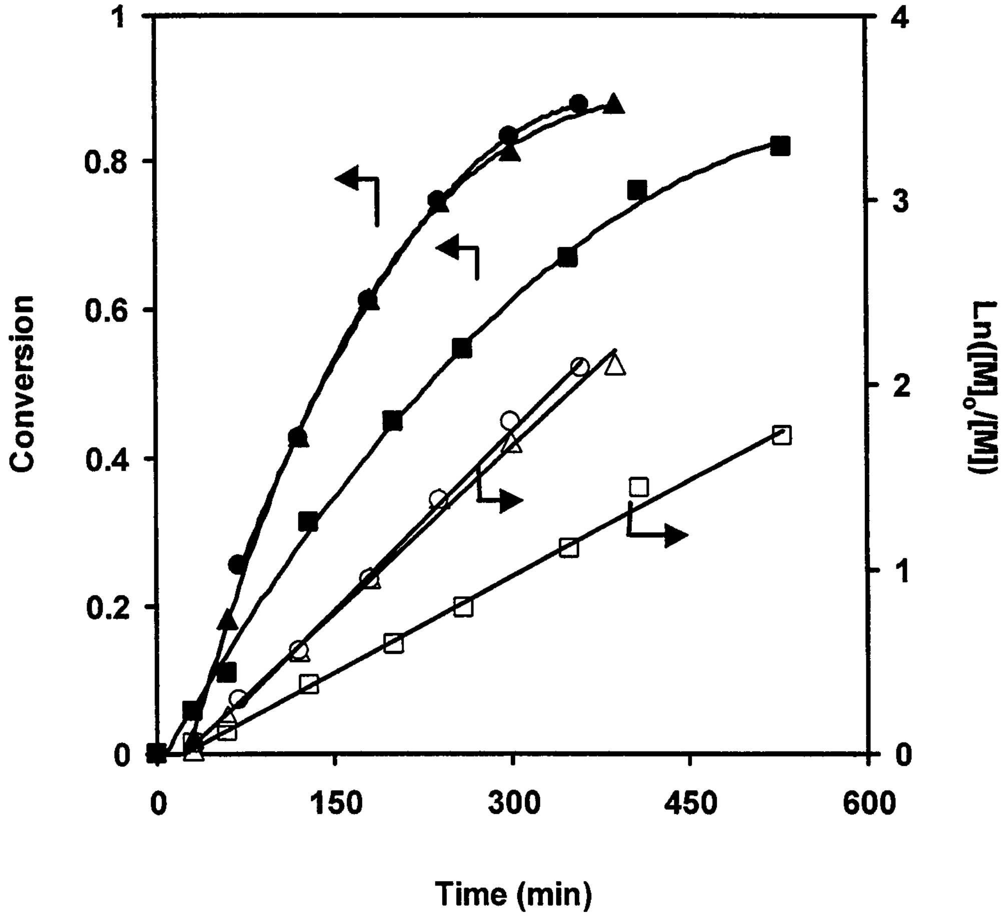

Figure 3.7 MMA polymerizations catalyzed by CuBr-HMTETA with different amounts of silica gel.

90 °C, [MMA]/[HMTETA]/[CuBr]/[Initiator] =100:0.5:0.5:1 (molar); toluene/MMA=2 (w/w); Silica gel/CuBr (w/w)= 2 (■,□); 5 (▲, △); and 10 (●, ○).

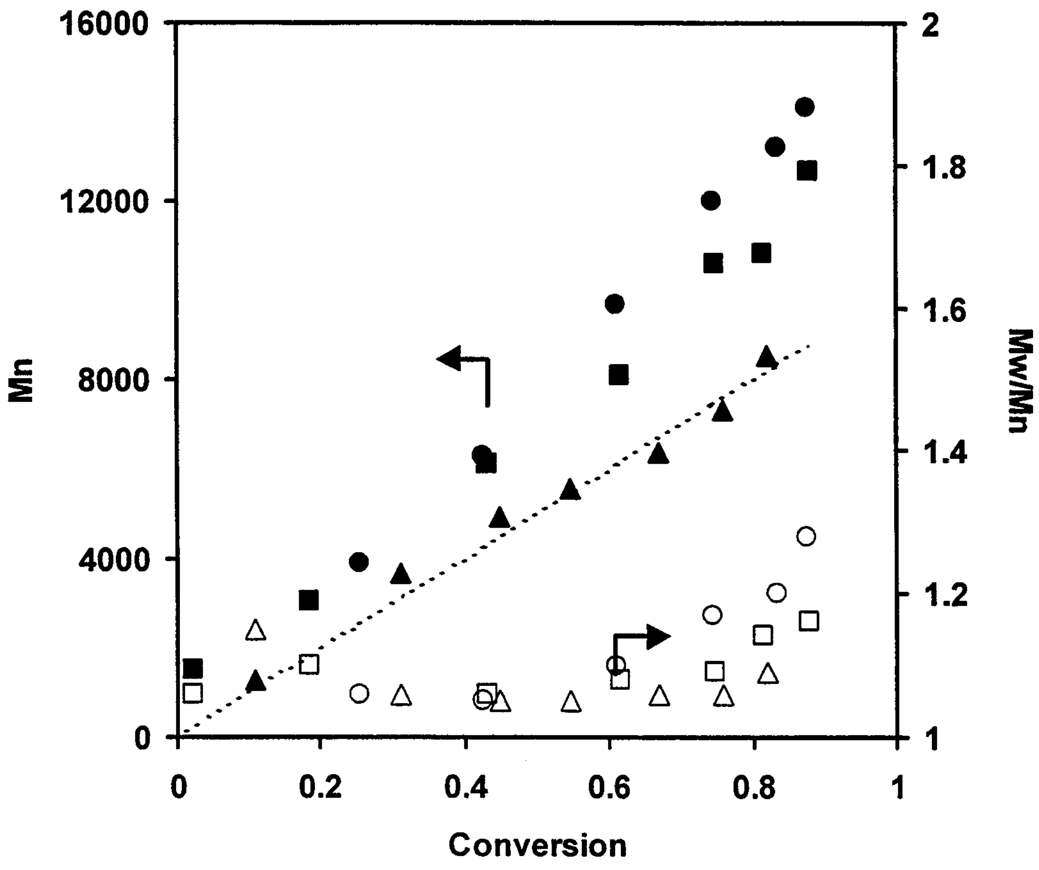

Figure 3.8 PMMA molecular weight and polydispersity as a function of conversion in the MMA polymerization catalyzed by CuBr-HMTETA in the presence of different amount of silica gel. See Figure 3.7 for the experimental conditions.

Silica gel/CuBr (w/w) = 2 (▲, Δ); 5(●, O); 10(■,□).

The polydispersities of PMMA were all lower than 1.15 at the conversions less than 70%. With silica gel/CuBr = 5 and 10 (w/w), the PMMA polydispersities increased at higher conversions, corresponding to the molecular weight increase. This was probably caused by slowed deactivation of the radicals by $CuBr_2$ due to limited diffusion of polymer radicals and silica gel supported catalyst in the viscous media at high MMA conversions.

3.3.1.4 Effect of MMA Concentration

In order to further understand the effect of viscosity on the polymerization, MMA was also polymerized using CuBr-HMTETA/2-silica gel at a high monomer concentration, while the monomer/catalyst molar ratio remained the same. Figure 3.9 shows the MMA polymerizations at two monomer concentrations. Using 33% MMA concentration (toluene/MMA = 2 (w/w)), the polymerization proceeded in a typical first order monomer kinetics throughout the polymerization, but at 50% MMA concentration (toluene/MMA = 1(w/w)), the polymerization followed the first order kinetics only at the early stage of the reaction, but deviated rapidly from the first order kinetics when the conversion was higher than 30%, indicating a rapid increase in the radical concentration based on $\ln([M]_o/[M]) = k_p[R^\bullet]t$ equation. Correspondingly, the PMMA molecular weight quickly deviated from predicted, and the polydispersity increased (Figure 3.10). The viscosity of 50% MMA polymerization media was found very high after about 30% conversion. This observation suggested that viscosity had an adverse effect and low monomer concentrations should be used for ATRP mediated by a supported catalyst system.

3.3.1.5 Catalyst Reuse

After the polymerization was complete, the catalyst was recovered for a second

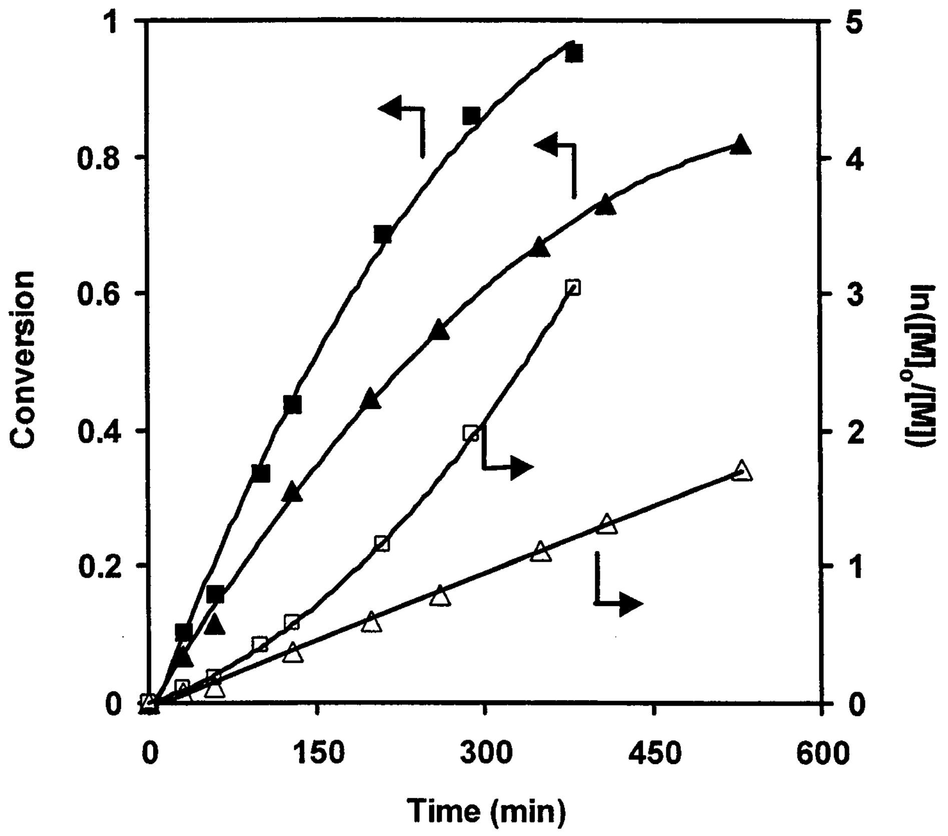

Figure 3.9 MMA polymerizations catalyzed by CuBr-HMTETA/2-silica gel with different monomer concentrations.

90°C, Silica gel/CuBr=2(w/w); [MMA]/[CuBr]/[HMTETA]/[Initiator] =100:0.5:0.5:1; toluene/MMA (w/w) = 1 (■,□); 2 (▲, △).

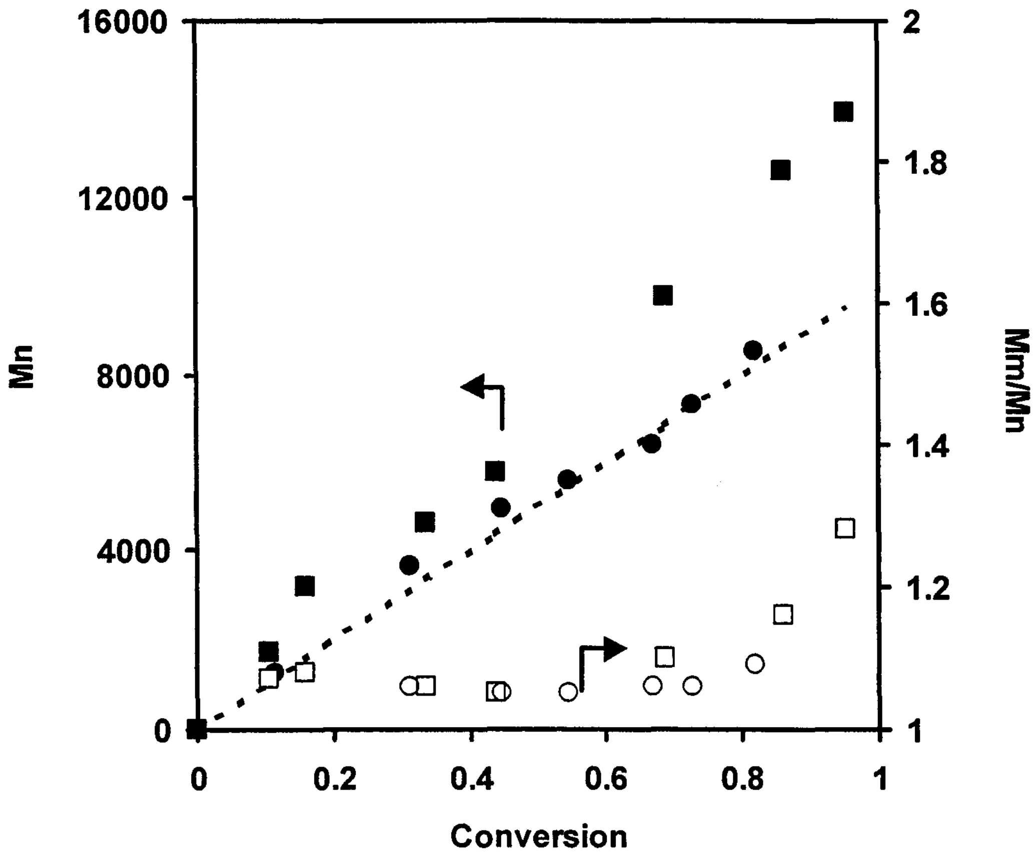

Figure 3.10 PMMA molecular weight and polydispersity as a function of conversion in the MMA polymerization catalyzed by CuBr-HMTETA/2-silica gel with different monomer concentrations. See Figure 3.9 for other experimental conditions.

Toluene/MMA (w/w) = 1 (■,□); 2 (●, O).

use. Figures 3.11, 3.12 and 3.13 show the MMA polymerization with the recycled catalysts. All the MMA polymerizations were still in a first order kinetics with respect to monomer concentration. All of the first recycled catalysts retained about 80% of their initial activities (k^{app} ratios). The reduction in activity was caused by a loss of some supported catalysts during the removal of polymer and by the presence of $CuBr_2$ that was produced in the previous polymerization run to equilibrate with CuBr. (Eq. 3.1). $CuBr_2$ can significantly decrease the polymerization rate even in the presence of small amount by driving the equilibrium (Eq. 3.1) to the dormant state of the polymer chains.[1]

After the second use for MMA polymerization, some CuBr-HMTETA/2-silica gel catalyst stuck on the surface of the flask, and thus it could not be recycled again. While CuBr-HMTETA/5-silica gel and CuBr-HMTETA/10-silica gel catalysts still readily settled down to the bottom for recycling. Therefore these catalysts could be re-used for a third time. Figure 3.13 shows that twice recycled CuBr-HMTETA/10-silica gel catalyst still had about 65% activity of the second used catalyst and 50% of the fresh catalyst.

The Mn of PMMA produced by recycled catalysts also increased linearly with conversion (Figures 3.14 and 3.15). The molecular weights of PMMA obtained from the re-used catalysts were actually much closer to the theoretical values than those by fresh catalysts (Figures 3.14 and 3.15). The polydispersities of PMMA prepared by the reused catalysts remained very low. These results clearly indicated that the recycled catalysts still effectively mediated the polymerizations in a living manner. The improvement in the molecular weight control of the recycled catalysts was benefited from $CuBr_2$, which produced in the first polymerization run to equilibrate with CuBr. It decreased the radical concentration, resulting in a lower polymerization rate but suppressed radical side reactions.

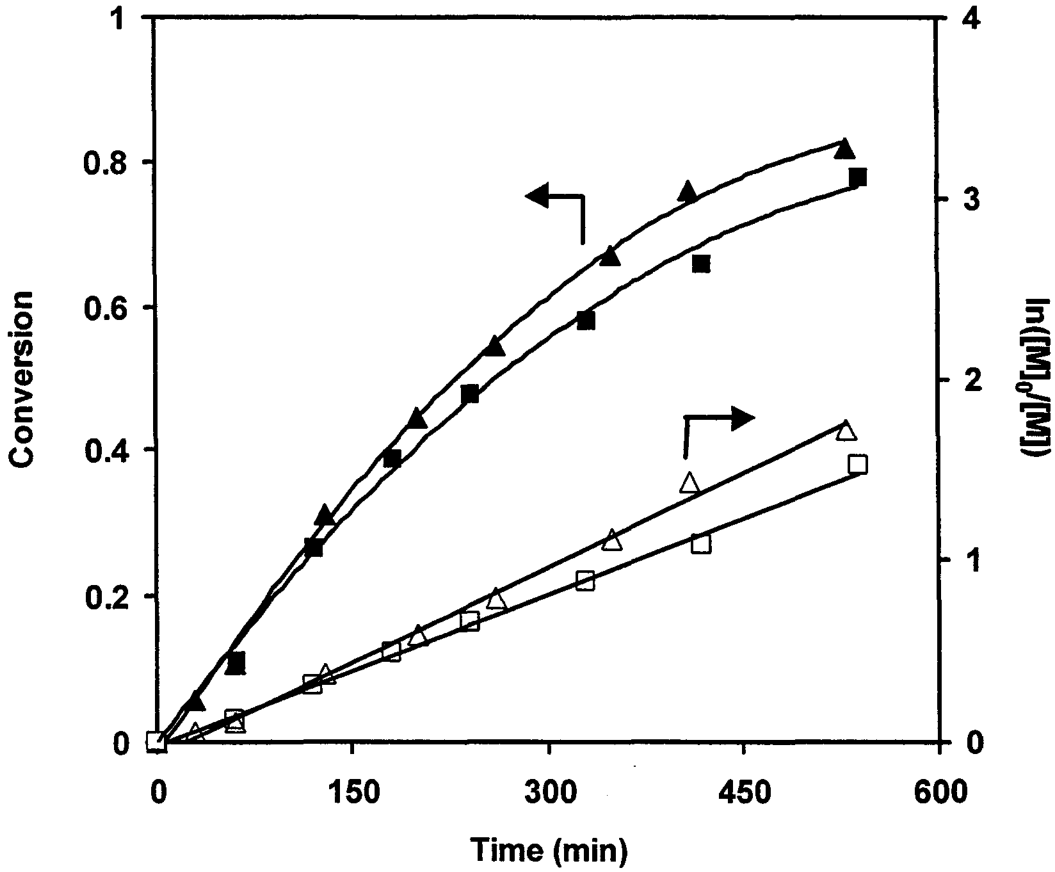

Figure 3.11. Reuse of CuBr-HMTETA/2-silica gel for the MMA polymerization.

90°C, toluene/MMA=2(w/w), silica gel/CuBr = 2(w/w), [MMA]/[CuBr]/[HMTETA]/[Initiator]=100:0.5:0.5:1. First use (▲, △); second use (■,□).

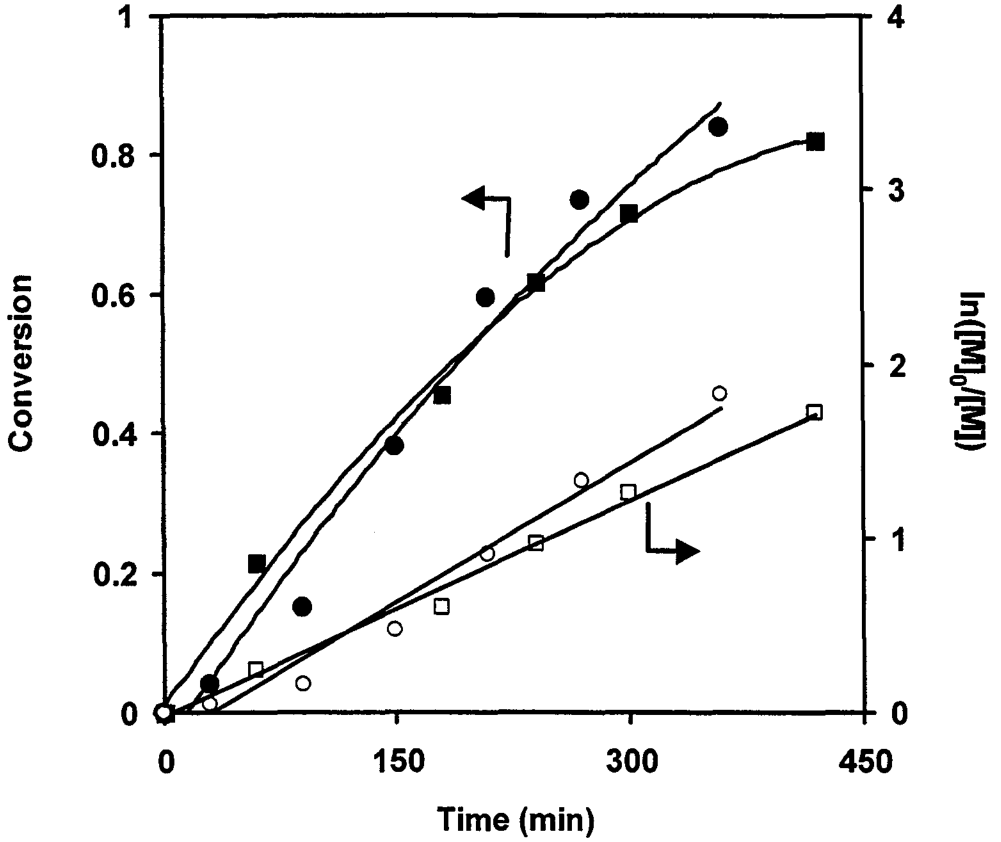

Figure 3.12. Reuse of CuBr-HMTETA/5-silica gel for the MMA polymerization.

90 °C, toluene/MMA=2 (w/w), silica gel/CuBr = 5(w/w), [MMA]/[CuBr]/[HMTETA]/[Initiator] = 100:0.5:0.5:1. First use (●, ○); second use (■,□).

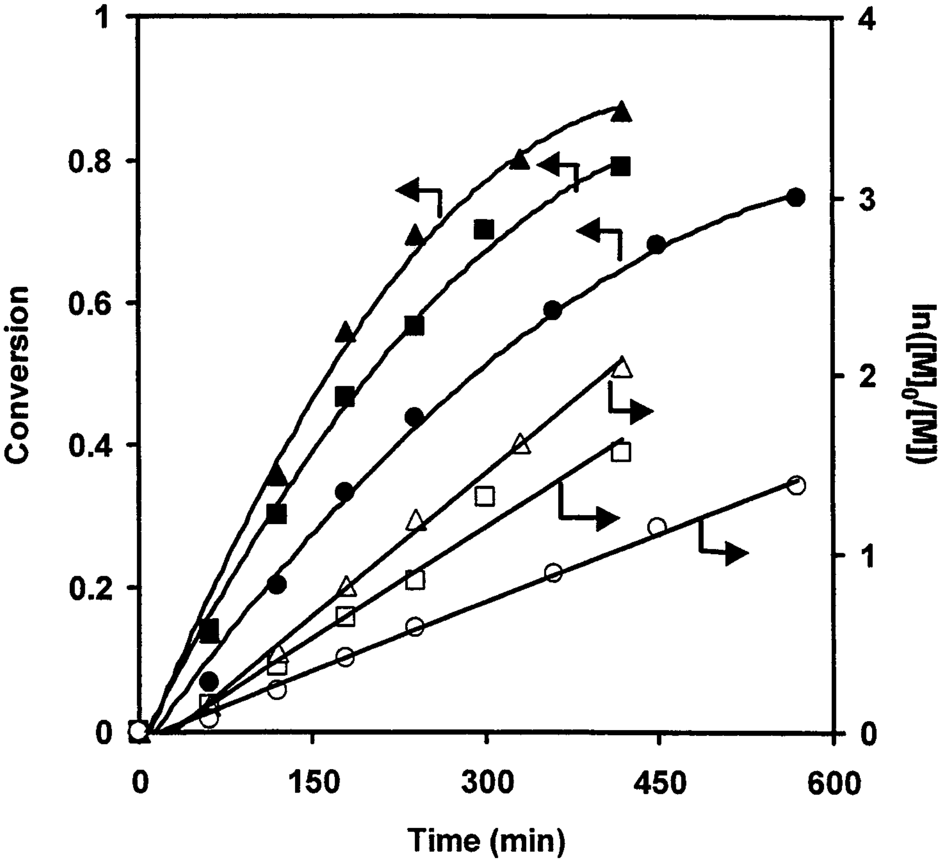

Figure 3.13. Reuse of CuBr-HMTETA/10-silica gel for the MMA polymerization.

90°C, toluene/MMA = 2 (w/w), silica gel/CuBr = 10(w/w), [MMA]/[CuBr]/[HMTETA]/[Initiator] = 100:0.5:0.5:1. First use (▲, Δ); second use (■,□) and third use (●, ○).

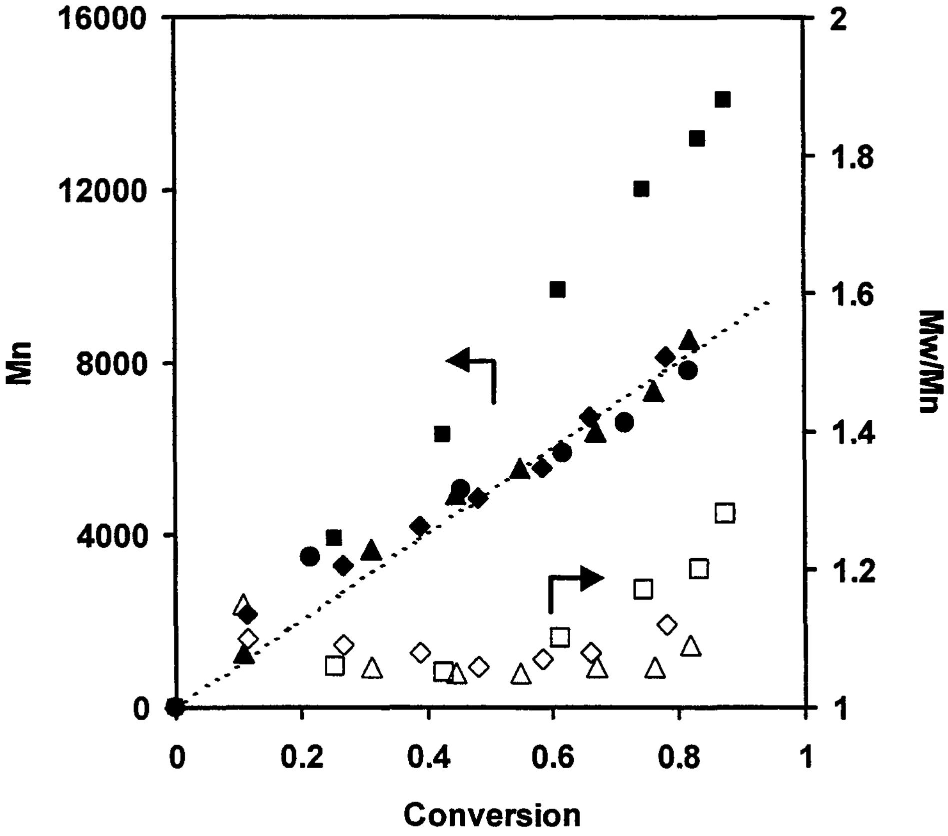

Figure 3.14. PMMA molecular weight and polydispersity as a function of conversion in the MMA polymerization catalyzed by CuBr-HMTETA/2-silica gel and CuBr-HMTETA/5-silica gel.

CuBr-HMTETA/2-silica gel: first use (▲, △), second use (◆, ◇); CuBr-HMTETA/5-silica gel: first use (■,□), second use (●, ○). Same conditions as in Figures 3.11 and 3.12, respectively.

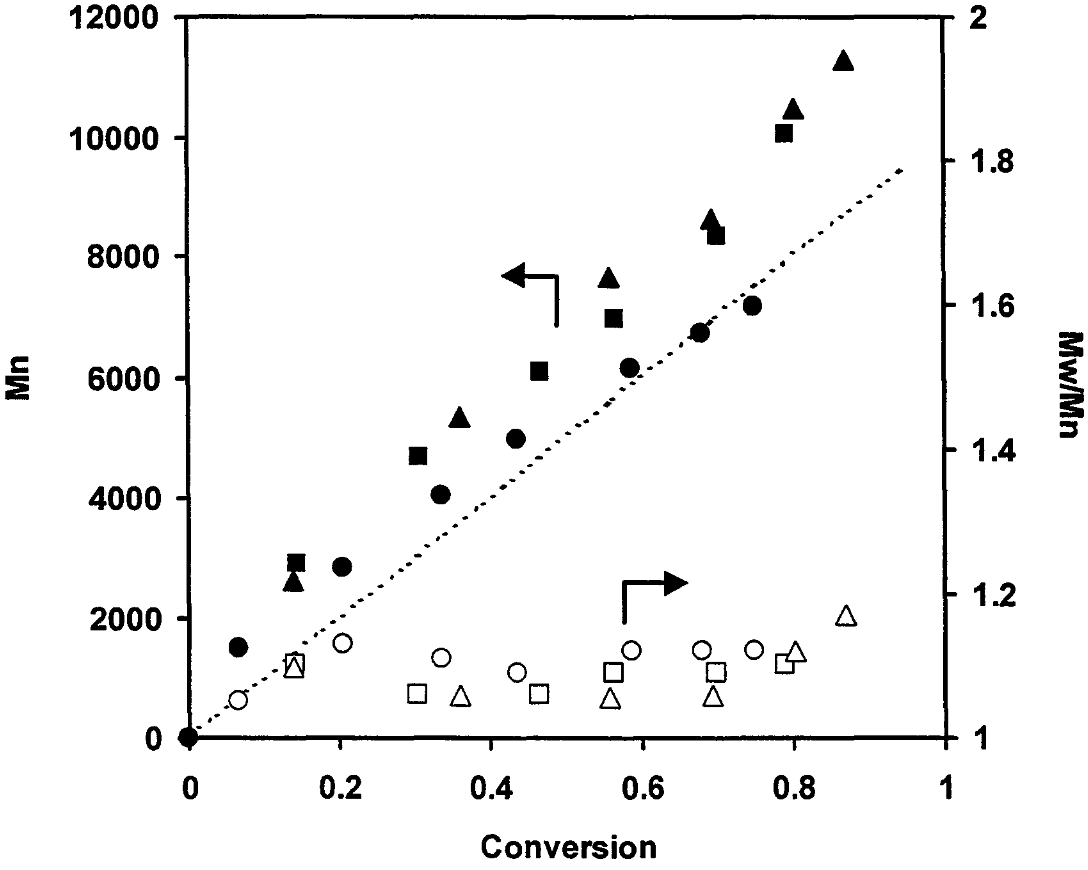

Figure 3.15. PMMA molecular weight and polydispersity as a function of conversion in the MMA polymerization catalyzed by CuBr-HMTETA/10-silica gel. Same conditions as in Figure 3.13.

First use (▲, △), second use (■,□); and third use (●, ○).

3.3.2 Macromonomer Synthesis by Supported Catalyst

3.3.2.1 MMA Polymerization

The synthesis of macromonomers by ATRP of MMA and DMAEMA mediated by the silica gel supported CuBr-HMTETA was assessed by using 2'-vinyloxyethyl 2-bromoisobutyrate (VBIB) or allyl 2-bromoisobutyrate (ABIB) as initiators used in Chapter 2. Figure 3.16 shows the MMA polymerizations using the two initiators at 70 and 90 °C. There was no difference in the polymerization rate with ABIB or VBIB as initiator respectively, which agreed with the fact that the initiating moieties of the two initiators were the same in their molecular structure. At 90 °C, the polymerization with VBIB as initiator proceeded much faster and achieved higher conversion than that at 70 °C. The MMA polymerizations proceeded in a first order kinetics with respect to monomer up to 60 % conversion. After this stage, the polymerization slowed down and deviated from the first order kinetics, suggesting that the radical concentration decreased after this conversion. This observation is very different from the MMA polymerization catalyzed by the same supported catalyst but with methyl α-bromophenylacetate (MBP) as initiator (Section 3.3.1), which was a first order reaction throughout the polymerization. This comparison suggests that the deviation from the first order kinetics

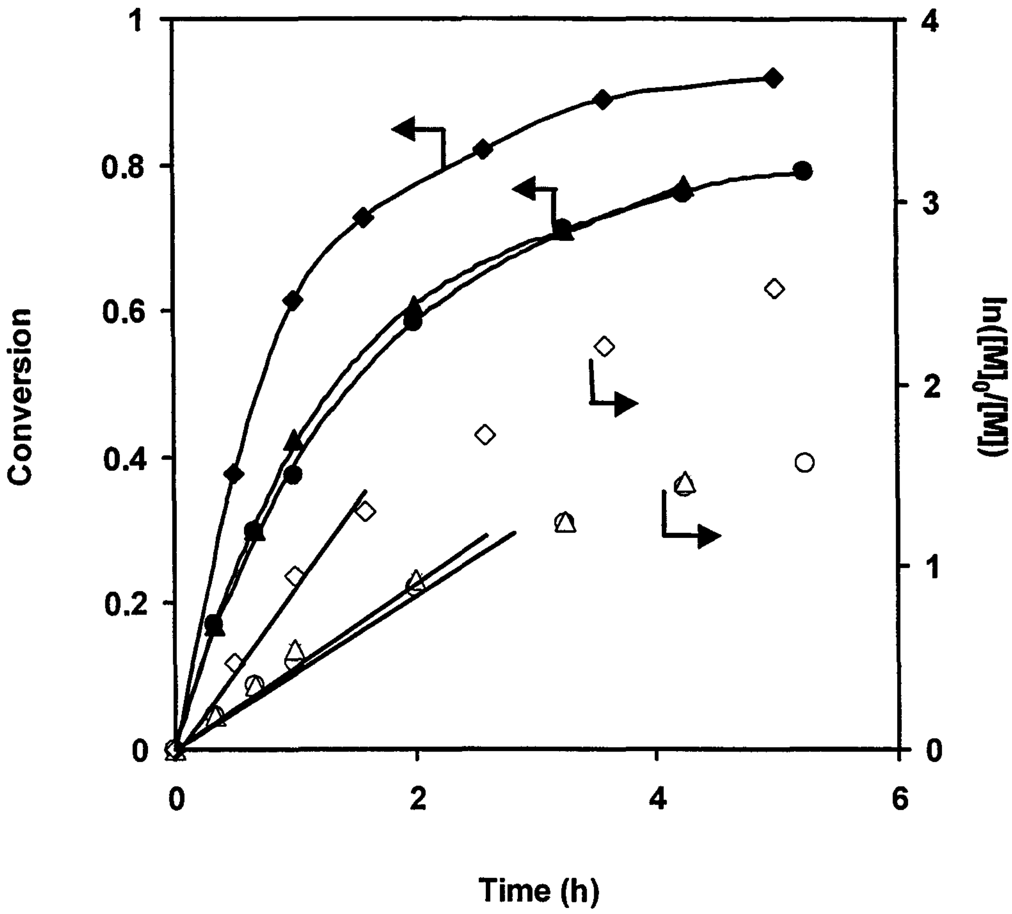

Figure 3.16. The MMA polymerization catalyzed by silica gel supported CuBr-HMTETA.

Toluene/MMA = 3 (w/w); Silica gel/CuBr=2/1(w/w), MMA/CuBr/HMTETA/Initiator = 100/1/1/1; Initiator: VBIB (●, O), 70 °C; VBIB (◆, ◇), 90 °C; ABIB (▲, Δ), 70 °C.

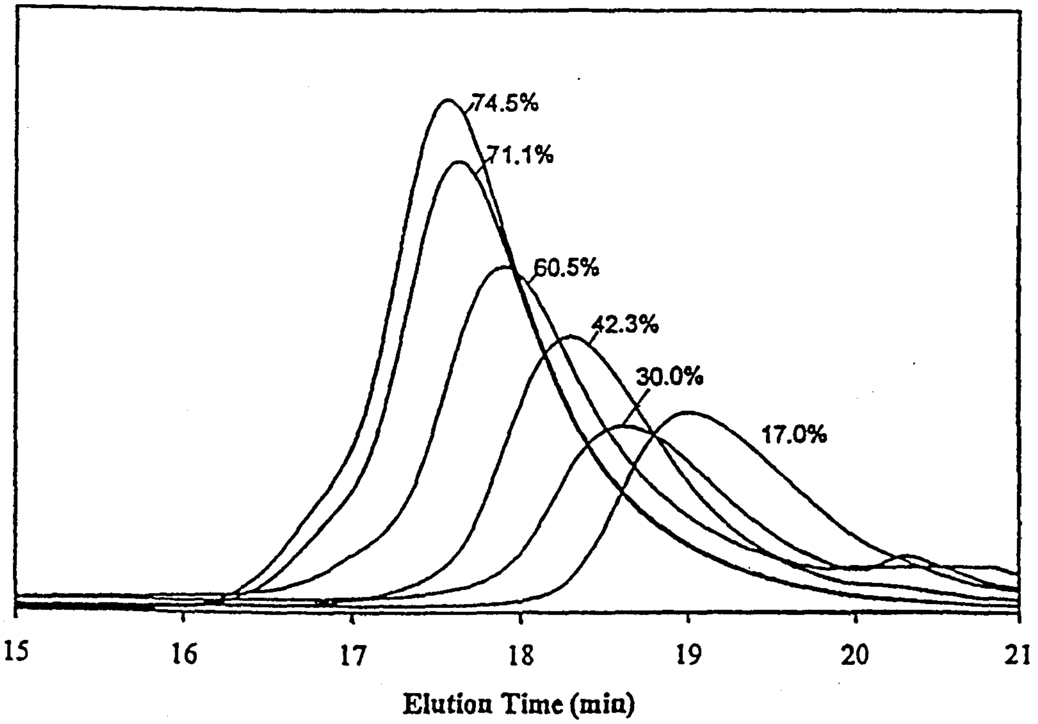

Figure 3.17. GPC traces of PMMA at different conversions polymerized at 70 °C with VBIB as initiator. See Figure 3.16 for the experimental conditions

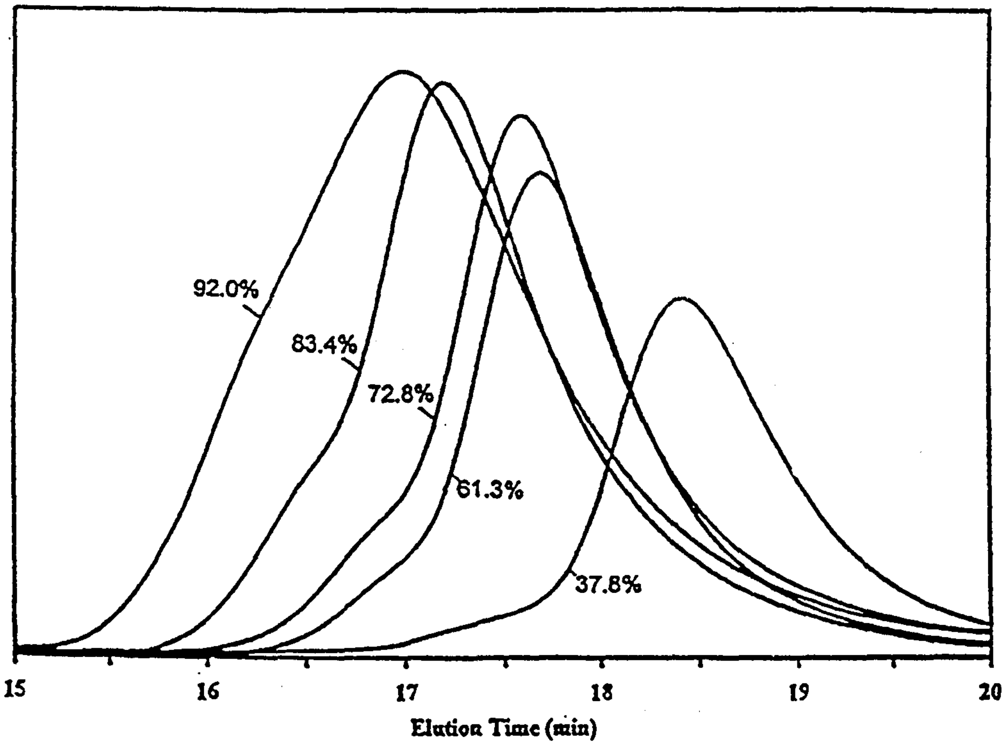

Figure 3.18. GPC traces of PMMA at different conversions polymerized at 90 °C with VBIB as initiator. See Figure 3.16 for the experimental conditions

of MMA polymerizations with the vinyl-containing initiators at high conversions was caused by the initiator type.

The GPC traces of resulting PMMA are shown in Figures 3.17 and 3.18. At the early stage, the GPC traces were typical Gaussian distribution without any shoulder peak. When the conversion reached around 70%, a shoulder peak appeared at the high molecular region. The intensity of the shoulder peak increased with conversion. The shoulder peak was more significant when the polymerization was carried out at 90 °C as shown in Figure 3.18. This phenomenon is very similar to the polymerization of acrylates initiated with VBIB (Section 2.3.3). This population of high molecular weight chains corresponding to the shoulder peak may be produced by reactions of propagating radicals with terminal vinyl moieties (Scheme 3.1), which yielded polymer chains with doubled molecular weights. Because it is very difficult to abstract the bromide atom in the produced C-Br (Section 2.3.3), the radical concentration subsequently decreased.

Figure 3.19 shows the dependence of molecular weight and polydispersity of PMMA on the MMA conversion. Before the conversion reached 60%, the molecular weights of PMMA for polymerization runs increased linearly with conversion and were very close to the theoretical values. The polydispersities at this stage were narrow, lower than 1.2. The molecular weight and polydispersity increased sharply at conversions higher than 70%. This was particularly true for the polymerization at 90 °C. It coincided

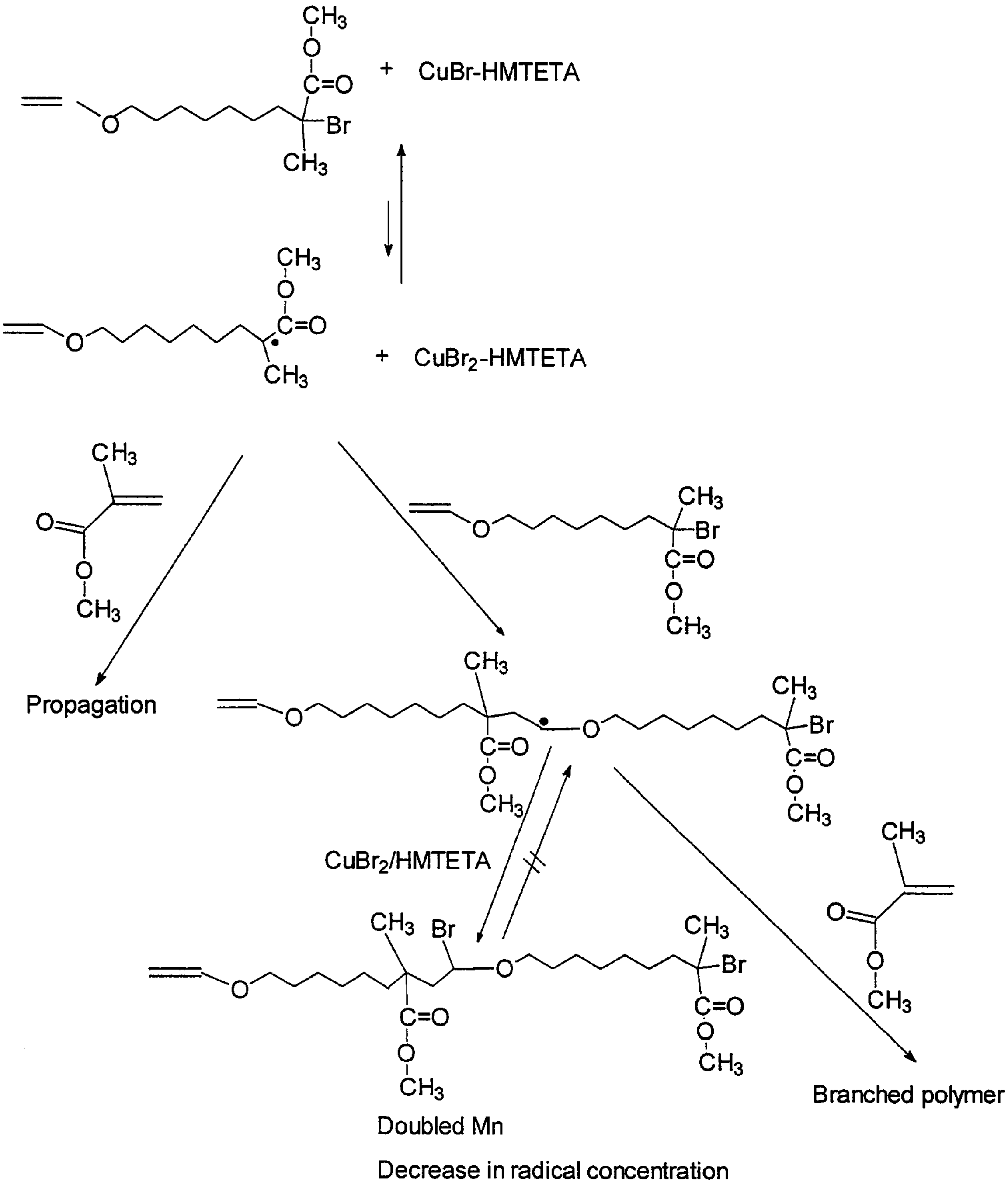

Scheme 3.1. The reaction of radicals with vinyl group of the initiator moiety

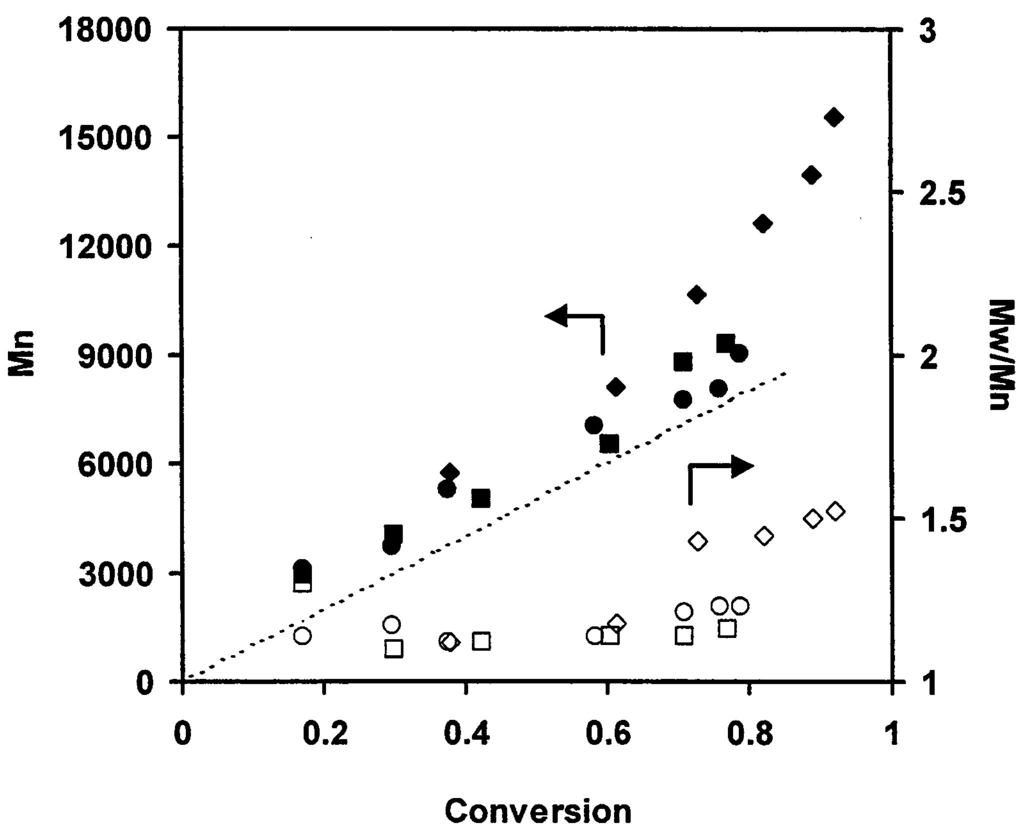

Figure 3.19. The PMMA molecular weight and polydispersity dependence on the MMA conversion. See Figure 3.16 for the experimental conditions.

Initiator: VBIB (●, ○), 70 °C; ABIB (■,□), 70 °C; VBIB (◆, ◇), 90 °C.

with the observation of GPC traces that a shoulder peak appeared and became more significant at higher conversions.

Comparison of this supported ATRP with its homogeneous counterpart with the same catalyst and initiator in Chapter 2 indicates that the supported catalysts mediated the polymerization less effectively. In a homogenous ATRP catalyzed by CuBr-HMTETA with VBIB as initiator, there was no reaction of vinyl moiety with polymer radical even at 80% conversion. However, in the heterogeneous ATRP catalyzed with the same catalyst and initiator, the polymer radical began to react with vinyl moieties even at 60% conversion. This was caused by a slowed deactivation of the radicals, leaving the polymer chain in its radical state for a relatively longer time and thus increasing the chance for the radical to react with vinyl moieties in the polymer ends.

3.3.2.2 DMAEMA Polymerization

The polymerization of DMAEMA with VBIB as initiator is shown in Figure 3.20. Different from the MMA polymerization, the DMAEMA polymerization catalyzed by the supported catalyst proceeded smoothly up to 80 % in a first order kinetics, indicating a constant radical concentration. The GPC traces of the resulting polyDMAEMA gradually moved to the high molecular weight region and only showed sign of shoulder peak at about 80 % conversion. The molecular weights of polyDMAEMA increased with

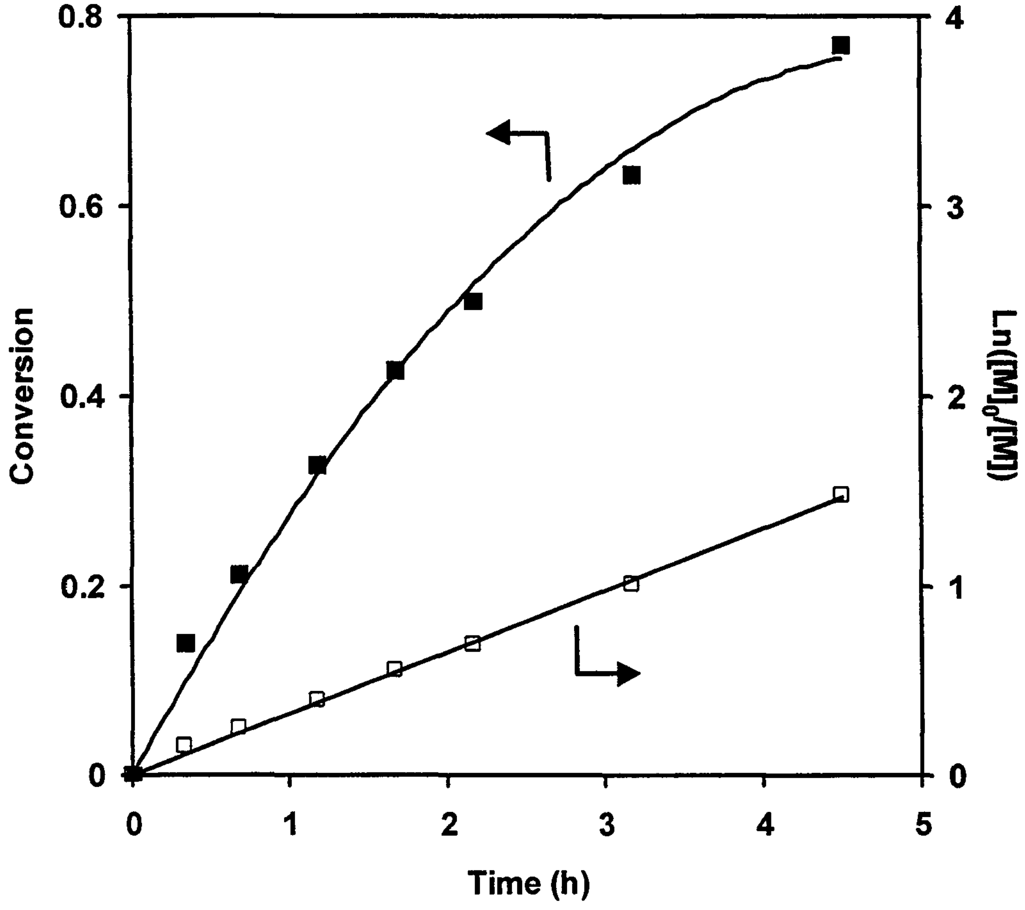

Figure 3.20. The DMAEMA polymerization catalyzed by silica gel supported CuBr-HMTETA.

Toluene/DMAEMA=3 (w/w); Silica gel/CuBr=2:1(w/w),

DMAEMA/CuBr/HMTETA/VBIB = 100/1/1/1, 70 °C.

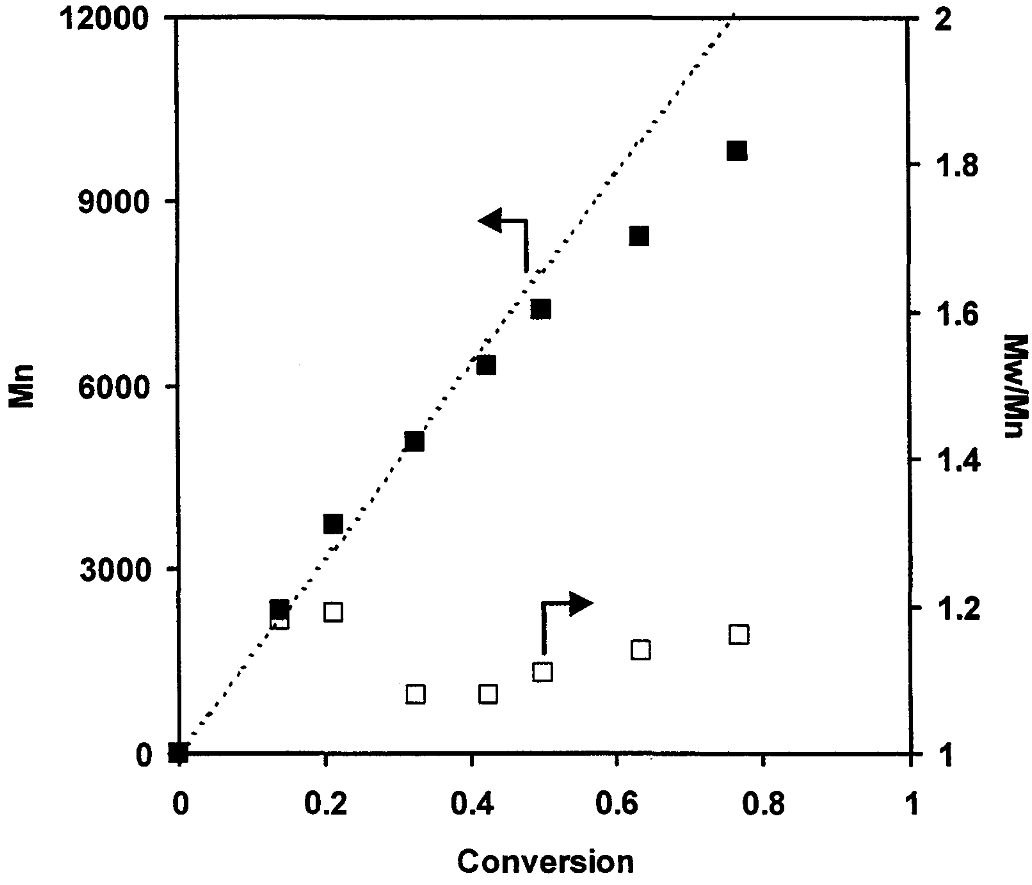

Figure 3.21. The polyDMAEMA molecular weight and polydispersity dependence on the DMAEMA conversion. See Figure 3.20 for the experimental conditions.

DMAEMA conversion and were very close to the theoretical values (Figure 3.21). The deviation of the experimental molecular weights of polyDMAEMA at high conversions may be due to the different hydrodynamic volumes of polystyrene standard in the GPC measurements and polyDMAEMA.

It was observed that the polymerization solution of DMAEMA was slightly green, suggesting that not all the catalyst was adsorbed on the silica gel. DMAEMA has a nitrogen atom that can coordinate with the catalyst like a ligand. Therefore, in the presence of DMAEMA monomer, silica gel could not adsorb all the catalyst from the solution. The improvement of the DMAEMA polymerization compared to the MMA polymerization with the same catalyst system thus derived from the catalyst that was not adsorbed onto the silica gel. The catalyst in solution lowered the radical concentration and thus reduced the chance for radicals to attack terminal vinyl groups of polymer chains.

3.3.2.2 Catalyst Reuse

After the polymerization was complete, the upper layer polymer solution was removed and green silica gel particles were recovered for the second run polymerization. Figure 3.22 shows the MMA polymerization catalyzed by the fresh and reused catalysts. The recycled catalyst retained some activity, about 15% of its original activity (the ratio of in the curve slopes). This is very different from the MMA polymerization with the same catalyst but using MBP as initiator. With MBP as initiator, the recycled CuBr-HMTETA supported on silica gel retained 80% original activity. The significant loss of

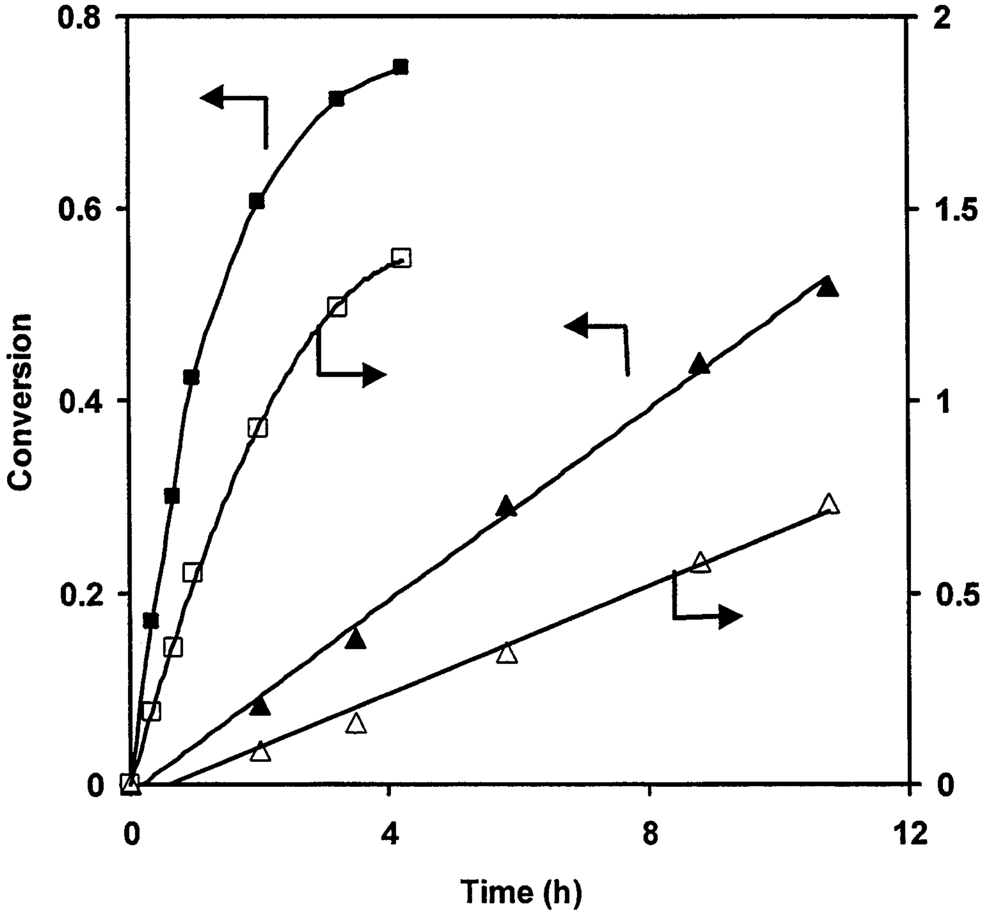

Figure 3.22. Reuse of CuBr-HMTETA/silica gel system for the MMA polymerization.

Toluene/MMA = 3 (w/w); Silica gel/CuBr=2/1(w/w), MMA/CuBr/HMTETA/Initiator = 100/1/1/1; VBIB as initiator, 70 °C. First use (■,□) and second use (▲, △).

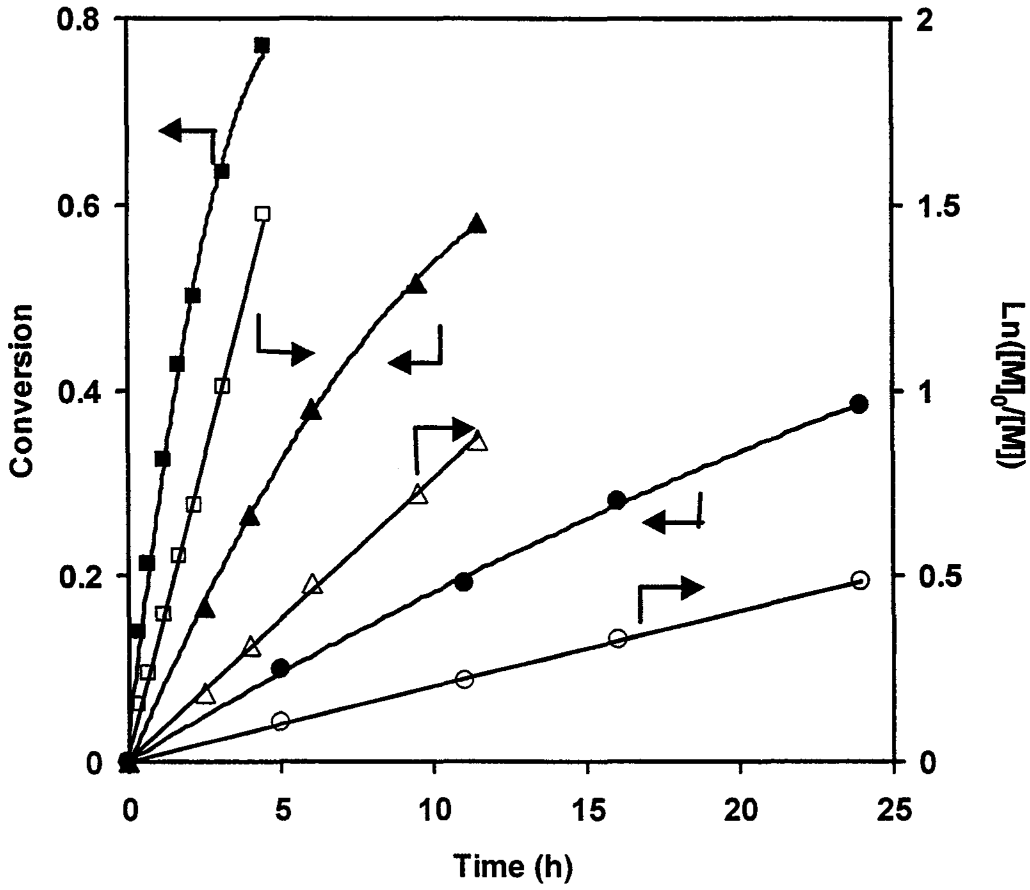

Figure 3.23. Reuse of CuBr-HMTETA/silica gel system for the DMAEMA polymerization.

Toluene/DMAEMA = 3 (w/w); Silica gel/CuBr=2/1(w/w),

MMA/CuBr/HMTETA/Initiator = 100/1/1/1, 70 °C. First use (■,□), second use (▲, Δ) and third use (●, O).

activity of the recycled catalyst with VBIB may be caused by the radical side reactions (Eq. 3.1), which produced extra $CuBr_2$. It was reported that small amount $CuBr_2$ could substantially decrease the polymerization rate by driving back the equilibrium (Eq. 3.1) and thus reducing the radical concentration.[1]

The DMAEMA polymerization catalyzed by the recycled catalyst from the DMAEMA polymerization is shown in Figure 3.23. Similar to the first run polymerization, the second and third runs were also in first order kinetics. However, the activity of the recycled catalyst substantially decreased. Each recycle catalyst retained only 25% of its original activity. This activity loss in the DMAEMA polymerization was caused by the loss of catalyst in recycling. Because only some catalysts were adsorbed on the silica gel in the presence of DMAEMA, the others were removed with the polymer when the solid was recovered from the polymer solution after the each run.

The dependence of molecular weight of PMMA and polyDMAEMA obtained by the recycled catalysts is shown in Figures 3.24 and 3.25 respectively. The molecular weights of PMMA or polyDMAEMA increased with the conversion. The molecular weight distributions of the resulting polymers were around 1.2. The GPC traces showed no shoulder peak in the polymer samples prepared by the recycled catalysts. These results indicate that the recycled catalysts still mediated living polymerization of MMA or DMAEMA, even though the activity of the recycled catalysts was low.

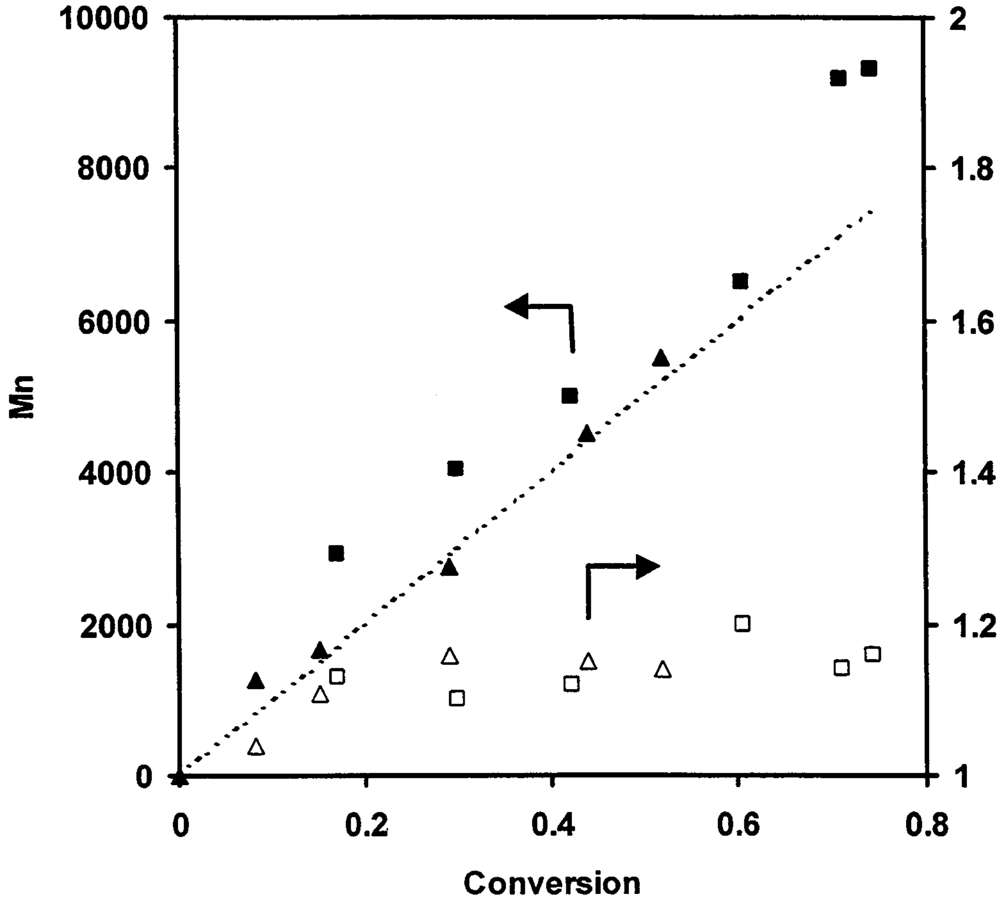

Figure 3.24. The PMMA molecular weight and polydispersity dependence on the MMA conversion catalyzed by fresh and recycled CuBr-HMTETA/silica gel catalysts.

First use (■,□), second use (▲, Δ), theoretical Mn (……). See Figure 3.22 for the experimental conditions.

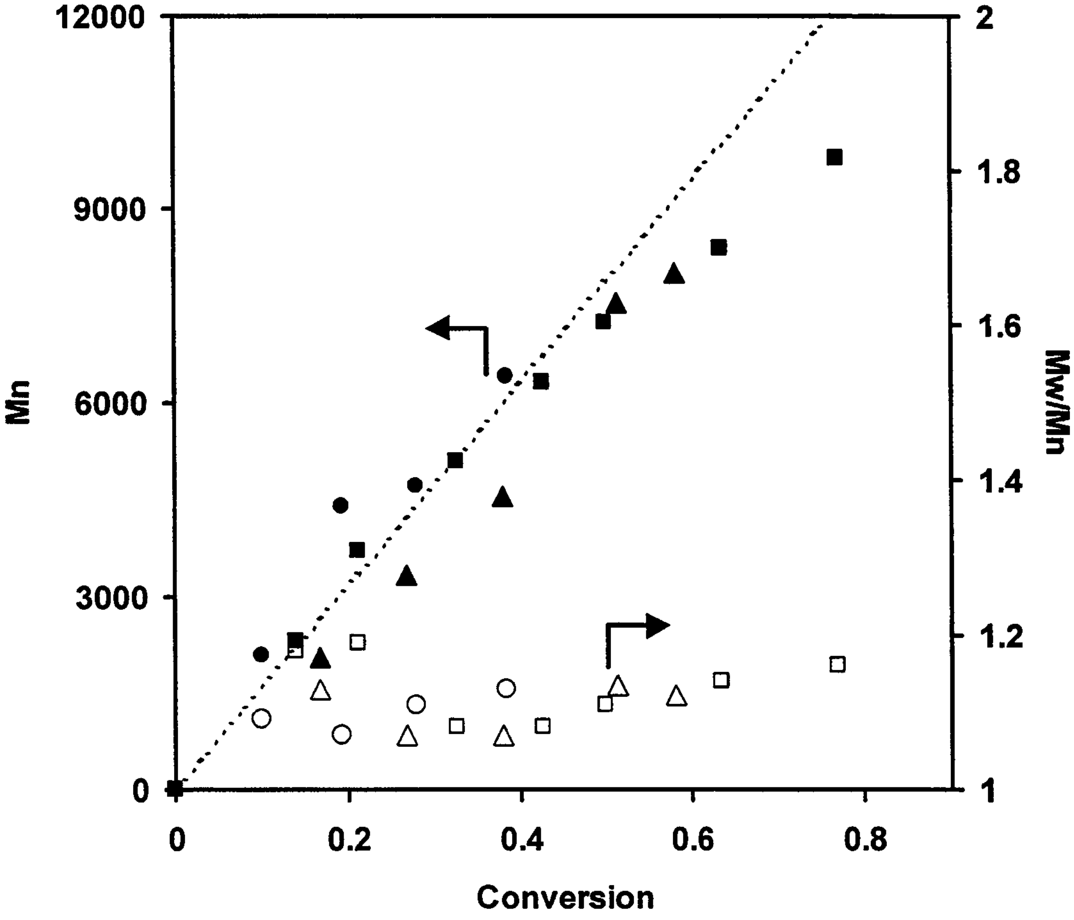

Figure 3.25. The polyDMAEMA molecular weight and polydispersity dependence on the DMAEMA conversion catalyzed by fresh and recycled CuBr-HMTETA/silica gel catalysts. First use (■,□); second use (▲, Δ) and third use (●, O), theoretical Mn (……). See Figure 3.23 for the experimental conditions.

3.3.2.3 Macromonomer Characterization

The PMMA and polyDMAEMA prepared with VBIB and ABIB as initiators were characterized by NMR. Figure 3.26 shows that in addition to the polymer backbone signals assigned in the figures, there were signals ascribed to the terminal groups. For both PMMA and polyDMAEMA prepared with VBIB, there was a same tetrad signal at 6.50~6.30 ppm attributed to the methine proton of the vinyl group ($=C\underline{H}-$). The methylene proton signals of the vinyl group ($C\underline{H_2}=CH-$) were also found at around 4.0 ppm in PMMA polymer, but were overlapped by those of the ester group ($-COOC\underline{H_2}-$) in polyDMAEMA. For PMMA prepared by ABIB as initiator, the signals of allyl group were appeared at 5.8 ppm (m, $CH_2=C\underline{H}-CH_2-$), 5.2 ppm (t, $C\underline{H_2}=CH-CH_2-$) and 4.45 ppm (d, $CH_2=CH-C\underline{H_2}-$). These observations proved that the prepared polymers contained the vinyl or allyl group from the initiator moieties.

The molecular weights of the polymers can also be calculated from the signal intensity ratio of polymer backbone to terminal unsaturated group. When the polymerization was terminated at relatively low conversions, the calculated Mn values by NMR were agreeable to the theoretical. For example, with VBIB as initiator, Mn of PMMA from one hour polymerization (yield, 38.6%) was 4,200 (Figure 4.26, A (1)), close to theoretical value of 3,860 (Mn_{Theor} = MMA/Initiator × 100 × yield). But if the polymerization was pushed to a high monomer conversion, the calculated Mn values from NMR were much higher than the theoretical, which is consistent with the GPC results.

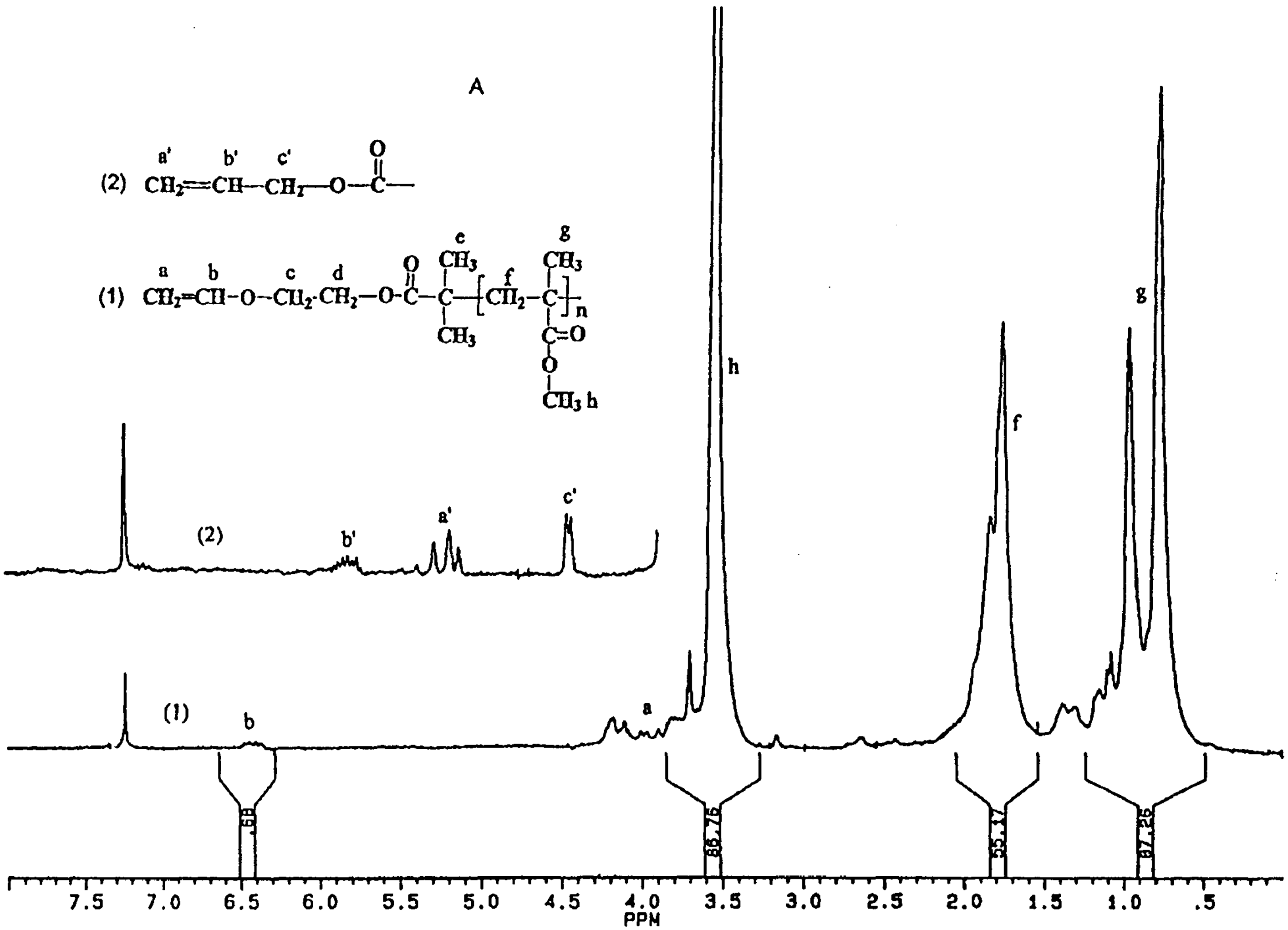
A
(2) CH2=CH—CH2—O—C(=O)—
a' b' c'
(1) CH2=CH-O-CH2-CH2-O-C(=O)-C(CH3)(CH3)-[CH2-C(CH3)(C=O-O-CH3)]n
a b c d e f g h
(2)
b'
a'
c'
(1)
b
a
h
f
g
.58
68.76
55.17
87.26
7.5
7.0
6.5
6.0
5.5
5.0
4.5
4.0
3.5
3.0
2.5
2.0
1.5
1.0
.5
PPM

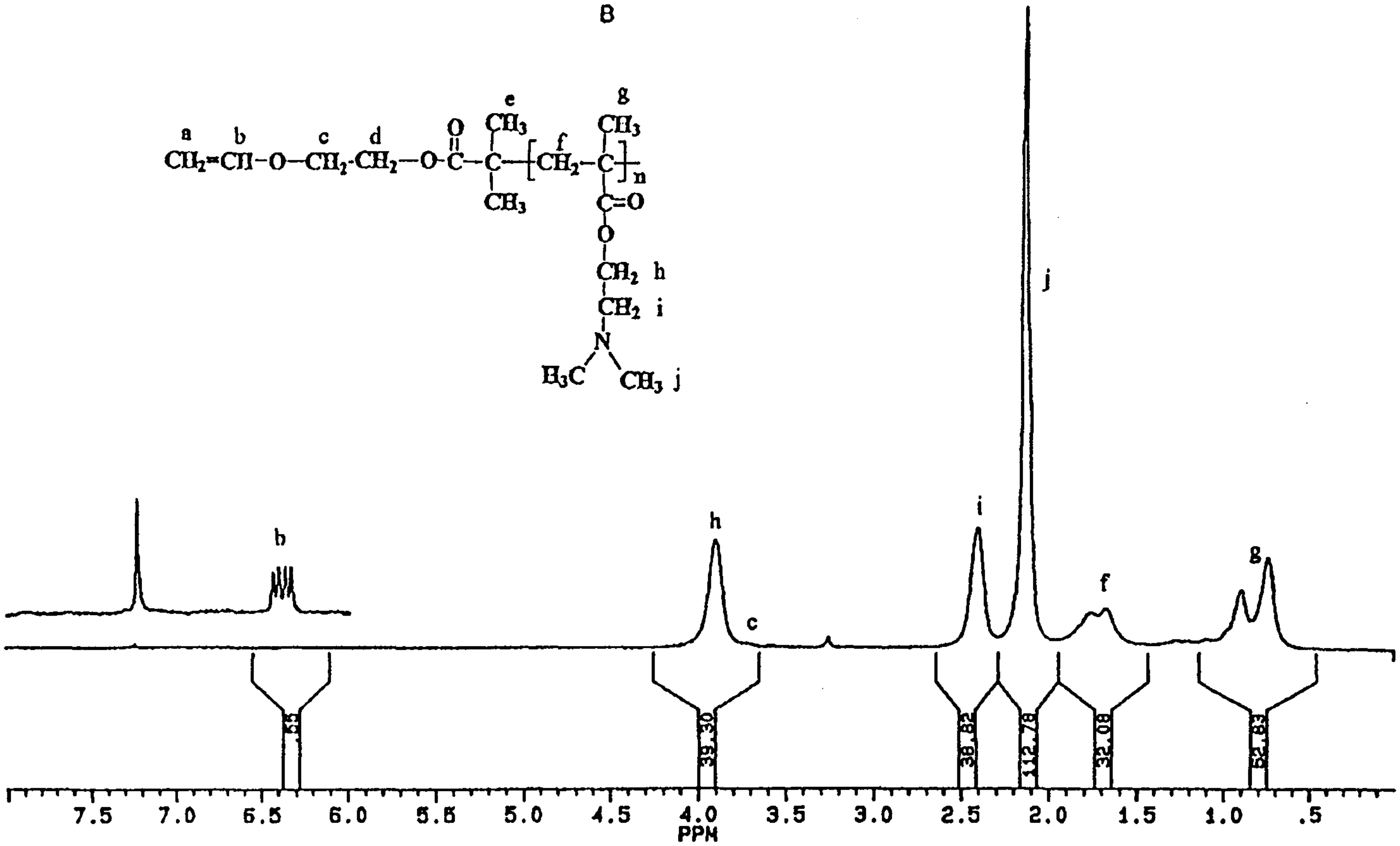
B
a
b
c
d
e
f
g
h
i
j
n
CH2=CH–O–CH2-CH2–O-C(=O)–C(CH3)2–[CH2–C(CH3)(C=O)]n
O
CH2 h
CH2 i
N
H3C
CH3 j
b
h
c
i
j
f
g
.55
39.30
38.82
112.78
32.08
52.83
7.5
7.0
6.5
6.0
5.5
5.0
4.5
4.0
3.5
3.0
2.5
2.0
1.5
1.0
.5
PPM

Figure 3.26. The ^{1}H-NMR spectra of PMMA and polyDMAEMA.

(A): PMMA: (1) VBIB and (2) ABIB as initiator, 70 °C, 60min; See Figure 3.16 for the experimental conditions.
(B) polyDMAEMA: VBIB as initiator, 70 °C, 70 min, See Figure 3.17 for the experimental conditions.

3.4 Conclusion

This chapter presents a simple but very efficient method to prepare supported catalyst for ATRP of MMA. CuBr-HMTETA adsorbed on silica gel was an efficient catalyst for ATRP of MMA, yielding polymers with well-controlled molecular weight and very low polydispersity. The supported catalyst was recycled for subsequent MMA polymerizations. It retained 80% activity in the second use and 50% activity in the third use. The recycled catalysts had improved control over the molecular weight of PMMA. The molecular weights of PMMA prepared by the recycled catalysts were closer to the theoretical values with narrower polydispersities.

Silica gel supported CuBr-HMTETA can also be used to the ATRP of MMA and DMAEMA for the synthesis of PMMA and polyDMAEMA macromonomers using allyl-(ABIB) and vinyl (VBIB)-containing initiators. In the MMA polymerization, the vinyl or allyl group survived when the conversion was less than 60 %. The recycled catalysts still showed catalytic activity and mediated a living polymerization of MMA or DMAEMA, but the activities of the recycled catalysts were relatively low because of the radical side reaction and catalyst loss.

3.5 Reference:

1. Matyjaszewski, K. Ed. *Controlled Radical Polymerization;* American Chemical Society: Washington, DC **1997**; ACS Symp. Ser. Vol. 685.
2. Wang, J.; Matyjaszewski, K. *J. Am. Chem. Soc.* **1995**, *117*, 5614.
3. Kato, M; Kamigaito, M.; Sawamoto, M.; Higashimura, T. *Macromolecules* **1995**, *28*, 1721.
4. Percec, V.; Barboiu, B; Neumann, A.; Ronda, J.C.; Zhao, M. *Macromolecules* **1995**, *29*, 3665.
5. Ando, T.; Kato, M; Kamigaito, M.; Sawamoto, M. *Macromolecules* **1996**, *4*, 371.
6. Haddleton, D. M.; Jasieczek, C. B.; Hannon, M. J.; Shooter, A. J. *Macromolecules* **1997**, *30*, 2190.
7. Percec, V.; Kim, H.-J.; Barboiu, B. *Macromolecules* **1997**, *30*, 8526.
8. Percec, V.; Barboiu, B.; Kim, H.-J. *J. Am. Chem. Soc.* **1998**, *120*, 305.
9. Sawamoto, M. and Kamigaito, M. *J. Macro. Sci-Pure Appl. Chem* **1997**, *A34(10),* 1803.
10. Matyjaszewski, K.; Wei, M.; Xia, J.; McDermott, N. E. *Macromolecules* **1997**, *30*, 8161.
11. Granel, C.; Teyssie, Ph.; Dubois, Ph.; Jerome, Ph. *Macromolecules* **1996**, *29*, 8576.
12. Uegaki, H.; Kotani, Y.; Kamigaito, M.; Sawamoto, M. *Macromolecules* **1998**, *31*, 6756.
13. Uegaki, H.; Kamigaito, M.; Sawamoto, M. *J. Polym. Sci., Part A: Polym. Chem.* **1999**, *37*, 3003.

14. Moineau, G.; Granel, C.; Dubois, Ph.; Jerome, R. and Teyssie, Ph. *Macromolecules* **1998**, *31*, 542.

15. Wang, X. S.; Jackson, R. A. and Armes, S. P. *Macromolecules* **2000**, *33*, 255.

16. Wang, X. S.; Lascelles, S. F.; Jackson, R. A., Armes, S. P. *Chem. Commun.* **1999,** 1817; Ashford, E.J.; Naldi, V.; O'Dell, R.; Billingham, N.C.; Armes, S.P. *Chem. Commun.* **1999**, 1285.

17. Nakagawa, Y. and Matyjaszewski, K. *Polym. J.* **1998**, *30*, 138.

18. Zeng, F.; Shen, Y.; Zhu, S. and Pelton, R. *Macromolecules*, **2000**; *33,* 1628.

19. Matyjaszewski, K.; Beers, K. L.; Kern, A.; Gaynor, S. G. *J. Polym. Sci.: Part A: Polym. Chem.***1998**, *36*, 823.

20. Shen, Y.; Zeng, F.; Zhu, S. and Pelton, R. H. *Macromolecules* **2000**, *33*, 5399..

21. Haddleton, D. M.; Waterson, C.; Derrick, P. J.; Jasieczek, C. B. and Shooter, A. J. *Chem. Commun.* **1997**, 683.

22. Coessens, V.; Matyjaszewski, K. *Macromol. Rapid Commun.* **1999**, *20*, 127.

23. Malz, H.; Komber, H.; Voigt, D.; Hopfe, I.; Pionteck, J. *Macromol. Chem. Phys.* **1999**, *200*, 642.

24. Matyjaszewski, K.; Pintauer, T.; Gaynor, S. *Macromolecules* **2000,** *33,* 1476.

25. Haddleton, D. M.; Duncalf, D. J.; Kukulj, D. and Radigue, A. P. *Macromolecules,* **1999**, *32*, 4769.

26. Haddleton, D. M.; Kukulj, D. and Radigue, A. P. *Chem. Commun* **1999**, 99.

27. Kickelbick, G.; Paik, H. and Matyjaszewski, K. *Macromolecules* **1999,** *32*, 2941.

Chapter 4

Supported Atom Transfer Radical Polymerization Mediated by CuBr-Grafted on Silica Gel Surface

4.1 Introduction to Catalyst Immobilization by Grafting

Chapter 3 has demonstrated that CuBr/HMTETA supported on silica gel by adsorption effectively mediated the MMA polymerization, allowed us to reuse the catalyst, and gave products with reduced concentration of catalyst residue. However, the catalyst has no covalent bond to silica gel particle. In a high polar solvent or in the presence of high polar monomer such as DMAEMA, only a part of the catalyst can be adsorbed onto particles. This caused significant catalyst loss during recycling and the polymer products were not free of catalyst residue.

Catalysts immobilized onto particles by covalent bonds have been widely used in small molecular reactions.[1-3] The same concept has been attempted for ATRP but was not very successful. Haddleton et al.[4] supported copper halide via alkylpyridylmethanimine onto silica gel/crosslinked polystyrene particles. This supported catalyst was used to polymerize methyl methacrylate with ethyl-2-bromoisobutyrate as the initiator, but could not control the molecular weight satisfactorily. Matyjaszewski et al.[5] immobilized CuBr onto multidentate amine-functionalized silica gel and cross-linked polystyrene particles for the polymerizations of styrene, methyl acrylates and methacrylates, but did not obtain a living polymerization. The molecular weights of the resulting polymers were significantly higher than predicted, and the polydispersities were over 1.5.

In this chapter, we grafted multidentate amine (N,N,N',N'-tetraethyl diethylenetriamine (TEDETA), di(2-picolyl)amine (DiPA)) onto silica gel to immobilize copper bromide to mediate ATRP of various monomers. In contrast to the non-living process mediated by CuBr on diethylentriamine-functionalized silica gel,[5] the MMA polymerization by CuBr on TEDETA-functionalized-silica gel demonstrated a feature of living polymerization, yielding PMMA with controlled molecular weight and narrow molecular weight distribution. Further study shows that the supporting spacer, through which the catalyst was immobilized onto the silica gel surface, had a very strong influence on the catalyst activity and the control of polymerization. Too short or too long spacer would deteriorate catalytic activity and control of the polymerization.

4.2 Atom Transfer Radical Polymerization of Methyl Methacrylate Mediated by CuBr-TEDETA Grafted on Silica Gel

4.2.1 Experimental Section

4.2.1.1 Materials

Methyl methacrylate (MMA) from Aldrich was distilled under vacuum and stored at –15 °C. N,N,N',N'-tetraethyldiethylenetriamine (TEDETA, 90%), CuBr, methyl α-bromophenylacetate (MBP, 99%), 3-(trimethoxylsilyl)propyl acrylate (92%) and phenyl ether also from Aldrich were used as received. Silica gel with 230-400 mesh and an average pore diameter of 60 angstroms was supplied by SiliCycle Inc.

4.2.1.2 Grafting Tetraethyldiethylenetriamine onto Silica Gel

TEDETA was grafted onto silica gel as shown in Scheme 4.1. TEDETA was first coupled with trimethoxysilylpropyl acrylate to synthesize N,N,N'N'-tetraethyl-N"-[3-(trimethoxysilylpropoxycarbonyl)ethyl]-diethylenetriamine (1). 3-(Trimethoxysilyl propyl) acrylate (20 g) was charged to a flask and cooled to 0 °C. TEDETA (22.6 g) was added dropwise to the flask with stirring for 10 h. The mixture was further stirred at room temperature until no vinyl signal of the acrylate was detected by NMR. The liquid was then subject to high vacuum to remove possible volatile species. A viscous liquid was finally obtained. IR: 2970 cm^{-1}, 2808 cm^{-1}, 1738 cm^{-1} (C=O), 1202 cm^{-1}, 1109 cm^{-1}; ^{1}H-NMR: 3.80 ppm (t, 2H, $COOCH_2$), 3.35 ppm (s, 9H, $SiOCH_3$), 2.60 ppm (t, 2H, CH_2COO), 2.30 ppm (m, 18H, NCH_2), 1.50 ppm (m, 2H, $SiCH_2CH_2$), 0.80 ppm (t, 12H, NCH_2CH_3). ^{13}C-NMR: 172.3ppm (C=O), 66.0 ppm ($COOCH_2$), 51.0 ppm (Si-OCH_3), 47.4 ppm (NCH_2), 32.3 ppm (CH_2C=O), 21.8 ppm ($CH_2CH_2CH_2$), 11.54 ppm (CH_3), 6.43 ppm ($SiCH_2$).

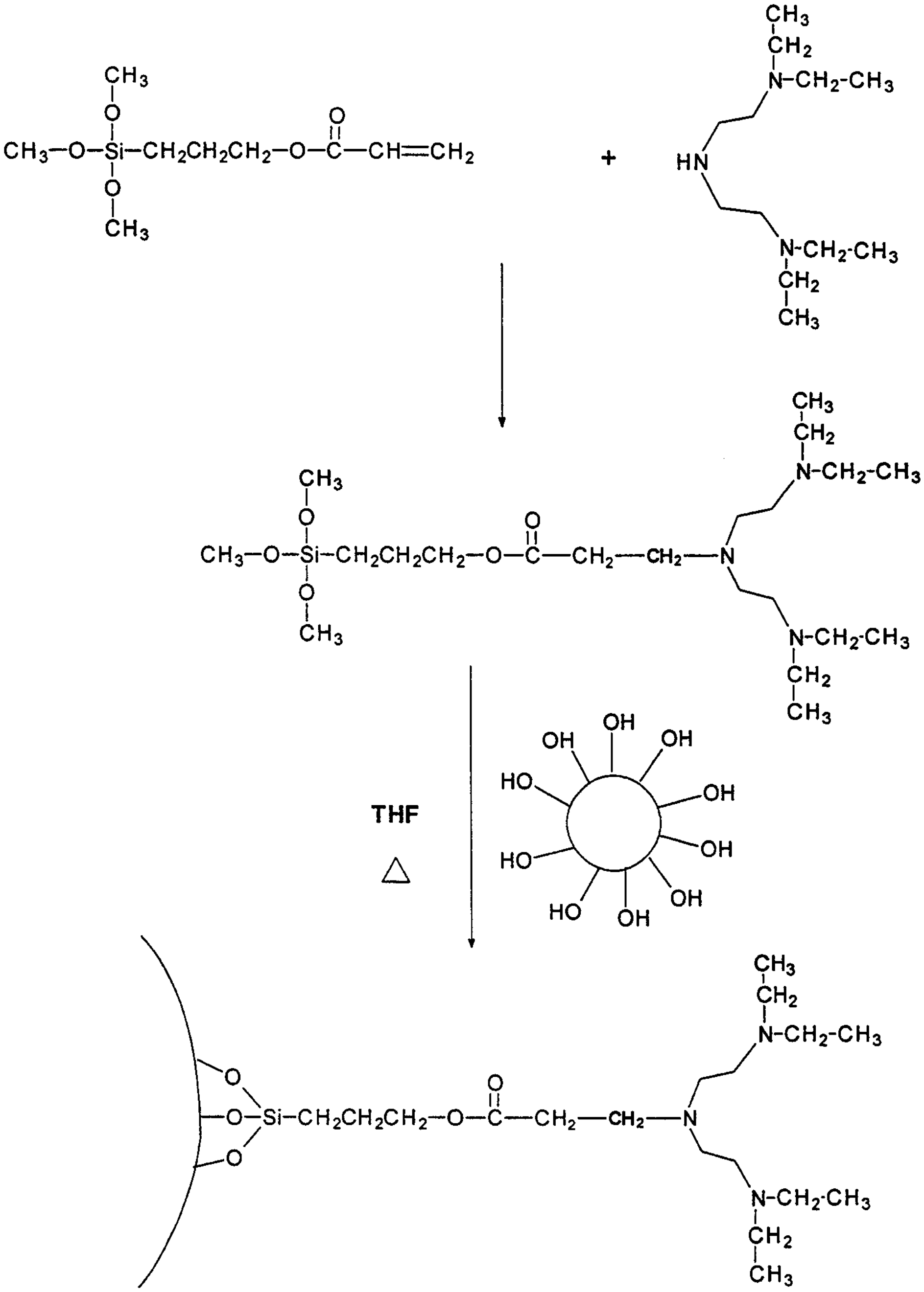

Scheme 4.1. Grafting TEDETA onto silica gel surface

The attachment of TEDETA ligand onto silica gel surface was via a reaction of silicon alkoxide with silanol group on the particle surface. Hydrophilic silica gel was dried in vacuum at 100 °C for 3 days. Dried silica gel (10 g), synthesized product (1) (5 g) and THF (50 mL) were charged to a flask. The mixture was refluxed for 48 h. Silica gel was separated from the solution by centrifugation and washed 6 times with THF. The silica gel was finally dried at 50 °C under vacuum for 24h. IR: 3440 cm^{-1} (Si-OH); 2959 cm^{-1}, 2923 cm^{-1}, 2877 cm^{-1}, 2841 cm^{-1}, 1736 cm^{-1} (C=O), 1457 cm^{-1}, 1377 cm^{-1}, 1109 cm^{-1} (Si-O-Si). The amount of ligand grafted onto silica gel was determined by thermogravimetric analysis (TGA) and elemental analysis. The calculated values from the two methods agreed very well. TEDETA concentration was 14.87%(w/w).

4.2.1.3 Polymerization

A typical polymerization process was as follows: CuBr (13.3 mg) and silica (133 mg) gel and phenyl ether (4g) were added to a Schlenk flask and was degassed by 5 vacuum-nitrogen cycles. Degassed monomer (1.84 g) was added to the flask with nitrogen-purged syringe and the mixture was bubbled with nitrogen for 1 min. The mixture was stirred at room temperature for 60 min. Degassed initiator (MBP) (9.7 μL) was then introduced dropwise to the flask with stirring. The flask was subsequently heated to 80 °C in an oil bath. At different time intervals, solution/catalyst mixture (0.05 mL) was withdrawn with nitrogen-purged syringe. The solution was diluted with $CDCl_3$. The conversion was measured with ^{1}H-NMR by calculating the intensity ratio of $OC\underline{H}_3$ signals in polymer (3.60 ppm) and in monomer (3.75 ppm). 50 μL of this solution was injected to gel permeation chromatography (GPC) to measure the molecular weight and polydispersity of the polymer.

4.2.1.4 Catalyst Reuse

When the polymerization was complete, the flask was lifted from the oil bath and centrifuged. The supernatant was carefully removed from cannula with nitrogen. The remaining solid in the flask was washed twice with 20 mL (total) degassed phenyl ether under nitrogen. The same amounts of degassed MMA, phenyl ether, and initiator, as in the first run, were added to the flask and reheated to 80 °C. The same procedure as that for the first run was repeated.

4.2.1.5 Catalyst Regeneration

After the polymerization was complete, the catalyst was recovered as described above. Phenyl ether and copper turnings (not powder) were charged to the flask under nitrogen. The mixture was stirred for 24 h at 35 °C. The catalyst suspension was transferred using a syringe with a B-D 22G1½ needle (copper turnings are thin copper foil slices, which can not pass this kind of needles) to a second degassed flask with 13.3 mg TEDETA-modified silica gel (10% of the first used modified silica gel). To this flask were charged the same amounts of degassed MMA and initiator. The flask was reheated to 80 °C. The same procedure as for the first run was repeated.

4.2.2 Results and Discussion

CuBr was immobilized to silica gel particles via TEDETA attached to the particle surface, as shown in Scheme 4.1. TEDETA firstly reacted with 3-(trimethoxylsilyl)propyl acrylate to introduce a trimethoxysilyl group. Excess amount of TEDETA was used to have a high conversion of the acrylate since TEDETA was easy to be removed under vacuum. Subsequent condensation reaction between trimethoxylsilyl group with silanol group on the silica gel surface attached TEDETA ligand onto the particle. In contrast to an almost instant complexation of unbound TEDETA with CuBr, the reaction of CuBr with immobilized TEDETA was very slow. The silica gel particles became blue after sufficient stirring. The blue particles turned to green upon the addition of the initiator MBP, but the color was much lighter than that of free TEDETA with CuBr under the exactly same conditions without silica gel.

4.2.2.1 Effect of Catalyst/Initiator Ratio

In a homogenous ATRP, the typical initiator/CuBr ratio is 1/1. Therefore, an equimolar initiator with respect to CuBr was first evaluated for MMA polymerization (Figure 4.1). The polymerization was fast at the beginning but slowed down quickly. The $\ln([M]_0/[M])$ *vs.* time plot was linear, but did not pass the zero point, indicating that the concentration of the propagating radical decreased (based on $\ln([M]_0/[M]) = k_p[R^*]t$) after an initial period. This result suggests that some initiator molecules were consumed by side reactions because of the high radical concentration at the early stage of polymerization. We thus reduced the initiator concentration to CuBr/initiator = 3/2 to decrease the radical concentration to minimize these side reactions. Figure 4.1 shows that with higher catalyst/initiator ratios, the polymerization proceeded smoothly to 80% conversion. The $\ln([M]_0/[M])$ *vs.* time plot was linear throughout the polymerization, demonstrating a typical first-order kinetics. It became clear that a high level of catalyst concentration was required for this silica gel-supported TEDETA/CuBr system to mediate a living polymerization. This is because that the heterogeneous reaction between the immobilized catalyst and polymer halide and polymer radical (Scheme 4.2) in the supported system mainly depended on the diffusions of the polymer species, in contrast to a molecular level homogeneity in a homogeneous system.

Figure 4.2 shows the molecular weight of PMMA as a function of conversion. The molecular weight of PMMA increased linearly with conversion for both CuBr/initiator ratios at 1 and 1.5. The molecular weights were higher than the predicted at the low conversions, but approached the theoretical values at the high conversions. The initiator efficiency at 80% was about 0.9. This result indicated that the MMA polymerization mediated by the silica gel-supported TEDETA/CuBr was a living process. The polydispersities of the resulting PMMA decreased with conversion and were about 1.4-1.5 for CuBr/initiator = 1.5 and about 1.6-1.7 for initiator/CuBr = 1. The values were higher than those from homogenous ATRP,[6] but much lower than multidentate amine-silica gel supported ATRP.[5] Figure 4.3 shows the GPC traces of PMMA prepared by CuBr/initiator = 3/2. The peak gradually moved to high molecular weight region with increase in conversion. In contrast to the symmetrical distribution of the GPC traces from the homogenous ATRP (Chapter 2), the GPC traces from the supported system had

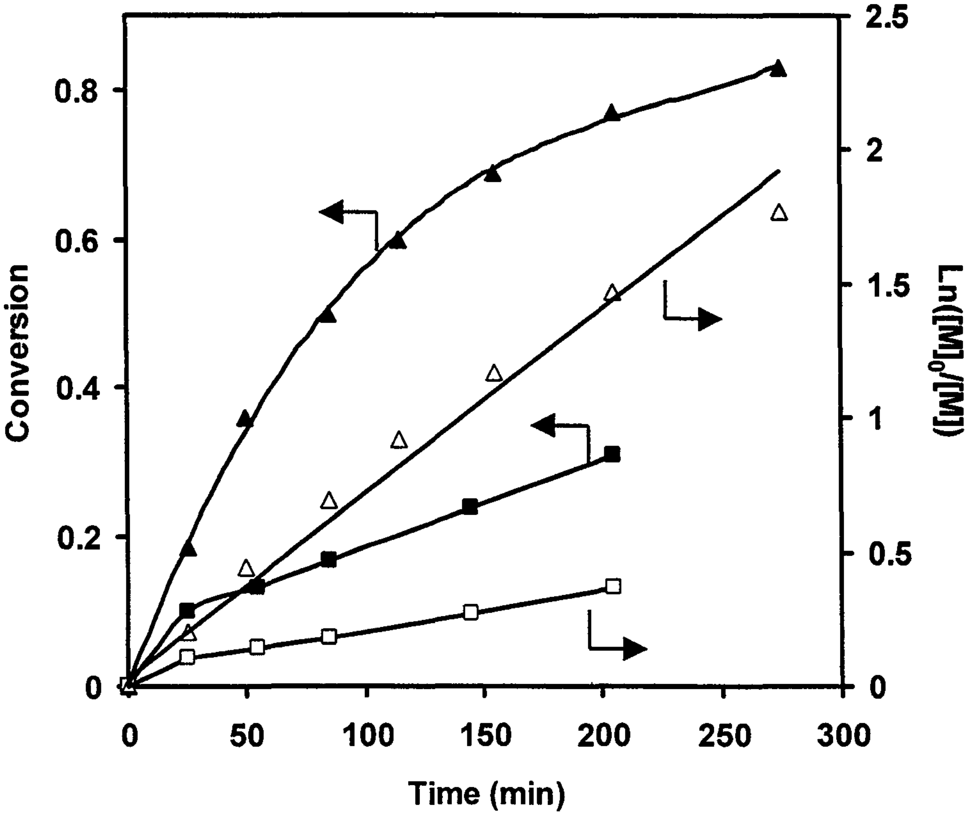

Figure 4.1. MMA polymerization in phenyl ether with different CuBr/initiator ratios catalyzed by CuBr-TEDETA supported on silica gel.

[CuBr] = 0.0158mol/L; MMA/CuBr (molar) = 300, Silica gel/CuBr = 10 (w/w) (TEDETA/CuBr = 1); CuBr/initiator (molar) = 1.5 (▲, △); 1.0 (■, □); 80 °C.

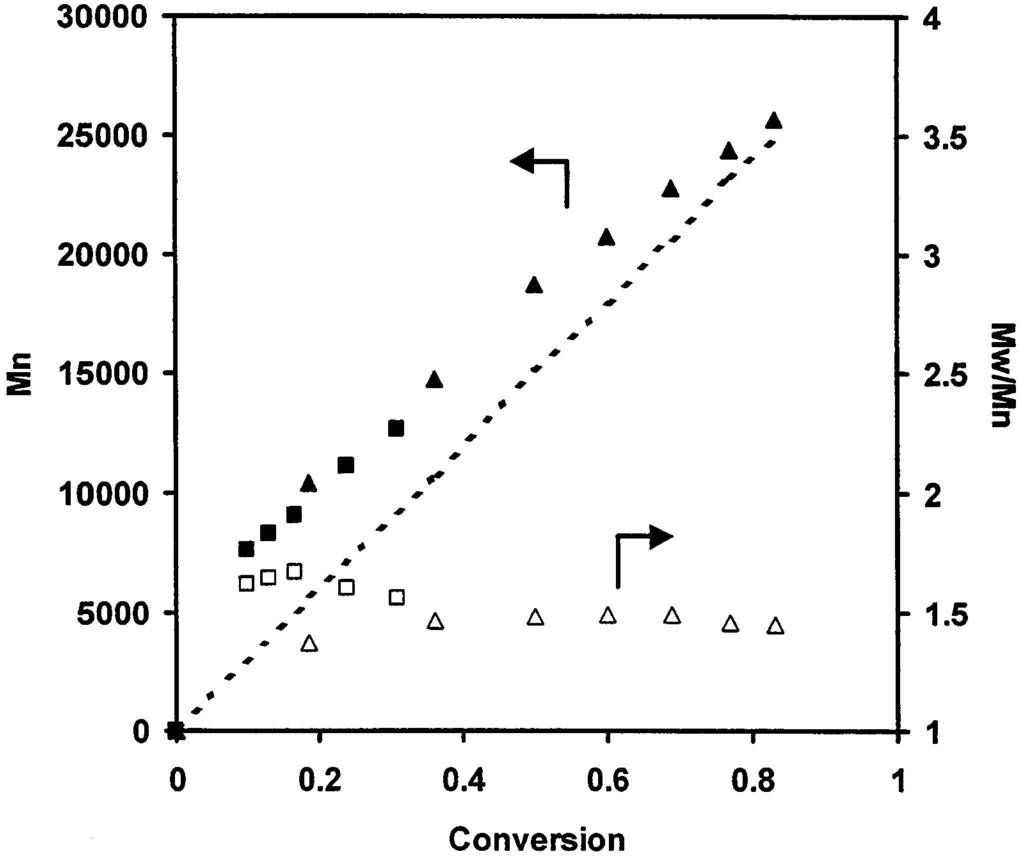

Figure 4.2. PMMA molecular weight and molecular weight distribution as a function of conversion for the polymerization of MMA in phenyl ether with different CuBr/initiator ratios catalyzed by CuBr-TEDETA supported on silica gel.

CuBr/initiator =1.5 (▲, △); 1(■, □); 80 °C. See Figure 4.1 for other experimental conditions.

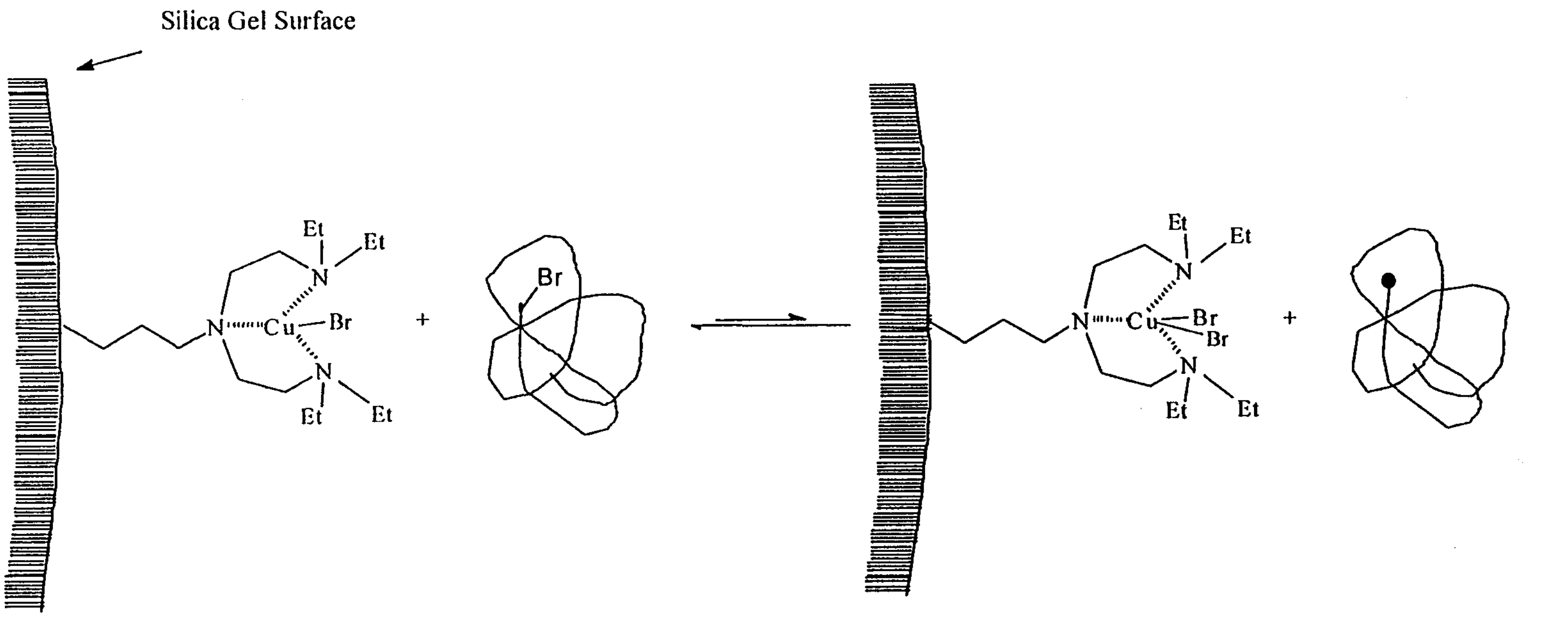

Scheme 4.2. The equilibrium in the ATRP of MMA by the supported catalyst

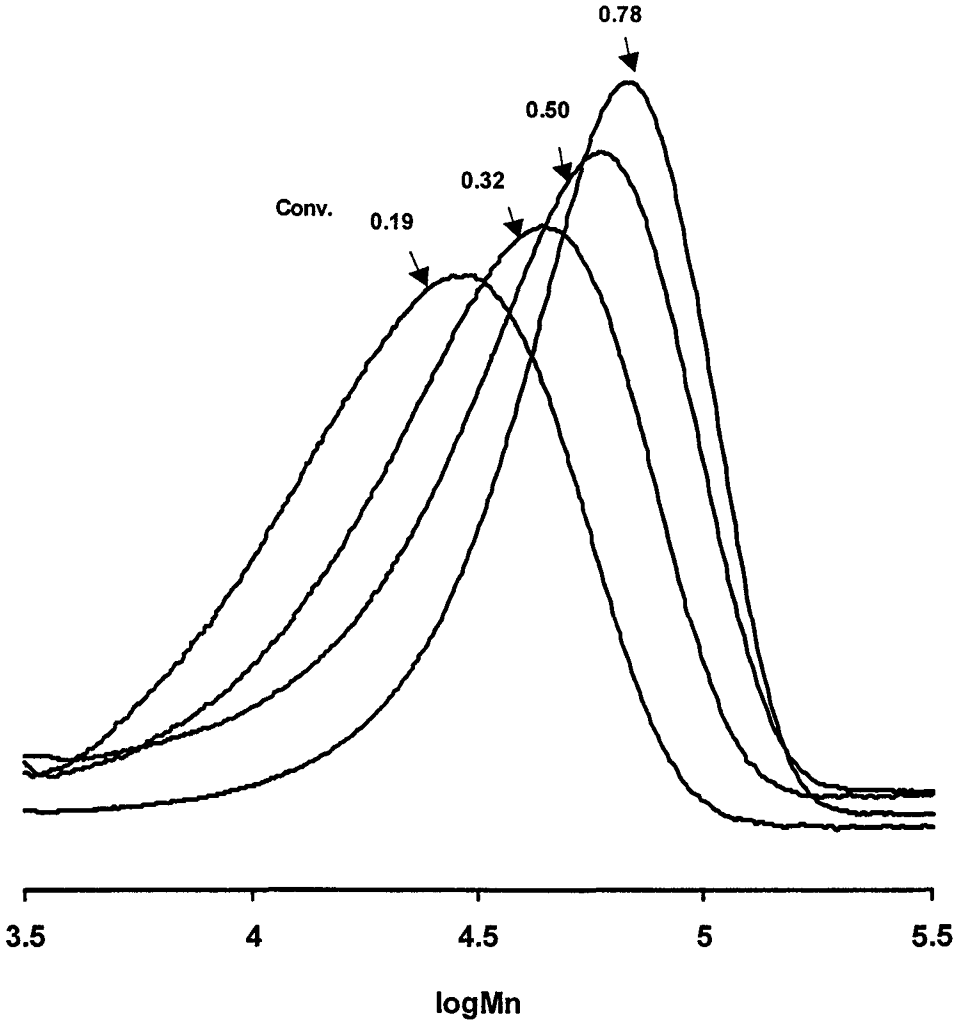

Figure 4.3. GPC traces of PMMA at different conversions.

See Figure 4.1 for the experimental conditions.

a tail in the low molecular weight region, which was the major reason for the high polydispersity values. This suggests that there were some terminations in the polymerization due to a slowed radical deactivation after the catalyst immobilized on solids. The low molecular weight fraction decreased as the conversion increased, and thus the polydispersity decreased as shown in Figure 4.2.

4.2.2.2 Effect of Silica Gel/Copper Bromide Ratio

Figure 4.4 shows the MMA polymerizations with silica gel/CuBr ratios of 5, 10, and 20. The polymerizations at different silica gel/CuBr ratios had almost the same rate in the early stage, but the rate curve leveled off at 40% for silica gel/CuBr = 5 and at 60% for silica gel/CuBr = 20. Correspondingly, the $\ln([M]_0/[M])$ *vs.* time plots for silica gel/CuBr = 5 and 20 deviated from linearity, indicating the decrease in the radical concentration. In contrast, the polymerization with silica gel/CuBr = 10 was smooth and its $\ln([M]_0/[M])$ vs. time plot was linear throughout the polymerization.

Figure 4.5 shows the PMMA molecular weight as a function of the MMA conversion. The molecular weights of PMMA prepared by silica gel/CuBr = 5 increased with conversion, but were much higher than the predicted. The initiator efficiency was about 50%, which means that almost 50% initiator was consumed by side reactions. The molecular weights of PMMA prepared by silica gel/CuBr = 10 and 20 were very close to the theoretical values. The initiator efficiencies were higher than 90%. The molecular weight distributions of the polymers were about 1.4-1.5, but became broader at high conversions for silica gel/CuBr = 5 system.

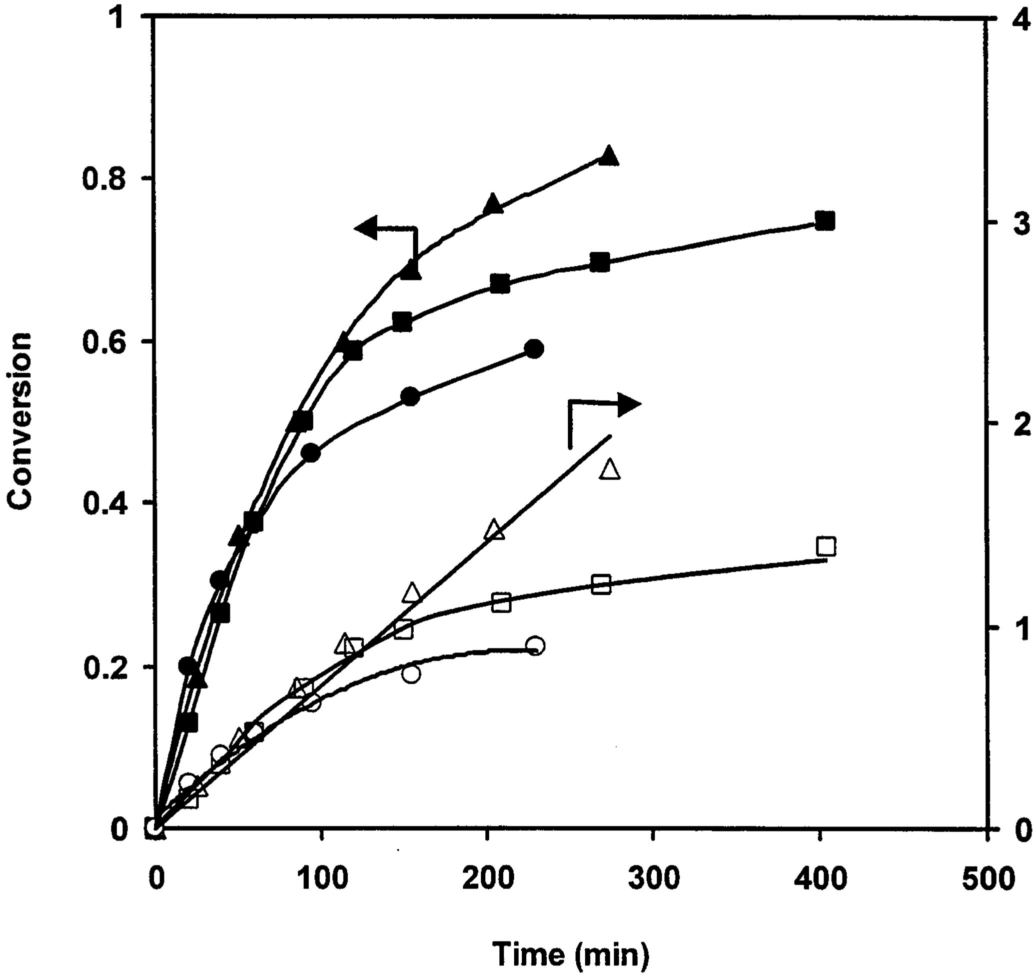

Figure 4.4. MMA polymerization in phenyl ether with different silica gel/CuBr ratios catalyzed by CuBr-TEDETA supported on silica gel.

[MMA] = 3.0 mol/L; [CuBr] = 0.0158mol/L; CuBr/initiator = 1.5; 80 °C.

Silica gel/CuBr (w/w) = 5 (●, ○); 10 (▲, △); and 20(■, □).

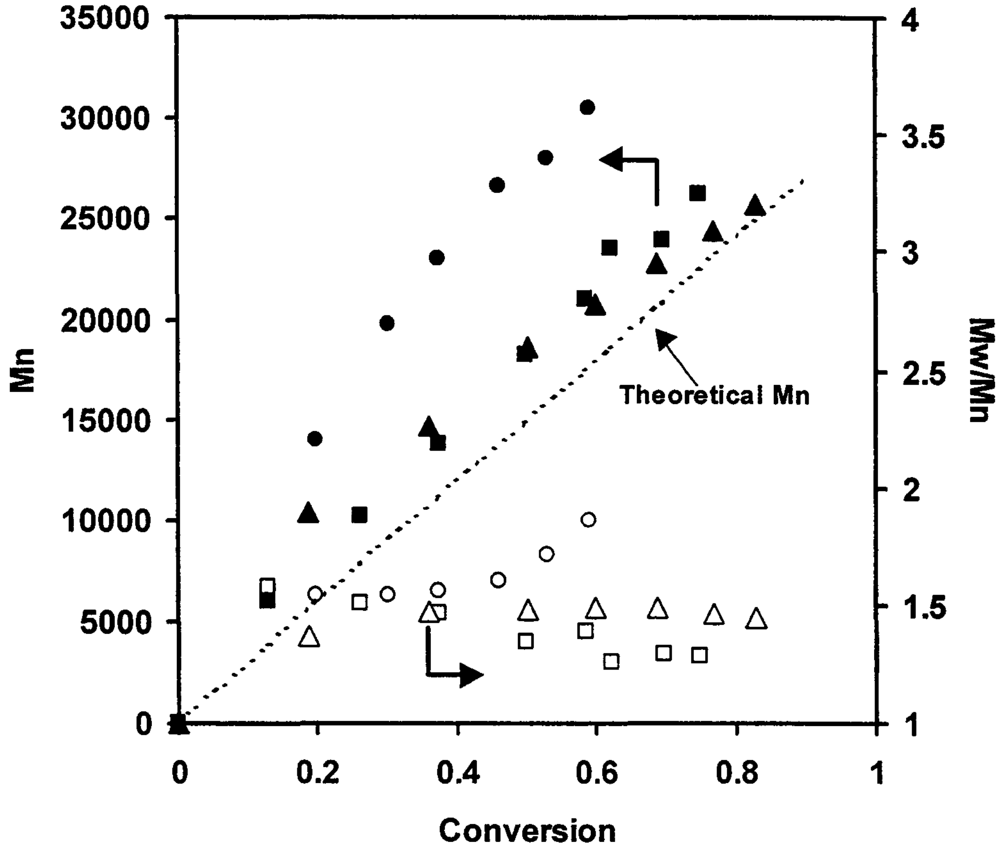

Figure 4.5. PMMA molecular weight and molecular weight distribution as a function of conversion for the polymerization of MMA in phenyl ether with different silica gel/CuBr ratios catalyzed by CuBr-TEDETA supported on silica gel.

Silica gel/CuBr (w/w) = 5 (●, ○); 10 (▲, △); 20(■, □). See Figure 4.4 for other experimental conditions.

It was estimated based on the TEDETA concentration grafted on silica gel that the silica gel/CuBr ratios of 5, 10, and 20 corresponded to the TEDETA/CuBr ratios of 0.5, 1, and 2, respectively. Therefore, there was no adequate ligand to complex with all catalyst molecules in the silica gel/CuBr = 5 system (i.e. TEDETA/CuBr = 0.5). Non-complexed CuBr was not a good catalyst for ATRP and thus caused its low initiator efficiency. In the case of silica gel/CuBr = 20 (i.e. the TEDETA/CuBr = 2), CuBr was well dispersed on the particle surface.

Chapter 3 shows that there was no significant effect of the excess multidentate amine on polymerization. Accordingly, the kinetic curvature of the silica gel/CuBr = 20 system was not caused by the excess TEDETA, but by silica gel. Silica gel increased the system viscosity. It was observed that during the polymerization with silica gel/CuBr = 20, the solution became very viscous and it was difficult to withdraw samples with syringe when the conversion reached 50%. Similar phenomena were also observed by Matyjaszewski et. al.[5] The high viscosity of the mixture reduced both mobility of silica gel and diffusion of polymer chains, resulting in a slower reaction between P-Br and catalyst, and thus a lower polymerization rate.

4.2.2.3 Polymerization at MMA/Initiator = 100

To synthesize low molecular weight PMMA, two approaches were examined. One was to increase the initiator concentration to three times (MMA/CuBr/MBP = 300/1.5/3) and the other was to reduce the monomer concentration to one-third

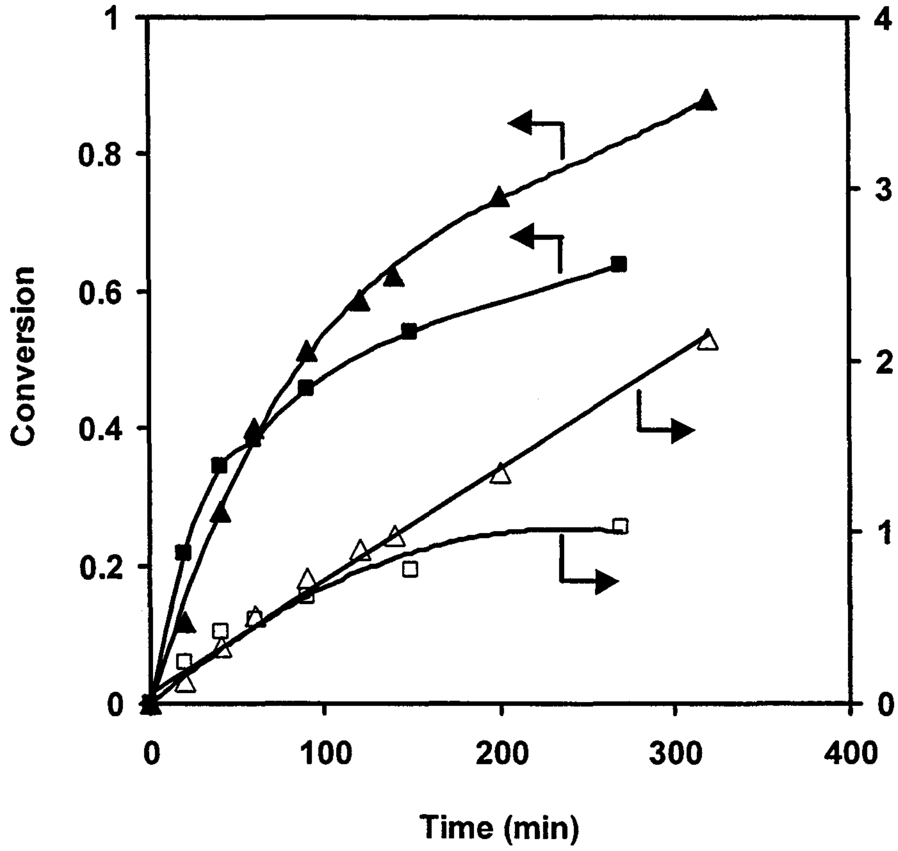

Figure 4.6. MMA polymerization in phenyl ether at monomer/initiator = 100 (molar) catalyzed by CuBr-TEDETA supported on silica gel.

[CuBr] = 0.0158mol/L; Silica gel/CuBr (w/w) = 10; 80 °C;

MMA/CuBr/initiator = 100/1.5/1 (▲, △) and 300/1.5/3 (■, □).

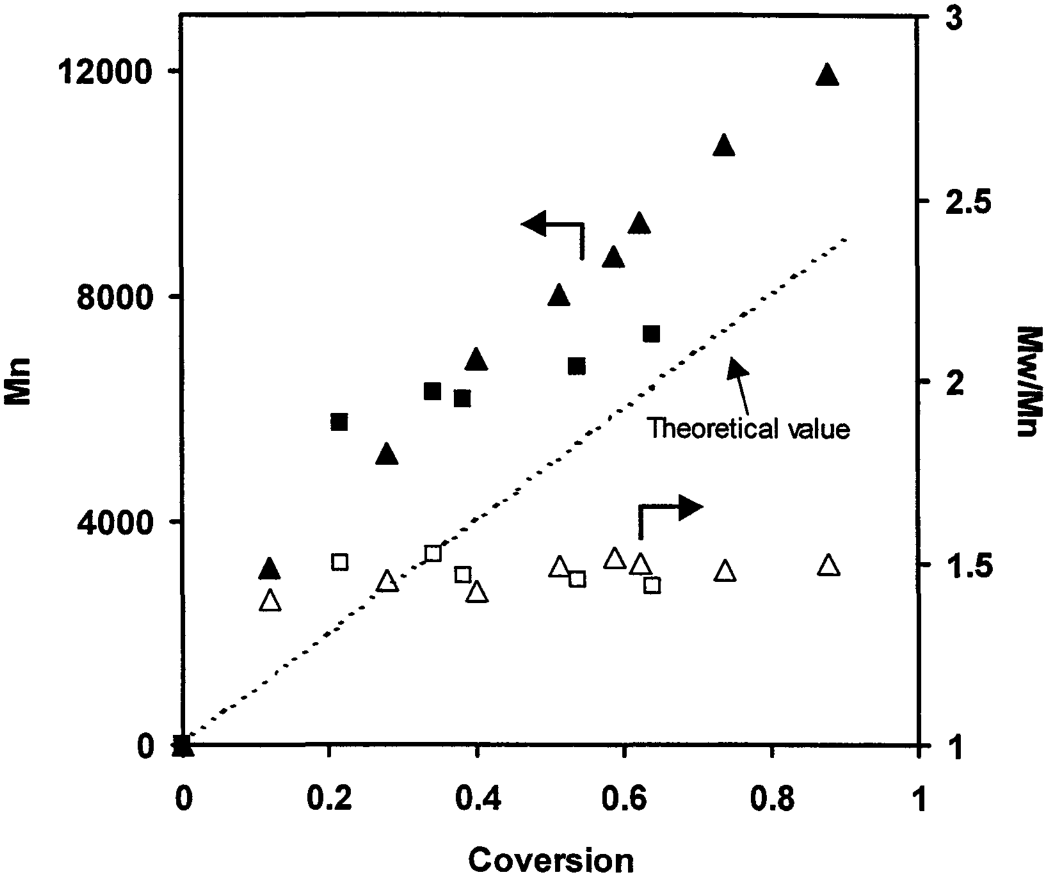

Figure 4.7. PMMA molecular weight and polydispersity as a function of conversion for MMA polymerization in phenyl ether at monomer/initiator = 100 (molar) catalyzed by CuBr-TEDETA supported on silica gel.

MMA/CuBr/initiator = 100/1.5/1 (▲, △); 300/1.5/3 (■, □). See Figure 4.6 for other experimental conditions.

(MMA/CuBr/MBP = 100/1.5/1) as used in Figure 4.1. Figure 4.6 shows that the former system had curvature in kinetic plot, suggesting significant radical termination in the initial stage. However, the latter showed a first-order kinetics with respect to the monomer concentration. Figure 4.7 shows that the former system initially produced PMMA with molecular weights much higher than the theoretical values and only a slight increase afterward. In contrast, the PMMA molecular weight obtained from the latter system increased linearly with the conversion (Figure 4.7). This result is in agreement with the above discussion that more catalyst with respect to initiator was required for a heterogeneous ATRP.

4.2.2.4 Catalyst Reuse.

Upon completion of the polymerization, the mixture was centrifuged. The clear solution was removed and green catalyst particles were separated. PMMA isolated from the solution was colorless. The catalyst was washed and used for subsequent polymerizations. Figure 4.8 shows the MMA polymerization catalyzed by the recycled silica gel/CuBr =10 system. The polymerizations with the recycled catalysts were also in a first order, but the activity of the recycled catalyst was reduced. The apparent polymerization rate constant, $k_p[P^\bullet]$, was 6.1×10^{-3} min^{-1} for the fresh catalyst, 3.1×10^{-3} min^{-1} for the second used catalyst, and 2.1×10^{-3} min^{-1} for the third used catalyst.

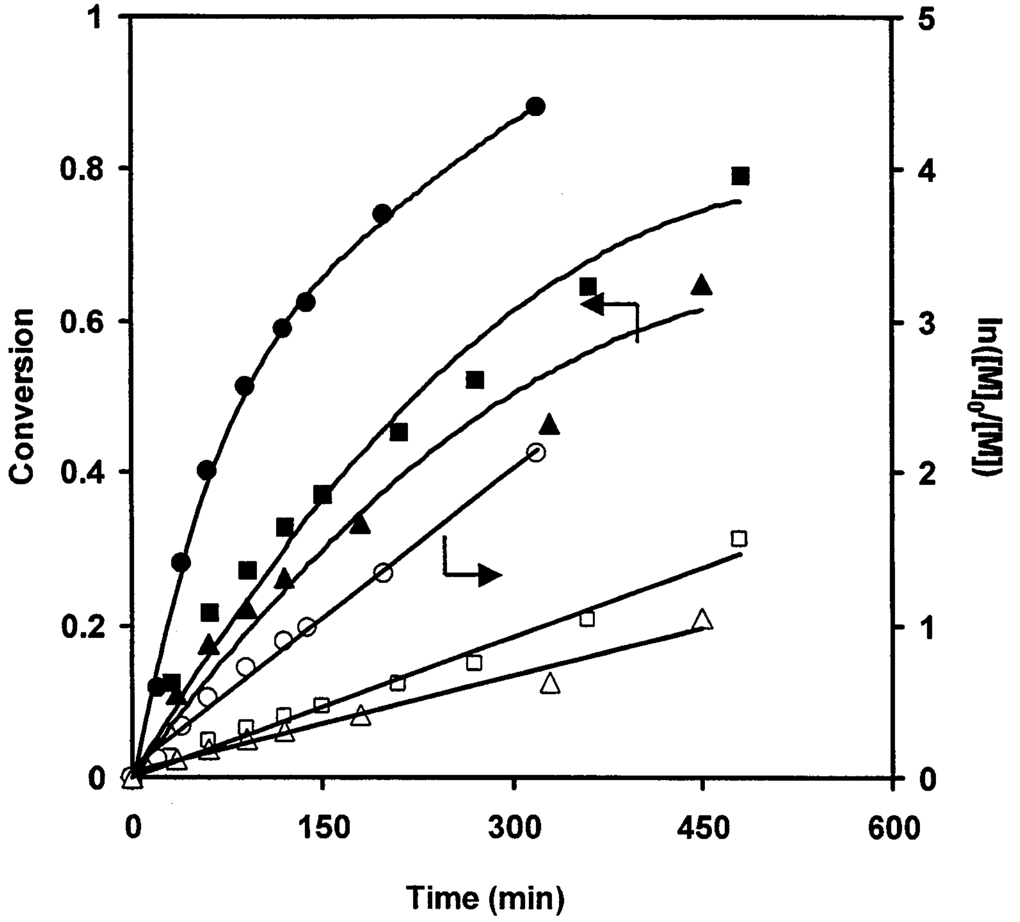

Figure 4.8. Reuse of CuBr-TEDETA/silica gel system for MMA polymerization.

[CuBr] = 0.0158mol/L; Silica gel/CuBr (w/w) = 10; MMA/CuBr/initiator = 100/1.5/1; 80 °C. First use (●, ○); Second use (■, □) and third use (▲, △).

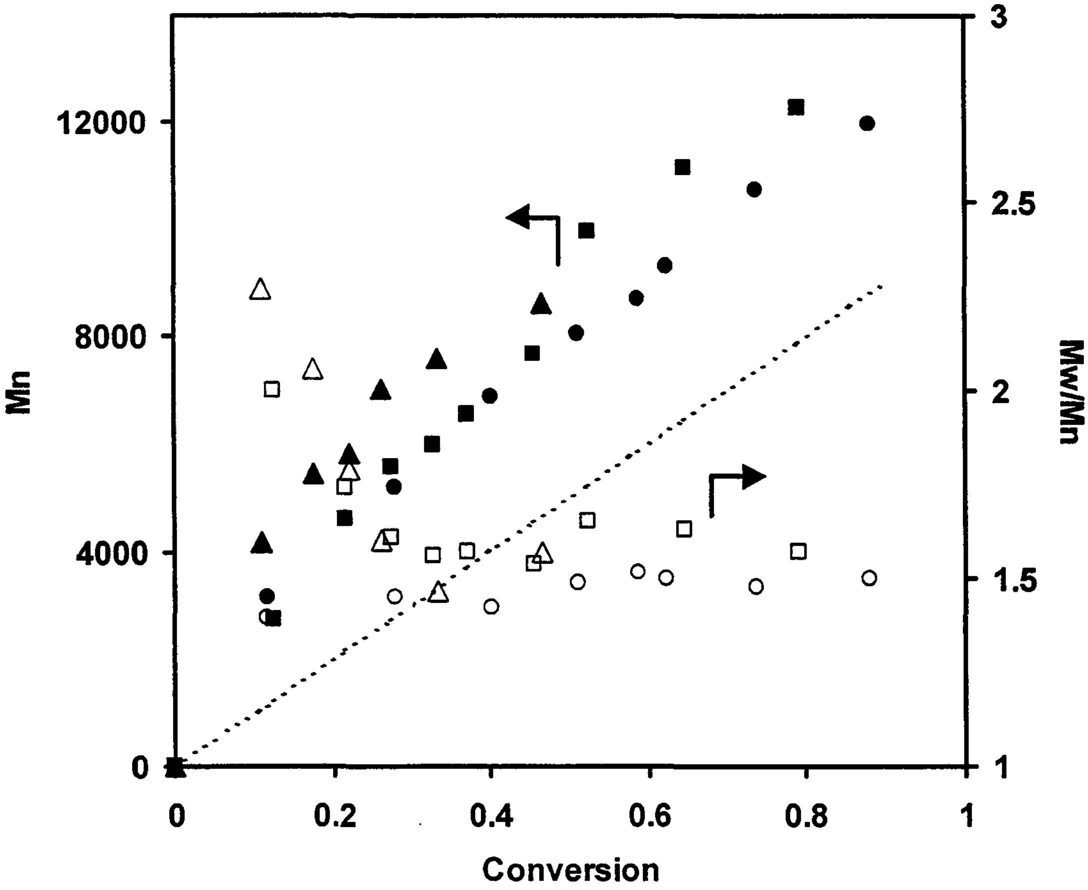

Figure 4.9. PMMA molecular weight and polydispersity as a function of conversion in the MMA polymerization catalyzed by fresh and recycled catalysts.

First use (●, O); Second use (■, □) and third use (▲, Δ). See Figure 4.8 for other experimental conditions.

The activity reduction was due to the formation of $CuBr_2$, as seen in the silica gel supported CuBr-HMTETA in Chapter 3. The presence of $CuBr_2$ in the recycled catalyst was fairly evident with its deep green color, which was a characteristic color of $CuBr_2$-multidentate amine complex, while the Cu(I)Br-TEDETA complex on silica gel was blue. It has been reported that the presence of a small amount of $CuBr_2$ substantially reduced the polymerization rate,[7] as discussed in Chapter 3. Figure 4.9 shows the molecular weight and polydispersity of PMMA as a function conversion in the MMA polymerization with the fresh and recycled catalysts. The initiator efficiency ($Mn_{.theoretical}/Mn_{.GPC}$) was less than 1, indicating that some initiator molecules were consumed by side reactions. As shown in Scheme 4.2, the radical consumption generated an excess $CuBr_2$ in the catalyst.

The molecular weights of PMMA produced by fresh and recycled catalysts were also controlled and increased linearly with conversion. The molecular weights of PMMA obtained in the second and third runs were slightly higher than those in the first run. These results indicate that the recycled catalysts still effectively mediated the polymerization.

4.2.2.5 Catalyst Regeneration

$$CuBr_2 + Cu \longrightarrow 2\,CuBr \qquad \text{(Eq. 4.1)}$$

We have ascribed the activity reduction in recycled catalysts to the presence of Cu(II), which equilibrated with Cu(I) in the first run polymerization. If this was the case, Cu(0) can reduce Cu(II) to Cu(I) [8] and the activity of recycled catalyst should be regained. We therefore used copper metal to regenerate the recycled catalyst (Eq. 4.1). Copper turnings were stirred with the catalyst at 35 °C for overnight. The green-colored recycled catalyst became blue again. This regenerated catalyst was used for the MMA polymerization. As shown in Figure 4.10, the regenerated recycled catalyst showed higher activity than the recycled catalyst without regeneration. This result confirms the presence of Cu(II) in the recycled catalyst. The regenerated catalyst mediated a first order polymerization. The molecular weights of PMMA from the regenerated catalyst were very close to the predicted with low polydispersities (Figure 4.11), similar to those from the fresh catalyst.

It is important to completely remove copper metal from the catalyst after regeneration. In the presence of copper metal, the regenerated catalyst had the same activity as the fresh one at the early stage of the polymerization, but leveled off later. This catalyst had no control over polymerization. The PMMA molecular weight decreased with conversion and had high polydispersity (Mw/Mn >1.7), indicating a typical conventional free radical polymerization. This may be because of the reaction between residual copper metal and Cu(II). The continuous reaction of Cu(II) with Cu(0) (Eq. 4.1) during the polymerization promoted forward reaction in Scheme 4.2 and resulted in a very low concentration of Cu(II), and thus the catalyst lost control over the polymerization. Therefore it is better to use copper turnings rather than copper powder. The latter is difficult to be separated from the catalyst. The fine silica gel particles suspended in phenyl ether were very easily separated from copper turnings by a syringe with a small-diameter needle.

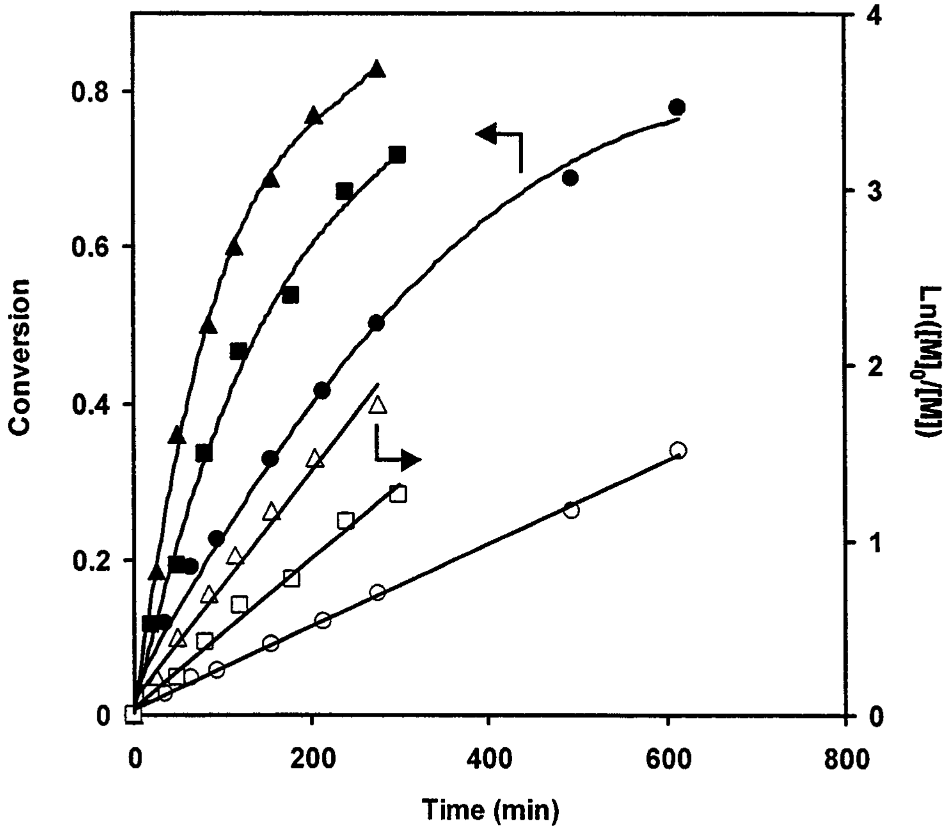

Figure 4.10. MMA polymerization catalyzed recycled and regenerated catalyst.

[MMA] = 3.0 mol/L; [CuBr] = 0.0158 mol/L; CuBr/initiator = 1.5; Silica gel/CuBr (w/w) = 10; 80 °C. Fresh catalyst (▲, △); recycled catalyst(●, ○); regenerated catalyst(■, □)

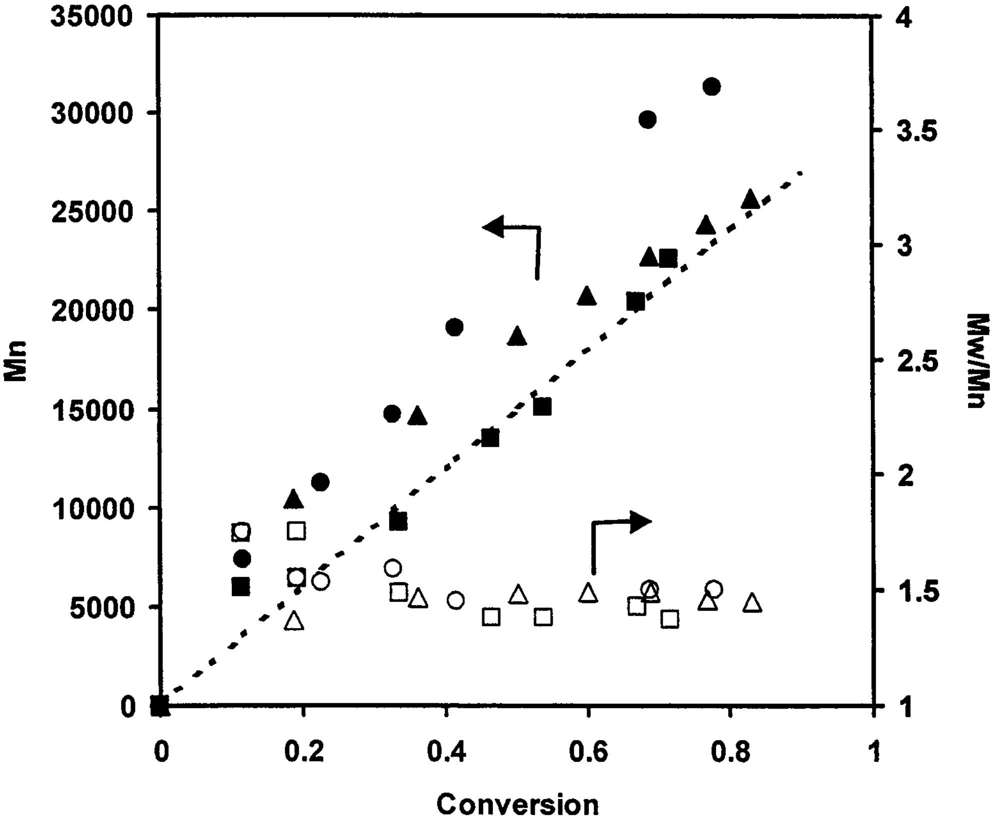

Figure 4.11. PMM molecular weight and polydispersity as a function of conversion in the MMA polymerizations catalyzed by fresh, recycled and regenerated catalysts

Fresh catalyst (▲, Δ); recycled catalyst(●, O); regenerated catalyst(■, □), See Figure 4.10 for other experimental conditions.

4.3 Effect of Ligand Spacer on Silica Gel Supported Atom Transfer Radical Polymerization

The above results show that the immobilized catalyst mediated a living polymerization of MMA, but its control over the polymerization is substantially decreased compared with the non-immobilized catalysts. This suggests that the deactivation reaction of radicals (reverse reaction in Scheme 4.2) is not efficient for supported catalyst mediated ATRP. ATRP is based on a fast reversible activation/deactivation process of radicals (Scheme 4.2).[7] It is critical for the generated radicals to be deactivated rapidly to maintain a very low radical concentration level and to protect the polymer chains; otherwise, the ATRP will behave like a conventional free radical polymerization.[7,9]

The deactivation depends on the diffusion of polymer radicals and that of catalyst. Because the diffusivity of a polymer chain is low due to its large molecular size, the deactivation reaction in an ATRP system is mainly determined by the catalyst diffusion. In a heterogeneous system, the supported catalyst molecules are confined on solid surface and thus lack of mobility. The diffusion limitation results in a slowed deactivation reaction by supported catalyst. Increasing the catalyst mobility on solid surface should favor the deactivation of polymer radicals, and thus favor the control of polymerization.

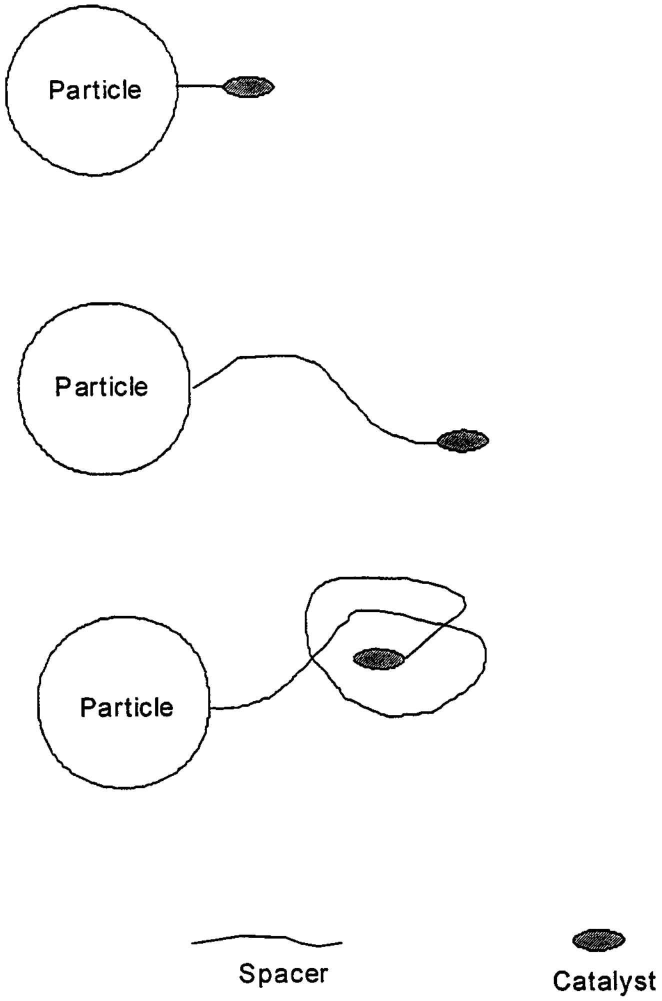

Scheme 4.3. The effect of spacer on catalyst mobility

It was therefore hypothesized that the supporting spacer, through which the catalyst is attached to particle surface, determines the catalyst mobility and accessibility. A short spacer confines catalyst due to a steric effect. A long and flexible spacer renders catalyst more mobility as illustrated in Scheme 4.3. However, an excess spacer length may embrace catalyst and thus impede the access of catalyst to polymer chain ends to facilitate reactions. The spacer length may strongly affect the catalyst activity and its controllability on ATRP. In this work, silica gels grafted with tetraethyl diethylenetriamine (TEDETA) and di(2-picolyl)amine (DiPA) via polyethylene glycol (PEG) spacers of different lengths have been synthesized for the polymerization of methacrylates to evaluate the spacer effect.

4.3.1 Experimental Section

4.3.1.1 Materials

Methyl methacrylate (MMA) and 2-(*N,N*-dimethylaminoethyl methacrylate (DMAEMA) from Aldrich were distilled under vacuum and stored at –15 °C. N,N,N',N'-tetraethyldiethylenetriamine (TEDETA, 90%), di(2-picolyl)amine (DiPA), CuBr, methyl α-bromophenylacetate (MBP, 99%), N^1-[3-(trimethoxylsilyl)propyl] diethylenetriamine (92%) and phenyl ether, polyethylene glycol diacrylates (Mn=275 (n=3.3) and 575 (n=10) respectively), also from Aldrich, were used as received. Silica gel with 100-200 mesh and an average pore diameter of 60 angstroms was supplied by SiliCycle Inc.

4.3.1.2 Synthesis Diethylenetriamine-Functionalized Silica Gel

The attachment of diethylenetriamine onto silica gel surface was based on the reaction of silicon alkoxides with silanol groups on the particle surface (Scheme 4.4). Hydrophilic silica gel was dried in vacuum at 60 °C for 3 days. Silica gel (10 g), N^1-[3-(trimethoxylsilyl)propyl]diethylenetriamine (5 g) and THF (50 mL) were charged to a flask. The mixture was refluxed for 48 h. The silica gel was separated from the solution by centrifugation and washed six times with THF. It was finally dried at 50 °C under vacuum for 24h. IR: 3433 cm^{-1}, 2975 cm^{-1}, 1733 cm^{-1}, 1567 cm^{-1}, 1032 cm^{-1}. The amount of diethylenetriamine grafted onto silica gel was determined by thermogravimetric analysis (TGA) and elemental analysis. The calculated diethylenetriamine concentration was 4.24 %(w/w).

4.3.1.3 Grafting TEDETA or Di(2-picolyl)amine (DiPA) onto Silica Gel

TEDETA or DiPA was grafted onto silica gel via polyethylene glycol spacer by two times of Michael reactions of acrylates with primary or secondary amines, as shown in Scheme 4.5. Diethylenetriamine–functionalized silica gel (10 g) was gradually added to polyethylene glycol diacrylates (30 g) with sufficient stirring. The mixture was stirred for 48 h at room temperature. It was then diluted with THF to 100 mL and centrifuged. The silica gel was washed with 60 mL THF 6 times to remove adsorbed PEG. About 0.2g silica gel was taken out and dried in vacuum for analysis. The left silica gel was stirred with 20 mL TEDETA for 48 h at room temperature. The silica gel was then separated by centrifugation and washed with THF seven times. Finally the silica gel was air-dried and then vacuum-dried at 50 °C for 24 h. DiPA functionalized silica gel supports were prepared by the same procedure. FTIR for silica gel grafted with TEDETA: 2970 cm^{-1}, 2808 cm^{-1}, 1738 cm^{-1} (C=O), 1202 cm^{-1}, 1109 cm^{-1}; for silica gel grafted with DiPA: 2926 cm^{-1}, 1735 cm^{-1} (C=O), 1596 cm^{-1}, 1109 cm^{-1} (Si-O-Si), 797 cm^{-1}. The ligand contents were analyzed by thermogravimetric analysis (TGA) and elemental analysis. The ligand contents on the silica gel with different spacers are shown in Table 1.

4.3.1.4 Polymerization

A typical polymerization procedure was as follows: CuBr, silica gel and phenyl ether were added to a Schlenk flask and was degassed by four vacuum-nitrogen cycles. Degassed MMA was added to the flask by a nitrogen-purged syringe. The mixture was stirred at room temperature for 20 min. A slightly blue suspension with a colorless solution was obtained. Degassed initiator (MBP) was dropwise added to the flask with stirring. The flask was subsequently heated to 60 °C in an oil bath. At different time intervals, about 0.05 mL of the solution/catalyst mixture was withdrawn with nitrogen-purged syringe. The solution was diluted with $CDCl_3$. The conversion was measured with ^{1}H-NMR by the intensity ratio of the OCH_3 signals in polymer (3.60 ppm) and monomer (3.75 ppm). The molecular weight and polydispersity were measured by GPC.

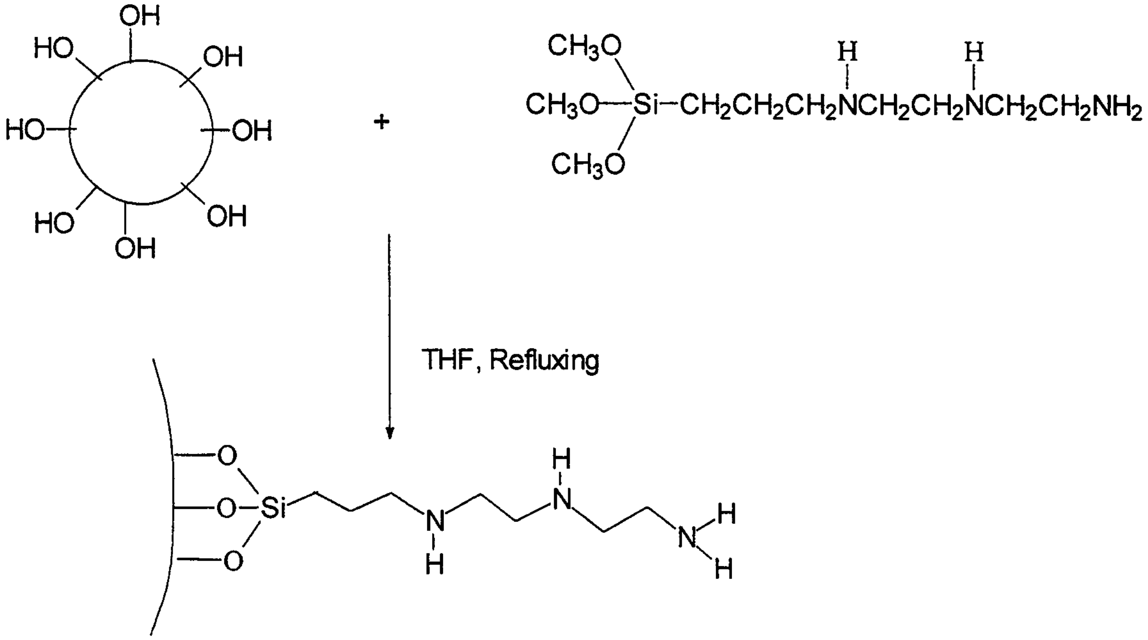

Scheme 4.4. Grafting diethylenetriamine onto silica gel

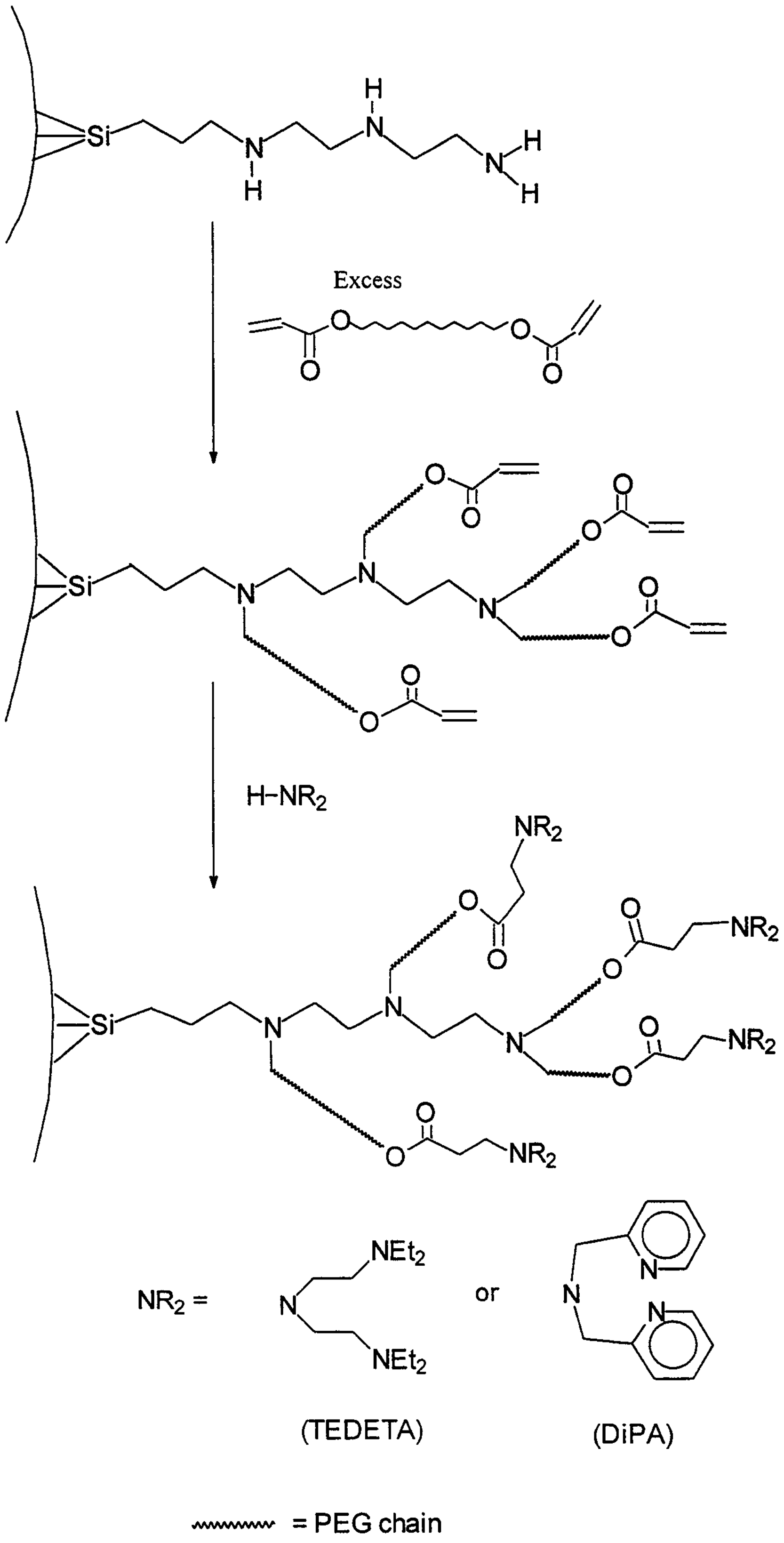
Si
N
H
Excess
O
H-NR2
NR2
NR2 =
NEt2
(TEDETA)
or
(DiPA)
= PEG chain

Scheme 4.5. Immobilizing ligand onto silica gel via polyethylene glycol spacer

Table 4.1. Ligand contents in synthesized silica gel supports

Support Name	PEG spacer units	Ligand	Ligand %(w/w)
SG-PEG$_1$-TEDETA	1	TEDETA	3.0
SG-PEG$_3$-TEDETA	3	TEDETA	1.43
SG-PEG$_{10}$-TEDETA	10	TEDETA	1.32
SG-PEG$_1$-DiPA	1	DiPA	2.97
SG-PEG$_3$-DiPA	3	DiPA	2.34
SG-PEG$_{10}$-DiPA	10	DiPA	1.1

4.3.1.4 Block Copolymerization

CuBr (7.0 mg), SG-PEG$_3$-TEDETA (700 mg), phenyl ether (3.15 g) were added to a Schlenk flask and degassed as described above. Degassed MMA(0.34 mL) and 6.3 μL of methyl α-bromophenylacetate were added. The mixture was immersed in a 60 °C oil bath for 6 h. A small amount of the mixture (0.05 mL) was withdrawn to analyze the conversion by NMR spectra (conversion = 75%) and molecular weight by GPC (Mn = 6900, Mw/Mn = 1.22). Then the flask was connected to vacuum to remove the volatile in the bottle. Degassed DMAEMA (0.5 g) was charged to the flask and stirred for 10 min. Then the flask was reheated to 60 °C for 8 h (DMAEMA conversion, 70%; Mn = 14700, Mw/Mn = 1.46; Mn(theor.) = 15700).

4.3.2 Results and Discussion

4.3.2.1 MMA Polymerizations by Catalysts Supported with Different Spacers

Figures 4.12 and 4.13 show the MMA polymerization mediated with CuBr supported on TEDETA or DiPA-modified silica gel via different PEG spacer lengths. The MMA polymerization rates are summarized in Table 4.2. The apparent polymerization rate constant k^{app} (i.e., $k_p[R^\bullet]$) increased with the spacer length in the following order: PEG$_1$< PEG$_{10}$ < PEG$_3$ (the subscripts are the numbers of EG units of the spacers). This suggests that when CuBr is immediately anchored on the silica gel surface, the catalyst has very limited mobility and therefore less chance to react

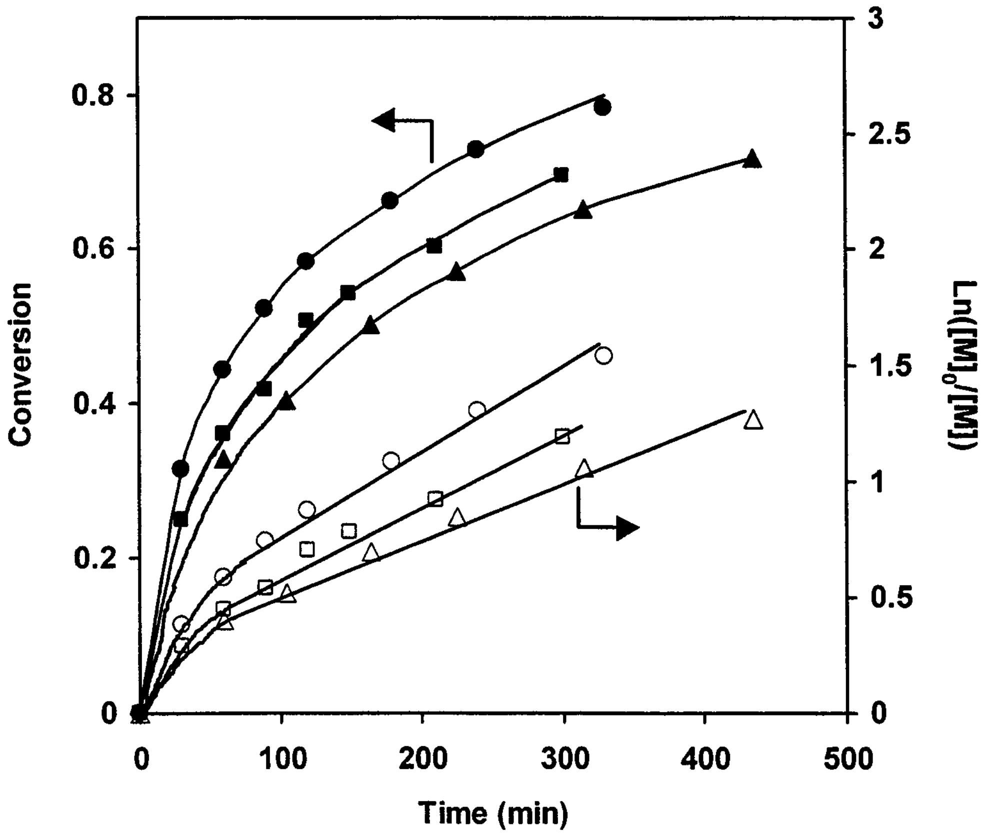

Figure 4.12. MMA polymerization in phenyl ether catalyzed by CuBr with TEDETA-functionalized silica gel support.

[MMA]=1.38 mol/L, [MBP]=9.2×10^{-3} mol/L, [CuBr]=1.39×10^{-2} mol/L, [TEDETA]/[CuBr] (molar) = 1, 60 °C; Support: SG-PEG$_1$-TEDETA (▲, △); SG-PEG$_3$-TEDETA (●, ○); SG-PEG$_{10}$-TEDETA (■, □).

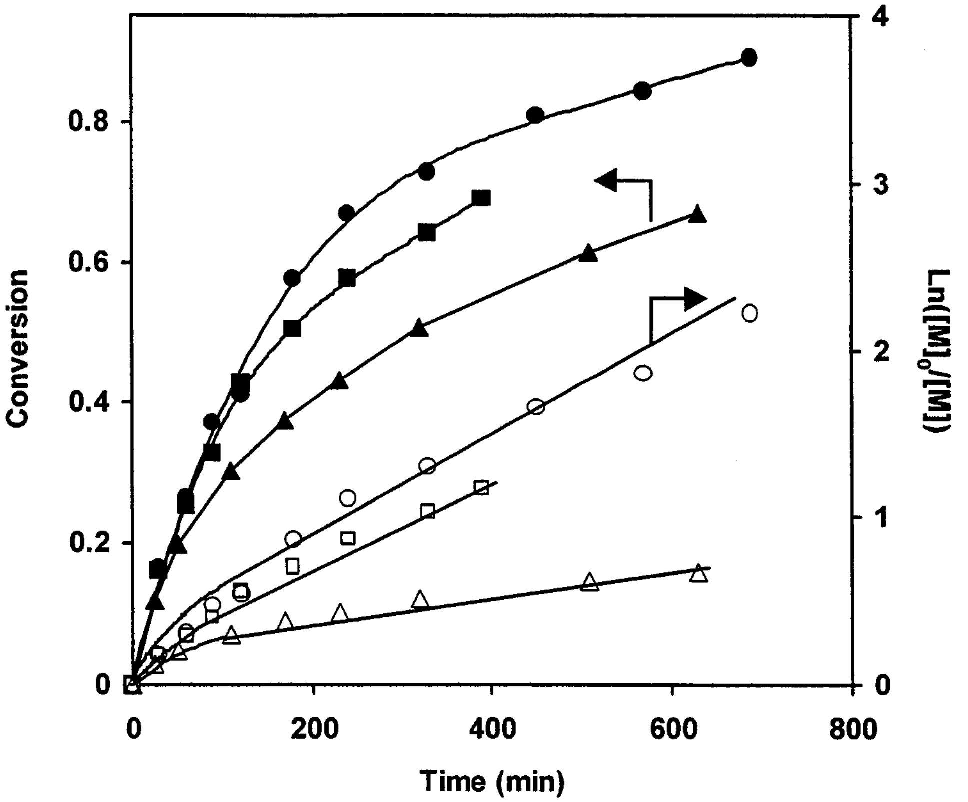

Figure 4.13. MMA polymerization in phenyl ether catalyzed by CuBr with DiPA-functionalized silica gel support.

[MMA]=1.38 mol/L, [MBP]=9.2 $\times10^{-3}$ mol/L, [CuBr]= 1.39×10^{-2} mol/L, [DiPA]/[CuBr] (molar) = 1; 60 °C; Support: SG-PEG$_1$-DiPA (▲, △); SG-PEG$_3$-DiPA (●, ○); SG-PEG$_{10}$-DiPA (■, □).

Table 4.2. The apparent rate constant of MMA polymerization catalyzed by CuBr immobilized on silica gel with different spacer lengths. [a]

Support	$k^{app}[R^{\bullet}]$ ($\times 10^{-3}$ min^{-1})
SG-PEG_1-TEDETA[b]	2.5
SG-PEG_3-TEDETA	3.8
SG-PEG_{10}-TEDETA	3.2
SG-PEG_1-DiPA	1.6
SG-PEG_3-DiPA	3.0
SG-PEG_{10}-DiPA	2.7

[a] [MMA]=1.38 mol/L, [MBP]=9.2×10^{-3} mol/L, [CuBr]= 1.39×10^{-2} mol/L, [TEDETA] or [DiPA]/[CuBr] (molar) = 1, 60 °C; Solvent: phenyl ether.

[b] The subscripts are the ethylene glycol unit numbers.

with the dormant centers (P-Br). However, when the spacer is too long, e.g. with 10 EG units, the PEG coils surrounding the catalytic site impedes the reaction of the catalyst with dormant active center (P-Br), as illustrated in Scheme 4.3. It becomes clear that the length of three EG units is optimal for immobilizing CuBr among these three supporting spacers.

The polymerizations in Figures 4.12 and 4.13 experienced an initial rate decrease before the $\ln([M]_0/[M])$ versus time curves became linear. This suggests a decrease in the radical concentration in the early stage of polymerization based on $\ln([M]_0/[M])= kp[R^\bullet]t$. This decrease was caused by radical termination reactions. At the early stage of the polymerization, the low Cu(II) concentration in solution favored the forward reaction (Scheme 4.2) and thus resulted in a high radical concentration. Consequently radical side reactions such as termination became significant. These side reactions consumed radicals and generated excess Cu(II) (Scheme 4.2). When a certain level of Cu(II) concentration was accumulated and the reverse reaction reached an equilibrium with the forward reaction (Scheme 4.2), the reaction proceeded smoothly in a constant radical concentration (i.e. a first order reaction).

Figures 4.14 and 4.15 show the number average molecular weight (Mn) and polydispersity (Mw/Mn) of the resulting PMMA. The molecular weights of PMMA increased linearly with the conversion, indicating a living process in all cases. The spacer

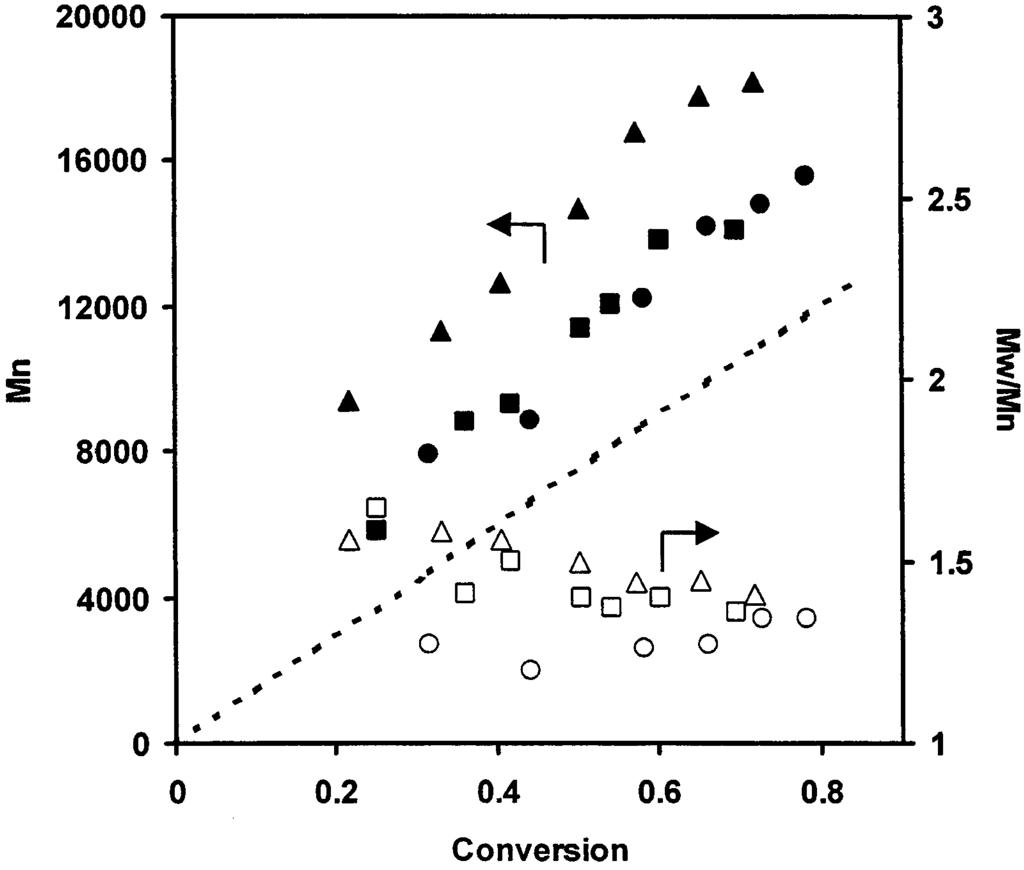

Figure 4.14. PMMA molecular weight and polydispersity as a function of conversion in phenyl ether with different TEDETA-functionalized supports. See Figure 4.12 for other experimental conditions.

SG-PEG$_1$-TEDETA (▲, △); SG-PEG$_3$-TEDETA (●, ○); SG-PEG$_{10}$-TEDETA (■, □); theoretical Mn (-------).

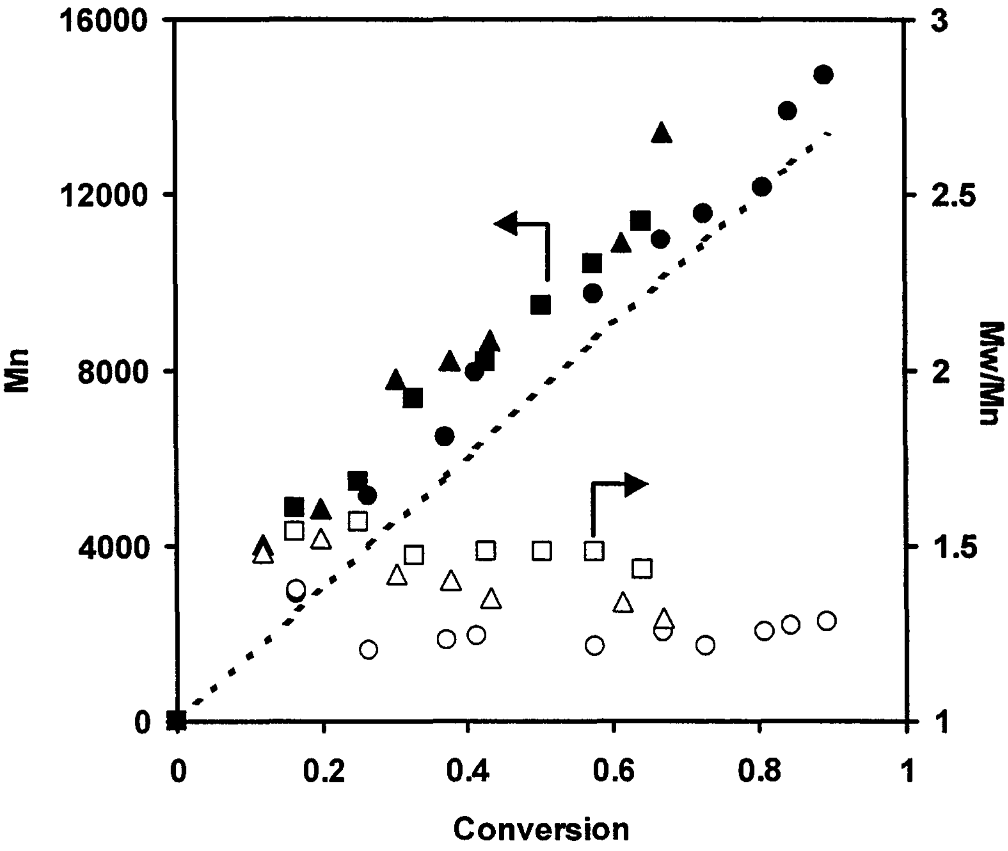

Figure 4.15. PMMA molecular weight and polydispersity as a function of conversion in phenyl ether with different DiPA-functionalized supports. See Figure 4.13 for other experimental conditions.

SG-PEG$_1$-DiPA(■, □); SG-PEG$_3$-DiPA (●, ○); SG-PEG$_{10}$-DiPA (▲, △); theoretical Mn (-------).

length of the catalyst support affected the initiator efficiency and polydispersity of PMMA. The initiator efficiency was 57% with SG-PEG$_1$-TEDETA, 75% with SG-PEG$_3$-TEDETA, and 70% with SG-PEG$_{10}$-TEDETA. The polydispersities of PMMA were in the range of 1.4-1.6 by SG-PEG$_1$-TEDETA, 1.2-1.4 by SG-PEG$_3$-TEDETA and 1.4-1.5 by SG-PEG$_{10}$-TEDETA. With DiPA as the ligand, there was little difference in initiator efficiencies of different systems, but the polydispersities of PMMA by SG-PEG$_3$-DiPA were the lowest. These results indicate that CuBr grafted with 3 units of PEG regulated the polymerization most effectively. A spacer longer or shorter than 3 EG units may slow the deactivation reaction of radicals ($P^\bullet$) and thus decrease the control of polymerization. This observation agrees with the kinetic data in Figures 4.12 and 4.13.

4.3.2.2 Temperature Effects

MMA was also polymerized at 80 °C using three different combinations of ligand and spacer for CuBr (SG-PEG$_3$-TEDETA, SG-PEG$_1$-DiPA, SG-PEG$_3$-DiPA). The polymerization rates were higher than those of 60 °C. However, the spacer effects on the polymerization rate and molecular weight control were not as significant. The polymerizations had almost the same rates below 60 % conversion (Figure 4.16), but the polymerization with CuBr/SG-PEG$_1$-DiPA slowed down rapidly after the 60% conversion, whereas that with SG-PEG$_3$-TEDETA remained almost a constant rate. This may be caused by too fast polymerization due to high radical concentration. A high

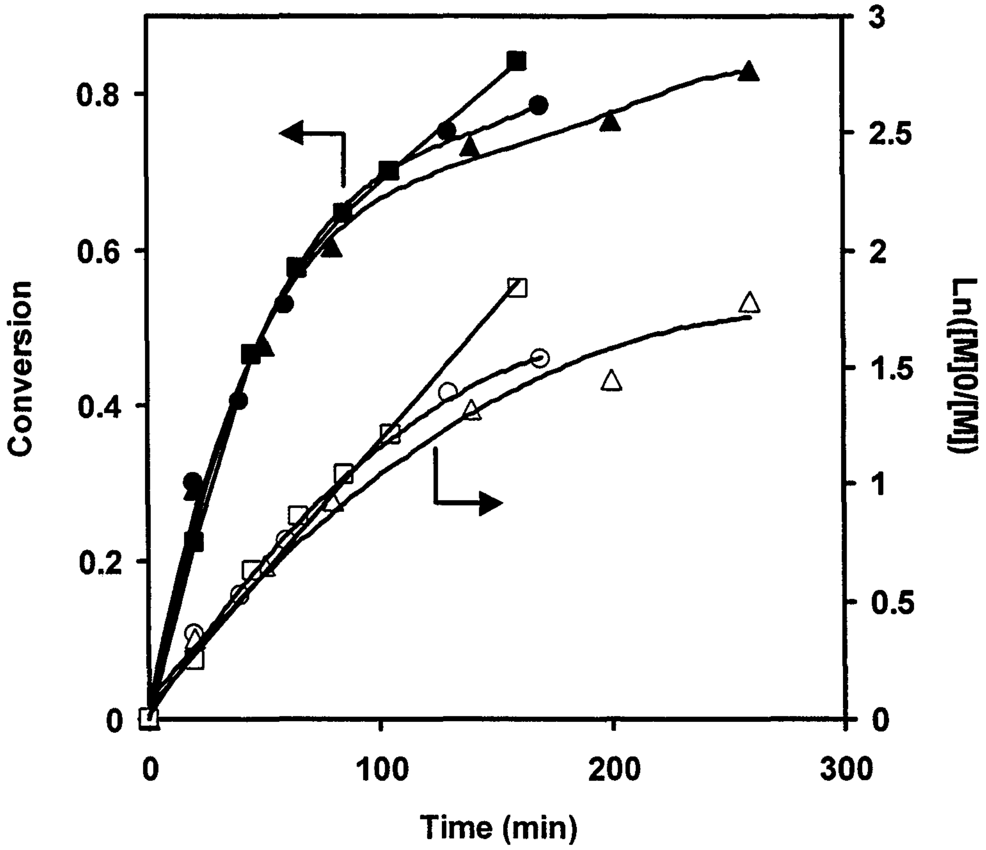

Figure 4.16. MMA polymerization in phenyl ether at 80 °C with silica gel support.

[MMA]=1.38 mol/L, [MBP]=9.2 $\times 10^{-3}$ mol/L, [CuBr]= 1.39×10^{-2} mol/L, [TEDETA] or [DiPA]/[CuBr] (molar) = 1, 80 °C; Support: SG-PEG$_3$-TEDETA (■, □); SG-PEG$_3$-DiPA (●,○); SG-PEG$_1$-DiPA (▲, △).

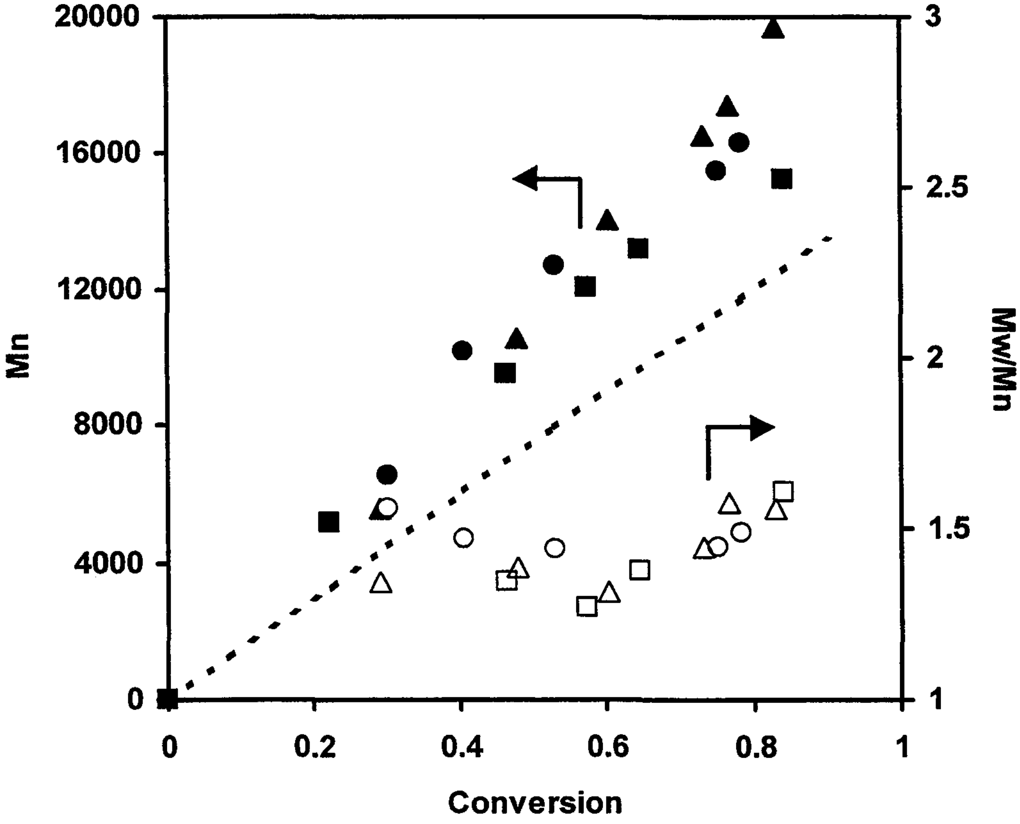

Figure 4.17. PMMA molecular weight and polydispersity as a function of conversion in phenyl ether at 80 °C with different TEDETA or DiPA -functionalized supports. See Figure 4.16 for other experimental conditions.

Support: SG-PEG$_3$-TEDETA (■, □); SG-PEG$_3$-DiPA (●, O); SG-PEG$_1$-DiPA (▲, Δ); theoretical Mn (-------).

radical concentration resulted in radical termination. This is particularly true for the catalyst immobilized by a short spacer length, which has slowed deactivation reaction rate.

The molecular weight developments of PMMA polymerized at 80 °C (Figure 4.17) were similar to those obtained at 60 °C. However, the polydispersities of PMMA at 80 °C were generally higher than those at 60 °C. The polydispersity in each case decreased gradually with the conversion and reached a minimal value at 60%, prior to its increase at high conversions. This broadening in molecular weight distribution was also caused by too fast polymerization rate. Equation 1.4 indicates that high polymerization rate caused high polymer polydispersity.

4.3.2.3 Catalyst/Initiator Ratio Effect

Figure 4.1 demonstrates that it was necessary to use excess catalyst of typical CuBr/initiator = 1.5 to mediate the polymerization for supported catalysts with a short spacer ($-CH_2-CH_2-CH_2-$ was used as the spacer) in order to achieve a controlled polymerization. However, the CuBr/initiator ratio could be lowered with longer spacers. Figure 4.18 shows the MMA polymerization using CuBr/initiator = 1 with SG-PEG_3-TEDETA or SG-PEG_1-TEDETA supports. The kinetic plots were similar to those of CuBr/initiator = 1.5 but the rates were slightly slower. The polymerization with SG-PEG_1-TEDETA was still slower than that with SG-PEG_3-TEDETA. At CuBr/MBP=1, the molecular weight control was improved and polydispersites were even lower than those with CuBr/initiator = 1.5 (Figure 4.19). Similarly the control of molecular weight

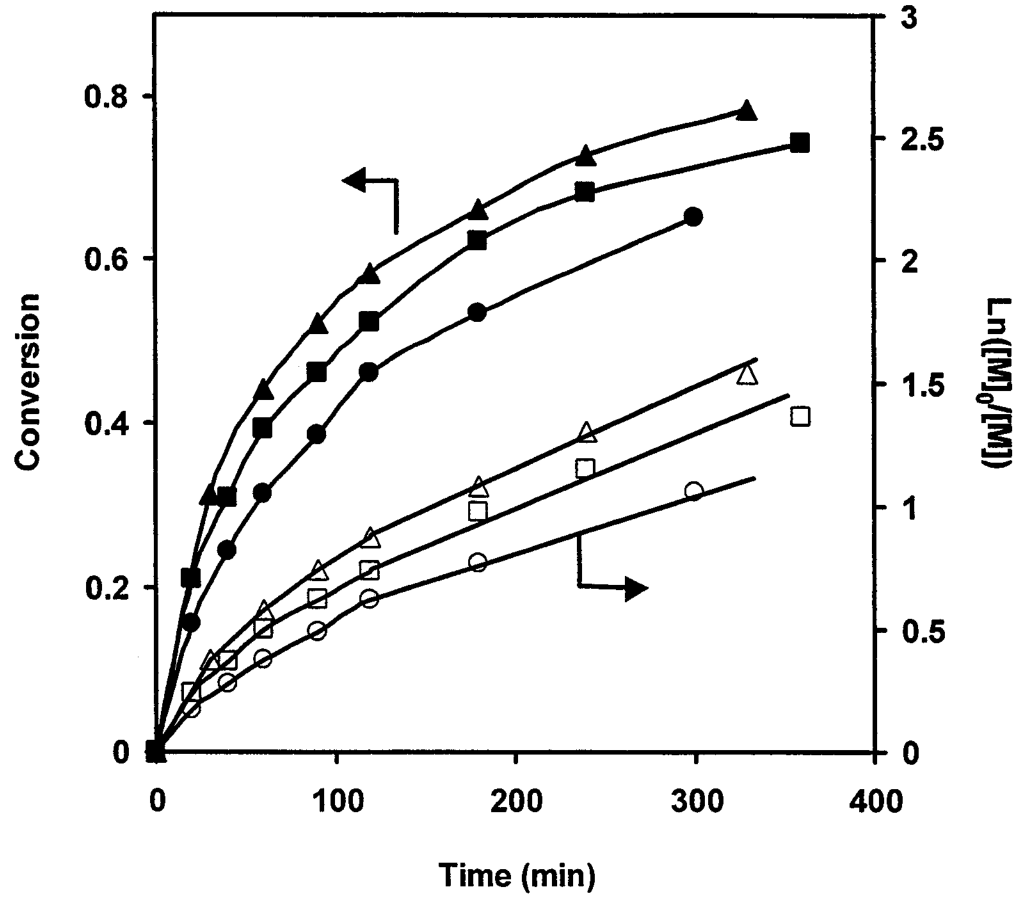

Figure 4.18. MMA polymerization with different CuBr/initiator ratios.

[MMA]= 1.38 mol/L, [MBP]= 9.2×10^{-3} mol/L, [TEDETA]/[CuBr] (molar) = 1, 60 °C, SG-PEG$_3$-TEDETA as support: [CuBr]= 9.2×10^{-3} mol/L (■, □), [CuBr]=1.39×10^{-2} mol/L (▲, Δ); SG-PEG$_1$-TEDETA as support: [CuBr]= 9.2×10^{-3} mol/L (●, O).

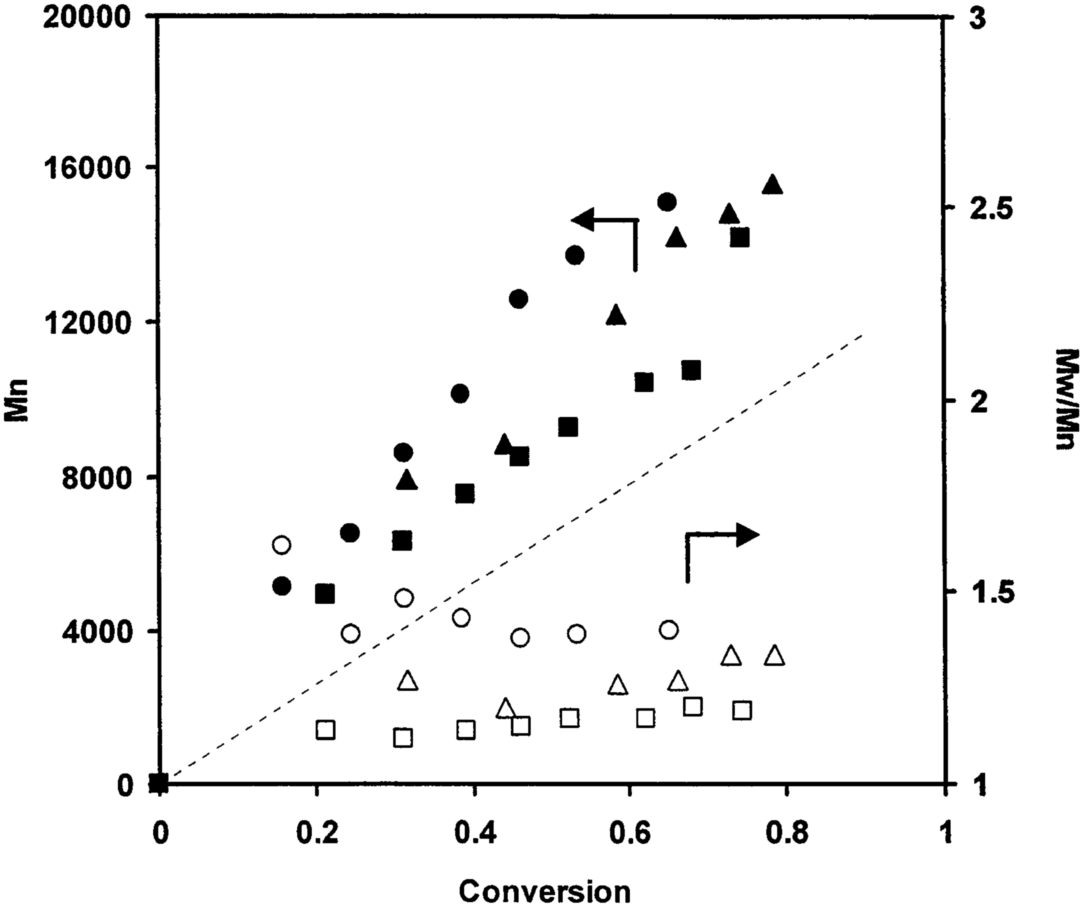

Figure 4.19. PMMA molecular weight and polydispersity as a function of conversion with different CuBr/MBP ratios. See Figure 4.18 for other experimental conditions.

SG-PEG$_3$-TEDETA as support: [CuBr]= 9.2×10^{-3} mol/L (■, □), [CuBr]=1.39×10^{-2} mol/L (▲, △); SG-PEG$_1$-TEDETA as support: [CuBr]= 9.2×10^{-3} mol/L (●, ○); theoretical Mn (------).

by CuBr/SG-PEG$_3$-TEDETA was better than that by CuBr/SG-PEG$_1$-TEDETA, in agreement with the results at CuBr/initiator=1.5. These comparisons suggest that the catalyst immobilized with PEG$_3$ spacer effectively mediated the MMA polymerization and did not require excessive catalyst (i.e., high CuBr/initiator ratio) to mediate the polymerization.

4.3.2.4 Catalyst Reuse

One of the major objectives of catalyst supporting is to recycle the catalyst. A series of catalyst recycling experiments were therefore carried out with SG-PEG$_1$-TEDETA and SG-PEG$_3$-TEDETA supports. The results are shown in Figures 4.20 and 4.21. MMA was first polymerized using silica gel supported catalyst. Upon completion, the reaction mixture was centrifuged and the solution was removed with cannula under nitrogen. The catalyst was washed three times with degassed phenyl ether. The same amounts of degassed solvent, MMA and initiator as in the first run were recharged to the recycled catalyst for a second run polymerization at 60 °C. Unlike the polymerization with fresh catalysts, the recycled catalysts had rather smooth curves without an initial decrease in rate. This is due to CuBr$_2$ in the recycled catalysts, which equilibrated with CuBr in the first run polymerization. The $\ln([M]_0/[M])\sim t$ plots with the recycled catalysts were linear throughout the polymerization and parallel to those with the fresh catalysts, indicating that the recycled catalysts had the same catalytic activity as the fresh ones in the late stage of polymerization.

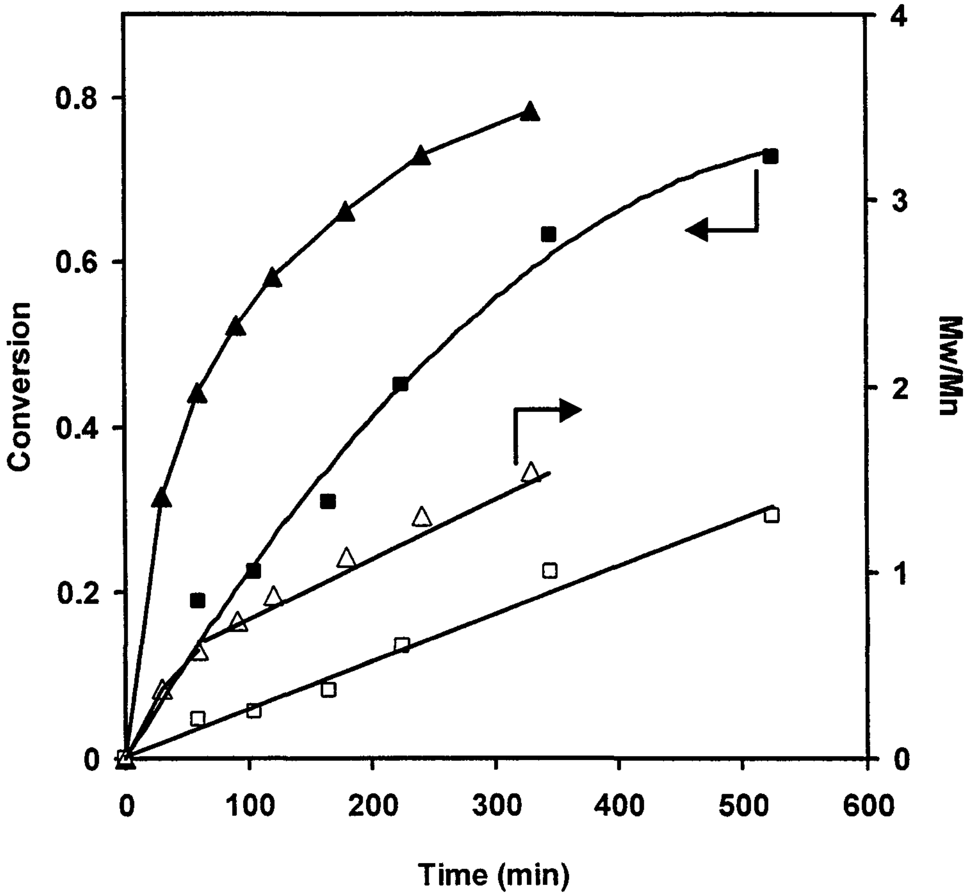

Figure 4.20. Reuse of SG-PEG3-TEDETA supported CuBr for MMA polymerization in phenyl ether.

[MMA] = 1.38mol/L, [MBP] = 9.2×10^{-3} mol/L, [CuBr] = 1.39×10^{-2} mol/L, [TEDETA]/[CuBr] = 1, 60 °C; fresh catalyst (▲, △); reused catalyst (■, □).

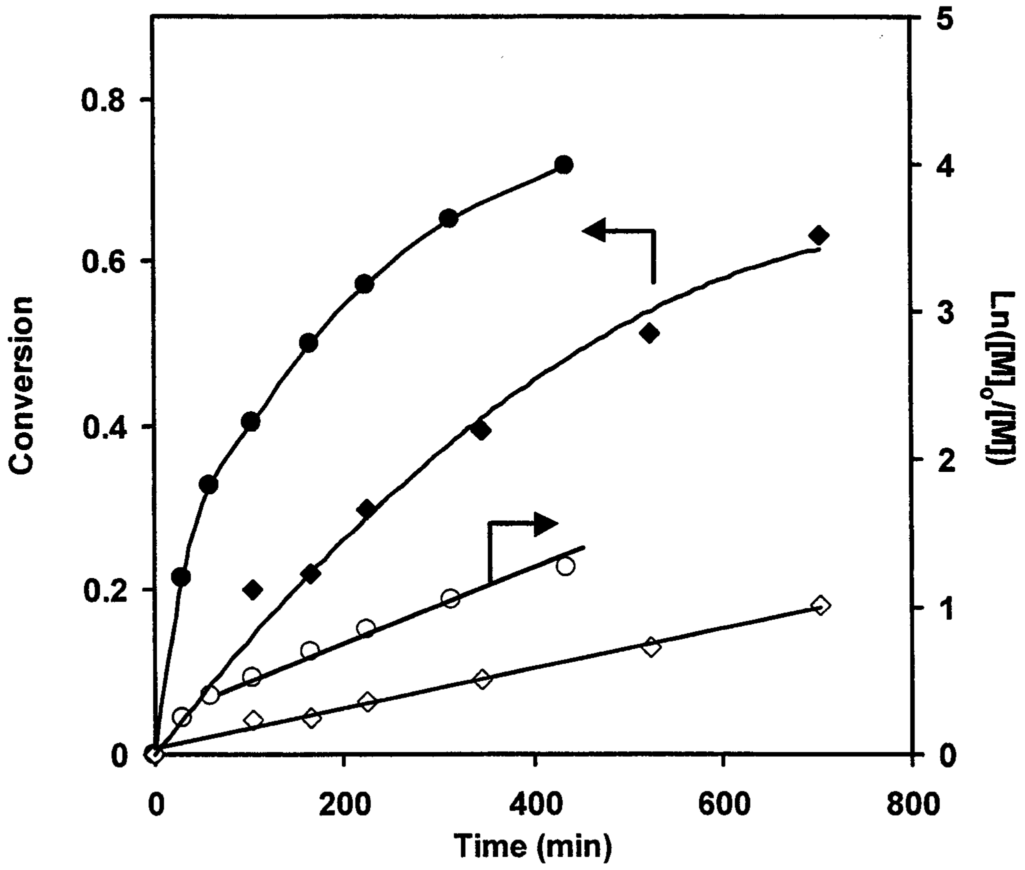

Figure 4.21. Reuse of SG-PEG$_1$-TEDETA supported CuBr for MMA polymerization.

[MMA] =1.38 mol/L, [MBP] = 9.2×10^{-3} mol/L, [CuBr] = 1.39×10^{-2} mol/L, [TEDETA]/ [CuBr] (molar) = 1, 60 °C; fresh catalyst (●, ○); reused catalyst (◆, ◇).

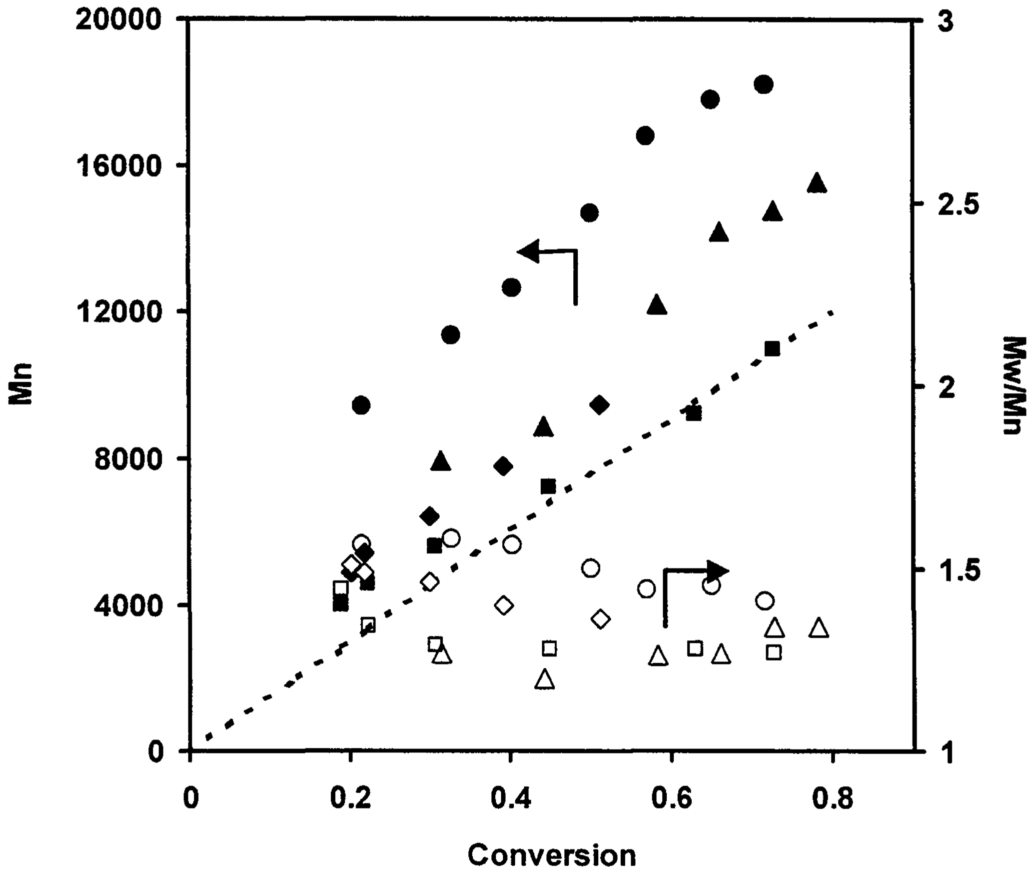

Figure 4.22. PMMA molecular weight and polydispersity as a function of conversion with fresh and recycled catalysts on different supports. See Figures 4.20 and 4.21 for experimental conditions.

SG-PEG$_3$-TEDETA: first use (▲, △); second use (■, □); SG-PEG$_1$-TEDETA: first use (●, ○); second use (◆, ◇); theoretical Mn (------).

Figure 4.22 shows the molecular weight and polydispersity of PMMA as a function of conversion with the fresh and recycled catalysts. In all cases, the molecular weights increased linearly with conversion. The molecular weights of PMMA prepared by the recycled catalysts were much closer to their theoretical values, i.e. higher initiator efficiencies. The initiator efficiency was about 100% catalyzed by the recycled CuBr/SG-PEG$_3$-TEDETA and 78% by the recycled CuBr/SG-PEG$_1$-TEDETA, compared to 75% and 57% by their corresponding fresh catalysts. These results indicate that the recycled catalysts had improved ability to regulate the chain growth. The improvement in the initiator efficiency was resulted from the Cu(II) in the recycled catalysts, which suppressed the radical termination by lowering the radical concentration.

4.3.2.5 Block Copolymerization of MMA with 2-(*N,N*-Dimethylamino)ethyl Methacrylate (DMAEMA)

The ability of the silica gel supported CuBr to mediate a block copolymerization was examined by sequential copolymerizing MMA and DMAEMA using re-initiation method. The DMAEMA polymerization by CuBr/SG-PEG$_3$-TEDETA was investigated first. Table 4.3 shows the DMAEMA polymerization with the CuBr/SG-PEG$_3$-TEDETA support. Similar to the MMA polymerization, the DMAEMA polymerization was also a first order reaction, but was much faster than the MMA polymerization. This is consistent with the higher ATRP polymerization rates in more polar solvents.[10,11] The molecular weights of poly(DMAEMA) were very closer to the predicted values with low polydispersities (1.2~1.4).

Table 4.3. DMAEMA polymerization catalyzed by CuBr supported on SG-PEG$_3$-TEDETA [a]

Time (min)	Conv.	Ln([M]$_0$/[M])	Mn(GPC)	Mn(Theor.)	Mw/Mn
20	0.27	0.31	8300	5525	1.21
50	0.44	0.58	10900	9016	1.24
80	0.56	0.82	13700	11402	1.23
110	0.69	1.16	15500	14027	1.31
170	0.75	1.37	16600	15209	1.28

[a] [DMAEMA= 1.38 mol/L, [MBP]=9.2 ×10^{-3} mol/L, [CuBr]= 1.39×10^{-2} mol/L, [TEDETA]/[CuBr] (molar) = 1, 60 °C; Solvent: phenyl ether.

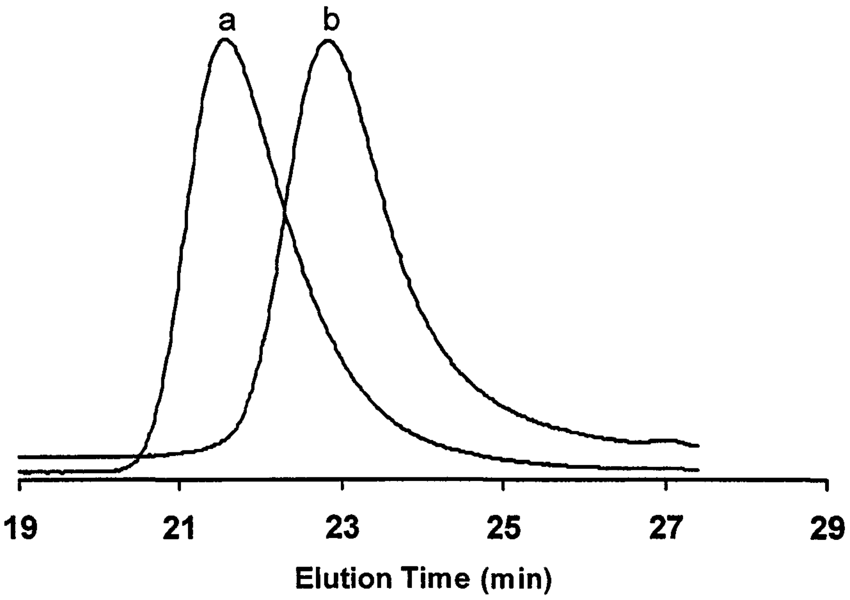

Figure 4.23. GPC traces of (a) Poly(MMA-b-DMAEMA) block copolymer and (b) PMMA macro-initiator.

[MBP]=9.2 $\times 10^{-3}$ mol/L, [CuBr]=1.39×10^{-2} mol/L, [TEDETA]/[CuBr] (molar) = 1, 60 °C; MMA/MBP (molar) = 80; DMAEMA/MBP (molar) = 80.

MMA (MMA/MBP=80) was first polymerized using CuBr/SG-PEG$_3$-TEDETA for 6 hours, yielding macro-initiator of PMMA with Mn=6900 and Mw/Mn= 1.22 (Mn theor = 6000) with 75 % conversion. The reaction was stopped and the unreacted MMA was removed by vacuum. DMAEMA was then added and the mixture was reheated to 60 °C for 8 hours. A block copolymer of Poly(MMA-b-DMAEMA) was isolated with 70% DMAEMA conversion. The resulting polymer had Mn of 14700 (Mn theor = 15700) and polydispersity of 1.46 without contamination of PMMA prepolymer (Figure 4.23). This demonstrates that the silica gel supported CuBr could be used for the block copolymerization.

4.4 Catalyst Residue Analysis

After the polymerization was complete, the flask was cooled to 20 °C and centrifuged at 4000 rpm. The green particles were recovered as described in *Catalyst Reuse* section. The clear polymerization solution (0.50 mL) was dissolved in 1.0 mL of H_2SO_4/HNO_3 (3/1 in v/v). While the mixture was heated at 100 °C, additional 2.5 mL of H_2SO_4/HNO_3 (3/1 in v/v) was gradually added. A clear yellowish solution was finally obtained and the solution was diluted to 50 mL with de-ionized water. The copper concentration in the aqueous solution was measured by Perkin Elmer Elan 6100 ICP-MS. The copper concentration in the polymerization solution was then calculated.

The measured copper concentration in the polymerization solution was about 13 ppm irrespective of the spacer used. For example, the copper concentration was 13.2 ppm when supported catalyst in Section 4.2 was used ($CH_2CH_2CH_2$ as spacer) and 12.9 ppm, 13.4 ppm, 12.7 ppm when SG-PEG$_3$-TEDETA-CuBr, SG-PEG$_1$-TEDETA-CuBr and SG-PEG$_3$-DiPA-CuBr were used as catalyst, respectively. This is equal to about 0.7% of the initial amount of the catalyst used. The precipitated PMMA from the solution was white without any color.

4.5 Conclusion

CuBr was immobilized on silica gel via grafted tetraethyldiethylenetriamine (TEDETA) for the ATRP of MMA. The supported CuBr mediated a living polymerization of MMA, yielding PMMA with controlled molecular weight and low polydispersity. The CuBr/initiator ratio significantly affected the polymerization. It is necessary to use more catalyst than initiator (CuBr/initiator >1) in order to achieve a living process for catalyst supported via a short spacer. The recycled catalyst still mediated a living polymerization of MMA, but had a reduced activity. The activity of recycled catalyst can be regained by reacting the catalyst with copper metal. The regenerated catalyst had a slightly lower activity than the fresh one, but mediated a living polymerization of MMA.

The spacer between the catalyst and its support strongly affected the ATRP polymerization rate and the control over molecular weight and polydispersity of the resulting polymers. For the supporting method reported in this work, the optimum spacer length was about 3 units of ethylene glycol, with which the supported catalyst had the highest activity and the best control over the molecular weight of PMMA. The recycled catalyst on these supports also retained much of its activity and improved the initiator efficiencies.

4.6 Reference

1. Hartley, F.R. *Supported Metal Complexes : A New Generation of Catalysts*, Boston, Kluwer Academic Publishers, **1985**.
2. Stiles, A. B. (ed), *Catalyst Supports and Supported catalysts : Theoretical and Applied Concepts*, Boston : Butterworths, **1987**.
3. Hodnett, B.K. et al. (ed), *Supported Reagents and Catalysts in Chemistry*, Cambridge, Royal Society of Chemistry, **1998**.
4. Haddleton, D. M.; Kukulj, D. and Radigue, A. P. *Chem. Commun,* **1999**, 99.
5. Kickelbick, G.; Paik, H.; and Matyjaszewski, K. *Macromolecules* **1999,** *32*, 2941.
6. Shen, Y.; Zhu, S.; Zeng, F. and Pelton, R. *Macromolecules* **2000**, *33*, 5399.
7. Matyjaszewski, K. Ed. *Controlled Radical Polymerization;* American Chemical Society: Washington, DC **1997**; ACS Symp. Ser. Vol. 685.
8. Matyjaszewski, K.; Coca, S.; Gaynor, S. G.; Wei, M.; Woodworth, B. E. *Macromolecules,* **1997**, *30*, 7348.
9. Zhu, S. *Macromolecular Theory and Simulations* **1999,** *8,* 29.
10. Matyjaszewski, K.; Nakagawa, Y.; Jasieczek, C. B. *Macromolecules* **1998,** *31*, 1535.
11. Percec, V.; Barboiu, B.; van der Sluis, M. *Macromolecules* **1998,** *31*, 4053.

Chapter 5

Atom Transfer Radical Polymerization on Soluble and Recoverable Supports

5.1 Introduction to Catalyst Support Effect

Chapters 3 and 4 and literature [1-6] demonstrated that catalysts immobilized on insoluble particles can be easily separated from the reaction mixture and be recycled and yield catalyst-free products. However, catalysts immobilized on insoluble particles less effectively control polymerizations. Generally, polydispersities of polymers produced by immobilized catalysts were higher then those of homogeneous systems and molecular weights were higher than the predicted (low initiator efficiency).

The study in Chapter 4 on the catalysts supporting spacer effect suggests that the lack of control of ATRP mediated by supported catalysts may be due to the heterogeneity of the reaction between supported catalysts and propagating radicals. A well-controlled ATRP is achieved only when generated radicals are deactivated quickly enough so that the radicals propagate only few units in each activating/deactivating cycle and the stationary radical concentration remains low.[7,8] Otherwise, the polymerization will proceed in a conventional free radical polymerization manner.[7,8] Compared with free catalyst molecules, the mobility and accessibility of the catalyst molecules bound on insoluble particles were substantially reduced. On the other hand, polymer chains adopt coil conformation in solution. The active polymer chain ends (terminal carbon-halide or radical) may be entrapped inside of these polymer coils and thus may have difficulty in accessing the catalytic sites on insoluble particle surface. These two factors limit the supported catalysts to efficiently deactivate radicals. It can thus be postulated that in a homogenous catalyst system, the catalyst molecules can diffuse more freely in solution and thus effectively regulate the chain growth. An ideal catalyst system is that the catalyst is soluble under reaction conditions to achieve a homogenous ATRP but precipitate at work-up condition for catalyst recycling.

Polyethylene (PE) is soluble in toluene at high temperature but insoluble at room temperature and thus was used as soluble recoverable support for small molecule reactions.[9-13] Brittain et al.[14] used it as support for ATRP of MMA. However, the polyethylene supported copper bromide was found to have very low activity even at 100 °C. The molecular weights of produced PMMA were controllable but the polydispersities were in the range of 1.4-1.5. We found that copper bromide supported on PE via polyethylene glycol (PEG) spacer had high activities for the polymerization of methacrylates and styrene, producing polymers with well-controlled molecular weights and low polydispersities. In this chapter, we investigated the PE support and PEG spacer effects on the MMA polymerization.

5.2 Experimental Section

5.2.1 Materials

Methyl methacrylate (99.9%, MMA) and 2-(*N,N*-dimethylamino)ethyl methacrylate (99.9%, DMAEMA), styrene (99.9%, St) from Aldrich were distilled under vacuum and stored at –15 °C. Polyethylene-*block*-poly(ethylene glycol) ($CH_3(CH_2CH_2)_x(OCH_2CH_2)_yOH$) with molecular weight of 875 (21%w/w of ethylene units) and 920 (50 % ethylene units) and α-hydroxylpolyethylene ($CH_3(CH_2CH_2)_mOH$) with molecular eight of 700 and 460 also from Aldrich were characterized by ^{1}H-NMR and the results were agreeable with the reported from Aldrich. They are designated as PE_{25}-PEG_4-OH, PE_{16}-PEG_{10}-OH, PE_{25}-OH, and PE_{16}-OH (the subscripts are the numbers of monomer units).

5.2.2 Supporting the Ligand onto the PE Support

The catalyst supporting procedure is shown in Scheme 5.1. Polyethylene-*block*-poly(ethylene glycol) (PE_{25}-PEG_4-OH, PE_{16}-PEG_{10}-OH) or α-hydroxyl-polyethylene (PE_{16}-OH, PE_{25}-OH) was end-capped with acryloxyl group by the reaction of terminal hydroxyl group with acrylic chloride. The Michael reaction of the acryloxyl group with tetraethyldiethylenetriamine (TEDETA) attached the ligand onto the support. The typical procedure is as follows:

PE_{25}-PEG_4-OH (20g, 0.0228 mole) was dissolved in toluene (200 mL) at 90 °C under nitrogen atmosphere. The solution was cooled slowly to room temperature. Precipitated PE_{25}-PEG_4-OH was centrifuged. The solid was dispersed in 200 mL THF-Et_3N (5/1 in v/v) at ambient temperature. Acryloyl chloride (3.6 mL, 0.0442 mole)

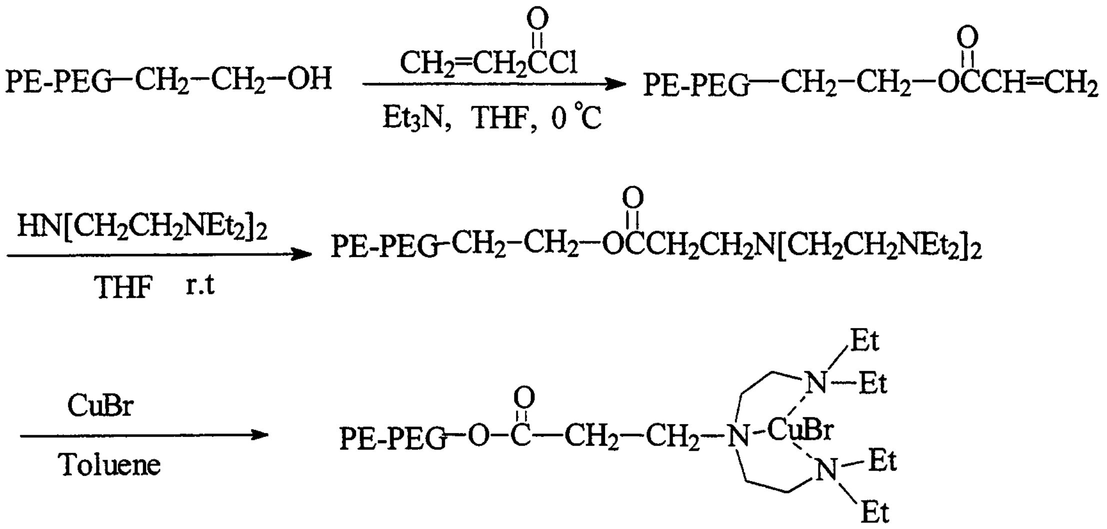

Scheme 5.1. Supporting the catalyst onto polyethylene via tetraethyldiethylenetriamine (TEDETA)

diluted in 10mL THF was dropwise added to this mixture. The mixture was stirred for overnight and then centrifuged. The solid was washed successively seven times with THF, ten times with water and twice with THF. The solid was then dispersed in 25 mL TEDETA and stirred for 48 h (Michael reaction) at ambient temperature. The solid was separated by centrifugation, washed with THF ten times and dried under vacuum at 30 °C. ^{1}H-NMR in deuterated toluene (80 °C, 300MHz):

$(CH_2\text{-}CH_2)_x(OCH_2CH_2)_yCH_2CH_2OC(O)CH_2CH_2N[CH_2CH_2N(CH_2CH_3)_2]_2$ (PE_{25}-PE_4-TEDETA)

1.3 ppm (CH_2 in PE segments), 3.65ppm(CH_2 in PEG segment), 4.2ppm ($COOCH_2$), 2.7ppm($OC(O)CH_2$), 2.5ppm (NCH_2), 1.0 ppm (NCH_2CH_3), 0.87ppm (CH_3 at the PE end). The intensity ratio is 108:21.1:2.69:2.67:13.1:9.1:4.0. 42% of PE_{25}-PEG_4-OH ends was capped with TEDETA ligand.

Similar method was used to synthesize other ligands: PE_{16}-PE_{10}-TEDETA (32.6% capped); PE_{16}-TEDETA (20.1% capped); PE_{25}-TEDETA (13.7% capped).

5.2.3 Polymerizations

In a typical polymerization run, CuBr (0.011g, 0.0764 mmole), PE_{25}-PEG_4-TEDETA (0.3g), toluene (5g) were charged to a Schlenk flask and degassed with several vacuum/nitrogen cycles. Then degassed MMA (1.0g) was introduced by syringe and stirred. After the PE_{25}-PEG_4-TEDETA support was thoroughly dispersed, degassed methyl α-bromophenylacetate (12 μL, 0.0757 mmol) was dropwise added to the mixture with stirring. The slightly yellowish solution immediately turned green. The mixture was further stirred at room temperature for 30 min. Then the flask was immersed in an oil bath (80 °C) for polymerization. The polymerization solution (0.05 –0.1 mL) was withdrawn at different intervals to analyze the conversion (by NMR) and molecular weight (GPC). For styrene polymerization a small amount of γ-butyrolactone was added as an internal reference for ^{1}H-NMR for conversion calculation.

5.2.4 Block Copolymerization

CuBr(0.011 g, 0.0764 mmol), PE_{25}-PEG_4-TEDETA(0.3 g) and toluene (2.5 g) were added to a Schlenk flask and degassed as described above. Degassed MMA (0.60 g, 6.0 mmol) and methyl α-bromophenylacetate (12 μL, 0.0757 mmol) were added. The mixture was immersed in an 80 °C oil bath for 10 h. A small amount of this mixture (~0.05 mL) was withdrawn to analyze the conversion by NMR (Conv. 90%) and molecular weight by GPC (Mn = 8500, Mw/Mn = 1.09). Then the flask was connected to vacuum to remove the volatiles. Degassed DMAEMA (1.26 g, 8.0 mmol) and toluene (2.5 mL) were charged to the flask and stirred for 10 min. Then the flask was reheated at 80 °C for 10 h (Conversion, 79%; Mn = 21000, Mw/Mn=1.26).

5.2.5 Catalyst Reuse

After the polymerization is complete, the flask was lifted from the oil bath and centrifuged at 0 °C. The supernatant was carefully removed by cannula with nitrogen. The leftover green solid in the flask was washed three times with 20 mL (total) degassed toluene under nitrogen. The same amounts of degassed MMA, toluene, and initiator, as in the first run, were added to the flask and reheated to 80 °C. The same procedure as that for the first run was repeated.

5.2.6. Catalyst Residue Analysis

After the polymerization was complete, the flask was cooled to 20 °C or 0 °C and centrifuged at 6000 rpm for 10 min. The precipitate was separated from the solution. The clear solution (0.50 mL) was dissolved in 1.0 mL of H_2SO_4/HNO_3 (3/1 in v/v). While the mixture was heated at 100 °C, additional 2.5 mL of H_2SO_4/HNO_3 (3/1 in v/v) was gradually added. A clear yellowish solution was finally obtained and the solution was diluted with 50 ml de-ionized water. The copper concentration in the aqueous solution was measured by Perkin Elmer Elan 6100 ICP-MS. The copper concentration in the polymerization solution was then calculated.

5.2.7 Measurements

Nuclear magnetic resonance (NMR) spectroscopy: Proton (^1H) NMR spectra were recorded on a Bruker ARX-200 or 300 spectrometer at 200 or 300MHz. ^1H NMR chemical shifts in $CDCl_3$ were reported downfield from 0.00 ppm using TMS as an internal reference.

Molecular weight measurements: Number and weight average molecular weights (M_n and M_w, respectively) were determined by gel permeation chromatography (Columns: TSK G2500HB, G3000HXL, 7000HXL) using THF-2% (v/v) triethylamine as solvent at 25 °C with a RI detector. Narrow polystyrene standards (Polysciences) were used to generate a universal calibration curve (K_{PS}=0.000128, α_{PS}=0.712; K_{PMMA}=0.000128, α_{PMMA}=0.69). Data were recorded and manipulated using the Windows based Millennium software package.

5.3 Results and Discussion

5.3.1 PE Support and PEG Spacer Effects

The MMA polymerization catalyzed by CuBr with PE or PE-b-PEG as supports is shown in Figures 5.1 and 5.2. N'-(n-butyloxycarbonyl)-N,N,N'',N''-tetraethyl diethylenetriamine (PE_2-TEDETA), which has the same structure as other PE-TEDETA but only two ethylene units, was also synthesized from n-butyl acrylate and TEDETA in order to compare the PE chain length effect. All catalysts immobilized on PE based supports completely dissolved in toluene solution of MMA at 70 °C or above, but only part of the catalyst dissolved in the toluene solution of MMA when PE_2-TEDETA was used as ligand. Therefore for PE_2-TEDETA-CuBr catalyzed MMA polymerization, a small amount of γ-butyrolactone was added in order to obtain a homogeneous polymerization as other systems did. Figure 5.1 shows that except PE_{25}-TEDETA-CuBr system, all the polymerizations proceeded at 80 °C in typical first order kinetics, suggesting a constant radical concentration throughout each polymerization run. The polymerization with PE_{25}-TEDETA-CuBr was also first order reaction at the early stage, but bent from the linearity after medium conversion, indicating a decrease in radical concentration.

The type of support strongly affected catalyst activity, as summarized in Table 5.1. Firstly, the PE chain length strongly affects on the polymerization rate (Table 5.1). For catalyst directly supported onto PE via TEDETA (PE_2, PE_{16}, PE_{25}), the catalytic

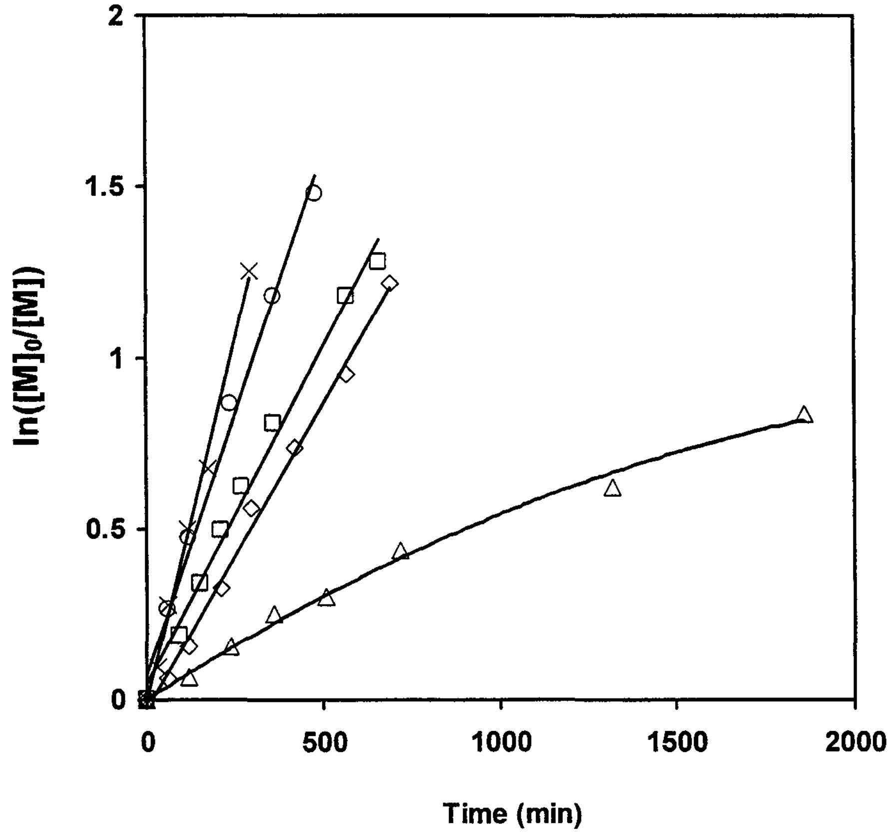

Figure 5.1. Polymerizations of MMA catalyzed by CuBr on different supports

[CuBr] = [MBP] = 0.0115 mol/L, PE-PEG-TEDETA or PE-TEDETA/CuBr = 1.5, [MMA]= 1.5 mol/L, 80 °C. PE_2-TEDETA (×); PE_{16}-PEG_{10}-TEDETA (○); PE_{25}-PEG_4-TEDETA (□); PE_{16}-TEDETA (◇); PE_{25}-TEDETA (△).

activity substantially decreased as the PE length increased. The apparent polymerization rate constant ($k_p[R^\bullet]$) was 4.2×10^{-3} min^{-1} with PE_2-TEDETA, 1.79×10^{-3} min^{-1} with PE_{16}-TEDETA, and only 0.66×10^{-3} min^{-1} with PE_{25}-TEDETA as support, respectively. The low activity was also found in Schiff-base CuBr system when PE with molecular weight of 2000 (71 units) was used as support.[14] Second, this deteriorating effect of PE support on catalytic activity could be minimized by supporting the catalyst on PE via PEG spacer, as shown in Figure 5.1 and Table 5.1. The polymerization rate constants with PE_{25}-PEG_4-TEDETA and PE_{16}-PEG_{10}-TEDETA were 1.97×10^{-3} min^{-1} and 3.04×10^{-3} min^{-1}, compared with 0.66×10^{-3} min^{-1} using PE_{25}-TEDETA and 1.79×10^{-3} min^{-1} using PE_{16}-TEDETA as support, respectively.

Figure 5.2 show the molecular weight of PMMA as a function of conversion in the MMA polymerizations mediated by CuBr on different supports. Generally the molecular weight of PMMA obtained from the different systems increased with conversion. The PMMA molecular weights obtained from the other systems except the PE_{25}-TEDETA-CuBr were very close to the theoretical values, but those by PE_{25}-TEDETA-CuBr were much higher than the predicted with an initiator efficiency about 0.50. The polydispersities of the prepared polymers were less than 1.2 at conversions less than 70%, similar to those prepared by CuBr complexed with small molecular ligand (Chapter 2) but much lower than those obtained by CuBr supported on insoluble particles (Chapter 4).[1-6] When the MMA conversion was higher than 70%, the polydispersity of PMMA increased rapidly with conversion.

Table 5.1. The apparent rate constants of MMA polymerizations with different supports [a]

Support	PE units	EG units in PEG spacer	k^{app} ($k_p[P^\bullet]$) $\times 10^3$
PE_{16}-PEG_{10}	16	10	3.04
PE-$_{25}$-PEG_4	25	4	1.97
PE_2	2	0	4.2
PE_{16}	16	0	1.79
PE_{25}	25	0	0.66

a: See Figure 5.1 for experimental conditions.

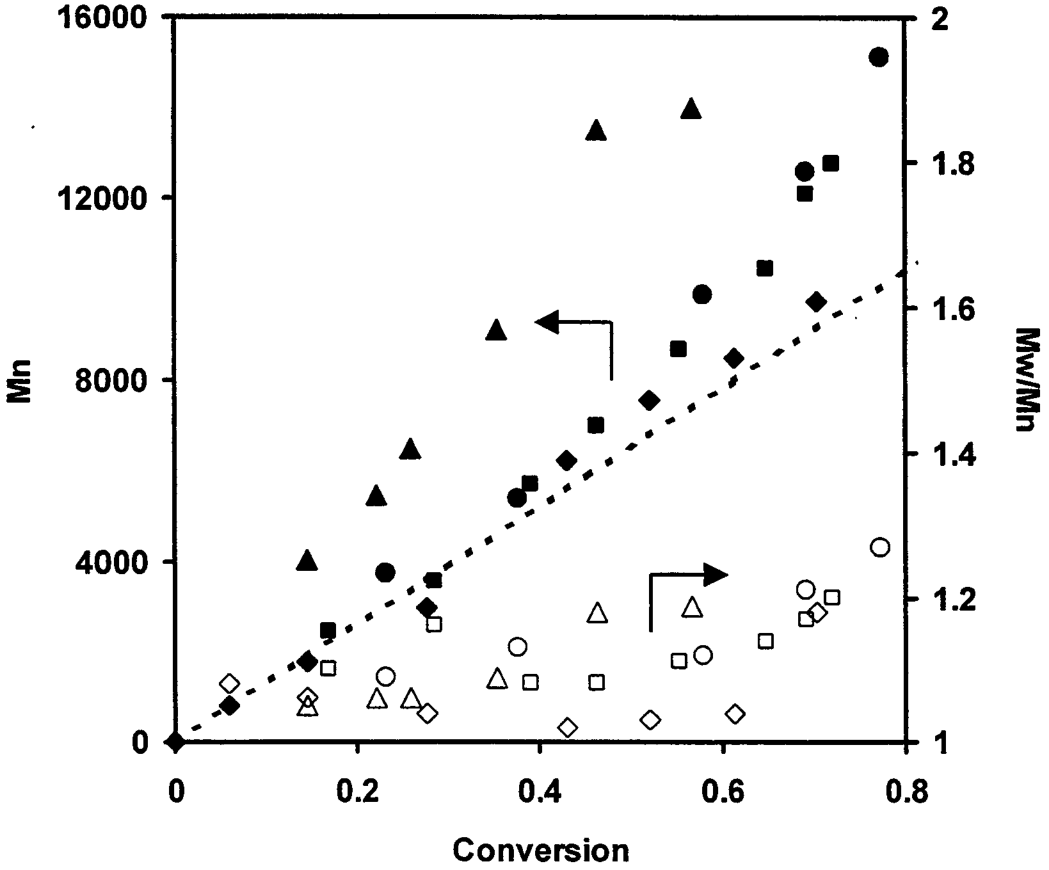

Figure 5.2. PMMA molecular weight and polydispersity as a function of conversion in polymerizations of MMA catalyzed by CuBr on different supports. See Figure 5.1 for the experimental conditions. PE_{16}-PEG_{10}-TEDETA (■,□); PE_{25}-PEG_4-TEDETA (●,○); PE_{16}-TEDETA (◆, ◇); PE_{25}-TEDETA (▲,△).

5.3.2 Influence of Temperature

Figure 5.3 shows the effects of temperature on the polymerization. The activity of the catalyst on PE_{25}-TEDETA support had a very strong temperature dependence, while the temperature dependence of catalyst on PE_{25}-PEG_4-TEDETA support was not so strong. The initial k^{app} of MMA polymerization by PE_{25}-TEDETA-CuBr increased from 0.65×10^{-3} min^{-1} to 3.75×10^{-3} min^{-1} with the temperature increasing from 80 °C to 100 °C, while the k^{app} for polymerization with PE_{25}-PEG_4-TEDETA-CuBr increased only by 50% with temperature increasing from 70 °C to 80 °C. On the other hand, while the polymerizations with PE_{25}-PEG_4-TEDETA-CuBr maintained a first order reaction at both 70 °C and 80 °C, the polymerization with PE_{25}-TEDETA-CuBr still experienced deviation from the first order reaction, i.e. decreasing radical concentration from the $\ln([M]_0/[M]=kp[R^\bullet]t$ equation, for conversions higher than 40%, as observed in the polymerization at 80 °C.

Temperature did not affect the polymer molecular weight control of PE_{25}-PEG_4-TEDETA-CuBr (Figure 5.4). However, the molecular weights of PMMA obtained by PE_{25}-TEDETA-CuBr at 100 °C were much closer to the theoretical values than those prepared at 80 °C, suggesting the much better control of the polymerization at 100 °C than the polymerization at 80 °C by PE_{25}-TEDETA-CuBr.

The above results demonstrated that supporting the catalyst to polyethylene via PEG spacer resulted in an increased polymerization rate and better control of polymer

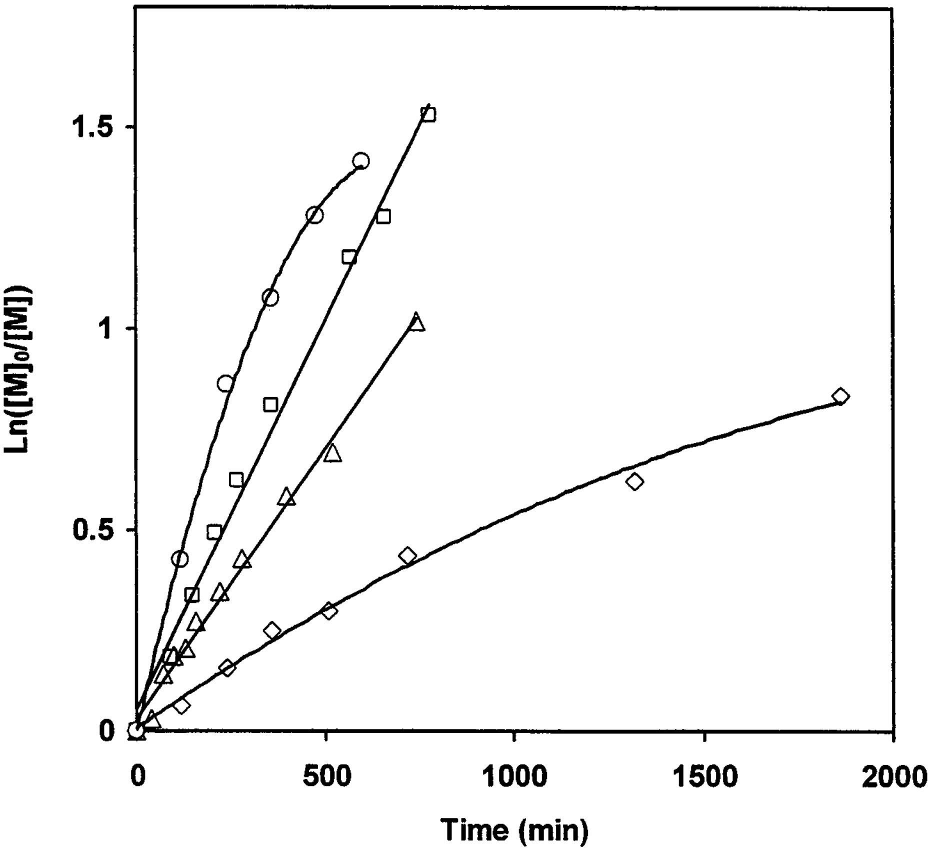

Figure 5.3. MMA polymerizations at different temperatures catalyzed by CuBr on PE_{25}-PEG_4-TEDETA and PE_{25}-TEDETA.

[CuBr] = [MBP] = 0.0115 mol/L, PE_{25}-PEG_4-TEDETA or PE_{25}-TEDETA/CuBr = 1.5, [MMA]= 1.5 mol/L, 80 °C. PE_{25}-PEG_4-TEDETA: 80 °C (□), 70 °C (Δ); PE_{25}-TEDETA: 100 °C (○), 80 °C (◊)

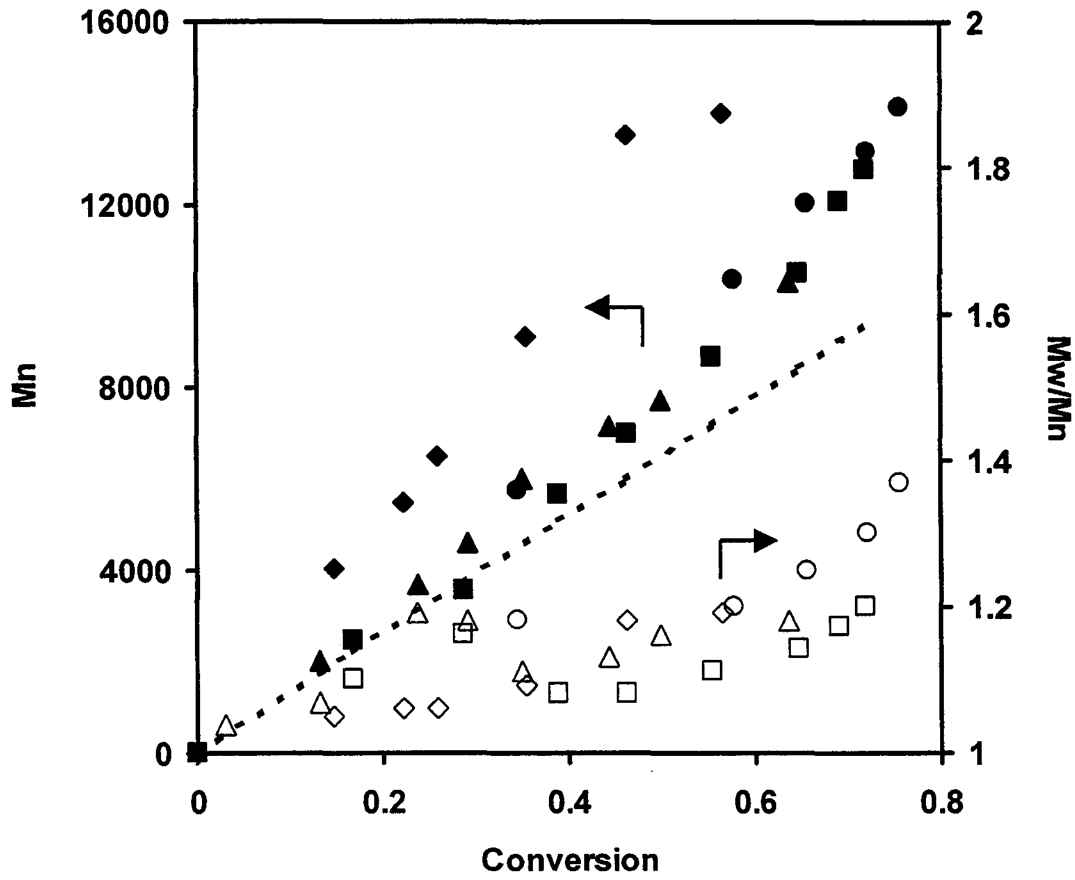

Figure 5.4. PMMA molecular weight and polydispersity as a function of conversion in MMA polymerizations at different temperatures catalyzed by CuBr on PE_{25}-PEG_4-TEDETA and PE_{25}-TEDETA. See Figure 5.3 for experimental conditions.

PE_{25}-PEG_4-TEDETA: 80 °C (■, □), 70 °C (▲, △); PE_{25}-TEDETA: 100 °C (●, ○), 80 °C (◆, ◇).

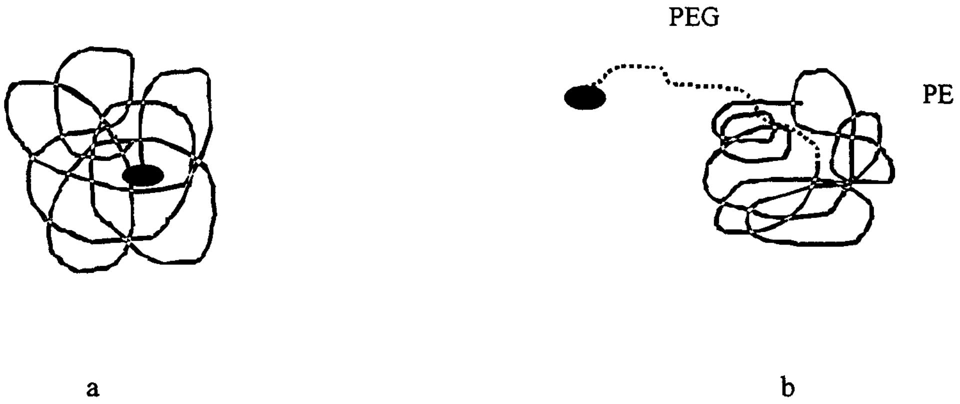

Scheme 5.2. The sketches of PE and PE-PEG supported catalysts

a: PE supported catalyst

b: PE-PEG supported catalyst

chain growth compared with grafting the catalyst directly to the PE support. Polyethylene has a high tendency to crystallize and thus dissolves in toluene only at higher temperature, e.g. 100 °C. Even though low molecular weight PE (PE oligomers) can dissolve in toluene at relatively lower temperature, e.g. 80 °C, their chains may not be in the configuration of extended coils in solvent but aggregate together. Therefore the catalyst directly attached on the PE chain may be trapped inside the compacted PE coils (Scheme 5.2a). Consequently, the catalyst would not be able to effectively activate dormant ends (P-Br), resulting in a low polymerization rate. The catalyst trapped in the PE coils may also not effectively deactivate the produced radicals ($P^\bullet$), resulting in radical terminations and consequently low initiator efficiencies. This was especially true at 80 °C, as seen in the MMA polymerization catalyzed by PE_{25}-TEDETA-CuBr at 80 °C (Figures 5.1 and 5.2). At 100 °C, the PE coils became less compacted. The catalyst could access to the dormant/active propagating ends easier and therefore had much higher activity and more effectively regulated the chain growth. As the PMMA chains grew longer, the propagating PMMA ends (P-Br and $P^\bullet$) might also be trapped in their own PMMA chain coils, which made the catalyst difficult to access the polymer propagating centers again, resulting in a slowed reaction between P-Br and thus slower polymerization (Figures 5.2 and 5.4).

When the catalyst is grafted to PE via PEG spacer, the flexible PEG chains render the catalyst more freedom. Therefore, the catalyst not only reacts more efficiently with the P-Br to have higher polymerization rate, but also deactivate radicals more quickly to

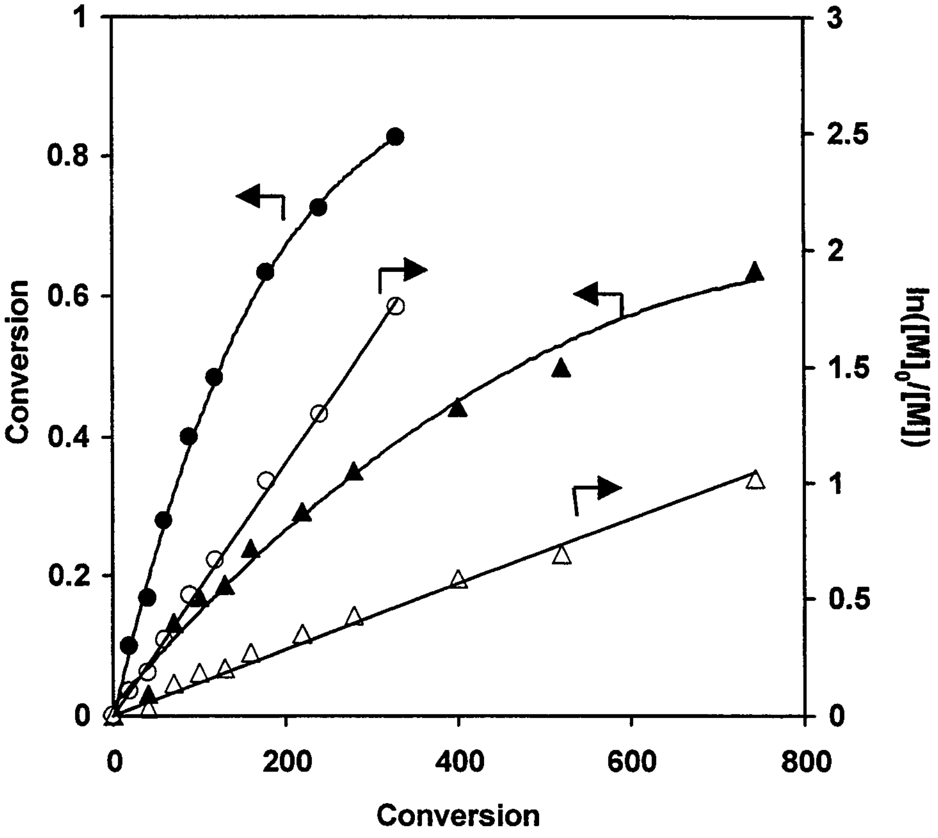

Figure 5.5. MMA polymerizations in different solvents.

[CuBr] = [MBP] = 0.0115 mol/L, PE_{25}-PEG_4-TEDETA /CuBr = 1.5, [MMA]= 1.5 mol/L, 70 °C. Solvent: toluene (▲, △), phenyl ether (●, ○).

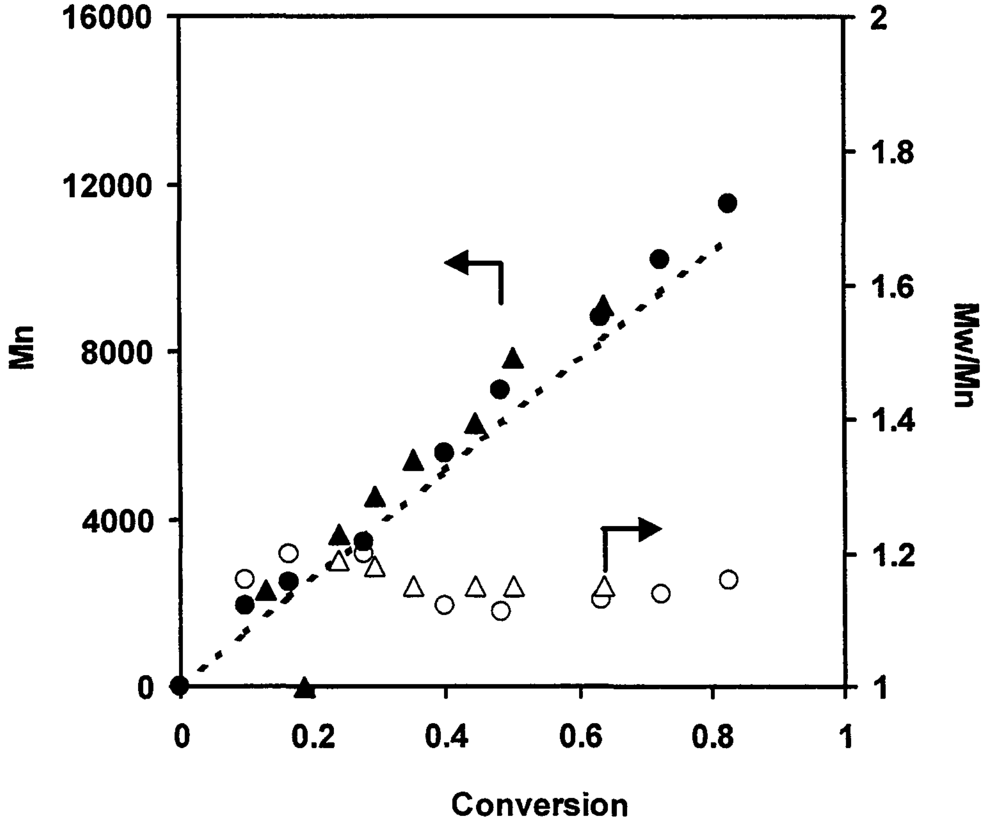

Figure 5.6. PMMA molecular weight and polydispersity as a function of MMA conversion in MMA polymerizations catalyzed by PE_{25}-PEG_4-TEDETA-CuBr in phenyl ether and toluene. See Figure 5.5 for experimental conditions.

Solvent: phenyl ether(●, ○); toluene (▲, △)

effectively regulate the chain growth. The similar spacer effect was also found in the PMMA polymerization mediated by silica gel supported catalysts (Chapter 4).

5.3.3 Solvent Selection

The polymerizations in different solvents catalyzed by PE_{25}-PEG_4-TEDETA-CuBr were also compared. The polymerization in polar solvent had faster polymerization rate than that in toluene. For example, the k^{app} of the polymerization in phenyl ether at 70 °C was 5.4×10^{-3} min^{-1}, compared with 1.4×10^{-3} min^{-1} in toluene (Figure 5.5). This agrees with the report that a polar solvent gave higher ATRP rate.[15,16] The molecular weights of PMMA prepared in phenyl ether were also well agreeable with the theoretical values (Figure 5.6). However, the catalyst in phenyl ether was found very difficult to be separated from the polymerization solution. The green catalyst suspended in solution like gel and could not precipitate from the solution even by centrifugation. Therefore toluene is a better solvent in terms of catalyst recycling.

5.3.4 Reuse of Catalysts on Different Supports

The recyclibility of the catalyst on each support was assessed using the recovered catalyst in a subsequent MMA polymerization run. After the polymerization was complete and the solution was cooled to zero degree, green solids precipitated from the solution were recovered by centrifugation. After washed with degassed toluene, the solids were mixed with monomer, solvent and initiator and the mixture was reheated to

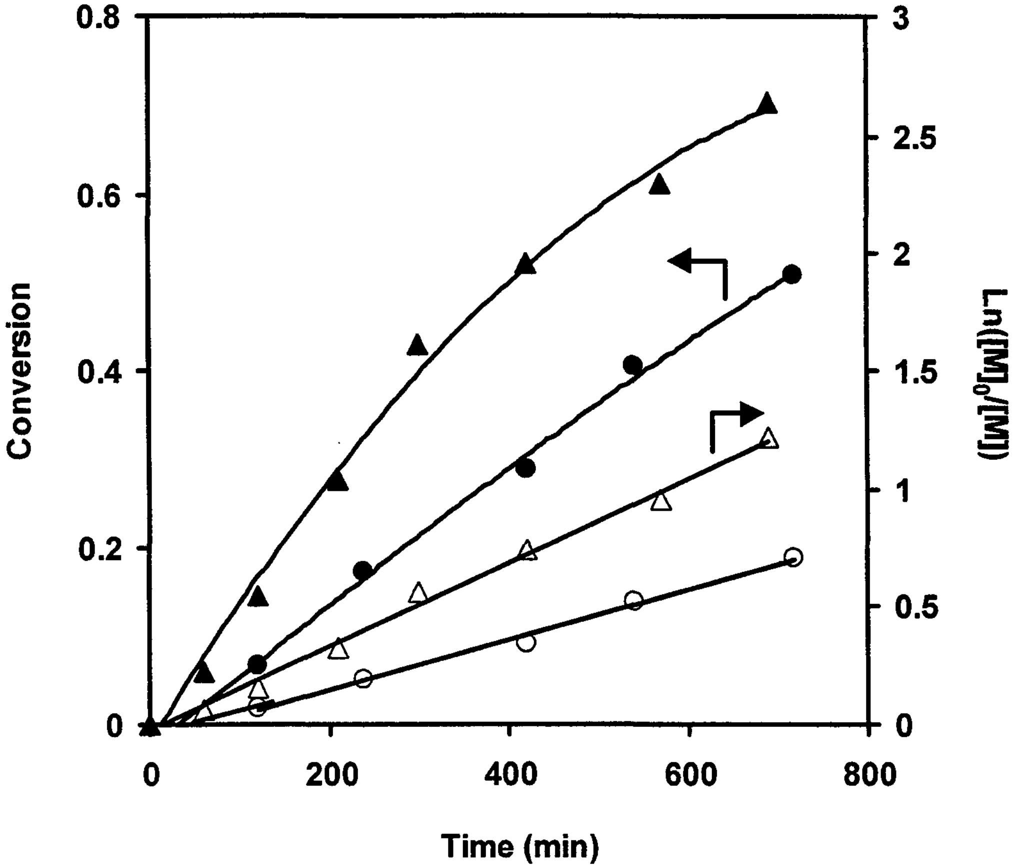

Figure 5.7. Reuse of PE_{16}-TEDETA-CuBr for the MMA polymerization.

[CuBr] = [MBP] = 0.0115 mol/L, PE_{16}-TEDETA/CuBr = 1.5, [MMA]= 1.5 mol/L, 80 °C; First use (▲, △) and second use (●, ○).

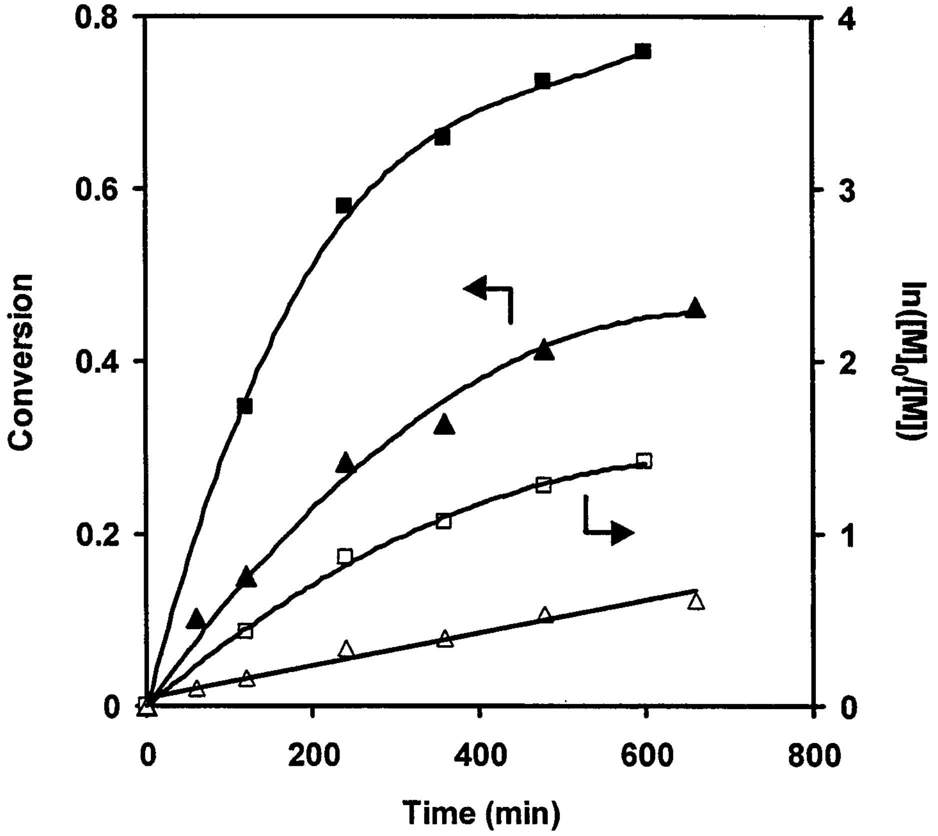

Figure 5.8. Reuse of PE$_{25}$-TEDETA-CuBr for the MMA polymerization.

[CuBr] = [MBP] = 0.0115 mol/L, PE$_{25}$-TEDETA/CuBr = 1.5, [MMA]= 1.5 mol/L, 100 °C; First use (■,□) and second use (▲, △).

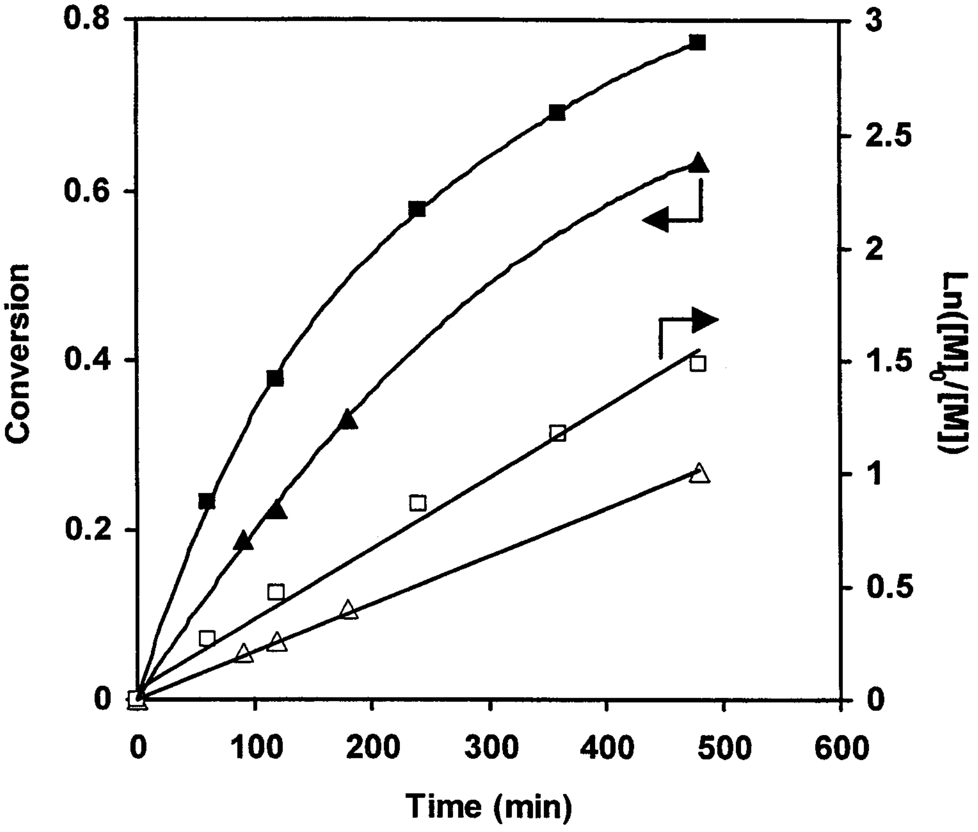

Figure 5.9. Reuse of PE$_{16}$-PEG$_{10}$-TEDETA-CuBr for the MMA polymerization. [CuBr] = [MBP] = 0.0115 mol/L, PE$_{16}$-PEG$_{10}$-TEDETA/CuBr = 1.5, [MMA]= 1.5 mol/L, 80 °C; First use (■,□) and second use (▲, Δ).

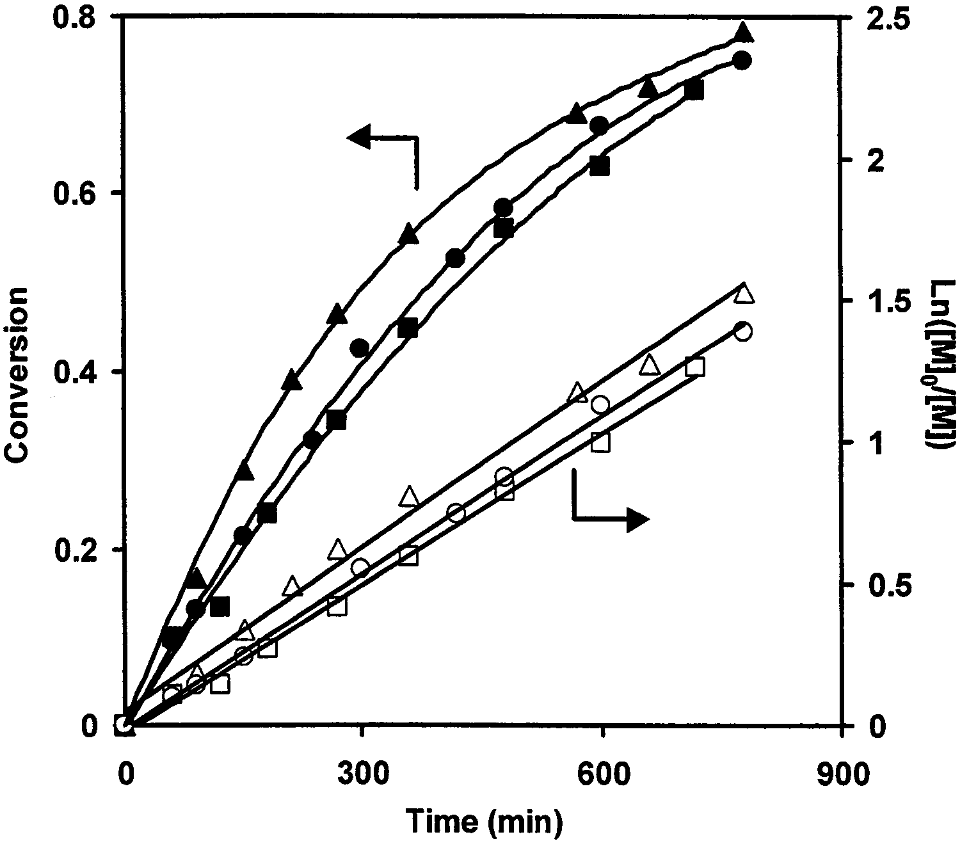

Figure 5.10. MMA polymerizations with fresh and recycled PE_{25}-PEG_4-TEDETA-CuBr catalysts.

[CuBr] = [MBP] = 0.0115 mol/L, PE_{25}-PEG_4-TEDETA/CuBr = 1.5, [MMA]= 1.5 mol/L, 80 °C; Fresh catalyst (▲, Δ), second used catalyst (● , O), third used catalyst(■,□).

80 °C or 100 °C (for PE_{25}-TEDETA support). Figures 5.7, 5.8, 5.9 and 5.10 are the MMA polymerizations with fresh and recycled catalysts on different supports. All the recycled catalysts on different supports still mediated first order reaction, but their catalytic activity retentions strongly depended on the supports used. The catalyst activity retained 61% of its fresh activity for PE_{16}-TEDETA-CuBr, 31% for PE_{25}-TEDETA-CuBr, 67% for PE_{16}-PEG_{10}-TEDETA-CuBr, and 90% for PE_{25}-PEG_4-TEDETA-CuBr, respectively.

The activity reduction of the recycled catalysts was generally found in other recycled supported catalysts for ATRP (Chapters 3 and 4). There were several reasons that might cause the decrease in the activity of recycled catalysts. First, in recycled catalysts there was some $CuBr_2$ produced in the first run polymerization, which equilibrated with CuBr during the first run polymerization. It has been demonstrated that a small amount of $CuBr_2$ could significantly decrease the catalytic activity.[7,8] This was also found in the silica gel supported catalysts, as reported in Chapters 3 and 4. Secondly, the loss of catalyst during recycling could also decrease the catalyst activity. The solubility of PE_{16}-TEDETA-CuBr and PE_{16}-PEG_{10}-TEDETA-CuBr was about 18 mg/g toluene, while the solubility of PE_{25}-TEDETA-CuBr and PE_{25}-PEG_4-TEDETA-CuBr was less than 0.15 mg/g toluene at 0 °C. Thirdly, there might some side reactions of the catalyst. This was particularly true for PE_{25}-TEDETA-CuBr system. It was noticed that after heated to 100 °C, the color of PE_{25}-TEDETA-CuBr catalyst turned to deep brown, in contrast to the green color of catalysts polymerized at 70 or 80 °C. Therefore the loss of catalyst during recycling due to high solubility also contributed to the catalytic activity reduction of recycled PE_{16}-TEDETA-CuBr and PE_{16}-PEG_{10}-TEDETA-CuBr. The reduction in catalytic activity of recycled PE_{25}-TEDETA-CuBr was mainly caused by side reactions at high temperature rather than catalyst loss.

PE_{25}-PEG_4-TEDETA-CuBr retained a high activity even in the third use (Figure 5.10). The first recycled catalyst retained 90% activity (slope ratio in Figure 5.10) of the fresh catalyst, while the second recycled catalyst had almost the same activity as the first recycled catalyst (97% activity). This activity retention was much higher than those of silica gel supported CuBr. The copper concentration in solution measured by UV (Figure 5.11) was less than 2-3% of the catalyst used and the PMMA isolated from the solution was colorless, which confirms very little catalyst loss during recycling. This result indicates that PE_{25}-PEG_4-TEDETA-CuBr is reusable catalyst.

Figures 5.12 and 5.13 show that the recycled catalysts still had good control of the PMMA molecular weight. The molecular weights of PMMA obtained by the recycled catalysts were closer to the theoretical values than those by the fresh catalysts. This improvement in control of polymer molecular weight was resulted from the $CuBr_2$ in the recycled catalysts, which equilibrated with CuBr during the first run polymerization. In particular, PMMA molecular weights from the first and second recycled PE_{25}-PEG_4-TEDETA-CuBr increased linearly with conversion and were very close to the theoretical values (Figure 5.13). The polydispersities were less than 1.2, similar to those from

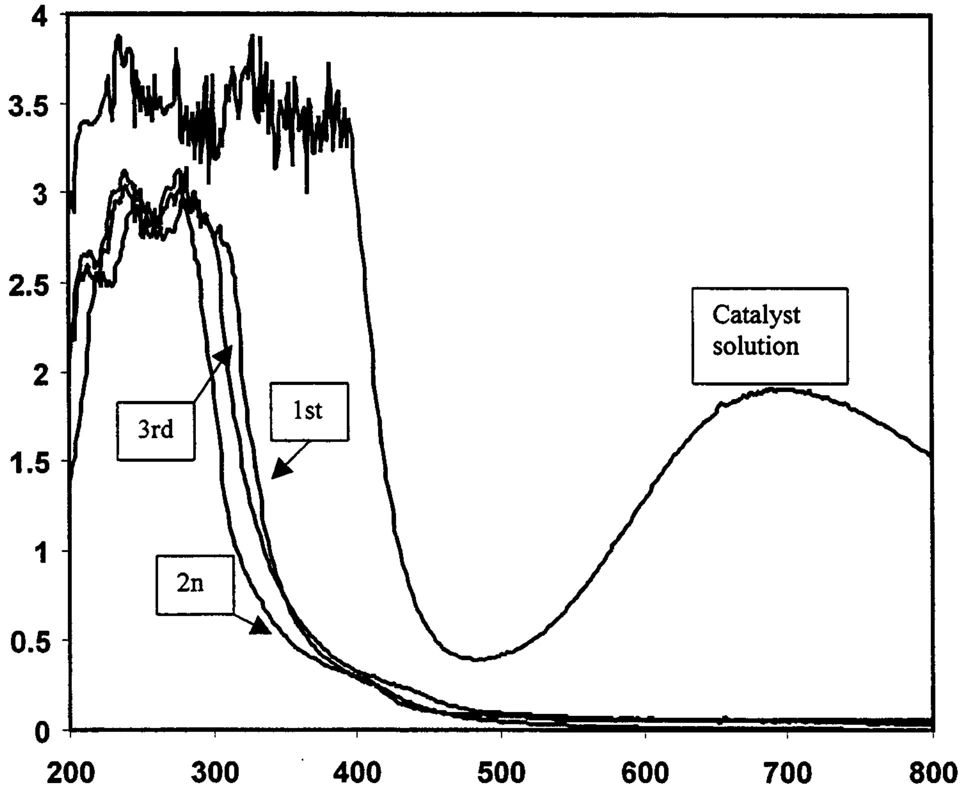

Figure 5.11. UV-VIS spectra of the polymerization solution catalyzed by PE_{25}-PEG_4-TEDETA-CuBr after the catalyst precipitated.

1st use: reaction solution after first run polymerization;

2nd use: reaction solution after second run polymerization;

3rd use: reaction solution after third run polymerization;

Catalyst solution: 0.011 g of CuBr, 0.041 g of tetraethyldiethylenetriamine, 5.0 g of toluene and 1.0 g of MMA, 12 μL MBP (as used in polymerization) were mixed and degassed.

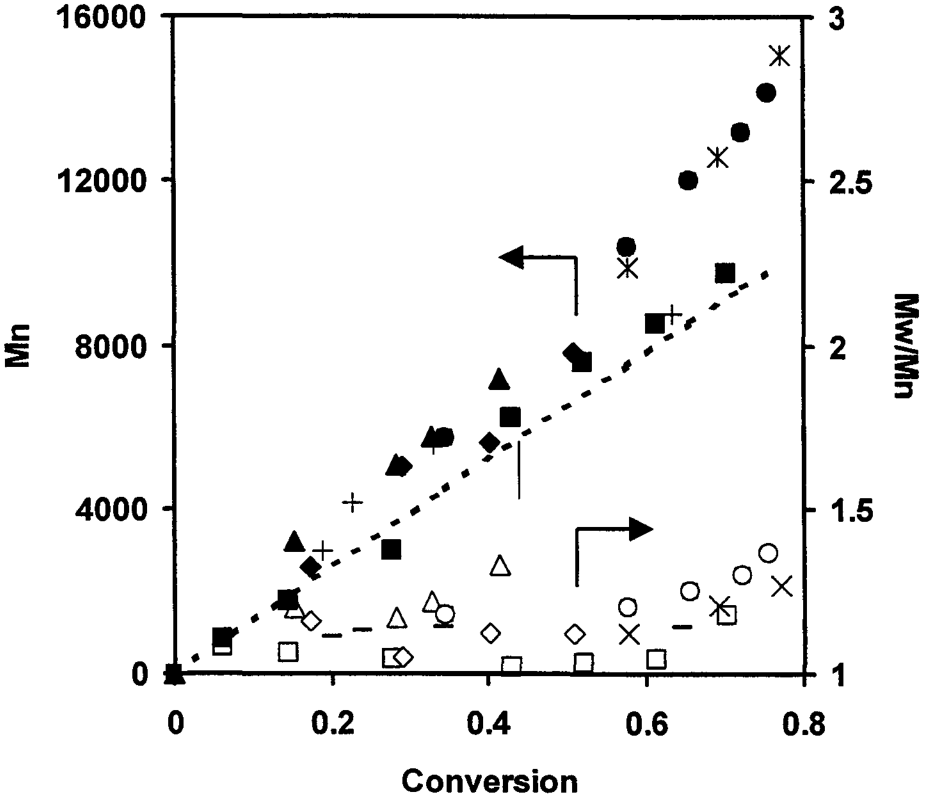

Figure 5.12. PMMA molecular weight and polydispersity as a function of MMA conversion catalyzed by fresh and recycled catalysts. See Figures 5.7, 5.8 and 5.9 for the experimental conditions, respectively.

PE$_{16}$-TEDETA-CuBr: First use (■, □), second use (◆, ◇); PE$_{25}$-TEDETA-CuBr: First use(●, O), second use(▲, Δ); PE$_{16}$-PEG$_{10}$-TEDETA-CuBr: First use (*,x); second use (+,-)

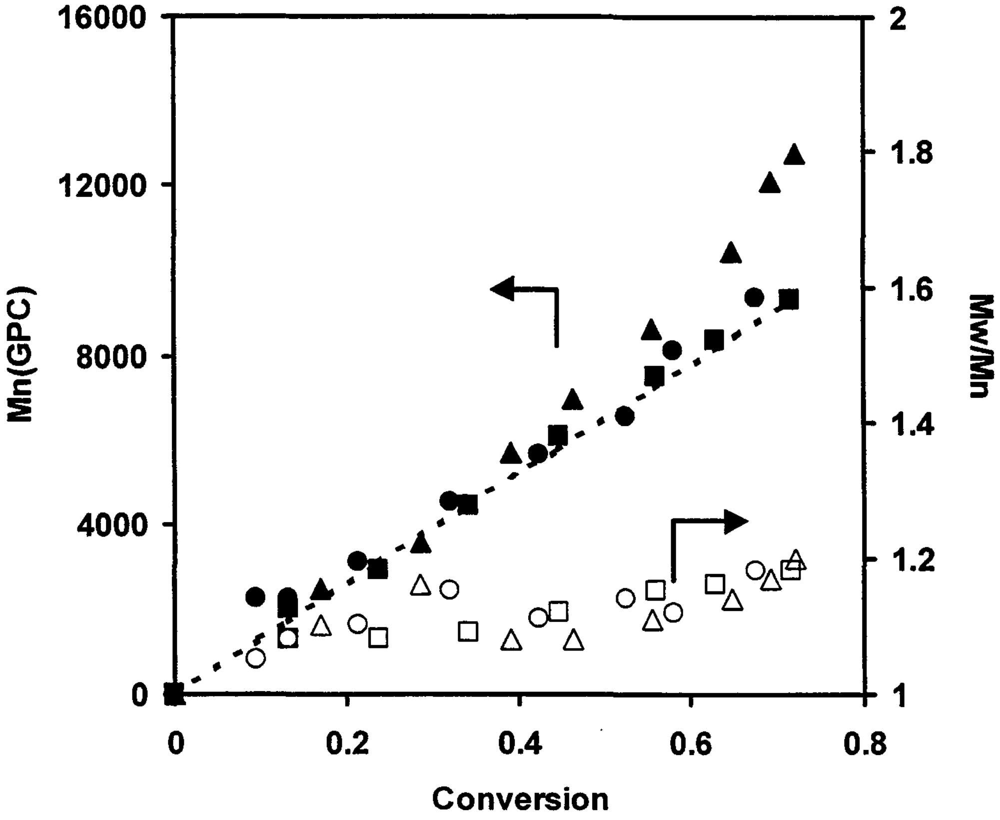

Figure 5.13. Molecular weight and polydispersity of PMMA as a function of conversion in MMA polymerization with fresh and recycled PE_{25}-PEG_4-TEDETA-CuBr. Fresh catalyst (▲, △), second used catalyst (●, ○), third used catalyst(■,□), theoretical Mn (-----). See Figure 5.10 for experimental conditions.

homogenous ATRP, and much narrower than those from heterogeneous ATRP of MMA. These results indicate that the PE_{25}-PEG_4-TEDETA supported CuBr is recoverable and reusable.

5.3.5 Polymerizations of Styrene and DMAEMA

The PE_{25}-PEG_4-TEDETA-CuBr also catalyzed the polymerizations of styrene and 2-(*N,N*-dimethylamino)ethyl methacrylate (DMAEMA), as shown in Table 5.2. The DMAEMA polymerization was faster than that of MMA. But the polymerization of styrene was the slowest. The molecular weights of the polymers were also close to the predicted with low polydispersities. The polydispersities increased slightly at high conversions, which might be caused by catalyst diffusion limitations as the solution became viscous. This indicates that the PE_{25}-PEG_4-TEDETA-CuBr is versatile for different monomers.

5.3.6 Block Copolymerization

The block copolymer of MMA with DMAEMA was prepared by a re-initiation method using PE_{25}-PEG_4-TEDETA-CuBr as catalyst. MMA (MMA/MBP=80) was first polymerized for 10 h, yielding PMMA of Mn=8500 with Mw/Mn=1.09 (Mn. Theor. = 7200). After the volatiles (toluene and unpolymerized MMA) were removed by vacuum, degassed toluene and DMAEMA were mixed with the remaining solid and reheated to 80 °C for 10 h. A block copolymer of P(MMA-b-DMAEMA) was isolated with Mn = 21100 (Mn.theor.= 21000) and PDI of 1.26 (Figure 5.14). This polydispersity is much

Table 5.2. DMAEMA and styrene polymerizations with PE_{25}-PEG_4-TEDETA-CuBr.[a]

Monomer	Time (h)	Conv [a] (%)	Mn×10^{-3} (Calc.)	Mn×10^{-3} (GPC)	Mw/Mn
DMAEMA[b]	1	18	3.64	3.70	1.16
	3	46	9.36	11.3	1.14
	6.6	74	15.1	16.6	1.20
Styrene[c]	11	31	4.20	4.30	1.11
	22	47	6.40	8.00	1.14
	74	70	9.50	12.1	1.21

[a] Conversion from integration of ^1H NMR; [CuBr]= [MBP]= 0.0115mol/L, PE_{25}-PEG_4-TEDETA/CuBr=1.5 (molar), [monomer] = 1.5mol/L. [b] 80 °C; [c]100 °C

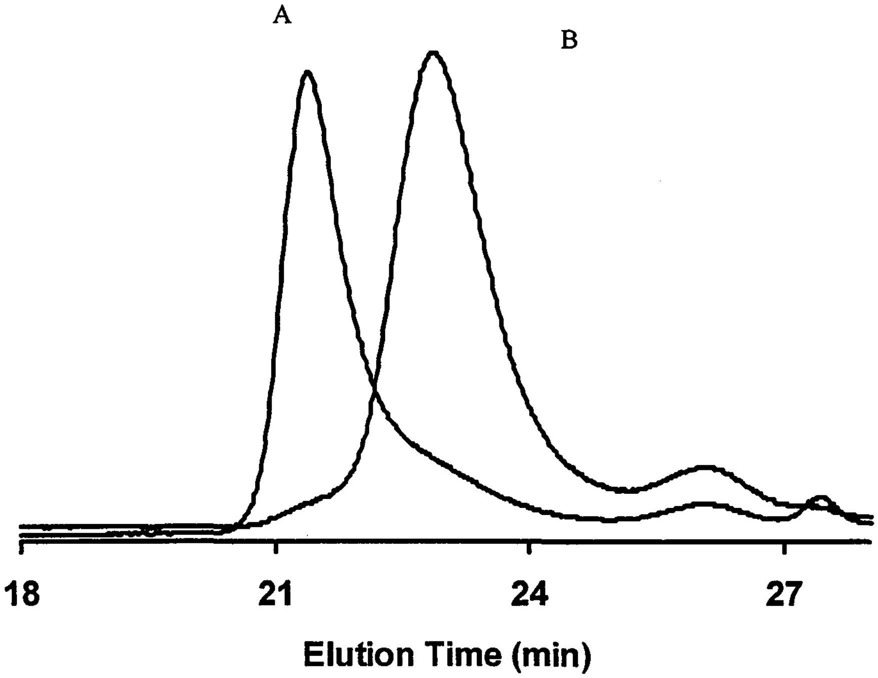

Figure 5.14. GPC traces of the PMMA-b-PDMAEMA (A) and PMMA prepolymer (B).

[CuBr] = [MBP] = 0.021 mol/L, PE_{25}-PEG_4-TEDETA/CuBr=1.5, [MMA] = 1.71 mol/L, 80 °C. Toluene was used as solvent.

lower than those produced by silica gel supported catalyst.[1-6] This further demonstrates that this soluble PE_{25}-PEG_4-TEDETA-CuBr can regulate ATRP as effective as unsupported catalysts.

5.3.7 Catalyst Residue

After the polymerization was complete, the catalyst was separated at 20 °C or 0 °C. The clear polymerization solution was dissolved in a concentrated H_2SO_4/HNO_3 (3/1 in v/v) solution. The copper concentration in the aqueous solution was measured by ICP-MS. The calculated copper concentration in the polymerization solution isolated at 0 °C was 12.6 ppm with PE_{25}-PEG_4-TEDETA-CuBr as catalyst, 33.4 ppm with PE_{16}-PEG_{10}-TEDETA-CuBr, 8.3 ppm with PE_{25}-TEDETA-CuBr and 21.3 ppm with PE_{16}-TEDETA-CuBr, equivalent to 0.77%, 2.0%, 0.51% and 1.3% respectively of the catalyst initially charged. This indicates that PE_{25}-PEG_4-TEDETA-CuBr and PE_{25}-TEDETA-CuBr had very low solubility in the polymerization solution, while those of PE_{16}-PEG_{10}-TEDETA-CuBr and PE_{16}-TEDETA-CuBr were higher. These results agreed with those of catalyst recycling. The catalysts had higher solubility at higher temperature. For example, the copper concentrations in the polymerization solution isolated at 20 °C were 21.6 ppm and 18.0 ppm with PE_{25}-PEG_4-TEDETA-CuBr and PE_{25}-TEDETA-CuBr as catalyst, respectively.

5.4 Conclusion

Polyethylene could be used as a soluble and recoverable support for ATRP of MMA, but the chain length of the polyethylene support strongly affected the catalyst activity and its control of the polymerization. Long PE chain decreased not only the catalyst activity but also the control of polymerization. Using polyethylene-*block*-polyethylene glycol (PE-PEG) as support, i.e. grafting the catalyst onto the PE support via PEG spacer, effectively minimized the deteriorating effects of PE support. The catalyst on PE-PEG support had higher catalytic activity and better control over the polymerization than that directly grafted on a PE support. The recycled catalysts on PE support had very low catalytic activity retention because of catalyst side reactions or loss of catalyst. PE_{25}-PEG_4 was found to be a good support for CuBr, on which the catalyst had a high catalytic activity retention and maintained a good control of the polymerization upon recycling.

5.5 References

1. Haddleton, D. M.; Duncalf, D. J.; Kukulj, D. and Radigue, A. P. *Macromolecules,* **1999,** *32,* 4769;
2. Haddleton, D. M.; Kukulj, D. and Radigue, A. P. *Chem. Commun,* **1999,** 99.
3. Kickelbick, G.; Paik, H.; and Matyjaszewski, K. *Macromolecules* **1999,** *32,* 2941.
4. Shen, Y.; Zhu, S.; Pelton, R. *Macromolecules* **2000,** *33,* 5427.
5. Shen, Y.; Zhu, S.; Zeng, F. and Pelton. R. *J. Polym. Sci. Part A: Polym. Chem,* **2001,** *39,* 1051.

6. Shen, Y.; Zhu, S.; Pelton, R. *Macromolecules, ASAP article, July 2001.*

7. Matyjaszewski, K. Ed. *Controlled Radical Polymerization;* American Chemical Society: Washington, DC **1997**; ACS Symp. Ser. Vol. 685.

8. Zhu, S. *Macromolecular Theory and Simulations* **1999,** *8,* 29.

9. Bergbreiter, D. E. *J. Polym. Sci.: Part A: Polym. Chem* **2001,** *39*, 2351.

10. Bergbreiter, D. E. *Cata. Today* **1998,** *42*, 389.

11. Bergbreiter, D. E.; Weatherford, D. A. *J. Org. Chem.* **1989,** *54,* 2726.

12. Bergbreiter, D. E.; Mariagnanam, V. M. *J. Am. Chem. Soc.* **1993,** *115,* 9295.

13. Bergbreiter, D. E.; Caraway, J.W. *J. Am. Chem. Soc.* **1996,** *118,* 6092.

14. Liou, S.; Rademacher, J. T.; Malaba, D.; Pallack, M. E.; Brittain, W. J. *Macromolecules* **2000,** *33,* 4295.

15. Matyjaszewski, K.; Nakagawa, Y.; Jasieczek, C. B. *Macromolecules* **1998,** *31*, 4053.

16. Percec, V.; Barboiu, B.; van der Sluis, M. *Macromolecules* **1998**, *31*, 4053.

Chapter 6

Continuous Atom Transfer Radical Polymerization Processes Using Packed-Column Reactor Technology

6.1 Introduction to Continuous Polymerization Process

The results in References [1-12] and Chapters 2-5 have been demonstrated that ATRP is a very useful process. The main drawbacks of ATRP are its low catalytic efficiency and deep color in final products due to its catalyst residue. Post-purification is thus required to remove catalyst from product.[13] Therefore, supporting ATRP has been developed to solve this problem: to directly remove catalyst from product and to recycle catalyst (references [14-18] and Chapters 3-5). In a typical supported ATRP batch process, the catalyst on particles is suspended in polymerization solution. After polymerization is complete, the mixture is left standing still for some time to let the particles to settle down. Then the supernatant solution is removed under nitrogen and the catalyst is washed and recovered for the next polymerization run. This batch polymerization could recycle the catalyst and avoid the post-purification step, but it is inefficient and time-consuming. A more efficient ATRP process is thus desirable for both academic and industrial interests.

Continuous processes are widely used in industry because of their high productivity and good quality control.[19] Chapter 3 demonstrated that CuBr-hexamethyl triethylenetetramine (CuBr-HMTETA) complex adsorbed on silica gel mediated a living polymerization of MMA. The recycled catalyst retained most of the fresh catalyst activity. More importantly, the reused catalyst had improved control over polymer molecular weight in its second and third polymerization runs. Therefore this catalyst is suitable for a continuous process. A continuous ATRP process has thus been developed by packing silica gel supported catalyst in a column reactor for the continuous ATRP of MMA.

6.2 Experimental Section

6.2.1 Materials

Methyl methacrylate (MMA) and *n*-butyl methacrylate (nBMA) from Aldrich were distilled under vacuum and stored at –15 °C before use. 1,1,4,7,10,10-Hexamethyl triethylenetetramine (HMTETA, ligand), CuBr and methyl α-bromophenylacetate (MBP, initiator) also from Aldrich were used as received. Toluene was distilled over CaH_2. Silica gel (100-200 mesh, Chromatographic Grade, Sargent-Welch Scientific Co.) was boiled in deionized water for 5 h and then air-dried and vacuum dried.

6.2.2 Apparatus

The polymerization system is shown in Scheme 6.1. The pump, solution flask, and column reactor were connected with 1mm diameter stainless tubing. The metering

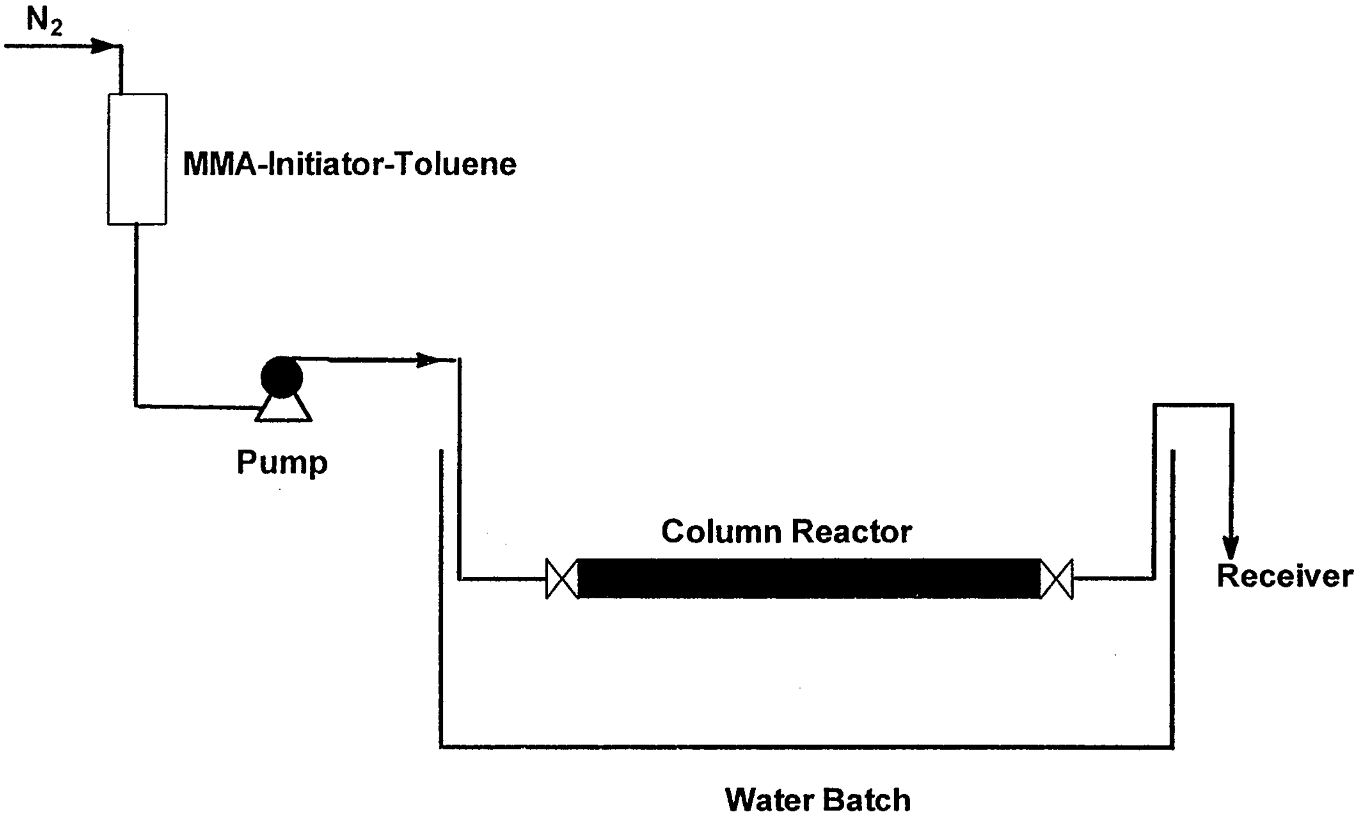

Scheme 6.1. The setup of the column reactor

pump was Gilson Model 302 with an adjustable flow rate at 0.01 mL/min. The flow rate was calibrated by a weight method. The column was made from stainless metal tubing of 900 mm length and 4.0 mm inner diameter. The pressure in the store flask was kept positive relative to the atmosphere pressure by ultra high purity nitrogen.

6.2.3 Catalyst Preparation and Reactor Packing

Boiled silica gel (12g) was weighted into a Schlenk flask and was degassed by vacuum-nitrogen for five cycles. Toluene (100 mL), CuBr (0.6 g) and HMTETA (0.96 g) were then added to the flask under nitrogen atmosphere. The mixture was bubbled with ultra high purity nitrogen for 10 min with efficient stirring. The blue mixture was further stirred for 3 h at room temperature. After the stirring, the silica gel became blue but the toluene solution was colorless. The blue silica gel was transferred to the column reactor under nitrogen atmosphere. The column was connected to the pump under nitrogen atmosphere.

6.2.4 Polymerization

A typical polymerization process was as follows. Degassed MMA-MBP-toluene polymerization solution (MMA/toluene =1/3 (w/w), MMA/MBP =100 (molar)) was added to the store flask. The flow rate was set and pump was then turned on. The column was then immersed into the water bath set at the required temperature. The outlet solution was collected at different time intervals and weighted to calibrate the flow rate. After the polymerization ran for 2~3 average residence times (τ), three parallel samples of 0.2~0.5 mL eluting out of the column were collected. The solution was diluted with $CDCl_3$. The conversion was measured with ^{1}H-NMR by calculating the intensity ratio of $OC\underline{H}_3$ signals in polymer (3.60 ppm) and monomer (3.75 ppm). The molecular weight and polydispersity of resulted PMMA were determined by GPC.

6.2.5 Block Copolymerization by Two Reactors in Series

Two reactors in series, as shown in Scheme 6.2, were used to carry out the block copolymerization of MMA and *n*-butyl methacrylate (nBMA). The toluene solution of monomer and initiator (MMA/MBP=30/1 in mole) was pumped to the first reactor immersed in water bath at 80 °C. The second monomer was pumped to the polymer solution eluting from the first reactor and the mixture was injected to the second reactor for polymerization. The solution eluting from the second reactor was collected and subject to NMR and GPC for measuring the conversion and molecular weight, respectively. The compositions of the block copolymers precipitated from the solution were determined by NMR.

6.2.6 Measurements

Nuclear Magnetic Resonance (NMR) Spectroscopy: Proton (^{1}H) NMR spectra were recorded on a Bruker ARX-200 spectrometer. ^{1}H NMR chemical shifts in $CDCl_3$ were reported downfield from 0.00 ppm using TMS an internal reference. The conversion was measured with ^{1}H-NMR by calculating the intensity ratio of $OC\underline{H}_3$ signals in polymer (3.60 ppm) and monomer (3.75 ppm).

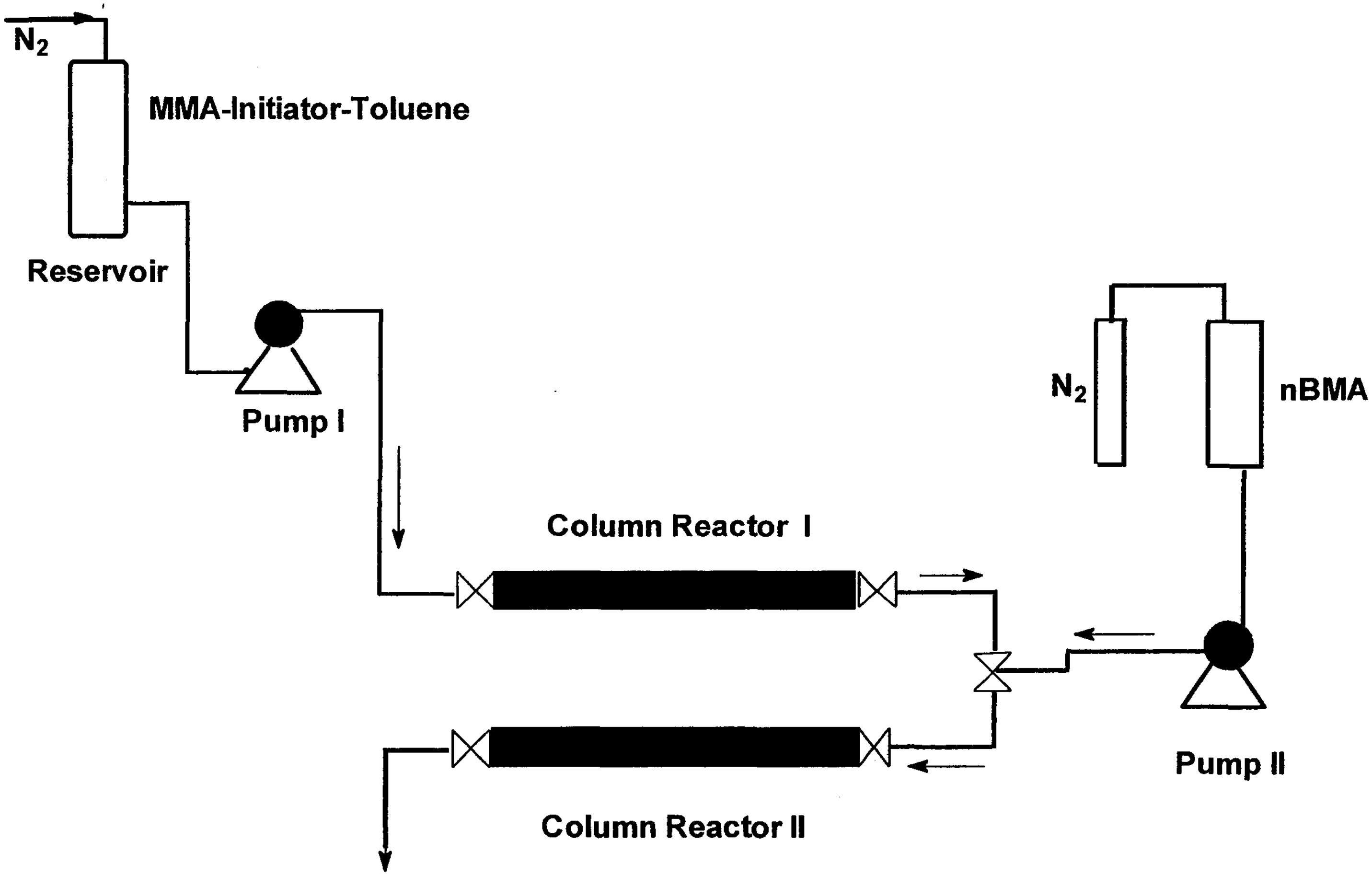

Scheme 6.2. Block copolymerization by two reactors in series

Molecular Weight Measurements: Number and weight average molecular weights (M_n and M_w, respectively) were determined by gel permeation chromatography (pore size: 500 Å, 1500 Å, 10000 Å) using THF-2% (v/v) triethylamine as solvent at a flow rate of 1.0 mL/min at 25 ^{o}C with a RI detector. Narrow polydispersed polystyrene standards (Polysciences) were used to generate a universal calibration curve. Data were recorded and manipulated using the Windows based Millennium software package.

Measurement of residence time distribution (RTD): The residence time distribution of the column reactor was measured as shown in Scheme 6.3 by injecting narrow dispersed polystyrene (Mn=2800, Mw/Mn=1.05; Mn=10,000, Mw/Mn=1.03, Polyscience) and PMMA (synthesized according to Reference 21; Mn=4,000, Mw/Mn=1.07; Mn=14,000, Mw/Mn=1.08). The reactor was packed with the same silica gel as used to support the catalyst. A refractive index detector used in the GPC measurement was used to determine the concentration of polymer eluting from the reactor. The signal was recorded and processed by Millennium Workstation for GPC. The variance was calculated by Equation 6.1:

$$\sigma^2 = \int_0^\infty (t-\tau)^2 E(t)dt \qquad \text{Eq. 6.1}$$

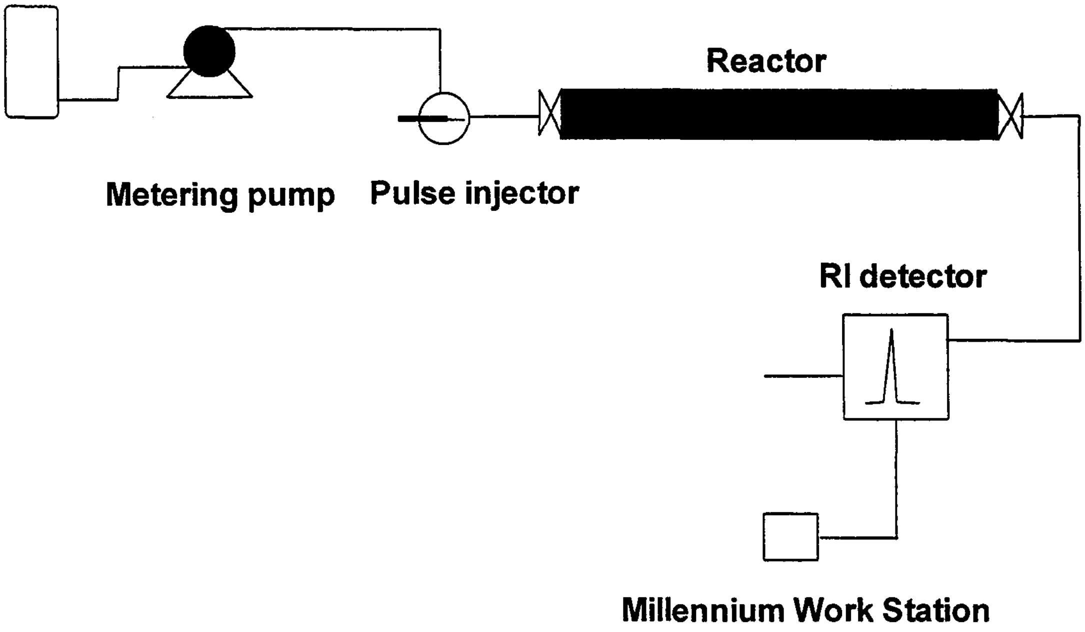

Scheme 6.3. RTD measurement by pulse injection

6.3 Results and Discussion

6.3.1 Reactor Stability

The conversion of MMA was used as an indicator for the reactor activity. The activity stability of the column reactor was evaluated at 80 °C and 90 °C by measuring the MMA conversion at a set flow rate. The reactor was run continuously at 1.2 mL/h and the eluting solution was sampled at different intervals (Figure 6.1). Figure 6.1 shows that the reactor activity was slightly low at the initial 10 hours but the system became stable up to 100 h at 90 °C and 120 h at 80 °C. In this time interval, the changes in the activity were within 7%. This suggests that the reactor had a good retention of the catalytic activity. After the stable period, the activity gradually reduced. This reduction was caused by an accumulation of copper dibromide and a loss of the catalyst. As we discussed in Chapters 3-5, in an ATRP system, copper dibromide is generated to equilibrate with copper bromide. If some radicals are consumed by side reactions such as radical coupling, the equilibrium shifts to the right side in Eq. 6.2 and thus generates an excess of $CuBr_2$. Figure 6.2 shows that the molecular weights of PMMA were always higher than the theoretical values ($Mn_{Theor.}$ = conversion × MW_{MMA}×MMA/MBP ratio),

$$\mathrm{CuBr/HMTETA} \quad + \quad \mathrm{P\text{-}Br} \rightleftharpoons \mathrm{CuBr_2/HMTETA} \quad + \quad \mathrm{P^{\bullet}}$$

Eq. 6.2

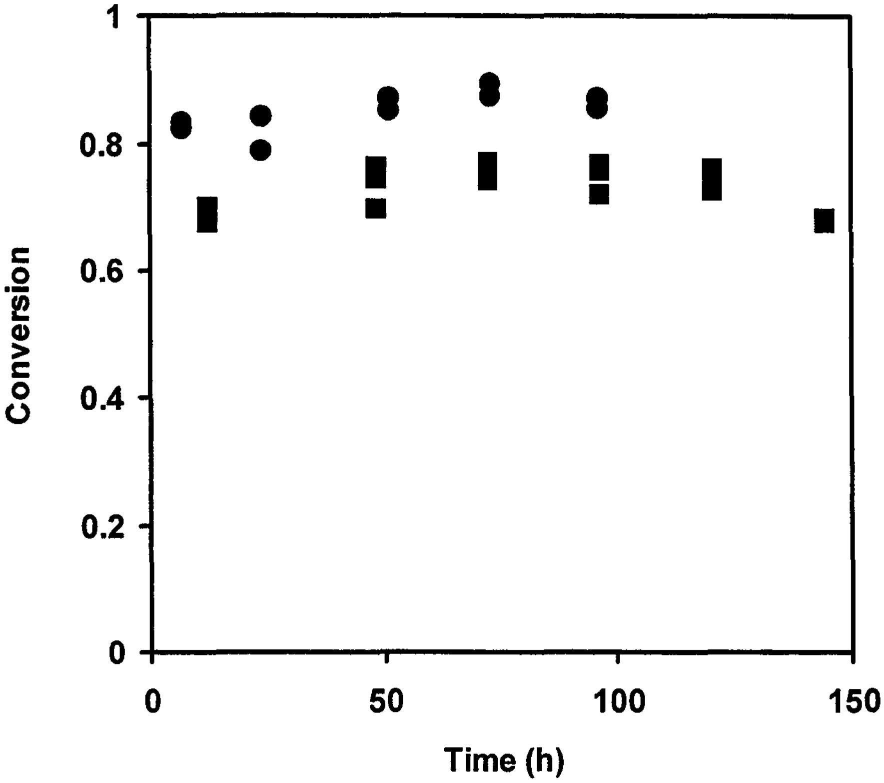

Figure 6.1. The stability of the column reactor packed with silica gel supported CuBr for ATRP polymerization of MMA: The MMA conversions at different times at the flow rate of 1.2 mL/h.

MMA/toluene = 1/3 (w/w), Silica gel/CuBr = 20(w/w), MMA/MBP = 100 (molar),

90 °C (●), 80 °C(■).

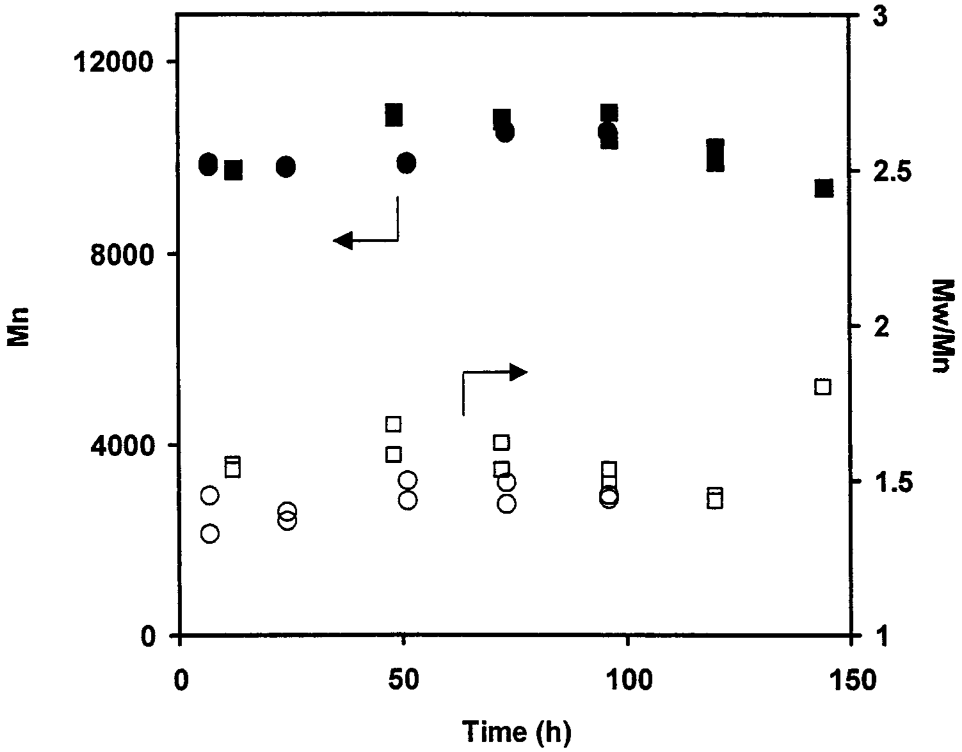

Figure 6.2. The molecular weight and molecular weight distribution of PMMA produced at different times by the column reactor at the flow rate of 1.2mL/h.

See Figure 6.1 for reaction conditions.

90 °C (●, ○), 80 °C (■,□).

i.e. the initiator efficiencies ($Mn_{Theoretical}/Mn_{Experimental}$) were less than 1. This indicates that some initiators were consumed by side reactions, such as radical coupling, leading to a gradual accumulation of $CuBr_2$ in the reactor. It has been demonstrated that $CuBr_2$ can shift the equilibrium to the left side and result in a lower radical concentration and thus a slower polymerization rate.[1] Meanwhile, the catalyst in this work was supported onto silica gel surface by physical adsorption. After reactor running for long time, some catalyst may be washed out of the reactor. Thus the loss of catalyst also contributed to the reduction in the reactor activity.

Figure 6.2 shows that the molecular weight of produced PMMA varied with the same trend as the reactor activity. At the initial stage, the molecular weight of resulting PMMA was slightly low and increased gradually to a maximum, and then became stable. It decreased gradually after about 120 h running, corresponding to the declination of MMA conversion in Figure 6.1. The variance of PMMA molecular weight in 120 h operation was also less than 7%, same as that of MMA conversion. These results indicate that the reactor was capable of producing PMMA with constant molecular weight in 120 h.

6.3.2 Effect of Silica Gel/CuBr on Reactor Stability

The stability of the reactors packed with catalysts of different silica gel/CuBr ratios at 80 °C is shown in Figures 6.3 and 6.4. The reactors packed with different silica gel/CuBr catalysts had quite different stability features. The activity of the reactor packed with silica gel/CuBr = 20 or 30 was slightly low at the early stage, but increased

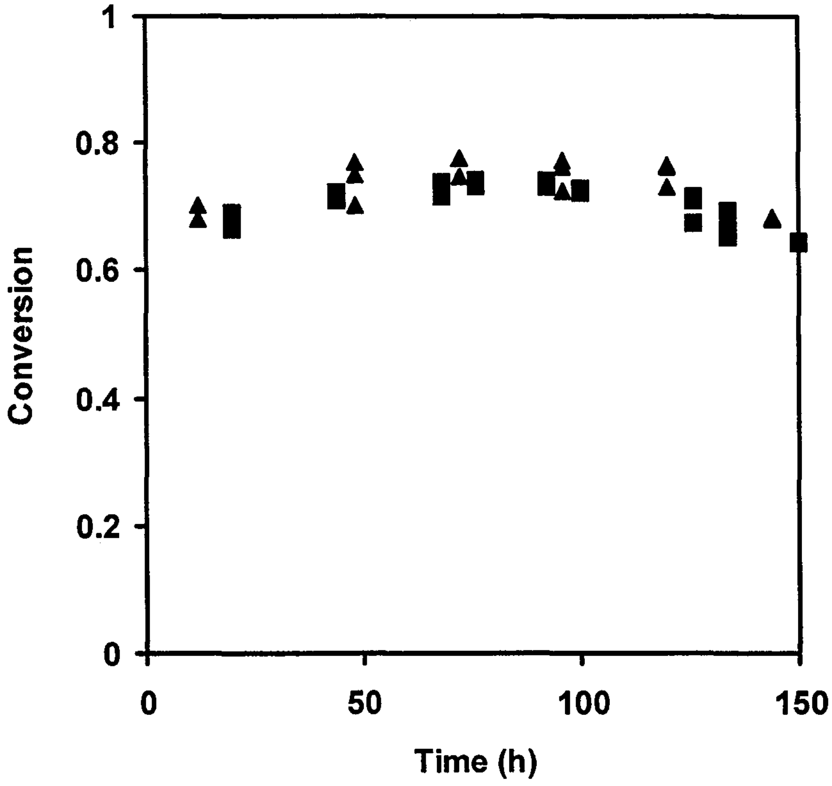

Figure 6.3. The activity stability of the column reactors packed with catalysts of different silica gel/CuBr ratios for the ATRP polymerization of MMA: The MMA conversions at different times at the flow rate of 1.2 mL/h.

MMA/toluene = 1/3 (w/w), MMA/MBP = 100(molar), 80 °C; Silica gel/CuBr(w/w) = 20 (▲), 30(■).

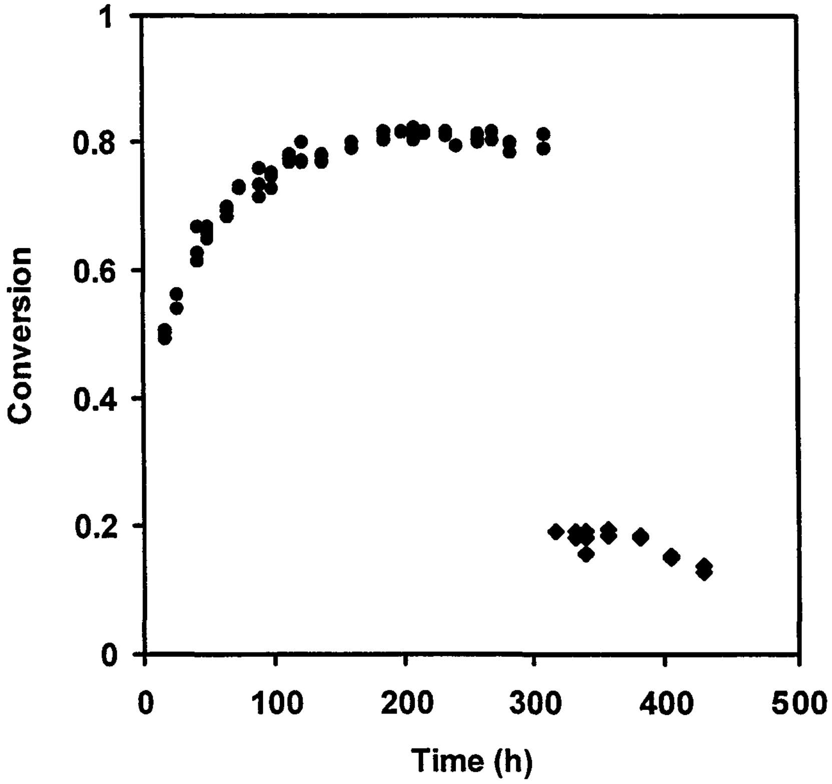

Figure 6.4. The stability of the reactor packed with catalyst of silica gel/CuBr = 10 for ATRP polymerization of MMA: The MMA conversions at different times at the flow rate of 1.2 mL/h(●) and 3.0 mL/h(◆)

MMA/toluene = 1/3 (w/w), MMA/MBP = 100 (molar), 80 °C; Silica gel/CuBr = 10(w/w).

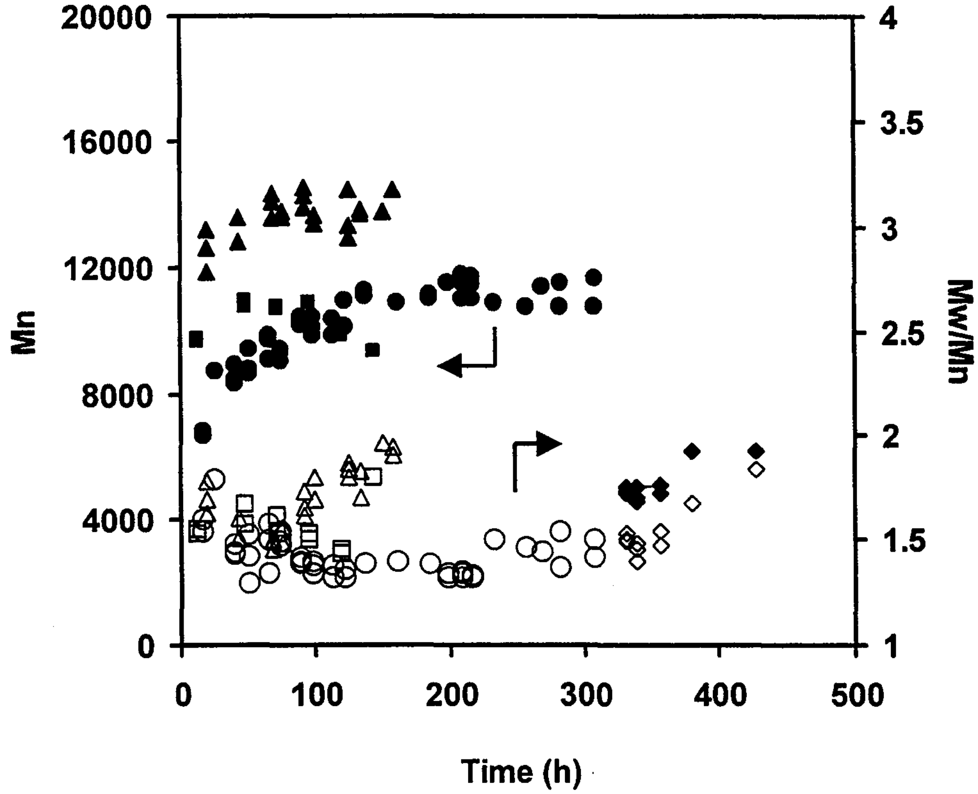

Figure 6.5. The molecular weight and molecular weight distribution of PMMA produced at different times by the column reactors packed with catalysts of different silica gel/CuBr ratios. See Figures 6.3 and 6.4 for conditions.

Silica gel/CuBr (w/w) = 10 (● , ○), 20(■,□), 30 (▲, Δ) at flow rate of 1.2 mL/h; Silica gel/CuBr (w/w) = 10 (◆,◊) at the flow rate of 3.0 mL/h; 80 °C.

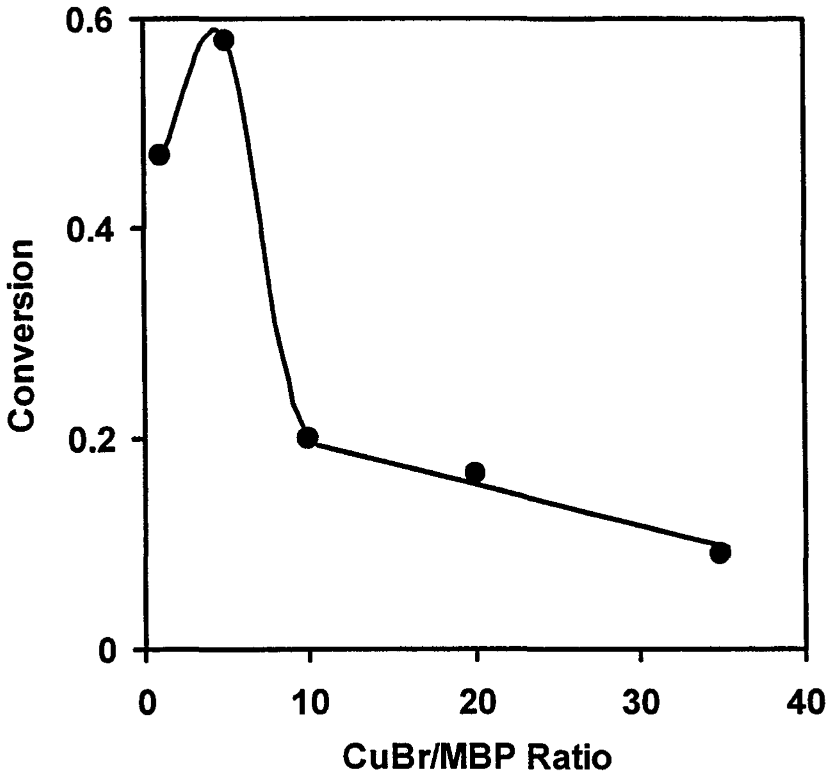

Figure 6.6. The effect of CuBr/initiator (MBP) ratio on the activity of the catalyst.

MMA/MBP = 100(molar), MMA/toluene = 1/3 (w/w), 80 °C, 4h.

quickly to a constant activity. The activity was stable up to 120 hours before it started to decrease. However, the initial activity of the reactor packed with silica gel/CuBr = 10 was much lower (50% conversion) than that with silica gel/CuBr = 20 or 30. It took about 100 hours for the system to gradually reach the stable activity. But once stabilized, the reactor remained the same activity for over 200 hours at a flow rate of 1.2 mL/h and an additional 80 hours at 3.0 mL/h. The molecular weight of the produced PMMA given in Figure 6.5 showed the same trend as the reactor activity. The molecular weight of PMMA produced by silica gel/CuBr = 20 and 30 systems increased slightly with time at the early stage of polymerization and became stable within 120 h. The molecular weight of produced PMMA by the silica gel/CuBr = 10 system increased gradually in the first 100 h, and then became stable for 200 h at the flow rate of 1.2 mL/h and a successive 80 hours at the flow rate of 3.0 mL/h.

It was surprising to observe that the reactor packed with silica gel/CuBr = 10, which had more catalyst in the reactor than with silica gel/CuBr = 20 or 30, had much lower activity at the beginning. The calculation of the catalyst/initiator ratio indicates that when the MMA-toluene-MBP solution flowed through the column reactor, by an average, each initiator molecule regulated by more than one catalyst molecule. For silica gel/CuBr = 10, 20, 30, the corresponding CuBr/MBP was 23.2, 11.6 and 7.7, respectively. The effect of excess CuBr on polymerization was thus evaluated in batch process, as shown in Figure 6.6. It can be seen that initially the polymerization rate increased as the CuBr/MBP ratio increased from 1 to 5 because more catalysts produced more radicals (Eq. 6.2) and thus increased the polymerization rate. However, further increasing CuBr/MBP ratio decreased the polymerization rate. This was caused by the fact that when there was too much excess of catalyst for each initiator, the equilibrium in Eq. 6.2 was pushed far right to produce a high concentration of radicals. The radical termination reaction thus became significant. This radical consumption produced a high concentration of $CuBr_2$ in the system (Eq. 6.2) and thus greatly slowed the polymerization.

Therefore, when the reactor was packed with catalyst of silica gel/CuBr=10, the excess of catalyst caused to produce a high concentration of $CuBr_2$ in the reactor and thus the reactor had low activity. But with continuous washing out of the catalyst, the catalyst concentration decreased and thus the activity increased gradually.

6.3.3 Effect of Flow Rate and Temperature on the Reactor Activity

The MMA conversion as a function of flow rate at 80 and 90 °C is shown in Figure 6.7. At both temperatures, the MMA conversion decreased with increasing the flow rate. For example, at 90 °C, the MMA conversion reached 87% at 1.2 mL/h but reduced to 23% at 9.6 mL/h. It was expected because the polymer chains flowed out of the reactor faster at a higher flow rate. At the same flow rate, lower temperature resulted in lower activity.

Figures 6.8 shows the dependence of MMA conversion on the mean residence time τ (the void column volume over volumetric flow rate). The MMA conversion

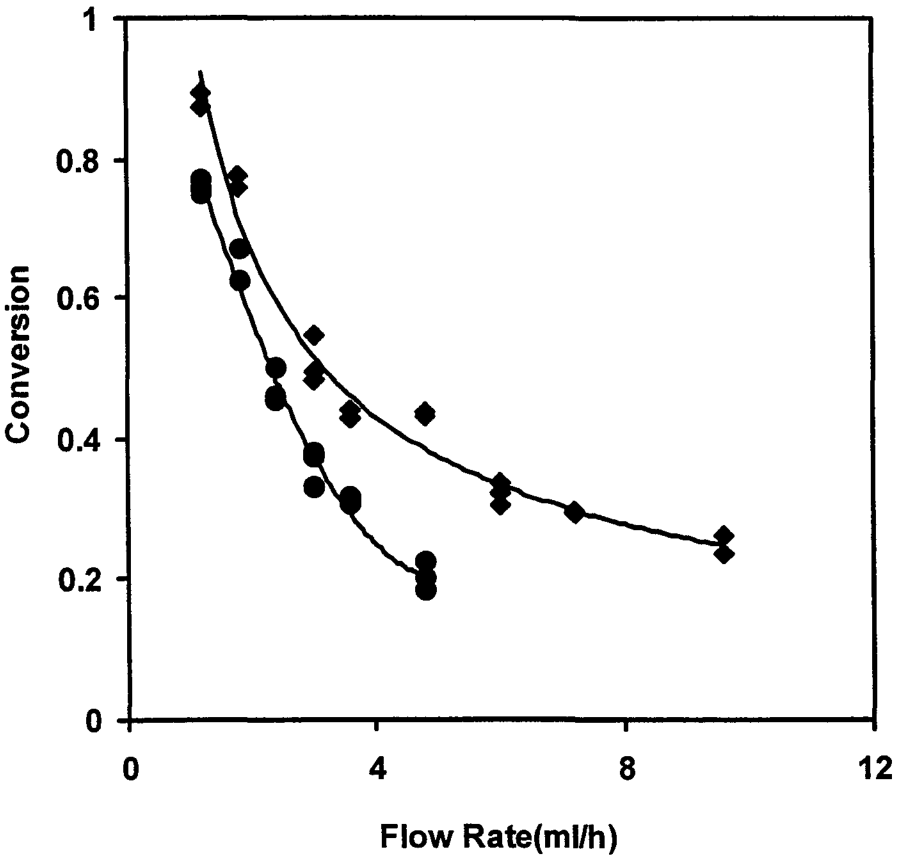

Figure 6.7. The MMA conversion as a function of flow rate for the polymerization of MMA in the column reactor at different temperatures.

MMA/toluene = 1/3 (w/w), MMA/MBP = 100 (molar), Silica gel/CuBr = 20 (w/w); 80 °C (●) and 90 °C (◆).

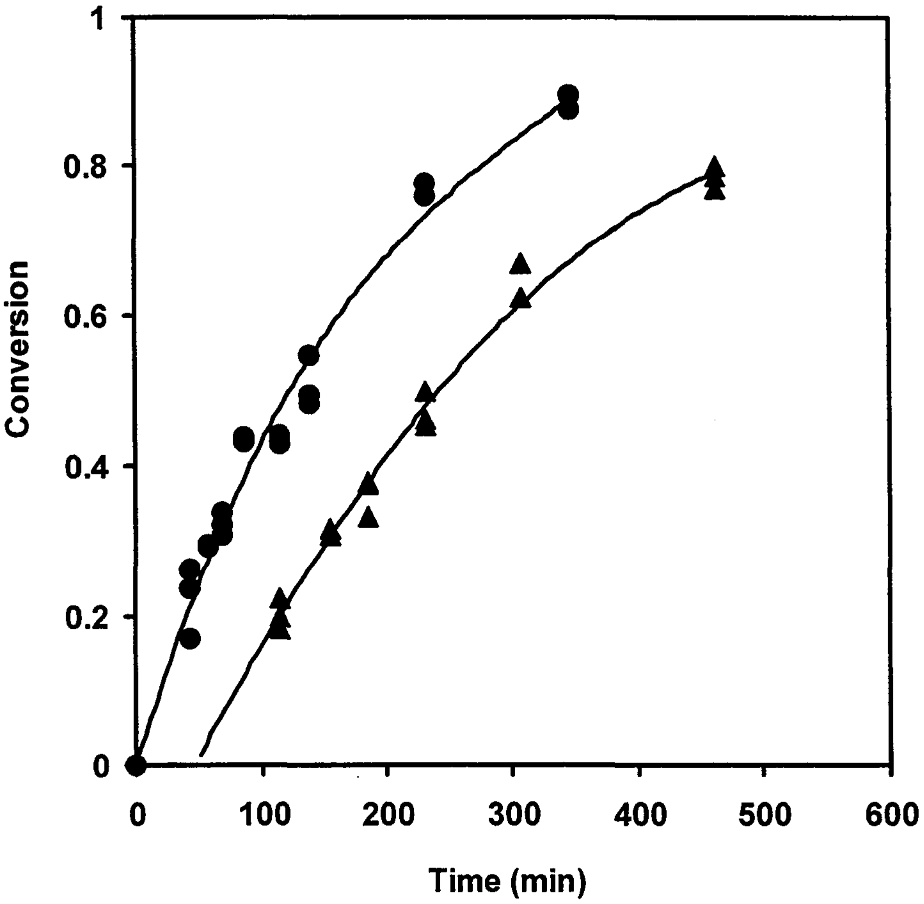

Figure 6.8. The MMA conversion as a function of residence time for the polymerization of MMA in the column reactor at different temperatures.

80 °C (▲) and 90 °C (●). See Figure 6.7 for the experimental conditions.

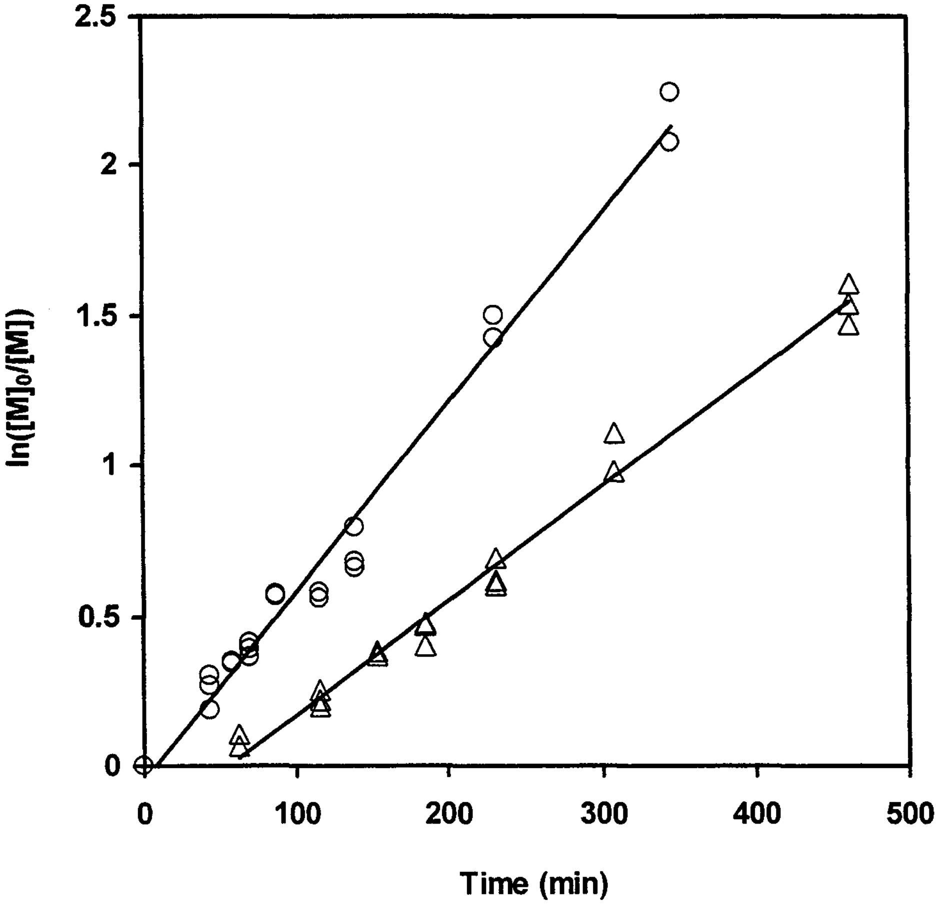

Figure 6.9. The kinetic plots of the MMA polymerization in the column reactor at different temperatures.

80 °C (Δ) and 90 °C (○). See figure 6.7 for the experimental conditions.

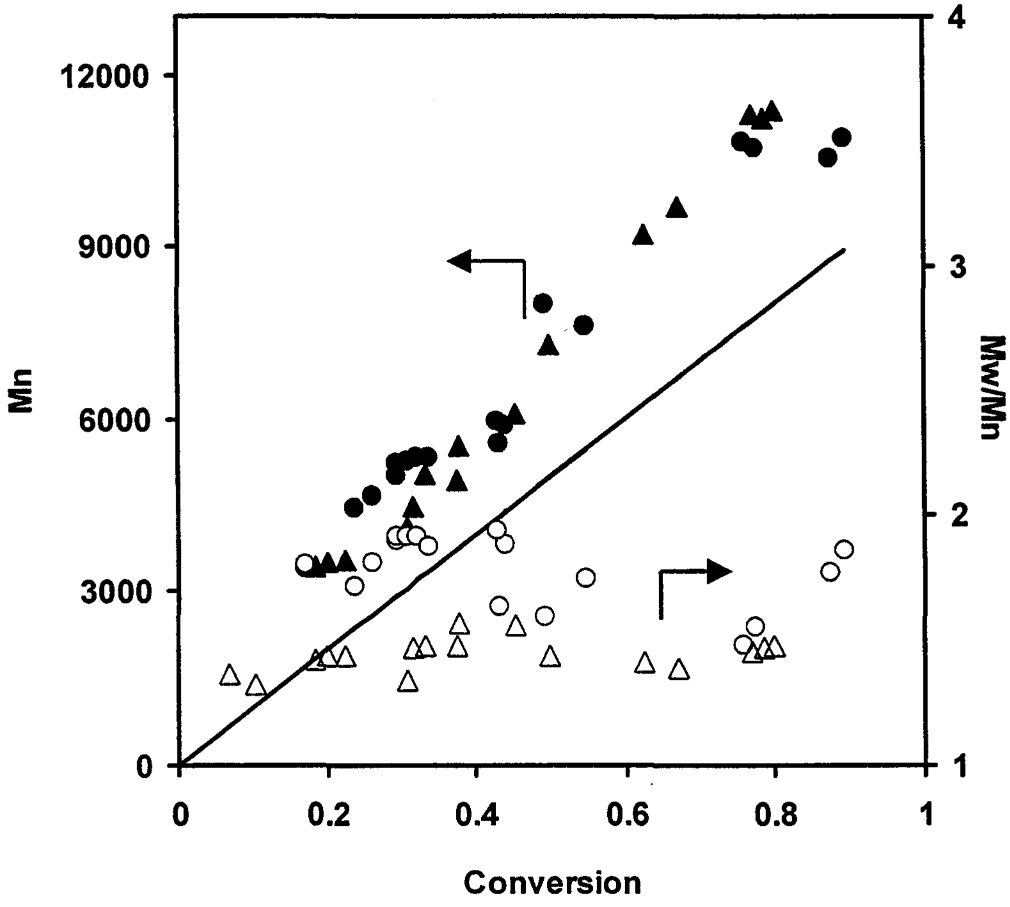

Figure 6.10 The molecular weight and molecular weight distribution of PMMA produced in the reactor as a function of conversion.

80 °C (▲, △) and 90 °C(●, ○), theoretical (—); See Figure 6.7 for conditions.

increased smoothly with the residence time. The $\ln([M]_o/[M])$ *vs.* time plots were linear at both temperatures (Figure 6.9), indicating that the MMA polymerization in the column reactor was in the first order kinetics with respect to monomer concentration, typical for an ATRP process. At 80 °C, the polymerization had a 50 min induction period.

Figure 6.10 shows the dependence of molecular weight and molecular weight distribution of PMMA on the MMA conversion. The molecular weight of the resulting PMMA increased linearly with the conversion, exhibiting the characteristic of a living polymerization process. This also confirms that the continuous polymerization inside the reactor proceeded via ATRP mechanism. The dormant polymer chains grew longer by reacting with catalyst on silica gel surface to propagate monomers (Eq. 6.2) while passing through the column reactor. It is also noticed that the PMMA molecular weights were higher than theoretical values with the initiator efficiency about 70%. This deviation from the theoretical prediction was typical when a high silica gel/CuBr ratio system was used (Chapter 3.) It was because some initiator molecules were consumed by radical side reactions such as coupling.

Since the molecular weight of PMMA is in a linear function of the MMA conversion (Figure 6.10) while the conversion is determined by the flow rate (Figure 6.7), the molecular weight of PMMA can thus be readily controlled by the flow rate. Figure 6.11 shows that at 80 and 90 °C, the PMMA molecular weight decreased with increasing the flow rate. Thus, this continuous ATRP process is clearly advantageous in preparing different polymer products of desirable molecular weights. A simple operation of adjusting flow rate produces polymers of different molecular weights.

The PMMA polydispersities (Mw/Mn) were about 1.5 for the samples prepared at 80 °C, and higher (~1.8) for those prepared at 90 °C. These distributions were much broader than the polymers prepared with the same supported catalyst system in batch processes (about 1.1) (Chapter 3). This broadening in the molecular weight distribution might be caused by different residence times for individual polymer chains spent in the reactor. The residence time distribution (RTD) of the reactor was measured by a pulse injection of monodispersed polystyrene (PS) and PMMA (Figure 6.12). The RTD of the reactor was rather broad. The variance σ^2 was 450 min^2 at the flow rate of 1.2 mL/h and 110 min^2 at the flow rate of 3.0 mL/h. This large difference in the residence time allowed some fraction of polymer chains to reside in the reactor for a long time and thus grow to high molecular weight, while some other fraction of chains exist the reactor too quickly with short chain length. The Peclet number calculated by Eq. 6.3 was 550 at the flow rate of 1.2 mL/h and 700 at the flow rate of 3.0 mL/h. This indicates that there was little dispersion probably due to low diffusion of polymer molecules.

$$\frac{\sigma^2}{\tau^2} = \frac{2}{\mathrm{Pe}_r} - \frac{2}{\mathrm{Pe}_r^{\,2}}(1 - e^{-\mathrm{Pe}_r}) \qquad \text{Eq. 6.3}$$

High viscosity of the reaction solution also contributed to the broadening in molecular weight distribution of PMMA. It was observed that even with 25% monomer

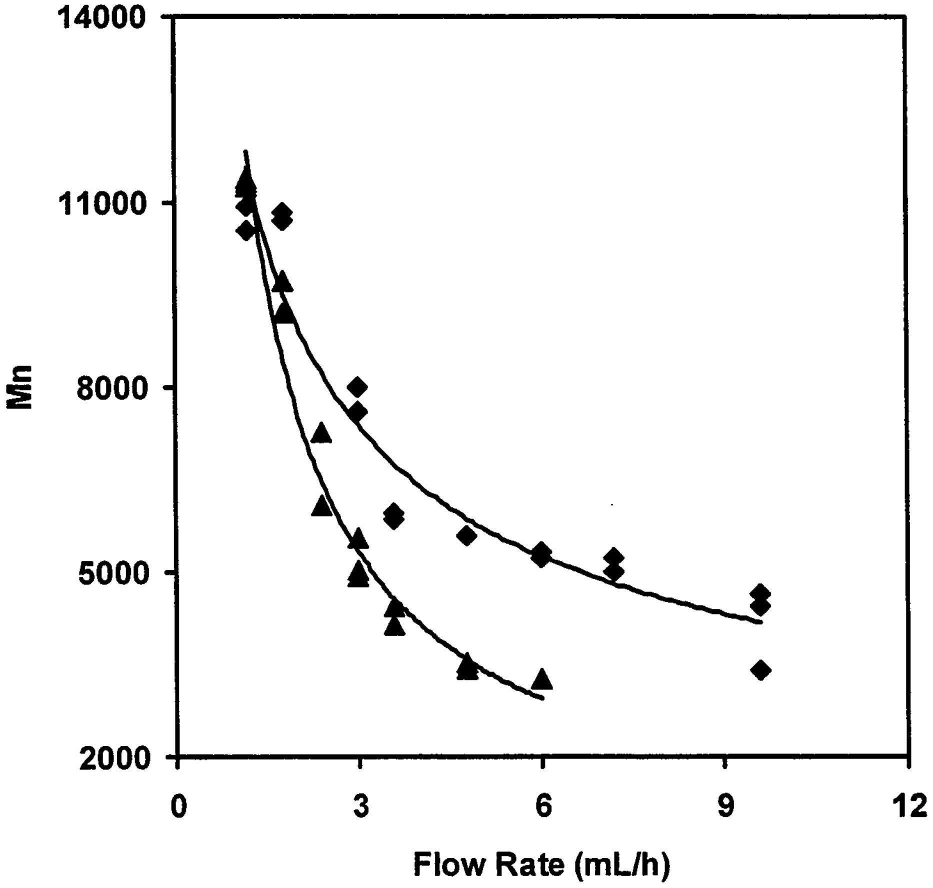

Figure 6.11. The molecular weight of PMMA produced in the reactor at 80 and 90 °C as a function of the flow rate. See Figure 6.7 for reaction conditions.

80 °C (▲) and 90 °C (◆).

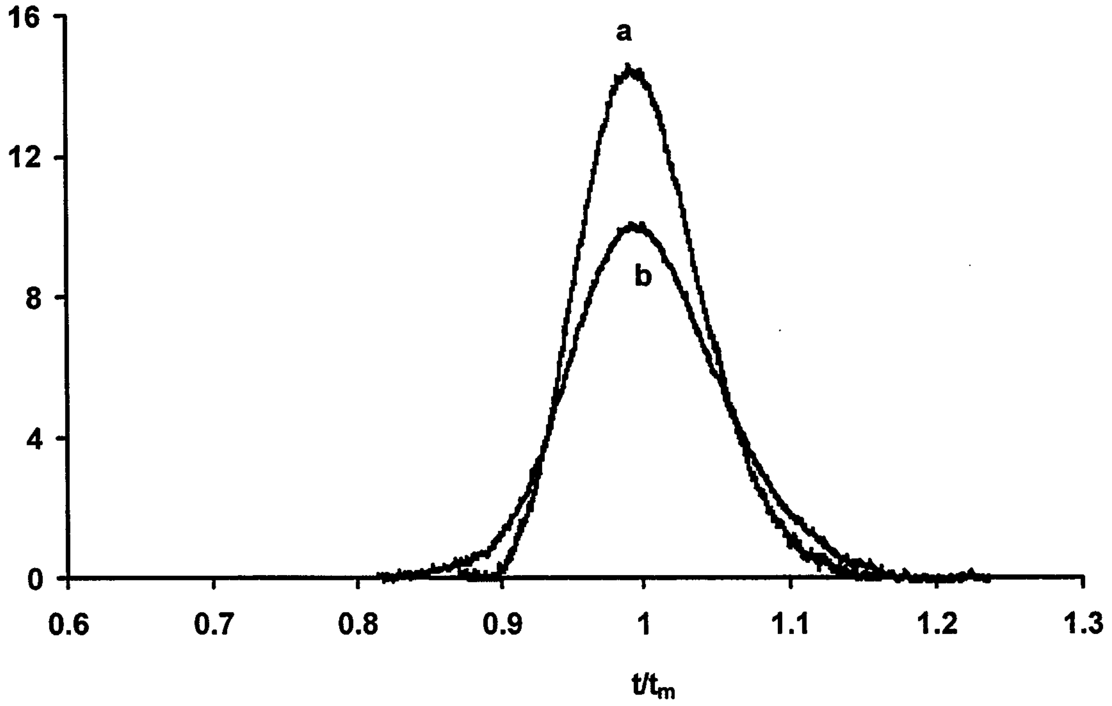

Figure 6.12. The residence time distribution of the reactor packed with silica gel by pulse injection of PMMA (Mn=4,000, Mw/Mn=1.08) at 25 °C at a flow rate of 1.2 mL/h (a) and 3.0 mL/h (b).

concentration (w/w) and at moderate conversions, the reaction solution eluting from the reactor was very viscous. This high viscosity imposed diffusion limitations on polymer chains (P-Br or $P^\bullet$) and made the chains difficult to access to the catalytic sites on silica gel surface. The propagating radicals ($P^\bullet$) were thus not deactivated quickly enough and propagated too many monomer units in each activation/deactivation cycle (Eq. 6.2). It has been shown that a fast radical deactivation so as to propagate only few monomers in each activation/deactivation cycle is essential for producing polymers of low polydispersity by ATRP.[1,22]

6.3.4 Polymerization with Different Monomer/Initiator Ratios

In addition to the flow rate, the monomer/initiator ratio was also used as a parameter to control the molecular weight of produced PMMA. Figure 6.13 shows the MMA conversion as a function of flow rate with monomer/initiator ratios of 100 and 200, respectively. The polymerization at MMA/Initiator = 200 was slower than that of MMA/Initiator = 100. This was because of the lower initiator concentration in the former system. Lower initiator concentration resulted in lower propagating radical concentration as shown in Eq. 6.2.

The molecular weight of PMMA increased linearly with the MMA conversion (Figure 6.14). At both ratios, the experimental molecular weights were higher than the theoretical values. The MMA/Initiator = 200 system yielded double molecular weight as that of MMA/Initiator = 100. For example, the Mn was 12,800 for PMMA produced with MMA/Initiator = 200 at 42% conversion, while it was 6,100 for MMA/Initiator =

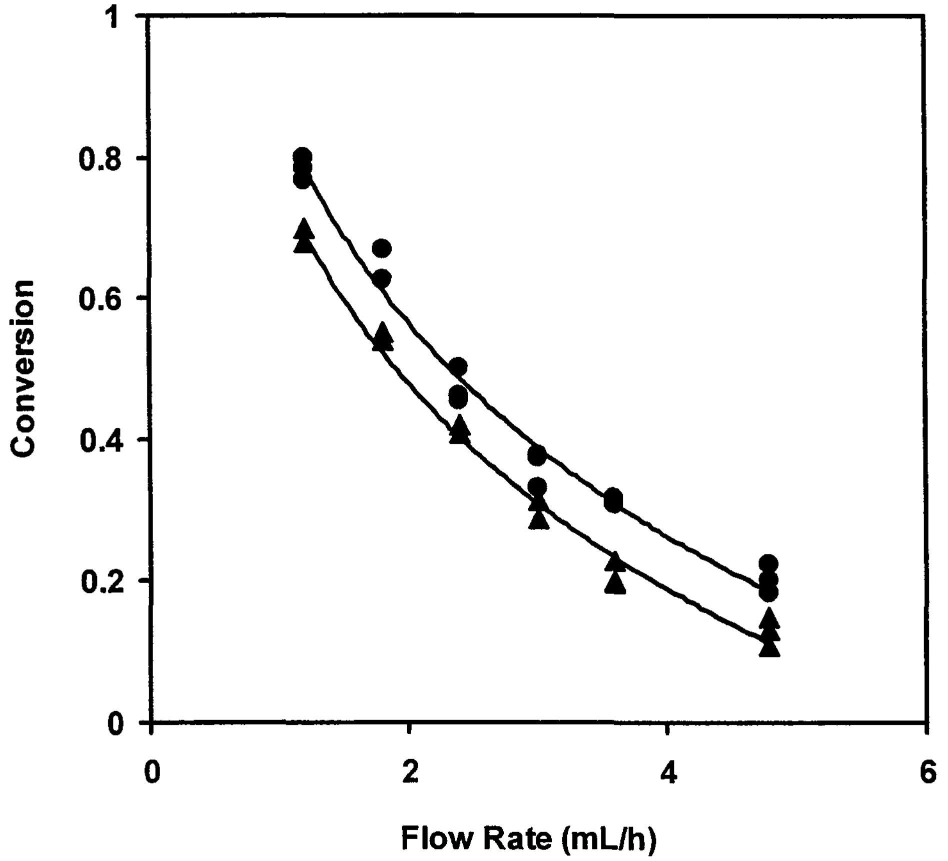

Figure 6.13. The MMA conversion as a function of the flow rate for the polymerization in the reactor at MMA/Initiator ratios of 100 and 200.

MMA/toluene =1/3 (w/w), Silica gel/CuBr = 20 (w/w), 80 °C;

MMA/MBP (molar) = 100 (●), 200 (▲).

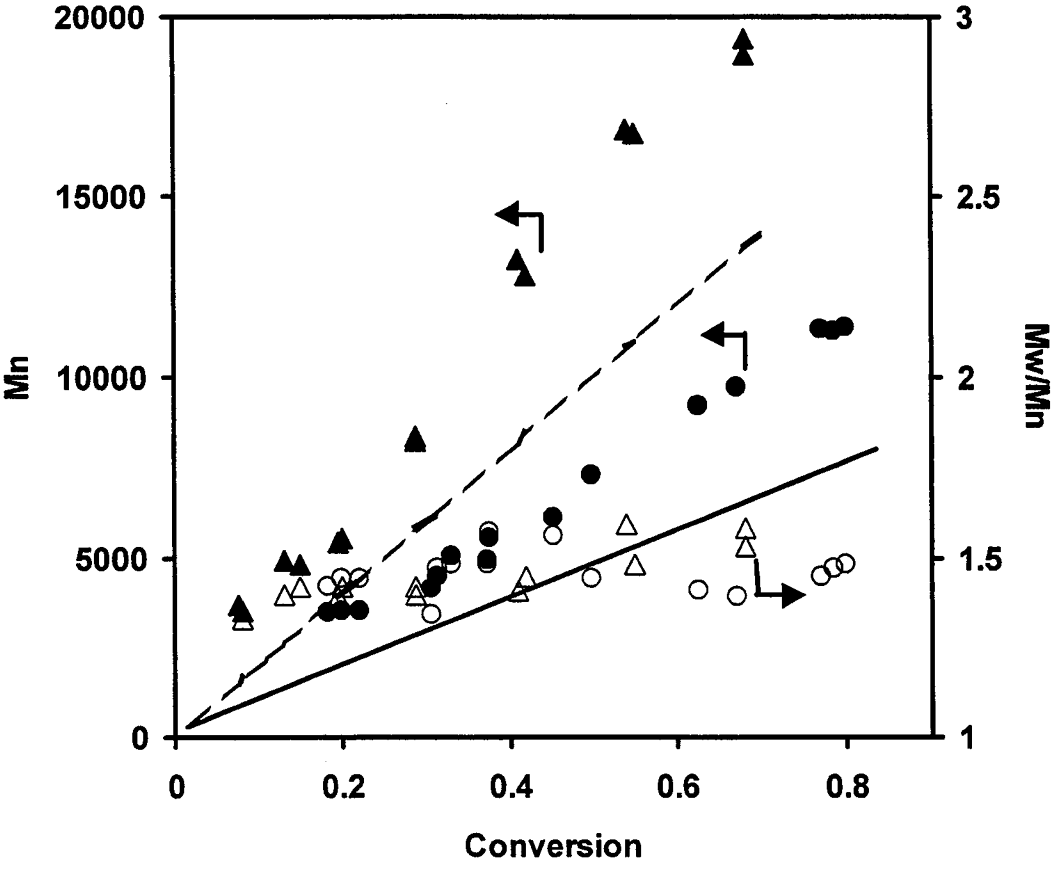

Figure 6.14. The dependence of the PMMA molecular weight and polydispersity on the conversion for the polymerizations of MMA at MMA/Initiator ratios of 100 and 200. See Figure 6.13 for reaction conditions;

MMA/MBP(molar) = 100 (●,○), 200 (▲, △); theoretical Mn: MMA/MBP = 100 (—), 200 (……).

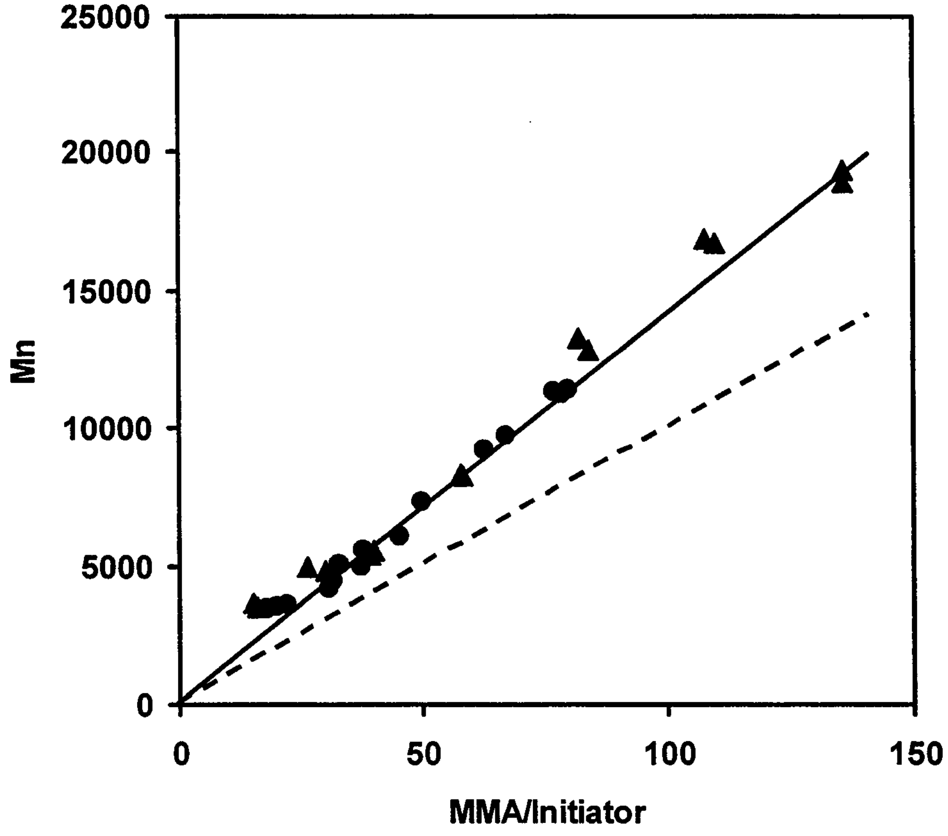

Figure 6.15. The molecular weight of PMMA as a function of MMA/initiator ratio for the polymerization. See Figure 6.13 for the reaction conditions.

MMA/MBP=100 (●), 200 (▲); Theoretical Mn (……).

100 at 45% conversion. The linearity in molecular weight of PMMA vs. MMA/MBP curves for these two systems gave a strong evidence for the livingness of the ATRP process inside the reactor. This also provides another approach to design polymer molecular weight in addition to the flow rate method (Figure 6.11).

6.3.5 Scaling Up

The polymerization of MMA was also carried out using two column reactors (500 cm long and 7.8 mm in diameter) in series packed with 2 g of CuBr supported on 40 g silica gel (compared to 0.6 g CuBr on 12 g silica gel). Figure 6.16 shows that the polymerization in the larger reactor had the same trend of MMA conversion with flow rate as that in Figure 6.7. The molecular weight of produced PMMA also increased with conversion (Figure 6.17), similar to the smaller reactor. These results indicate that the continuous ATRP can be scaled up to have high productivity.

6.3.6 Reproducibility

The data reproducibility was examined by repeating experiments with two sets of column reactors packed with catalyst of silica gel/CuBr = 20 at 80 °C. Figure 6.18 shows that the rate curves of the two experiments were the same. The difference in the apparent rate constants was 5.2% (3.8×10^{-3} min^{-1} and 3.6×10^{-3} min^{-1} respectively). The molecular weights of the PMMA prepared by the two experiments were also very close (see Figure 6.19). This result indicates that the continuous ATRP process had a very good reproducibility.

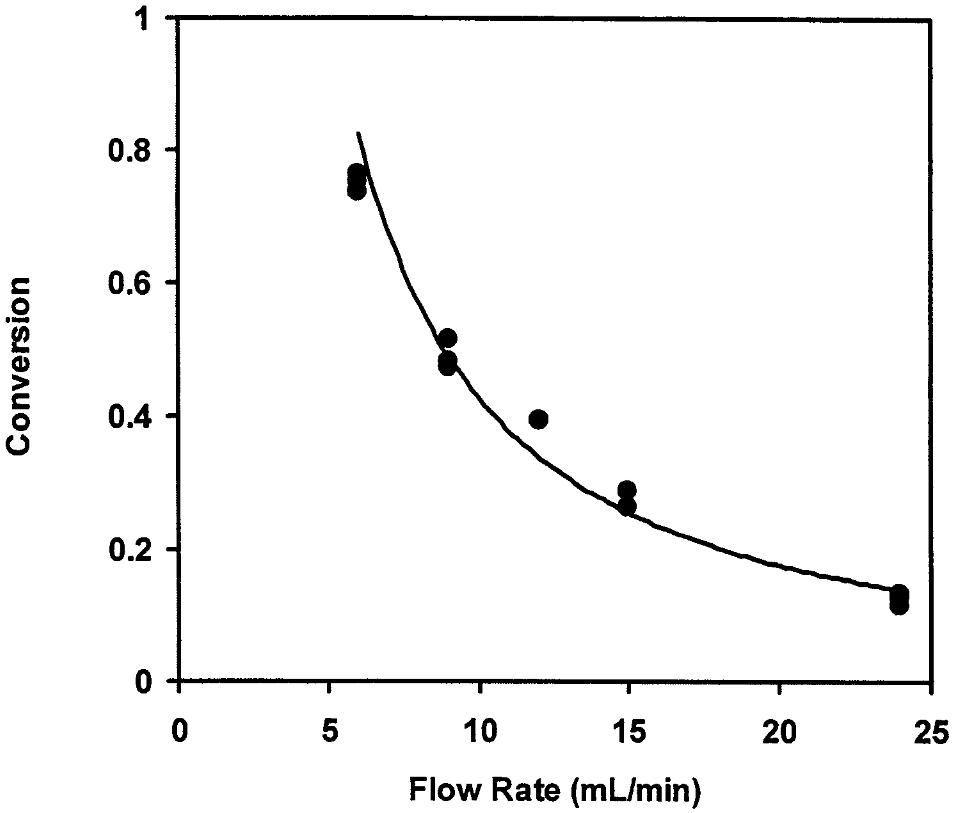

Figure 6.16. The MMA conversion as a function of flow rate for the polymerization of MMA in two larger column reactors in series.

MMA/toluene = 1/3 (w/w), MMA/MBP = 100(molar), Silica gel/CuBr = 20 (molar); 80 °C.

Reactor: 500 cm in length, 7.8 mm in diameter

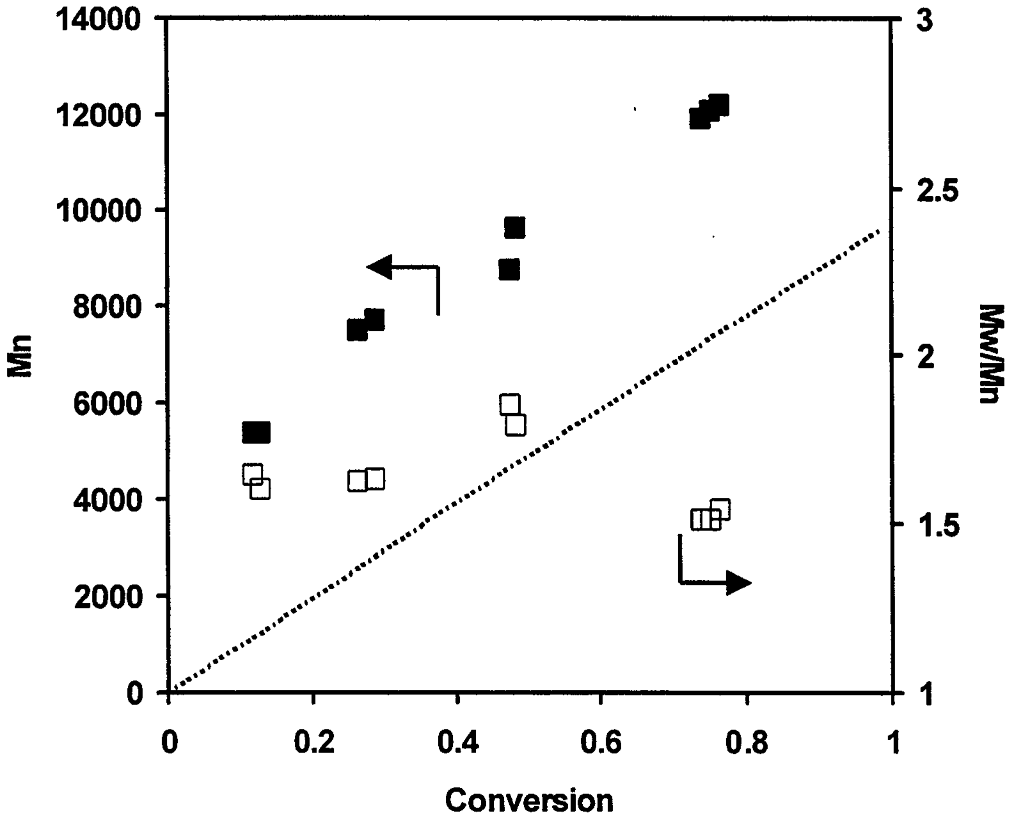

Figure 6.17. The molecular weight of PMMA as a function of MMA conversion for the polymerization in the two larger reactors. See Figure 6.16 for reaction condition. Theoretical Mn (.........).

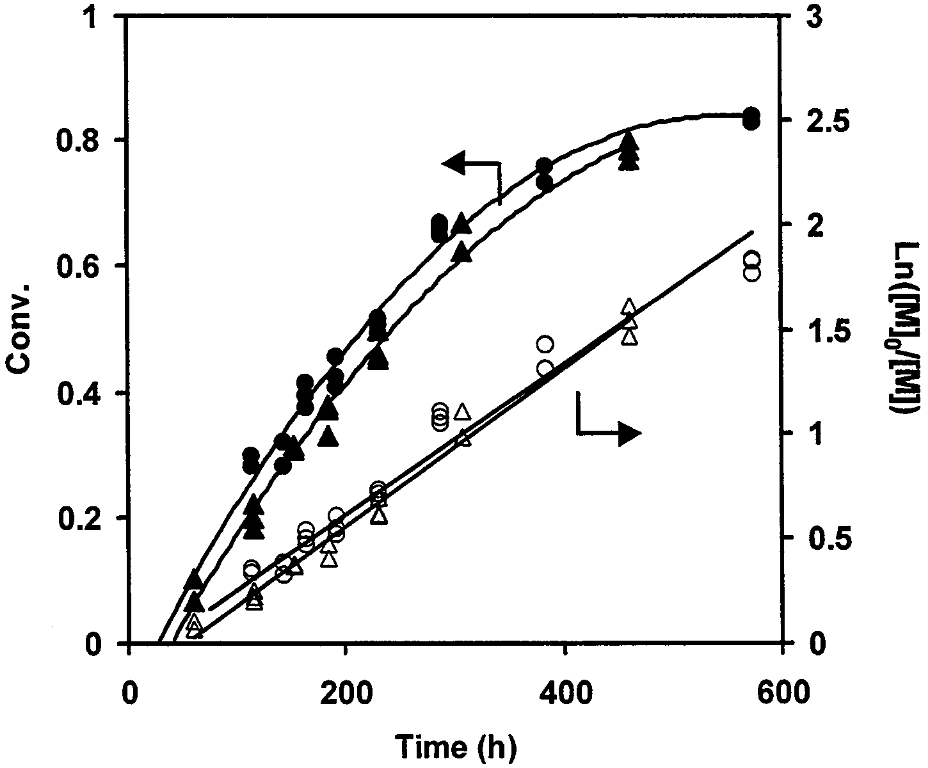

Figure 6.18. The kinetic plots of MMA polymerization in different runs.

MMA/toluene = 1/3 (w/w), MMA/MBP = 100, Silica gel/CuBr = 20; 80 °C.

Run 1(●, ○), run 2 (▲, △).

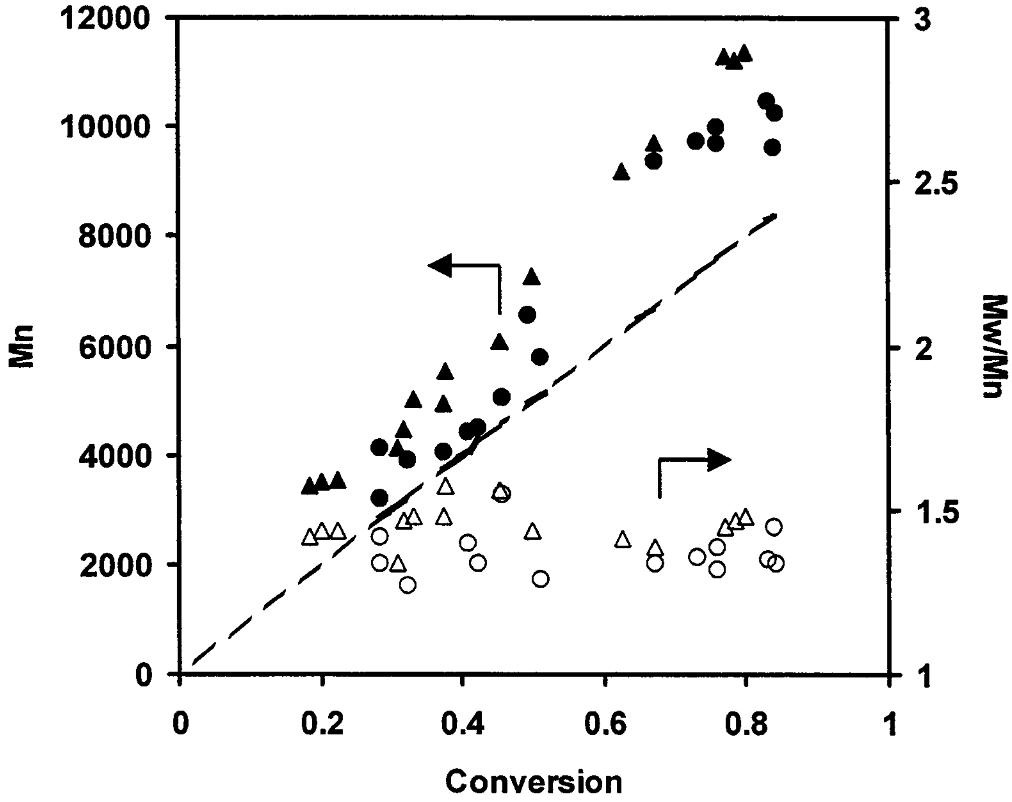

Figure 6.19 The molecular weight and polydispersity of PMMA produced in different runs. See Figure 6.18 for experimental conditions.

Run 1(●, ○), run 2 (▲, △), Theoretical Mn (.........).

6.3.7 Block Copolymerization of MMA with nBMA

The block copolymerization by supported ATRP in a batch process has been studied.[23,24] This work reports the continuous block copolymerization of MMA with nBMA carried out in two column reactors packed with catalyst in series, as shown in Scheme 6.2. MMA and initiator (MMA/initiator = 30) were delivered to Reactor I to produce prepolymer PMMA. The PMMA prepolymer eluting from Reactor I was mixed with the second monomer n-butyl methacrylate (nBMA) and the mixture was pumped into Reactor II for block copolymerization. The produced block copolymers were analyzed by GPC (see Figure 6.20) and their compositions were analyzed by NMR spectra (Table 6.1).

The molecular weight of PMMA prepolymer obtained from the first reactor was 4,000 with 80% conversion. When nBMA was injected at the flow rate of 1.2 mL/h, a block copolymer of molecular weight of 11,000 was produced. Increasing the nBMA flow rate to 1.8 mL/h yielded a block copolymer of molecular weight of 18,000. There were no prepolymer shoulder peak in the GPC traces of the block copolymer samples, indicating little contamination of the PMMA prepolymer and that the prepolymer PMMA chains eluted from the first reactor initiated the nBMA polymerization in the second reactor. These results further confirmed that the continuous supported ATRP in the reactor proceeded in a living manner. This work also demonstrated that the series tubular reactor system is a feasible technology for synthesizing block copolymers with their block molecular weights readily adjustable by changing the two monomer flow rates.

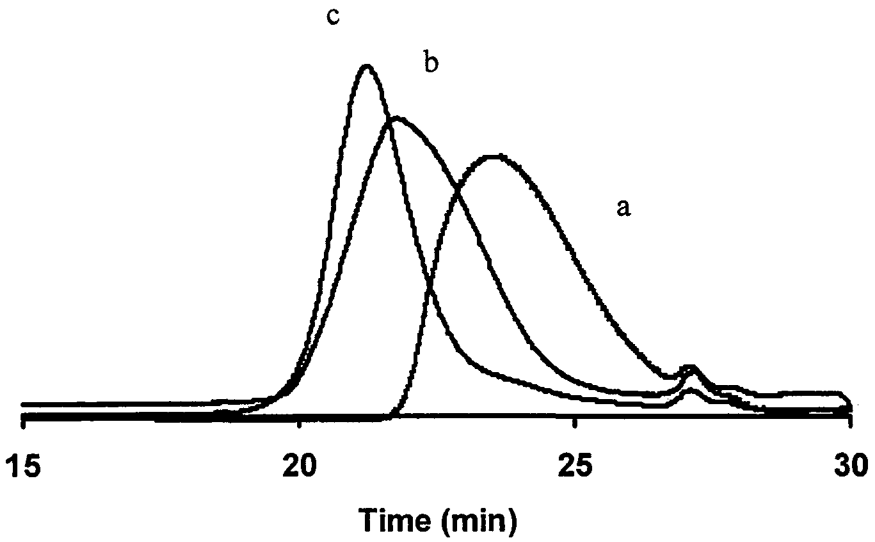

Figure 6.20. The block copolymerization of MMA and nBMA by two reactors in series.

PMMA prepolymer (a) produced in Reactor I: MMA/toluene = 1/4 (w/w), MMA/MBP = 30 (molar), Silica gel/CuBr = 20 (w/w); 80 °C, flow rate = 1.2 mL/h;

Reactor II: Silica gel/CuBr = 20 (w/w); 80 °C, pure nBMA, flow rate = 1.2 mL/h (b), 1.8 mL/h (c).

Table 6.1. The block copolymerization of MMA with nBMA in the two column reactors in series

nBMA Flow rate	MMA Conv. (%)	nBMA Conv.(%)	Mn	Mw/Mn	MMA/nBMA In copolymer
0	82	-	4,000	1.38	100/0
1.2	85	40	11,000	1.70	43/57
1.8	86	40	18,000	1.84	32/68

See Figure 6.20 for experiment conditions.

It should be pointed out that there are also some challenges remain to be solved for this newly developed continuous supported atom-transfer radical polymerization technology (C-SATRP). First, the conversions of the second monomer were low. This was caused by the high flow rate in the second reactor due to the combined flows from the first reactor and that of nBMA. There was also some percentage of MMA units in the second block due to the presence of residual MMA in the flow eluting from the first reactor. Further developments should be directed to increase the second monomer conversion using a reactor having higher mean residence time and/or to remove the unreacted MMA from the prepolymer solution to avoid its contamination to the second block composition.

6.4 Summary

The column reactor system packed with silica gel supported CuBr-HMTETA catalyst was demonstrated to be very useful for continuous homo- and block copolymerization of MMA. The system had good stability with respect to both reactor activity and PMMA molecular weight. Various product grades of polymers having different molecular weights can be readily prepared by adjusting the monomer flow rate and/or by changing the monomer/initiator ratio. The block copolymerization of MMA with n-butyl methacrylate (nBMA) using two column reactors connected in series was useful for preparing block copolymers with controlled molecular weight and block distribution.

6.5 References

1. Matyjaszewski, K. Ed. *Controlled Radical Polymerization;* American Chemical Society: Washington, DC **1997**; ACS Symp. Ser. Vol. 685.
2. Wang, J.; Matyjaszewski, K. *J. Am. Chem. Soc.* **1995**, *117*, 5614.
3. Percec, V.; Barboiu, B; Neumann, A.; Ronda, J.C.; Zhao, M. *Macromolecules* **1995,** *29*, 3665.
4. Kato, M; Kamigaito, M.; Sawamoto, M.; Higashimura, T. *Macromolecules* **1995**, *28*, 1721.
5. Matyjaszewski, K.; Wei, M.; Xia, J.; McDermott, N. E. *Macromolecules* **1997**, *30*, 8161.
6. Granel, C.; Teyssie, Ph.; Dubois, Ph.; Jerome, Ph. *Macromolecules* **1996**, *29*, 8576.
7. Uegaki, H.; Kotani, Y.; Kamigaito, M.; Sawamoto, M. *Macromolecules* **1998**, *31*, 6756.
8. Lecomte, P.; Drapier, I.; Dubois, P.; Teyssie, P.; Jerome, R. *Macromolecules* **1997**, *30,* 7631.
9. Matyjaszewski, K.; Beers, K. L.; Kern, A.; Gaynor, S. G. *J. Polym. Sci.: Part A: Polym. Chem.* **1998**, *36*, 823.
10. Haddleton, D. M.; Waterson, C.; Derrick, P. J.; Jasieczek, C. B. and Shooter, A. J. *Chem. Commun.* 1997, 683.
11. Zeng, F.; Shen, Y.; Zhu, S. and Pelton, R. *Macromolecules*, **2000**; *33,* 1628.
12. Shen, Y.; Zhu, S.; Zeng, F. and Pelton, R. *Macromolecules,* 2000, *33,* 5399.
13. Matyjaszewski, K.; Pintauer, T.; Gaynor, S. *Macromolecules* **2000,** *33,* 1476.

14. Kickelbick, G.; Paik, H.; and Matyjaszewski, K. *Macromolecules* **1999,** *32*, 2941.

15. Haddleton, D. M.; Duncalf, D. J.; Kukulj, D. and Radigue, A. P. *Macromolecules,* **1999**, *32*, 4769.

16. Shen, Y.; Zhu, S.; Pelton, R. *Macromolecules* **2000,** *33,* 5427.

17. Shen, Y., Zhu, S.; Pelton, R. *Journal of Polymer Science Part A: Polymer Chemistry,* **2001**, *39*, 1051.

18. Shen, Y., Zhu, S.; Pelton, R *Macromolecules* **2001,** *34,* 5812.

19. Pietro, T. *Continuous flow methods in organic synthesis* New York: Ellis Horwood, **1991**.

20. Zhu, S.; Shen, Y.; Pelton, R. *US Patent* 2,307,438.

21. Shen, Y.; Zhu, S.; Pelton, R. *Macromolecules* **2000**, *33*, 5399.

22. Zhu, S. *Macromolecular Theory and Simulations* **1999,** *8,* 29.

23. Davis, K. A. and Matyjaszewski K. *Macromolecules* **2001**, *34*, 2101;

24. Davis, K. A. and Matyjaszewski K. *Macromolecules* **2000,** *33*, 4039.

Chapter 7

Summary of the Thesis and Recommendations for the Future Work in This Field

7.1 Summary of the Thesis

This thesis systematically studied the macromonomer synthesis by ATRP and the catalyst supporting approaches for the catalyst contamination reduction in ATRP products by batch and continuous processes.

Chapter 1 generally introduced the concept of ATRP and its applications in synthesis of polymers of controlled molecular weights, block copolymers, star and hyperbranched polymers. The challenges of ATRP and objectives of this thesis are presented

Chapter 2 studied the macromonomer synthesis by ATRP. Four vinyl-containing initiators: 2′-vinyloxyethyl 2-bromoisobutyrate (VBIB), 3′-vinyloxypropyl 2-bromoisobutyramide (VBIBA), 2′-vinyloxyethyl 2-bromopropinate (VBP) and 3′-vinyloxylpropyl trichloroacetamide (VTCA) were synthesized and screened for the preparation of vinyl-terminated macromonomers of different monomers by ATRP. With copper bromide/hexamethyltriethylenetetramine (HMTETA) as catalyst, VBIBA and

VBP initiated ATRP of methyl methacrylate (MMA) and 2-(*N,N*-dimethylamino)ethyl methacrylate (DMAEMA) but produced polymers with high polydispersities due to slow initiation reaction. VBIB and VTCA initiated ATRP of MMA and DMAEMA, and VBIB initiated styrene polymerization in a first order monomer kinetics, producing polymers with controlled molecular weight and low polydispersity. The GPC traces showed no consumption of the vinyl moieties from the initiators at monomer conversions up to 80% during the polymerizations of DMAEMA, MMA and styrene. The polymerizations of methyl acrylate and butyl acrylate with VBIB as initiator initially were in a first order monomer kinetics, but the kinetics deviated its first order at a conversion around 50%. The GPC results indicated that the vinyl moieties on the polymer chain ends started to participate in the polymerization at this conversion. ^{1}H-NMR showed that the molecular weights of PMMA, poly(DMAEMA) and polystyrene agreed well with the theoretical values, confirming that all polymer chains contained terminal vinyl groups derived from the initiators, i.e. corresponding macromonomers. The polymerizations of acrylates terminated at the early stage also produced corresponding polyacrylate macromonomers with controlled molecular weights, but polymerization of acrylates at high conversions consumed most of the vinyl moieties.

Chapter 3 reported the catalyst supporting by physical adsorption to reduce the catalyst contamination in the product and to recycle the catalyst. The adsorption experiment showed that copper bromide-hexamethyltriethylenetetramine (CuBr/HMTETA) complex was adsorbed onto silica gel surface rapidly due to the high affinity of the complex to the hydrophilic silica gel surface. Therefore, the complex was supported on silica gel by physical adsorption for the ATRP of methyl methacrylate (MMA) in toluene. The supported complex mediated a living polymerization of MMA, yielding polymers with controlled molecular weights and low polydispersities. A low level of catalyst concentration was found essential to have high initiator efficiency. The MMA and silica gel concentration significantly influenced the polymerization behavior. At higher monomer concentration (e.g., 50% w/w) the polymerization was less controlled due to diffusion limitations of the supported catalyst in viscous media. Therefore low monomer concentration was required for supported ATRP. Increasing silica gel concentration resulted in a higher polymerization rate but lower initiator efficiency. The supported catalysts were recycled for second and third uses. The recycled catalysts retained 80% in the second use and 50 % in the third use of its initial activity. The recycled catalysts had improved control over the polymer molecular weights benefited from Cu(II) in the recycled catalysts. This supported catalyst could also be used for the macromonomer synthesis, but the vinyl moieties from the VBIB initiator began to participate in the polymerization at a medium monomer conversion. In the polymerization of 2-(*N,N*-dimethylamino)ethyl methacrylate, only a fraction of the catalyst was adsorbed to silica gel surface due to the high polarity of the monomer.

Chapter 4 investigated the catalyst supporting via chemical binding for the polymerization of polar monomers and/or in polar solvents. Silica gel particles grafted with tetraethyldiethylenetriamine (TEDETA) were used as a support for CuBr for heterogeneous atom transfer radical polymerization of MMA. The immobilized CuBr mediated a living polymerization of MMA, demonstrated by a linear increase in molecular weight with conversion and low polydispersity. An excessive amount of catalyst, typically CuBr/initiator = 1.5, was required to achieve a living process due to limited mobility of the supported catalyst. The concentration of silica gel had a strong effect on the polymerization. Lower or higher silica gel deteriorated the control of polymerization. The recycled catalyst still mediated a living process, but had a reduced catalytic activity, which was caused by the presence of Cu(II). After regenerated with Cu(0), the catalyst regained some activity.

The catalyst supporting spacer, the portion between catalyst and silica gel, affected the catalyst diffusion and thus the catalyst activity and the control of polymerization. Silica gels grafted with tetraethyldiethylenetriamine (TEDETA) and di-(2-picolyl)amine (DiPA) via polyethylene glycol (PEG) spacers of different chain lengths were synthesized, and used as CuBr support for ATRP of MMA to investigate the spacer effects. Catalyzed by CuBr immobilized on the silica gel, the MMA polymerization rate increased with spacer length in the order of $PEG_1 < PEG_{10} < PEG_3$ (the subscript is the number of the EG units). Copper bromide supported via 3-unit PEG (SG-PEG_3-TEDETA and SG-PEG_3-DiPA) had the best control over the MMA polymerization, producing PMMA with controlled molecular weights (initiator efficiency ca. 75%) and low polydispersities (Mw/Mn ~1.2-1.4), while a longer or shorter spacer length decreased the catalyst activity and control of polymerization. The recycled catalysts had activities similar to the fresh ones at the late stage of polymerization with improved initiator efficiencies. This catalyst also initiated the polymerization of 2-(*N*,*N*-dimethylamino)ethyl methacrylate. The PMMA-*block*-poly(2-(*N*,*N*-dimethylamino)ethyl methacrylate) with well-controlled molecular weight and low polydispersity was also synthesized by this support system.

Chapter 5 developed a soluble and recoverable support for the ATRP catalyst to overcome the adverse effects of insoluble support on the control of polymerization. A catalyst on soluble-and-recoverable support can dissolve in solution to have a homogeneous reaction at polymerization temperature but precipitate from the solution for catalyst recycling. Polyethylene (PE_{2}, PE_{16}, PE_{25}) and polyethylene-*block*-polyethylene glycol (PE_{16}-PEG_{10}, PE_{25}-PE_{4}) (the subscripts are the monomer units) grafted with tetraethyldiethylenetriamine (TEDETA) were used as soluble and recoverable supports for copper bromide for ATRP of methyl methacrylate. The effects of PE chain length and polyethylene glycol (PEG) spacer on the catalytic activity and control of the polymerization were investigated in detail. With PE as support, the catalytic activity and control of the polymerization were low and decreased as the PE chain length increased. This deteriorating effect of the PE support was minimized by using polyethylene glycol (PEG) as spacer to graft the catalyst onto the PE support. The PE_{25}-PEG_{4}-TEDETA-CuBr was found to effectively mediate the ATRP of MMA. The recycled catalysts on PE supports had low activity because of catalyst side reactions or loss of catalyst, but the catalyst with PE_{25}-PEG_{4}-TEDETA-CuBr retained 90% activity of its fresh catalyst with a good control over the polymerization. PE_{25}-PEG_{4}-TEDETA-CuBr was also versatile for other monomers such as styrene and DMAEMA. The block copolymer prepared by this supported catalyst had well-controlled molecular weight and low polydispersity.

Chapter 6 developed the first continuous ATRP process for homo- and block-copolymerization of MMA using column reactors packed with silica gel supported copper bromide (CuBr) -hexamethyltriethylenetetramine (HMTETA). The reactor showed a good stability (>100 h) in both catalyst activity and molecular weight of produced poly(methyl methacrylate) (PMMA). The silica gel/CuBr ratio strongly affected the stability of the reactor. The reactor packed with catalysts of silica gel/CuBr = 20 or 30 had a constant activity over 120 h, but the reactor packed with silica gel/CuBr = 10 had very low initial activity. The monomer conversion decreased as the flow rate increased or temperature decreased. The polymerization in the reactor was also in a first order kinetics with respect to monomer. The molecular weights of resulting PMMA increased linearly with MMA conversion, exhibiting a characteristic of living polymerization. Thus, the reactor readily produced PMMA of desirable molecular weight by simply adjusting the flow rate of MMA, which in turn determined the MMA conversion. In addition, the monomer/initiator ratio was also used as a parameter to control the polymer molecular weight. This process can be scaled up to have a higher productivity by using larger reactors. The block copolymerization of MMA with *n*-butyl methacrylate (nBMA) was carried out by using two reactors in series. The produced block copolymers had little contamination of PMMA prepolymer. The chain length of nBMA block could be adjusted by the flow rate of nBMA in the second reactor.

7.2 Recommendation for Future Work

The novel batch and continuous supported ATRP developed in this thesis work have good potentials for industrial applications. The further developments are recommended in the following:

7.1.1 To Improve the Stability of the Reactor.

The stable period of this current continuous ATRP process is about 100 h. The stable period has to be improved to a much longer time one, say 1000 h, to be cost effective for possible industrial uses. The accumulation of Cu(II) in the reactor and the catalyst loss are the main reasons for the activity reduction. Cu(II) is produced by persistent radicals due to radical termination, as evidenced by low initiator efficiency (60-70%). The radical termination can be suppressed by adding Cu(II) to the catalyst system and thus prevents the Cu(II) accumulation. The loss of catalyst in the current CuBr/HMTETA system is caused by continuous washing the catalyst out of the reactor due to no covalent binding between the catalyst and silica gel surface. One way to solve this problem is to supply a small amount of catalyst in the monomer solution to make up this loss to maintain the reactor activity. Another way to avoid this catalyst loss is to use grafting-supported catalyst described in Chapter 5, which the catalyst is immobilized onto silica gel surface by covalent binding to resist washing out of the reactor.

7.2.2 To Narrow the Polymer Polydispersity

The polydispersities of the polymers prepared by the current reactors is about 1.4-1.8, much higher than those prepared by batch processes with the same catalysts. This broadening is caused by the broad residence time distribution of the reactor, as discussed in Section 6.3.3. The size of silica gel we used ranged from 60-150 μm with various shapes. This allowed the packed column reactor to easily develop channels or dead zones, which resulted in broad residence time distribution. Therefore using mono-dispersed particles to support the catalyst may improve this aspect. These mono-dispersed particles can be silica gel. If mono-dispersed silica gel is not readily available, mono-dispersed cross-linked polystyrene particles with functionalized surface may be used. It is easy to synthesize mono-dispersed polystyrene spheres.

7.2.3 To Increase the Second Monomer Conversion in the Copolymerization and to Purify the Second Monomer Block of the Copolymer.

The conversion of the second monomer in the second reactor for the copolymerization by the reactors packed in series was low due to the combined flows from the first and second reactors. One way to increase the second monomer conversion is to use a larger reactor so as to have longer mean residence time for the polymer chains to grow in the second reactor. There was also a fraction of MMA units in the second block due to the presence of residual MMA in the flow eluting from the first reactor. A process, e.g. vacuum process, must be designed to remove the un-reacted MMA from the prepolymer solution to avoid its contamination to the second block.

7.2.4 Reactor Scaling-Up

The column reactors used in this work are small and for demonstration purposes. Section 6.3.5 has demonstrated that using larger reactor can have a higher productivity. Much larger sized columns are needed for full-scale industrial processes. A pilot plant sized reactor system is needed to be built for the study of the transport phenomena involved in the process. The scale-up work involves the principles of fluid dynamics, mass transfer, heat transfer, and reactor engineering. As discussed in Chapter 6, the viscosity of the polymerization solution eluting from the reactor was higher after the monomer conversion reached 80% or higher. High viscosity limits the transfer process, especially mass transfer, which limits the access of polymer chains to the catalytic sites for chain growth and thus results in high polymer polydispersity. Therefore special attention has to be paid to design the reactor to facilitate mass transfer inside the reactor.